Specific Targeting of Human Caspases with DARPins

Dissertation

zur Erlangung der naturwissenschaftlichen Doktorwürde

(Dr.sc.nat.)

vorgelegt der

Mathematisch-naturwissenschaftlichen Fakultät

der

Universität Zürich

Von

Thilo Schroeder

Aus

Deutschland

Promotionskomitee

Prof. Dr. Markus Grütter (Vorsitz)

Prof. Dr. Ben Schuler

Prof. Dr. Jürgen Rühe

Zürich 2012

CONTENTS

CONTENTS I
SUMMARY IV
ZUSAMMENFASSUNG VI
LIST OF FIGURES VIII
LIST OF TABLES IX
LIST OF ABBREVIATIONS IX
1. INTRODUCTION 12
1.1 Apoptosis 12
1.1.1 Apoptosis in physiology and pathologies 13
1.1.2 Signal transduction leads to the activation of a complex proteolytic network 14
1.1.2.1 The intrinsic pathway 15
1.1.2.2 The extrinsic pathway 16
1.1.3 Activation of caspases leads to severe morphological changes 17
1.1.3 Targeting apoptosis 20
1.1.3.1 Targeting the receptors 22
1.1.3.2 Regulating the regulators 23
1.1.3.3 Targeting peptidases 23
1.2 Caspases 25
1.2.1 Caspases – The main mediators of apoptosis 25
1.2.1.1 History 25
1.2.1.2 Classification 25
1.2.1.3 Architecture 26
1.2.1.4 Sequence and homology 27
1.2.1.5 Catalytic mechanism 28
1.2.2 Caspase regulation – From zymogen to the active peptidase 30
1.2.2.1 Activation of executioner caspases 30
1.2.2.2 Activation of initiator caspases - proximity induced activation 30
1.2.3 Activation platforms 31
1.2.3.1 The apoptosome – a soluble receptor 32
1.2.3.2 The DISC – a membrane receptor 34
1.2.4 Structure and biochemistry of caspases 36
1.2.4.1 Caspase structure 36
1.2.4.2 Active site architecture 38

1.2.4.3 Substrate recognition 39
1.2.4.4 Peptide specificity 40
1.2.5.1 Exosites 41
1.2.5.2 Caspase phosphorylation 42
1.2.5.3 Allosteric mechanisms 43
1.3 Targeting and analyzing caspases 44
1.3.1 General strategies of caspase inhibitor design 44
1.3.2 Alternative strategies for the development of caspase inhibitors 46
1.3.3 Specific inhibition of caspases 47
1.3.4 Specific activation of caspases 49
1.3.5 Specific analysis of caspase activities 50
1.4 Designed Ankyrin Repeat Proteins and their applications 52
1.4.1 Antibodies and the rise of alternative scaffolds 52
1.4.2 Design of DARPins based on ankyrin repeat proteins 54
1.4.3 Stability and folding of DARPins 57
1.4.4 Target directed DARPin selection with display techniques 58
1.4.5 Recent Applications of DARPins 61
1.4.6 Applications and future perspective 64
2. Expression, purification and kinetic characterization of human caspases 68
3. Development of a caspase specific microarray using DARPins as capture reagents 102
Introduction 102
Results 104
Discussion 119
Material and Methods 123
4. Specific inhibition of caspase-3 by a competitive DARPin 128
5. A DARPin activator of caspase-8 176
Introduction 176
Results 178
Discussion 190
Material and Methods 194
6. APPENDIX 200
HIV-1 protease inhibition potential of functionalized polyoxometalates 200
7. BIBLIOGRAPHY 210
8. CURRICULUM VITAE 218
9. ACKNOWLEDGEMENTS 220

SUMMARY

Programmed cell death (apoptosis) is an important process in development and tissue homeostasis of multicellular organisms. Apoptosis is triggered by various stimuli that lead to signal transduction and the activation of a complex proteolytic network consisting of cysteine aspartate-specific peptidases (caspases). Caspases cleave tetra peptide sequences with an absolute requirement of an aspartic acid in P_1, while the remaining three amino acids contribute to the specificity of the caspases; yet, overwhelming evidence indicates that the eleven caspase family members have overlapping sequence specificities. This latter feature has long been ignored in the design of putative caspase specific peptide substrates and inhibitors which are commonly used to dissect the apoptotic pathway.

In order to overcome the limited specificity of active-site directed compounds we have used designed ankyrin repeat proteins (DARPins) which are able to recognize their target proteins with high specificity. Based on a panel of DARPins that were selected against nine different caspases we aimed to develop novel strategies to specifically inhibit, activate and analyze caspases.

To this end, we first established expression protocols and a comprehensive kinetic characterization procedure for caspase-1 to -9. These caspases were used as target proteins for the selection of DARPins with ribosome display. The selected DARPins were systematically characterized using high throughput techniques such as ELISA, protein arrays and surface plasmon resonance. In total, over 200 DARPins selected against nine caspases were evaluated and ranked according to their kinetic properties and specificity.

Through this approach we identified two DARPins that inhibit the catalytic activity of caspase-3 with high affinity (K_D=9.6 or 3.4 nM) and specificity. Both DARPins were found to inhibit caspase-3 while not affecting the catalytic activity of the closely related caspase-7 (57% sequence identity). This example demonstrates that specificity can be achieved by using larger proteins instead of small active-site directed molecules. Our structural and kinetic description of this protein inhibitor complex revealed a competitive inhibition mechanism involving a direct interaction with the peptide binding

interface. Interestingly, we found that this DARPin mediates inhibition via a similar mechanism used by the natural inhibitor XIAP and the peptide inhibitor DEVD.

Furthermore we have found a DARPin which specifically interacts with caspase-8 leading to an significant increase of the activity. Based on a high resolution structure we were able to uncover the molecular basis of this finding. The interaction increases the activity of caspase-8 by locking loop1 in a substrate bound conformation leading to formation of a caspase-8 dimer. This study provides new evidence on the dynamic nature of caspase-8 active site loops and the link with dimer formation.

Taken together, this thesis describes a set of comprehensive protocols for the expression and characterization of caspases as well as presents evidence for, the selection of DARPins specific for each of the caspase family member. We have identified caspase inhibitors, activators and high resolution structures allowing us to uncover the molecular basis of the functional DARPin/caspases interactions.

ZUSAMMENFASSUNG

Programmierter Zelltod (Apoptose) ist ein wichtiger Prozess in der Entwicklung und Homöostase mehrzelliger Organismen. Verschiedene Reize können Apoptose auslösen, dies führt wiederrum zu der Aktivierung eines proteolytischen Netzwerkes, welches von den sogenannten Caspase gebildet wird. Caspasen schneiden ihre Substrate an definierten Tetra-Peptid Sequenzen hinter Asparaginsäure in Position P_1. Die Erkennung der weiteren drei Aminosäuren tragen zur Spezifität der Caspases bei, wobei die elf humanen Caspasen stark überlappenden Sequenzspezifitäten aufweisen. Diese Tatsache wurde in der Entwicklung und Verwendung von Caspase Substraten oder Inhibitoren oft nur unzureichend berücksichtigt da sie nach wie vor als „caspase-spezifisch“ bezeichnet werden. Während meiner Doktorarbeit habe ich neue Strategien entwickelt um Caspasen spezifisch zu detektieren, zu inhibieren oder zu aktivieren. Als Technologie haben ich sogenannte „designed ankyrin repeat proteins“ (DARPins) verwendet und habe neun verschiedene humane Caspasen in meine Studie mit einbezogen.

In einer ersten Studie haben wir ein umfassendes Protokoll für die Expression und der kinetischen Charakterisierung von Caspase-1 bis -9 entwickelt. Gegen diese Caspases haben wir DARPins unter der Verwendung von Ribosome Display selektioniert und anschliessend systematisch charakterisiert. Insgesamt wurden ca.200 DARPins aufgrund ihrer Bindungseigenschaften und Spezifität gegen jeden Caspase klassifiziert.

In diesem Ansatz haben wir zwei DARPins identifiziert, welche Caspase 3 mit hoher Affinität bindet (K_D=9.6 und 3.4 nM) und gleichzeitig inhibiert. Beide DARPins sind spezifisch für Caspase-3 und erkennen weder die homologe Caspase-7 (57 % Sequenzidentität) noch andere Caspasen. Desweiteren haben wir diesen Proteinkomplex mittels Röntgenstrukturanalyse aufgeklärt und können so den kompetitiven Inhibitionsmechanismus und die Grenzfläche der Interaktion beschreiben. Interessanterweise verwenden die DARPins einen ähhnlichen Inhibitionsmechanismus wie diese auch bei den natürlichen Inhibitoren DEVD.fmk und XIAP beobachtet wurde.

Des Weiteren haben wir einen DARPin identifiziert, welcher Caspase-8 spezifisch bindet (K_D=5.2 nM) und gleichzeitig die Aktivität von Caspase-8 steigert. Aufgrund einer Kristallstruktur haben wir

den molekularen Mechanismus, welcher die Aktivität steigert, beschreiben können. Der DARPin bindet Loop1 in einer Konformation die einer Bindung des Substrates begünstig und die Dimerisierung des Enzyms unterstützt.

Insgesamt betrachtet haben wir eine umfassende Strategie für die Expression und Charakterisierung humaner Caspasen erstellt, aufgrund welcher wir DARPins gegen neun Caspasen selektioniert haben. Diese DARPins haben wir systematisch unter der Verwendung von Hochdurchsatz-Screening Methoden wie Protein Microarrays und surface plasmon resonance (SPR) evaluiert. Aus dieser „Library“ konnten wir interessante DARPins identifizieren und Strategien zur Inhibition oder Aktivierung von Caspasen entwickeln. Röntgenstrukturanalysen dieser Caspase/DARPin Komplexen haben es uns ermöglicht die molekulare Grundlagen dieser funktionellen DARPins aufzuklären.

LIST OF FIGURES

Figure 1-1: Apoptosis 13
Figure 1-2: Apoptotic cascade 17
Figure 1-3: Common damages of an apoptotic cell. 20
Figure 1-4: Targeting apoptosis 22
Figure 1-5: The Caspase family. 26
Figure 1-6: Catalytic mechanism of cysteine peptidases 29
Figure 1-7: Apoptotic activation plattforms 33
Figure 1-8: Protein structure of Caspases. 37
Figure 1-9: Caspase substrate specificity 40
Figure 1-10: Caspase inhibitors 45
Figure 1-11: Caspase inhibition strategies by nature 47
Figure 1-12: Specific allosteric inhibition of caspase-2 by a DARPin 48
Figure 1-13: Overview of selected alternative scaffolds 54
Figure 1-14: Architecture of a DARPin 56
Figure 1-15: Protein display technologies 60
Figure 1-16: Crystal structures of DARPins 63
Figure 1-17: Possible applications of DARPins. 66
Figure 3-1: Workflow of the selection and characterization of DARPins. 103
Figure 3-2: Selection of DARPins. 105
Figure 3-3: SPR analysis of DARPins 107
Figure 3-4: SPR specificity analysis 108
Figure 3-5: Protein microarrays 114
Figure 3-6: Optimization of protein microarrays 116
Figure 3-7: Specificity of DARPins tested on microarrays 117
Figure 3-8: Potential formats for a caspase specific DARPin microarray 120
Figure 3-9: Overview of the RD selection strategy 124
Figure 5-1: DARPin selection against caspase-8 178
Figure 5-2: Analysis of DARPin binding to caspase-8 181
Figure 5-3: Crystal structure of caspase-8 in complex with DARPin_8.4 184
Figure 5-4: Caspase-8 superimposition 187
Figure 5-5: Caspase-8 activity is influenced by DARPin_8.4 188
Figure 5-6: Diagrammatic representation of caspase-8 monomer-dimer equilibrium 192

LIST OF TABLES

Table 3-1: DARPins selected against caspases 111
Table 3-2: Association, dissociation kinetics and K_D-values of selected DARPins for each caspase. 118
Table 5-1: Kinetic data obtained by ITC and SPR 179
Table 5-2: Crystallization and refinement statistics of the caspase-8/D8.4 crystal structure. 182
Table 5-3: Analytical Ultracentrifugation 189

LIST OF ABBREVIATIONS

ADP	Adenosine Di-Phosphate
AIF	Apoptosis-Inducing Factor
Akt	Serine/Threonine Protein Kinase
AML	Acute Myeloid Leukemia
Amp	Ampicillin
Apaf-1	Apoptotic Protease Activating Factor 1
APH	Aminoglycoside Phosphotransferase (3')-IIIa
AR	Ankyrin Repeat
ATP	Adenosine Tri-Phosphate
Bak	Bcl-2 Homologous Antagonist/Killer
Bax	Bcl-2–Associated X Protein
Bcr	Breakpoint Cluster Region
BSA	Bovine Serum Albumin
CAD	Caspase-Activated DNAse
Cam	Chloramphenicol
CARD	Caspase Recruitment Domain
CASBAH	Caspase Substrate Data Base Homepage
CED	Cell Death Abnormal
CHAPS	3-[(3-Cholamidopropyl)dimethylammonio]-1-propanesulfonate
CTL's	Cytolytic T Lymphocytes
DARPin	Designed Ankyrin Repeat Protein
DD	Death Domain

DED	Death Effector Domain
DIABLO	Direct Inhibitor of Apoptosis Binding Protein with Low pI
DISC	Death-Inducing Signaling Complex
DNA	Deoxyribonucleic Acid
DTT	Dithiothreitol
ELISA	Enzyme-linked Immunosorbent Assay
FADD	Fas-Associated Death Domain
Fas	Apoptosis Stimulating Fragment
FasR	Fas receptor
fmk	Fluoromethylketone
GdmCl	Guanidiniumchlorid
HEPES	4-(2-Hydroxyethyl)-1-piperazineethanesulfonic Acid
Her2	Human Epidermal Growth Factor Receptor 2
HIV	Human Immunodeficiency Virus
HTS	High-Throughput Screen
ICAD	Inhibitor of CAD
ICE	Interleukin-1β-Converting Enzyme
IgG	Immunoglobulin G
IL-1β	Interleukin-1-Beta
IMAC	Immobilized Metal-ion Affinity Chromatography
IPTG	Isopropyl-1-thio-β-D-galactopyranosid
ITC	Isothermal Titration Calorimetry
Kan	Kanamycin
LRR	Leucin Rich Repeat
MBP	Maltose Binding Protein
NACHT	NAIP, CIITA, HET-E, and TP1 domain
NF-κB	Nuclear Factor 'kappa-light-chain-enhancer' of Activated B-cells
NK	Natural Killer
NMR	Nuclear Magnetic Resonance
PARP	Poly(ADP-ribose)polymerase
PDB	Protein Data Bank

RD	Ribosome Display
ROCKI	Serine/Threonine Kinase rho-Associated Kinase I
scFv	Single Chain Variable Fragment
SHP-1	Tyrosine Phosphatase-1
SMAC	Second Mitochondria-Derived Activator of Caspases
SPR	Surface Plasmon Resonance
TNF-1	Tumor Necrosis Factor-1
TNFR	Tumor Necrosis Factor Receptor
TRAIL	TNF-Related Apoptosis Inducing Ligand
XIAP	X-linked Inhibitor of Apoptosis Protein

1. INTRODUCTION

1.1 Apoptosis

During the evolutionary development of multicellular organisms it became crucial to maintain the size and form of the body and organs. This process is important in development and growth but also in tissue homeostasis in order to counterbalance cell proliferation in bone marrow and the intestine with billions of cells dying every hour. This removal of unwanted cells is known as programmed cell death where cells activate an intracellular protein cascade to kill themselves in a controlled manner. In 1972 Currie and colleagues termed this suicide program Apoptosis (from the Greek term “dropping of leaves from a tree”) to describe morphological features that are observed when cells die [1]. These distinct morphological features include cell shrinkage, chromatin condensation, DNA fragmentation and plasma membrane blebbing (Figure 1.1) [2, 3]. Several years later, researchers began to understand the molecular principles of apoptosis after the discovery of distinct proteases that are involved in programmed cell death of the nematode worm *Caenorhabditis elegans* by Horovitz and colleagues [4]. This finding led to the discovery of the first human apoptotic peptidases, “interleukin-1β-converting enzyme” ICE which was later renamed Caspase-1 [5, 6]. These fundamental discoveries represent the starting point of 20 years of intensive research in the field of apoptosis with over 200.000 scientific articles in the field. Although apoptosis is by far the most important and best described form of programmed cell death, other mechanisms and pathways have been described. Necrosis, necroptosis, caspase independent mitotic death and autophagy are the most common alternative forms; however in the context of this thesis, these processes will not be further described.

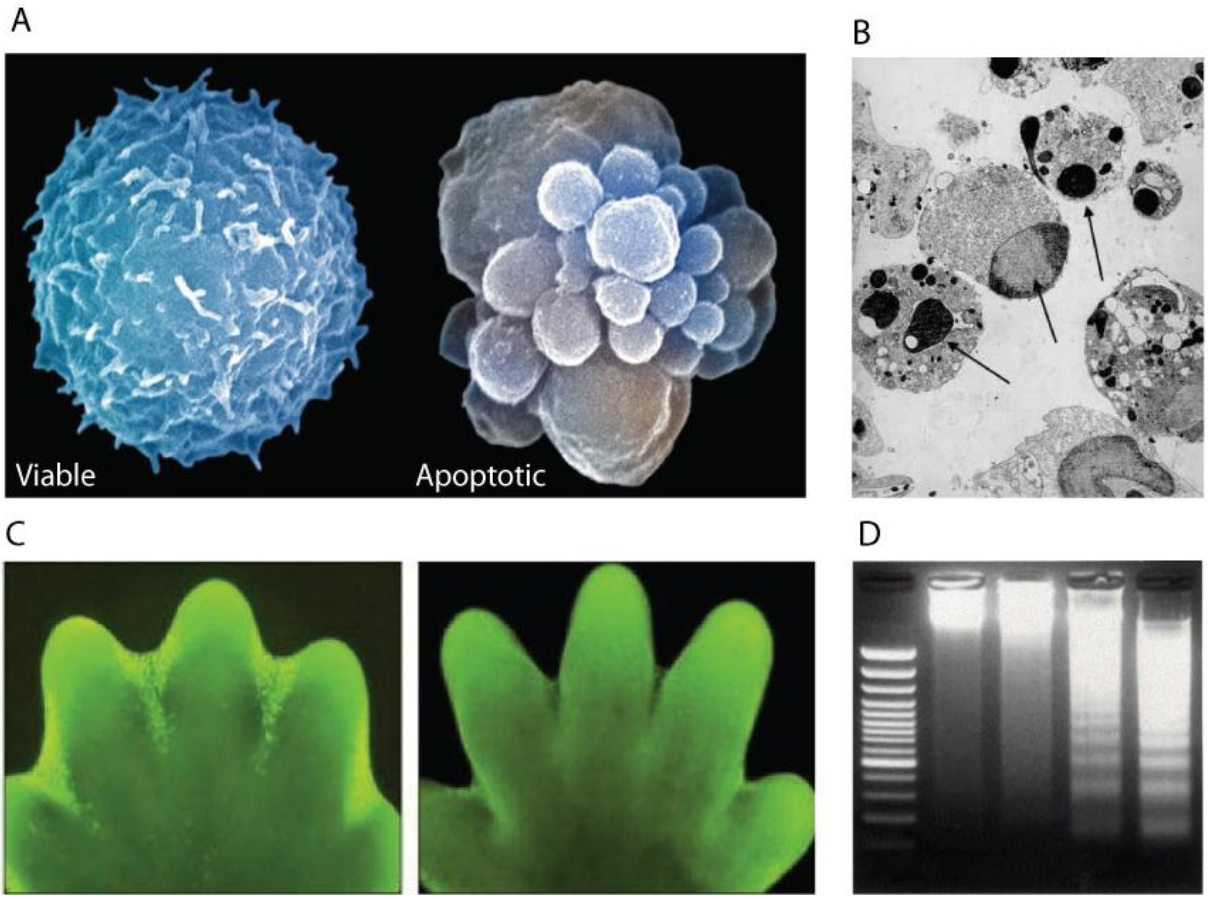

Figure 1-1: Apoptosis
(A) Morphological changes of a cell after induction of apoptosis shows cell shrinkage and membrane blebbing [3]. B) Nuclear morphology of a virus induced apoptotic cell shows shrinkage of the nucleus (arrows) due to loss of volume regulation [7]. C) Paw during embryonic development (left). Green fluorescing cells undergo apoptosis to remove unwanted tissue leading to separation of fingers (right)[8]. D) Agarose gel electrophoresis of apoptotic DNA fragments after treatment of cells with arsenic. DNA is cut into fragments of 180bp, a typical feature of apoptotic cells [9].

1.1.1 Apoptosis in physiology and pathologies

Although apoptosis occurs in a multitude of processes in physiology and pathogenesis the principle sequence of events remains the same. Cells receive an apoptotic stimulus which activates a complex proteolytic network leading to severe morphological changes and destruction of the cell. At the same time, the surface of an apoptotic cell becomes modified leading to a display of ligands that promote their engulfment by phagocytosis. Most of the proteins that are cleaved during apoptosis are believed to be essential for cell survival, however recent studies suggest that caspase mediated proteolysis also acts as a switch to dampen proinflammatory properties as it was shown for Interleukin-33 [10]. Thus Apoptosis

is not only responsible for cell death but plays a crucial role in cell removal, deactivation of proinflammatory proteins and survival of neighboring cells unlike necrosis which triggers an inflammatory response in the surrounding tissue. Apoptotic cells, even when large numbers of cells have died, are rapidly cleared and thus difficult to detect. For this reason researchers have for many years overlooked apoptosis and still underestimate its extent today [8].

The life of multicellular organisms is unthinkable without apoptosis. It is most critical in processes such as defining and shaping of embryos, development of the immune system, hematopoiesis and counterbalance of proliferating cells. Mutations of individual proteins in the apoptotic cascade lead to severe phenotypes or even death. The activation of apoptosis must be highly regulated as this process is irreversible once activated. Consequently evolution has derived a highly balanced system of pro apoptotic molecules and intrinsic inhibitor to orchestrate the activation of apoptosis in a spatial and time dependent manner. The complexity of this regulation is still poorly understood and further understanding is absolutely necessary because deregulation of apoptosis leads to many human diseases. It is generally accepted that too little apoptosis can lead to cancer and autoimmunity while inappropriate activation of apoptosis causes tissue damage and functional decline in acute diseases (tissue injury, stroke, myocardial infarction) and chronic diseases such as diabetes and Alzheimer's [11]. In order to target apoptosis a profound knowledge of intracellular and extracellular processes is required.

1.1.2 Signal transduction leads to the activation of a complex proteolytic network

Studies by Horvitz and colleagues in the nineties led to the discovery of the apoptotic pathway in the nematode *Caenorhabditis elegans*. The execution of apoptosis is controlled by a simple and elegant pathway which involves only four genes (Egl1, Ced-9, Ced-4 and Ced-3) [12, 13]. The general principle of signal transduction is conserved in the mammalian apoptotic mechanism and several functional homologues for each *C. elegans* apoptotic gene can be found in humans. It is thought that mammalian ced-like genes arose through gene

duplication and have evolved during evolution to meet the challenges complex multicellular organisms face [11].

In both, *C. elegans* and mammalians, four sequential events control the onset of apoptosis and result in the activation of a proteolytic network of caspases which is entirely represented by CED-3 in nematodes. The activation of these peptidases is mediated by an upstream adaptor protein (CED-4) which oligomerizes in the absence of CED-9, an upstream regulator of apoptosis. This negative regulation of CED-4 and CED-9 is controlled by EGL-1 which is again transcriptionally activated by various cell death stimuli [14]. This pathway can be considered as a simplified view of the more complex human pathway which involves a multitude of proteins and crosstalk's between different pathways (Figure 1.2). The numerous gene duplications during evolution allowed the development of functional specification so that different regulators can respond to different pro-apoptotic stimuli. These stimuli are either intracellular or extracellular and lead to the activation of the intrinsic and extrinsic pathway respectively.

1.1.2.1 The intrinsic pathway is triggered by different signals from various intracellular events such as DNA damage, oncogene activation, cell stress, hypoxia, and cell cycle defects [15]. These events lead to the permeabilization of the outer mitochondrial membrane regulated by the proapoptotic members of the Bcl family [16]. The disruption of the outer mitochondrial membrane then releases several proteins into the cytoplasm to trigger the apoptotic machinery. Among those proteins are cytochrome c, SMAC (second mitochondria-derived activator of caspases)/DIABLO (direct inhibitor of apoptosis binding protein with low pI) and AIF (apoptosis-inducing factor)[14, 17]. Cytochrome c and ATP-dependent oligomerization of Apaf-1 allows the recruitment of Caspase-9 into a large heptameric protein complex known as the apoptosome [18, 19]. Caspase-9 is recruited via the caspase recruitment domain (CARD) forming a homotypical CARD-CARD interaction. The resulting high local concentration of caspase-9 in the apoptosome favors dimerization and leads to the

formation of a catalytic active site. Active caspase-9 can now cleave other downstream caspases such as caspase-3, -6 and caspase-7 to execute apoptosis by cleaving specific substrates essential for cell survival.

1.1.2.2 The extrinsic pathway is sensitive to extracellular stimuli and involves binding of a death ligand to a death receptor. Currently 6 different death receptors are known including Fas (CD95/APO-1), TNF-1, TRAMP, TRAIL and DR6 with Fas representing the most important receptor [20]. The ligand of Fas (FasL) is a type-II transmembrane homotrimeric protein which is expressed in different cells such as cytolytic T lymphocytes (CTL's) and natural killer (NK) cells. Binding of the trimeric FasL to the Fas receptor (FasR) induces a potent apoptotic signal through the trimerization of the FasR and the subsequent recruitment of Fas-associated death domain (FADD) [21]. FADD forms a complex with FasR via a DD homotypic interactions [22] which frees the death effector domain (DED) of FADD to interact with the DED domain of the inactive caspase-8 monomer. This oligomeric death-inducing signaling complex (DISC) activates the recruited caspase-8 by a proximity induced dimerization with subsequent linker cleavage to obtain active and dimeric caspase-8 [23, 24]. As in the intrinsic pathway, the initiator caspase cleaves caspases-3, -6 and -7 to execute apoptosis.

The biological relevance of both pathways is highlighted by Weinberg and colleagues who claim that the required resistance of apoptosis is a hallmark of most if not all types of cancer cells [25].

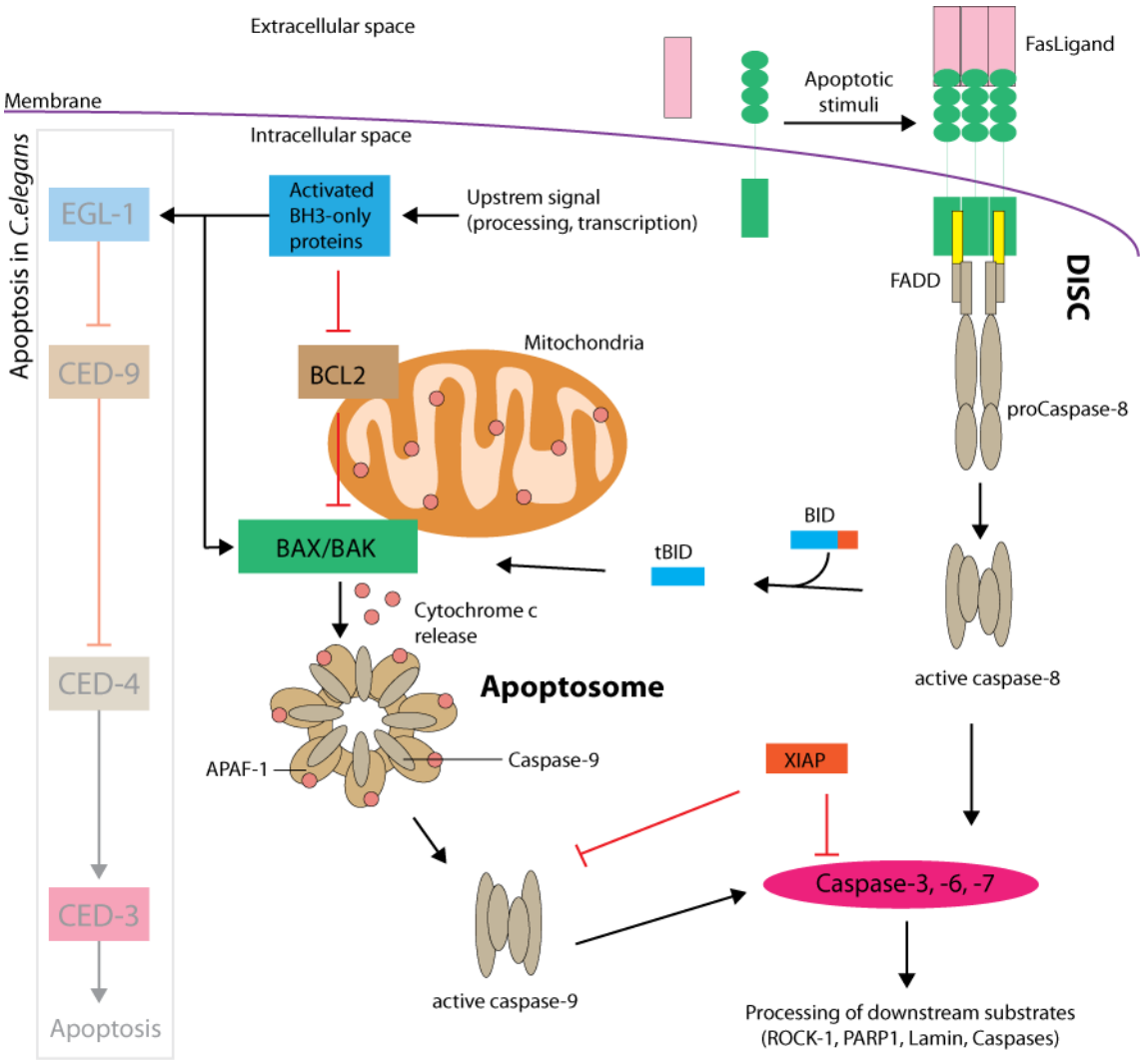

Figure 1-2: Apoptotic cascade
Apoptotic pathway in mammalian cells aligned with the apoptotic pathway in the nematode *C.elegans*. Figure adapted from [11].

1.1.3 Activation of caspases leads to severe morphological changes

The ultimate outcome of the intrinsic or extrinsic pathways is the activation of executioner caspases including caspase-3, -6 and -7. Executioner caspases are responsible to cleave a large set of proteins that are required for cell survival, proliferation and integrity of the cell. Apoptotic cells share many morphological features which are distinct from features observed in necrotic cell death. Eliminating or inhibiting caspases using pharmacological inhibitors can slow down or even prevent apoptosis [26]. Caspases cleave their target proteins at very specific sites and possess the absolute requirement of an aspartic acid, rather then degrading

proteins randomly. The preferred peptide sequence for executioner caspases is V/D-E-X-D followed by a small non charged residue. There has been extensive research over the last decade to analyze caspase substrate specificity, but to date no caspase structure has been solved in complex with a target protein. All target proteins that have been characterized structurally, reveal that the site of cleavage is in disordered mobile loop regions. The potential cleavage sites map to highly flexible and exposed linkers that are accessible to caspases. Thus all speculations about the secondary structure and nature of caspase cleavage sites remains speculative and most probably caspases cleave their natural substrates probably even without the need for exosite interactions [27].

The substrate specificity that has been defined by two independent research groups [28, 29] and subsequent proteomic analysis of whole apoptotic cell extracts based on the consensus recognition sequence suggest a multitude of caspase substrate *in vivo*. Two databases that are available online and offer a searchable list of verified and potential caspase substrates:

- The CASBAH: 777 entries (April 2011), http://bioinf.gen.tcd.ie/casbah/ [30]

- CutDB: 820 entries (April 2011), http://cutdb.burnham.org/ [31]

The number of possible caspases substrates is somewhere in the several hundred, but only few of those assigned target proteins have been carefully studied. The large majority probably simply represent `innocent bystanders` or false assignments [27]. In addition, some of the `legitimate targets` have been analyzed *in vitro* at totally arbitrary concentrations that may have no physiological relevance [30]. A preferred substrate sequence has been defined for each caspase, but due to the high homology within the caspase family, a single caspase can cleave almost any of the proposed sequences if the concentration of the caspase is high enough. This indicates the problem of physiological relevance and specificity of caspase cleavage events to distinguish between `legitimate targets` and `innocent bystanders` that are unavoidable regarding the complexity of the human proteome.

Nonetheless a handful of caspase substrates have been analyzed rigorously and affect mainly four classes of proteins: structural proteins, regulators of transcription/translation, kinases and signaling intermediates and Caspases themselves. Cleavage of those proteins generally results in gain-of-function or loss-of-function which is illustrated in Figure 1.3 and by some of the following examples.

Poly(ADP-ribose)polymerase (PARP) catalyzes ADP-ribose ligation to acceptor proteins in response to damaged DNA and thus plays a crucial role in DNA repair mechanisms. PARP is cleaved by caspase-3 and -7 resulting in a two fragments that have lost their function in DNA repair.

The serine/threonine kinase rho-associated kinase I (ROCK I) is a rather well studied substrate of executioner caspases and is thought to play an important role in two distinct apoptotic morphologies: nuclear fragmentation and plasma membrane blebbing [32, 33]. ROCK I is expressed as a zymogen with an auto inhibitory C-terminal domain and caspase mediated cleavage of the C-terminal domain results in a constitutively active kinase, an example for gain-of-function. Active ROCK I can phosphorylate myosin light chain kinase which leads to beaking of the nuclear envelope and contraction of microfilaments.

Interleukin-33 (IL-33) has been assigned to be cleaved by the inflammatory caspase-1 similar to IL-1β and IL-18 but only recently it was found that IL-33 is cleaved by executioner caspases in order to inactivate this inflammatory protein. Inactivation of IL-33 and other alarmins is a beautiful example of how caspase mediated proteolysis acts as a switch to dampen proinflammatory properties [10, 34].

The multiple cleavage events that occur during apoptosis lead to several distinct morphological changes that can be attributed to apoptosis only and has been first described almost 40 years ago [1]. The characteristic morphologic pattern show chromatin condensation and nucleosomal fragmentation followed by cell shrinkage, fragmentation of the nucleus and blebbing of the plasma membrane (Figure 1.1) [35]. The apoptotic cell forms apoptotic bodies

with maintained integrity and are ingested by neighboring cells. Most of these morphological changes can be completely blocked by inhibition of Caspase activity which indicates that they are specifically induced by Caspase directed limited proteolysis.

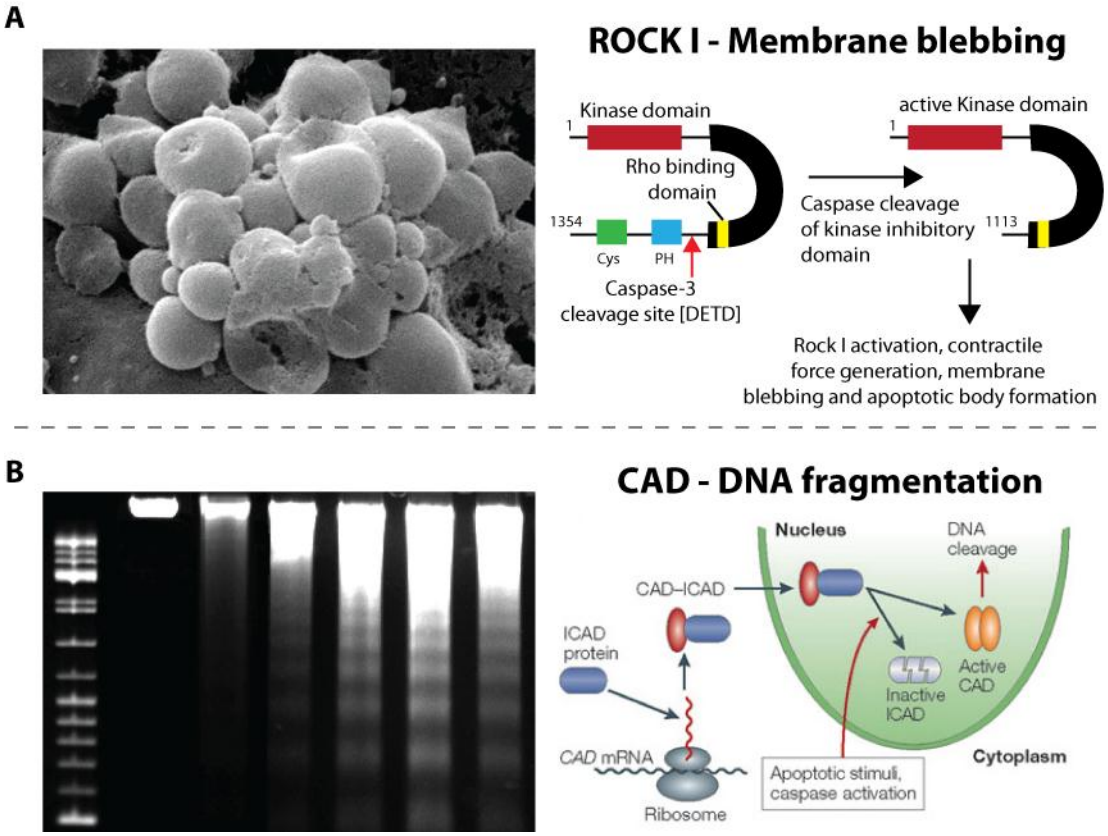

Figure 1-3: Common damages of an apoptotic cell.
A) Membrane blebbing is a characteristic phenotype of apoptotic cells and lead to the formation of apoptotic bodies. The phenomenon is based on the activation of the Kinase domain in ROCK-I by Caspase-3 cleavage. Cleavage of Caspase-3 releases the autoinhibitory domain leading to phosphorylation of several protein involved in cell contraction. CYS, Cysteine rich domain; PH, pleckstrin-homology domain. The picture and the schematic drawing are adapted from [32]. B) DNA fragmentation is a key feature of apoptotic cells. After the activation of endogenous endonucleases (Caspase-activated DNAse, CAD), the DNA is cleaved into fragments of 180 bp or multiples thereof. CAD is constitutively inhibited by Inhibitor of CAD (ICAD). Inactivation of ICAD through limited proteolysis of Caspases releases CAD which then cleaves DNA between the nucleosomes leading to the characteristic well defined DNA fragments. The schematic figures was copied from [36].

1.1.3 Targeting apoptosis

A review by Nicholson DW published in 2000 summarized possible targets in the apoptotic pathway and stated that practical therapeutics that modulate apoptosis will "no doubt appear in the clinic or on the shelf in the next few years" [37]. Until today more than 140,000 articles have been published on molecules that mediate the apoptotic cascade also due to the

substantial interest to therapeutically modulate this pathway [38]. Despite this large effort no drug that targets the apoptotic pathway has been approved to date. In order to understand why exhaustive research efforts have not yet been met with success a closer look is warranted on the principles and possible targets leading to therapeutic benefits.

As described in chapter 1.1.1, deregulation of Apoptosis is implied with several human diseases including cancer, autoimmunity, tissue damage in acute diseases, diabetes and Alzheimer to name a few. In addition apoptotic proteins such as caspase-3 have been connected to infection of human pathogens such as propagation of the human influenza virus and maturation of *Salmonella enterica* [39, 40]. Resisting cell death has been described as a hallmark of cancer and commonly involves signaling imbalances and attenuated apoptosis leading to hyper-proliferation and resistance to therapy [41]. In contrast, tissue damage often occurs in acute diseases such as stroke and myocardial infarction where it would be desirable to prevent apoptosis. From these two examples we can derive two directions of possible therapeutic strategies, selective activation or blocking of apoptosis (Figure 1.4).

The apoptotic pathway involves various types of proteins including, cell surface receptors and their respective ligands (Fas and FasL), transcription factors (NF-κB), tumor suppressors (p53) regulatory proteins (BCL-2), adaptors or oligomerization platforms (FADD, APAF-1), inhibitors (IAPs), heme proteins (Cytochrome C), proteases (Caspases) and even ions such as Calcium. Every single molecule plays a decisive role on the cascade and reveals many opportunities for apoptosis modulation. Instead of discussing the potential of every single protein involved in apoptosis I would like to highlight four major strategies in modulating apoptosis.

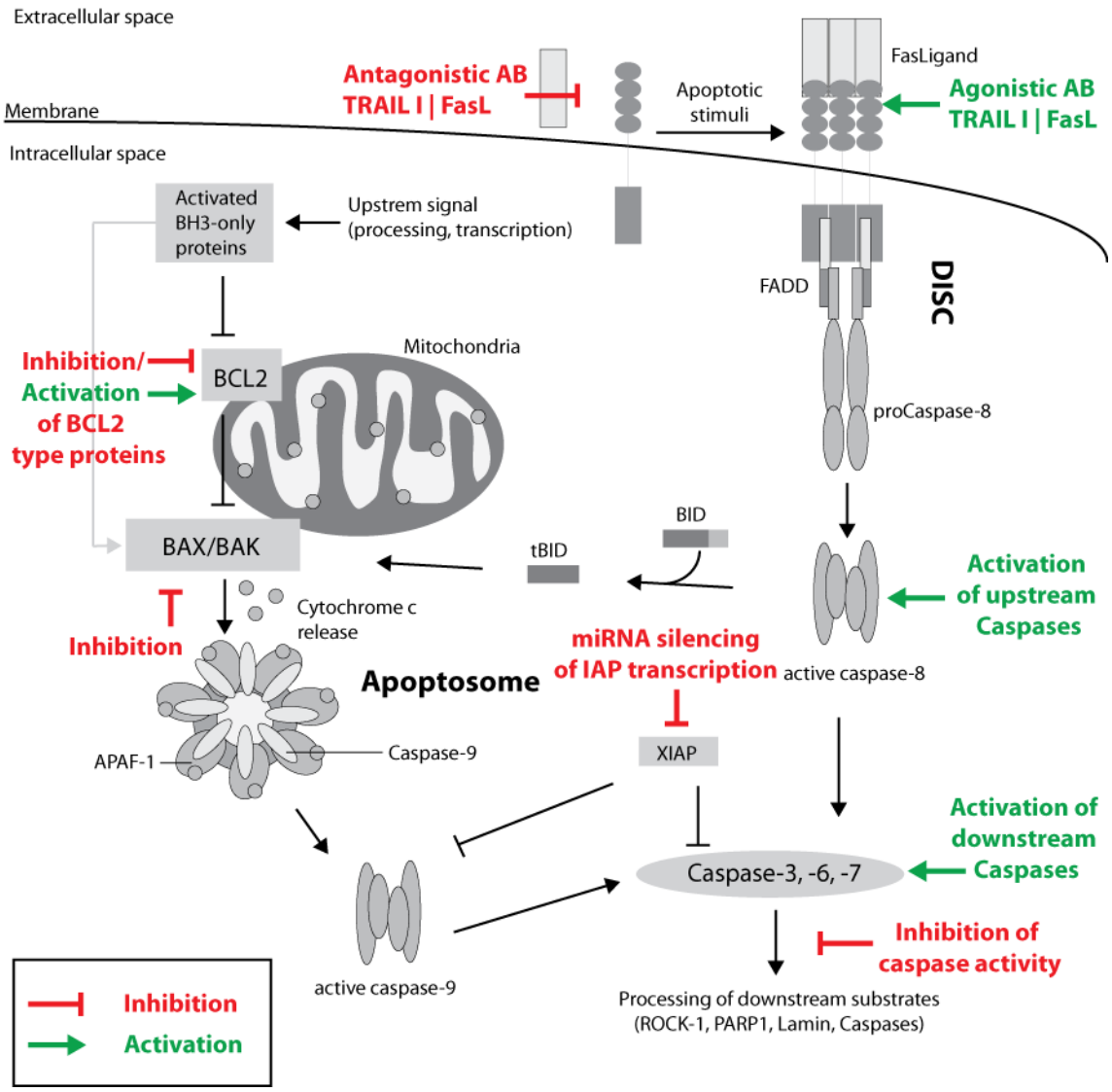

Figure 1-4: Targeting apoptosis
The main therapeutic strategies that have been pursued in the last decade are highlighted green or red for activation and inhibition of the apoptotic pathway respectively.

1.1.3.1 Targeting the receptors

The starting point for the extrinsic pathway (also known as death receptor pathway) is trimerization of receptors that are presented on the cell surface including FasR, TNF receptors or death receptor 4 and 5 (DR4/DR5 or TRAILR1/TRAILR2). These receptors are attractive targets to promote cancer because they are extracellular and can be targeted by their natural ligand or antibodies with no need of traversing the cellular membrane. Their activation would ultimately result in the activation of the apoptotic pathway independent of apoptotic resistance of cancer cells by p53 inactivation or Bcr-2 overexpression [42]. Multiple studies in recent

years showed that soluble TNF and agonistic anti-FAS antibodies have toxic side effects limiting their therapeutic use mainly because these drugs do not discriminate between healthy and malignant cells [43]. An alternative target are the TRAIL receptors, type II transmembrane proteins which are able to trigger the death receptor pathway. Agonistic antibodies against both TRAIL receptors and truncated TRAIL ligand have been made and are in phase I/II clinical trials for the treatment of cancer. These antibodies induce apoptosis in cancer cells but not in normal cells and are able to slow the growth of tumours without toxic side effects [42].

1.1.3.2 Regulating the regulators

BCL-2 family proteins are the main regulators of apoptosis and represent a switch that controls the activation of the intrinsic apoptotic pathway. Some BCL-2 homologs are pro-apoptotic including BH3-only proteins (BAX/BAK/BID/SMAC) whereas others are anti-apoptotic (BCL-2/BCL-XL). BAK and BAX activate the release of cytochrome-c by mitochondria. BCL-2 in contrast inhibits BAK/BAX and thus controls their activity. BCL-2 is overexpressed in many types of cancer leading to a resistance of cell death and various treatments including radiotherapy and cytotoxic agents [42]. In order to overcome the deregulation of the apoptotic regulators one could inhibit overexpression of BCL-2 with the aim to activate apoptosis or inhibit BAK/BAX leading to inhibition of apoptosis. Different kinds of drugs are currently in clinical trials including Bcl-2 antisense oligonucleotides and small molecule BCL-2 family inhibitors for the treatment of leukemia and solid tumours.

1.1.3.3 Targeting peptidases

Caspases, the main executioners of apoptosis are present as zymogens within the cell and require activation through dimerization and/or linker cleavage. This secured apoptotic regulation sometimes fails which leads to diverse disorders. In addition it is extremely attractive to activate caspases specifically to combat diseases that involve cells which are resistant to apoptosis as described in this chapter. Caspases were one of the most obvious targets in modulating apoptosis and soon after their discovery and characterization, active-site

mimetic peptide ketones (e.g. z-VAD.fmk) were developed [44]. These inhibitors are very unselective and do not only target caspases but also other neutrophil-containing peptidases leading to undesired off-target effects.

In preclinical studies, inhibition of caspases has shown remarkable effects e.g. treatment of ischaemia-reperfusion injury [37], which highlights the tremendous potential of caspase inhibitors. Despite this, active site directed approaches so far have not led to appropriate drugs because of poor drug like properties and pharmacological constraints [45].

1.2 Caspases

1.2.1 Caspases – The main mediators of apoptosis

1.2.1.1 History

The first caspase discovered was the human protease involved in activating the precursor of interleukin-1β and was called ICE (Interleukin-1β-converting enzyme) [5]. Shortly after, scientists discovered a role in apoptosis for the *C.elegans* gene CED3 which is homologous to ICE [46]. This link prompted many research groups to search for ICE homologous that are involved in human cell death and led to the discovery of several different peptidases. The frenetic pace of discovery of new homologous has let to multiple names for these enzymes until a common nomenclature was found in 1996 – caspases [47]. The name caspase is based on the catalytic properties with "c" representing the catalytic active site residue cysteine and "asp" for the absolute specificity of aspartic acid in P_1. The subsequent number of each caspase represents the order of discovery. The first caspase crystal structure was solved and published in 1994 and revealed that caspase-1 is a dimer consisting of two subunits - the "caspase fold" was born [48]. To date eleven different caspases have been discovered with different roles in inflammation, apoptosis and keratinocyte maturation. Nine out of these fourteen caspases have been described structurally.

1.2.1.2 Classification

Caspases are classified into the clan CD, family C14 according to the MEROPS peptidase database (http://merops.sanger.ac.uk/) or referring to IUBMB; caspases are cysteine endopeptidases with caspase-1 in the category: 3.4.22.36.

The caspase family with its eleven members can be divided into different groups depending on sequence homology, function or substrate specificity. Caspase-1, -4 and -5 represent the inflammatory caspases whereas all other caspases are involved in apoptosis except for caspase-14 being involved in keratinocyte maturation. The apoptotic caspases are subdivided

into initiator- (caspase-2, -8, -9 and -10) and executioner caspases (caspase-3, -6 and -7)(Figure 1.5).

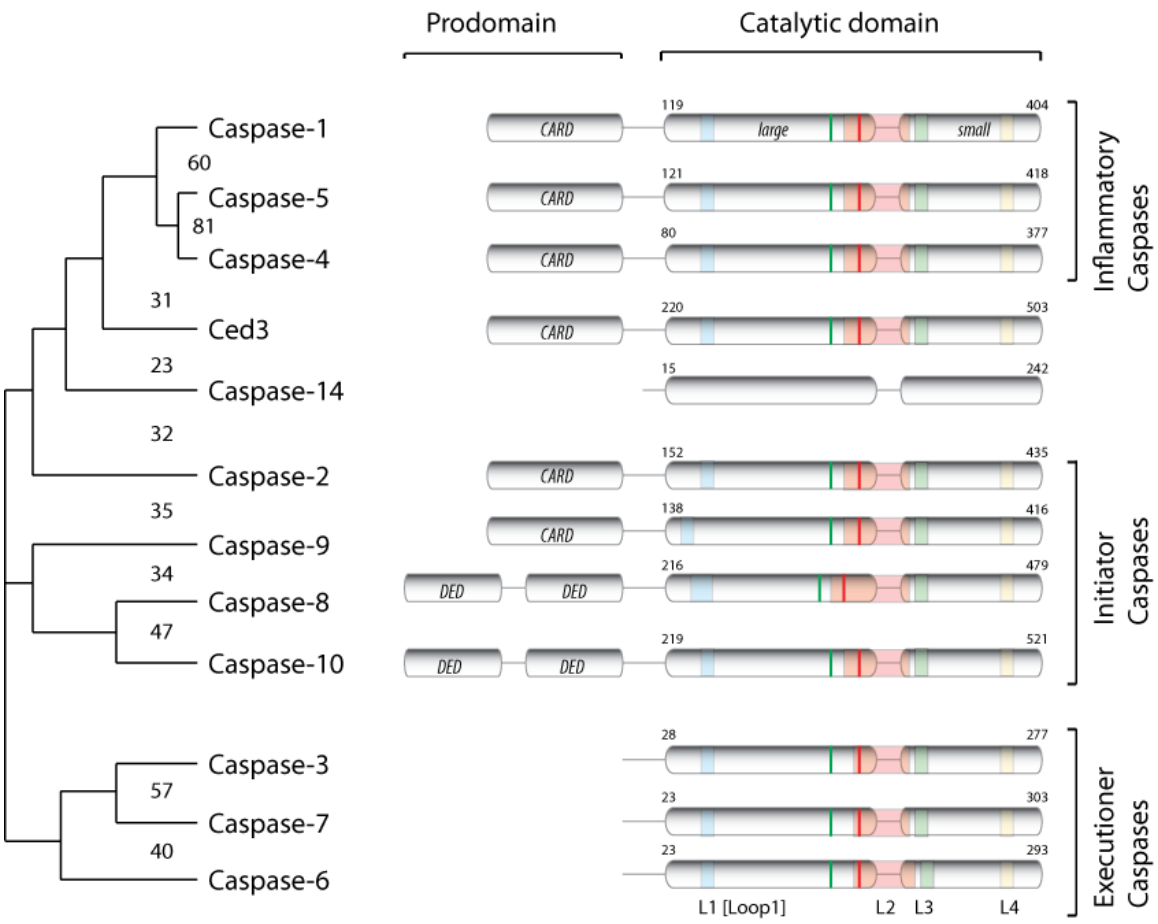

Figure 1-5: The Caspase family.
The domain architecture of all human caspases and Ced3 are shown. Loop1, -2, -3 and -4 are indicated in the respective color and the catalytic residues His237(green) and Cys285 (red) are marked by a line on the large subunit. The phylogenetic tree shows the evolutionary conservation within the caspase family. Numbers between two caspases within the tree represent the sequence homology of the respective caspases.

1.2.1.3 Architecture

Caspases are expressed as inactive zymogens and have a highly conserved sequence and domain architecture. All caspases have a large (p20) and a small (p10) subunit connected with a short linker. This catalytic domain contains all domains and residues of the catalytic machinery. Two of the active site forming loops (L3 and L4) are situated in the small subunit whereas loop1 (L1) is in the large subunit. Loop2 (L2) including the catalytic cysteine (Cys285) residue is mainly located in the large subunit but reaches to some extend into the

small subunit. The linker connecting the small and large subunit within L2 is relatively short with around ten amino acid residues and is cleaved upon activation of the caspase. Executioner caspase have a short N-terminal sequence with a length of 23 to 28 amino acids which is also cleaved upon activation. It is believed that this unstructured domain is involved in subcellular targeting [49]. The N-terminal prodomain of initiator caspases contains homotypic interaction motifs such as the caspase-recruitment domain (CARD) or death effector domain (DED) [14](Figure 1.5). Both domains are distantly related and are implicated in homophilic interactions with other CARD or DED domains in order to be recruited to multimeric caspases activation platforms. Activation of the procaspase by dimerization and/or proteolytic cleavage separates both subunits and removes the prodomain. The active site and the catalytically active enzyme are then formed in a homodimer with each monomer consisting of a small and large subunit. The homodimerization is mediated through a large hydrophobic interface with an antiparallel β-strand. The dimeric caspase has twelve continuous β-stands building the hydrophobic core and is surrounded by several α-helices leading to a globular fold. Loop1 to loop4 form the active sites which are located at two opposite ends.

1.2.1.4 Sequence and homology

Caspases are evolutionary highly conserved and have the same fold, quaternary arrangement and catalytic mechanism by which they cleave their substrates [50]. Based on multiple sequence alignments and similarity determinations it is observed that the catalytic core of all caspases is highly conserved especially around the catalytic residues His238 and Cys 285 [51]. There are additional highly conserved features such as the peptide binding pockets, the oxyanion hole, the dimer interface and cleavage sites that are essential for activation (Figure 1.6 and 1.8). Highest sequence similarity is found within the distinct groups where inflammatory caspase have an overall homology of 60%, initiator caspases 40% and executioner caspases 50%. The overall sequence identity is about 30% with the main differences between apoptotic and inflammatory caspases (less than 25%) due to a greater

evolutionary distance. The phylogenetic tree of the caspase family is a beautiful example of the relation between sequence homology and functional relationship (Figure 1.5). The inflammatory caspases segregate well from others caspases and other caspases that have partly redundant activity and the same sequence specificity group into distinct classes. A good example are caspase-3 and -7 which play a combined role in the execution of apoptosis and caspase-8 and -10 which play a similar role in receptor stimulated activation of apoptosis. Caspase-2 remains an enigmatic protein with an unclear functional role which is also illustrated by the position within the phylogenetic tree being close to inflammatory caspases with a suggested role in apoptosis [52].

1.2.1.5 Catalytic mechanism

Mutational studies revealed that Cysteine285 and Histidine237 are the catalytic residues in the active site. The similarity of chemical groups involved in peptide catalysis suggests a similar mechanism as in serine and other families of cysteine proteases [53, 54]. The catalytic mechanism (Figure 1.6) is based on a S_N1 mechanism with Cysteine285 and His237 representing the nucleophile and active site base respectively. Binding of a peptide in the substrate pockets and the carbonyl oxygen into the oxyanion hole is followed by a nucleophilic attack of the Cys285 sulfur atom on the highly electrophilic carbonyl carbon (1). His 237 then protonates the a-amino group of the leaving peptide product and thus avoids the reformation of the peptide bond (2). The formed acyl-enzyme complex is then deacylated by the deprotonated His237 which abstracts a proton from a water molecule, which is then activated to attack the thioester bond. This represents the second tetrahedral intermediate (4) with a nucleophilic attack of the hydroxyl group on the carbonyl carbon. The N-terminal peptide product is then bound to the enzyme non-covalently and is released eventually leaving the free enzyme (5) [53].

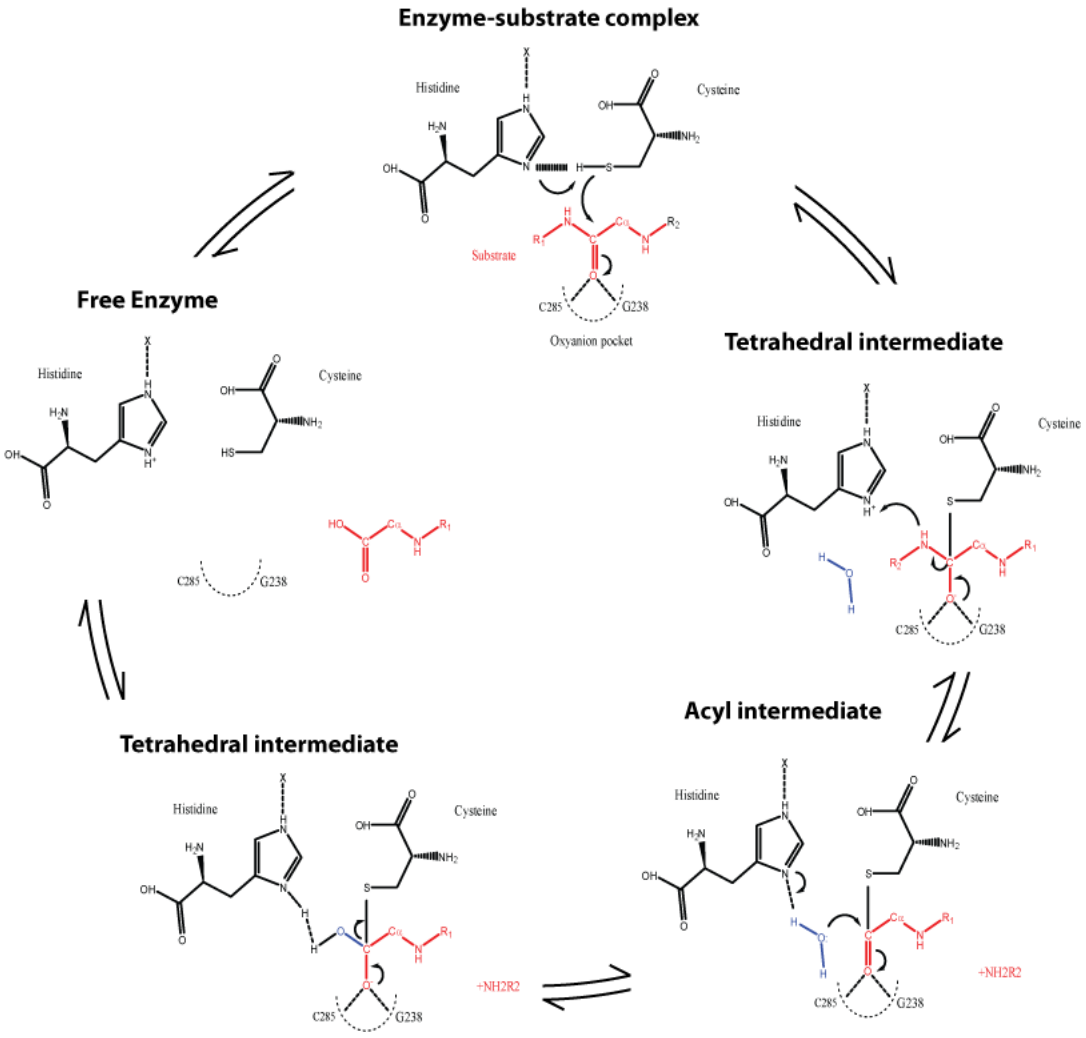

Figure 1-6: Catalytic mechanism of cysteine peptidases

1.2.2 Caspase regulation – From zymogen to the active peptidase

1.2.2.1 Activation of executioner caspases

Executioner caspases are expressed as dimeric procaspases containing the N-terminal domain and the linker connecting both subunits. Although they are in a stable dimeric form they do not possess any catalytic activity and need to be activated by apical caspases in order to form the active site. The activation occurs through processing of the N-terminal domain and the linker leading to structural rearrangements and formation of the active site. This mechanism has been deduced from crystal structures of active caspase-7 in complex with an inhibitor and caspase-7 zymogen [55, 56]. The active site in the active caspase is formed by L1 – L4 where L3 and L4 are rather flexible. L2 contains the active site cysteine and is additionally stabilized by L2'. The procaspase-7 zymogen structure in contrast shows that L2' is locked in a closed conformation and occludes it from stabilizing the active site. Only cleavage of the inter-chain allows L2 and L2' to place the cysteine and stabilize the active site. In addition L3 is very flexible and steric hindrance with the inter-chain linker prevents positioning of the active conformation of L3. These predictions were also confirmed for caspase-3 and -6 and are believed to be the general mechanism for executioner caspases [14].

1.2.2.2 Activation of initiator caspases - proximity induced activation

Active site formation upon inter-chain cleavage most likely also accounts for the activation of initiator caspases; however the situation here is fundamentally different since they are present as monomeric inactive precursors. They have to dimerize in order to become active by autoproteolysis, leading to interchain and linker processing, active site formation and dimerization. Furthermore there is evidence that association with multimeric complexes such as the apoptosome are essential for full catalytic activity [57].

The induced proximity model for the activation of apical caspases was proposed by two independent groups [24, 58] and has later been corrected to the more accurate term proximity-induced activation [59-61]. The model is based on two main observations. First, apical caspases are activated by adaptor-mediated clustering of inactive zymogens followed by

dimerization due to the high local concentration. In a second step it is believed that residual autocatalytic activity is sufficient for proteolysis of the inter-chain linker that is required to stabilize and activate dimeric caspases. As it accounts for executioner caspases, the cleaved linker allows the formation and stabilization of the active site leading to catalytic activity. The relative order of these events remains a hypothesis but recent structural and functional studies on monomeric caspase-8 zymogen by solution NMR have revealed novel insights [23]. It was proposed that dimerization is required to relocate the cleavage motifs to become accessible for the neighboring monomer and initiated pre-building of the active site which finally forms upon substrate binding [23, 62]. Thus dimerization, relocation, active site formation, cleavage and release of DISC seem to be a highly dynamic but well controlled process. Whether the exact same model is also valid for caspase-9 is unclear but the basic mechanism seems to be similar. It was for example shown, that inter-chain cleavage of caspase-9 is not necessary for inducing apoptosis [19]. In addition caspase-9 possesses only full activity when associated with the apoptosome suggesting that activation of procaspase-9 has little to do with inter-chain cleavage but requires apoptosome-mediated enhancement of the catalytic activity [60].

1.2.3 Activation platforms

The apoptotic machinery is a two-step proteolytic cascade that results in the activation of executioner caspases. In order to activate this cascade, an upstream signal is required which senses an apoptotic (or inflammatory) stimulus and translates it into caspase activation. This process is implemented by multimeric protein complexes which oligomerize and recruit the according caspase via recruitment domains such as DED or CARD. Four different activation platforms have been defined to date which are related to either apoptosis or inflammation. The first to be discovered was the death-inducing signaling complex (DISC) in 1995 by Peter Krammer and colleagues who identified an oligomeric assembly of FasR (APO-1/CD95) which recruits other molecules to start an apoptotic cascade [63, 64]. Later on the apoptosome was defined to be the starting point of intrinsic apoptosis [65, 66] and Juerg Tschopp and

colleagues discovered two additional multimeric complexes involved in apoptosis and inflammation, the inflammasome [67] and the Piddosome [68].

Structural information of an entire complex is so far only available for the apoptosome, where x-ray structures of the single components were positioned into a single particle Cryo-Electron Microscopy structure determined at 9.5 Å [19, 69]. The single components of the DISC have also been structurally described but their precise arrangement and the stoichiometry of the complex remains controversial to date. However, current knowledge of these two multimeric complexes presents a solid basis for the understanding of how apoptosis is triggered.

1.2.3.1 The apoptosome – a soluble receptor

The formation of the apoptosome is dependent of upstream events that are regulated by proteins of the bcl-2 family. They sense apoptotic events and control the release of cytochrome c from mitochondria which is then translated into the activation of the death cascade. The death cascade largely depends on the cofactor Apaf-1 which exists in a monomeric and auto inhibited state in the absence of an apoptotic signal. Apaf-1 has a rather complex domain structure comprised of CARD, a nucleotide-binding and oligomerization domain (NB-ARC/NOD) and two WD40 repeats. CARD is clearly involved in caspase recruitment and WD40 is responsible for cytochrome-c binding. NB-ARC with its three subdomains is involved in ATP binding and formation of the apoptosome. The first trigger of apoptosome formation is binding of cytochrome-c to the WD40 domain which unlocks the locked state of Apaf-1. This involves large structural rearrangements, (d)ATP hydrolysis and leads to a semi-open, auto-inhibited state. The complex of Apaf-1, cytochrome c and ADP is still monomeric, unable to bind caspase-9 and requires a second signal to proceed. This control device is believed to be (d)ADP – (d)ATP exchange so that apoptosome formation will only occur if enough unlocked Apaf-1 molecules co-localizes with (d)ADP – (d)ATP exchange [70]. After exchange of (d)ADP with (d)ATP, all described components form a heptameric wheel-like structure built on seven Apaf-1 molecules. The most recent structure reveals how the CARD domains assemble in a circular arrangement, which is the key

platform for the recruitment and activation of caspase-9 [69]. Recruitment at this platform via homotypic CARD – CARD interactions between Apaf-1 and monomeric procaspase-9 leads to high local concentration above the K_D for dimerization resulting in activation of caspase-9 by the proximity-induced model.

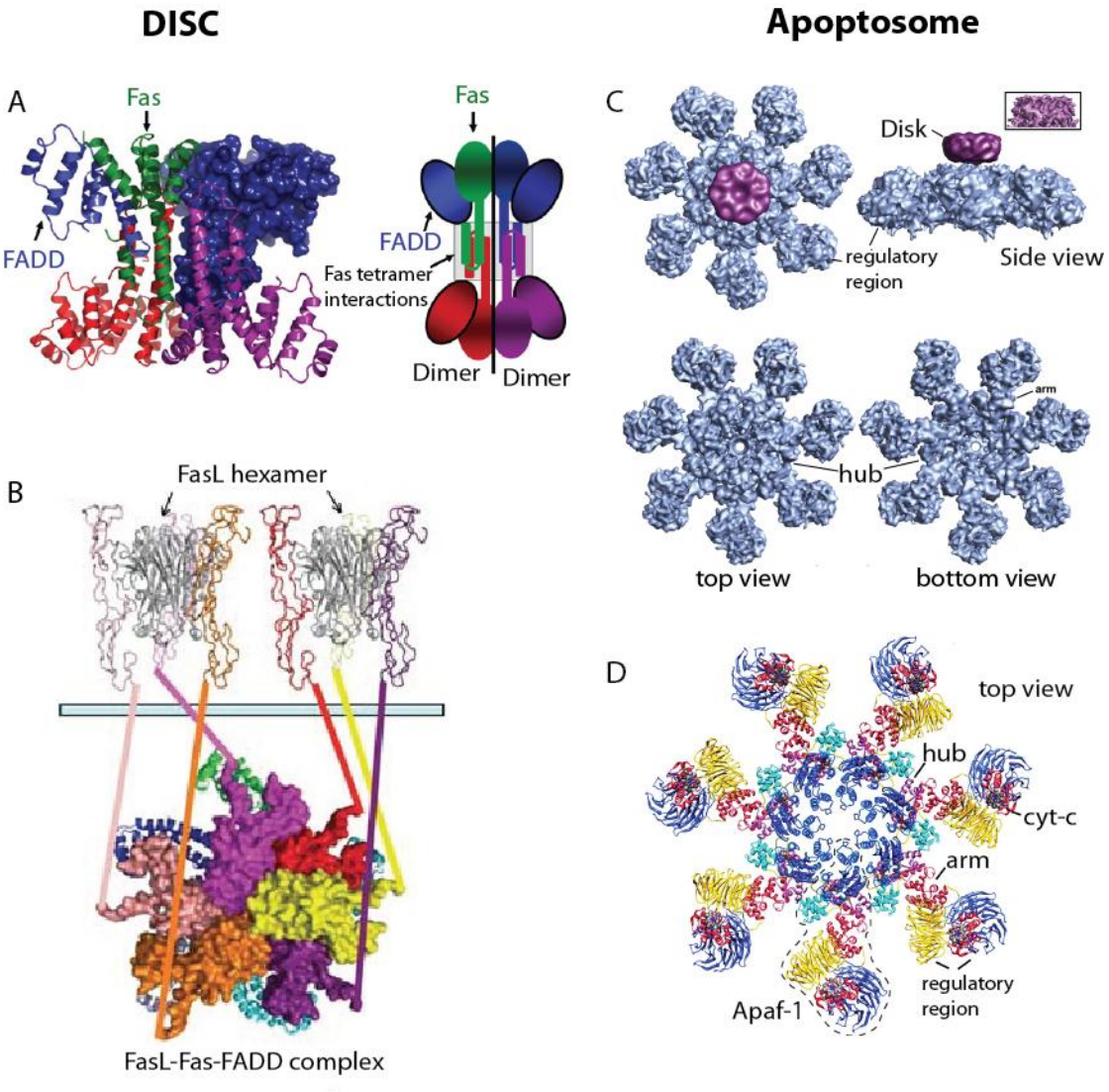

Figure 1-7: Apoptotic activation plattforms
(A) Crystal structure schows a tetrameric arrangement of the FAS/FADD complexbuilding the core of the DISC. Here the receptor signaling is supposedly only regulated by oligomerization and clustering events [71](B) Proposed asymmetric arrangement of the Fas/FADD complex is composed of 5 to 7 FAS DD and 5 FADD domains [72] (C) Structure of the apoptosome at a resolution of 27 Å. The wheel like structure (blue) is formed by Apaf-1 and cytochrome-c with a 7-fold symmetry. Caspase-9 is recruited to the CARD domain Disk (violet) [69] (D)Domain arrangement within the apoptosome.

1.2.3.2 The DISC – a membrane receptor

The DISC is a classic example of a ligand-dependent transmembrane signaling receptor and represents a standard solution that is used by cells to transduce signals from outside to the inside. Many other receptors such as TRAIL or TNF are believed to function in a similar way [70]. The formation of the DISC requires two trimeric or an engineered hexameric FasL complex [73]. This signal leads to oligomeric clustering of the FasR and their intracellular death domains (DD) which bind the homotypic DD of FADD, an adaptor protein which comprises a DD and a DED domain. The DED domain of FADD then recruits the N-terminal DED domain of caspase-8 leading to an increased local concentration and thus proximity induced activation of the apical procaspase. The general sequence of oligomerization and recruitment remains still highly controversial and to a large extent it is unknown how precisely this clustering is regulated and formed. In one model [74] a tetrameric arrangement of four FADD death domains bound to four Fas death domains is proposed. Fas undergoes structural rearrangements upon FasL binding and binds FADD in an open conformation which stabilizes the complex. This leads to a processive interlinked DISC formation and clustering upon sufficient stimulus. The proposed mechanism is solely based on clustering events and prevents accidental DISC formation. A second proposed mechanism [72] claims that the Fas-FADD complex forms an asymmetric oligomeric structure composed of 5 – 7 Fas DD and 5 FADD DD. Wang and colleagues further revealed that Fas lacks larger structural rearrangements upon FADD binding.

Although these two studies conclude different models they both describe experimental observations of higher order clustering events (Figure 1.7). Whether the DISC actually has a precise stoichiometry is unclear and might not be necessary provided that caspase-8 is specifically activated by a well-controlled mechanism. The DISC also shows the often observed highly dynamic and transient nature of regulatory complexes which is also believed

to be the case for the inflammasome and the PIDDosome where no structural information is available at all.

1.2.4 Structure and biochemistry of caspases

1.2.4.1 Caspase structure

Active caspases are homodimers with each monomer containing a large (~20 kDa) and small (~10 kDa) subunit. To date several crystallographic structures have been solved and they all show the same basic globular fold, also termed 'caspase fold' (Figure 1.8). In this caspase fold, both subunits are packed into an ellipsoid of approximate dimensions 25 Å x 50 Å x 30 Å. The catalytically active dimer is arranged by a twofold symmetry axis and each monomer derives from a single procaspase. The two active sites are found at opposite site ends of the dimer. Each monomer contains the entire apoptotic machinery and folds into αβα sandwiches forming a compact cylinder. The center is built with 6 stranded β-strands surrounded by five helices [51]. Two monomers assemble into a dimer through hydrophobic interactions, forming an antiparallel β-sheet at the interface. This generated a continuous 12-stranded β-sheet, a highly conserved and characteristic feature in all caspases.

Initiator or inflammatory caspases contain N-terminal domains such as caspase recruitment domains (CARD) or death effector domains (DED) (Figure 1.5). These domains play a crucial role in caspase activation by recruiting the procaspase to large oligomerization platforms via homophilic interactions, as described in chapter 1.2.1.3. Although these domains have no or very low sequence similarity they share a common fold which is also found in other protein binding domains such as LRRs, DDs and NACHT domains. These globular domains are mainly composed of six antiparallel α-helices, with helices α1 – α5 building an α-helical Greek key motif [53]. Executioner caspases in contrast, have short unstructured N-terminal peptides.

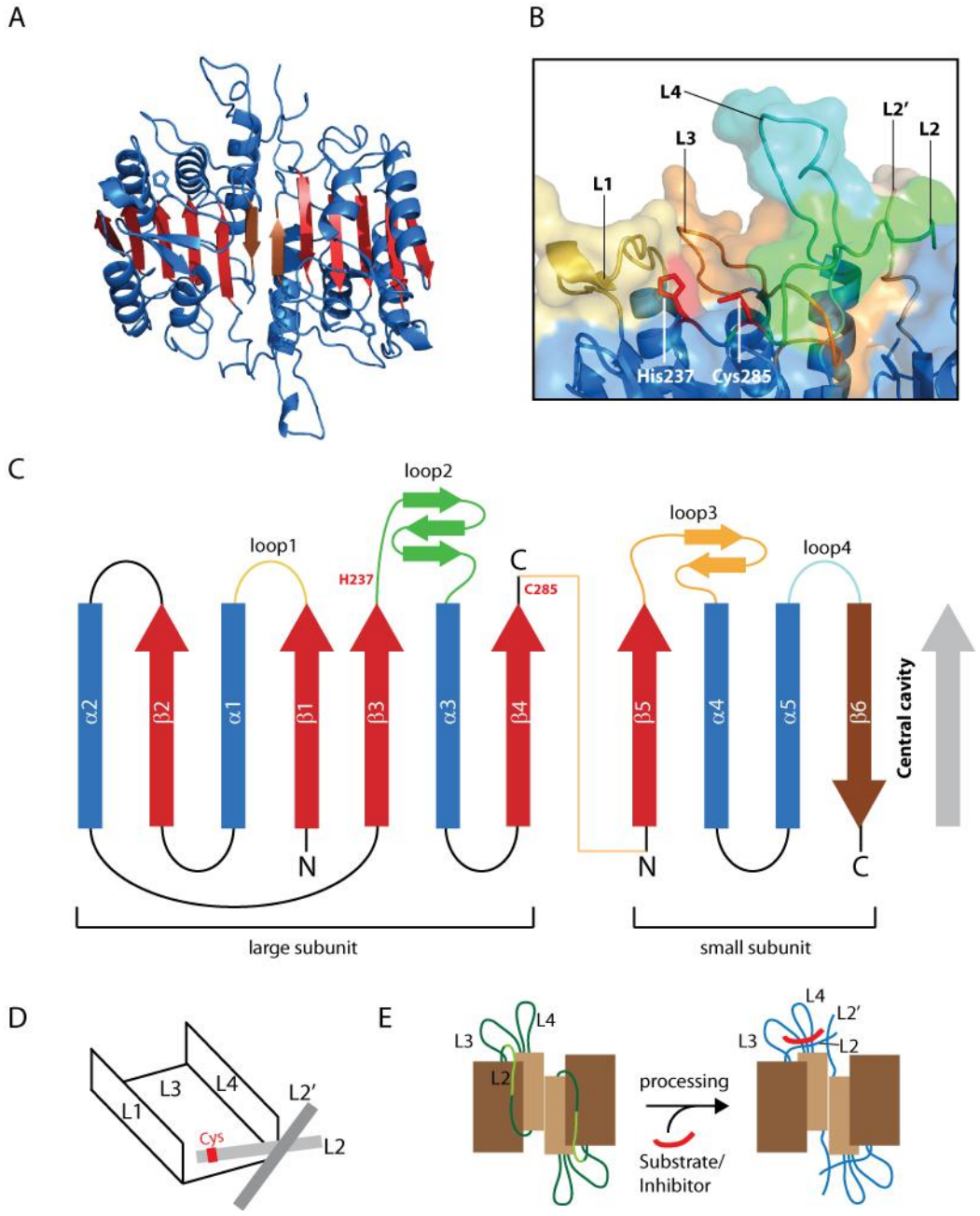

Figure 1-8: Protein structure of Caspases.
A) The structure of caspase-3 with continuous12 stranded β-sheets (red) surrounded by α-helices (blue) is shown (pdb entry code 2DKO). The antiparallel β-sheet in brown forms the dimer interface. B) The active site of a caspase monomer is shown in a cartoon and transparent surface representation with a distinct color for each loop forming the active site. The catalytic residues His237 and Cys285 are shown in red. C) Secondary structure of a caspase monomer with a small and large subunit is represented in this sketch. The α-helices and β-sheets and the loop are colored according to the colors used in (A and B). The linker connecting the large and small subunit is illustrated in light orange but is not present in the crystal structure shown in (A). D) The substrate binding groove is conserved in all caspases as illustrated by the diagram. L1 and L4 are flanking the active site and L3 serves as the base with crucial residues in substrate recognition. L2 positions the catalytic Cys and is stabilized by L2' after linker cleavage. E) Rearrangement of loops in executioner caspases is illustrated. L2 has drastic conformational changes after cleavage while L3 and L4 have only minor rearrangements. Part C, D and E have been adapted from [14, 53]

1.2.4.2 Active site architecture

A common rule for enzymes is that the active site is often found at 'topological switch points', meaning that the active site residues are positioned close to the C-terminal of the central β-sheet [75]. This general rule is also true for caspases where both catalytic residues, His237 and Cys285 are located at the C-terminal of β-strand 3 and β-strand 4 respectively. The majority of caspase structures that have been solved show the caspase in complex with a peptide inhibitor and thus show the active site in a substrate bound conformation. The two active sites are formed by four protruding loops (L1 to L4) in each monomer and are additionally stabilized by L2' by the neighboring monomer. The backbone configuration of the active site is highly conserved and L1 and L4 form the two sides of the substrate-binding groove [76] (Figure 1.8D). L3 forms the base of the active site with critical residues for substrate recognition. L2 which is cleaved during caspase activation is critical for active site formation and positions the catalytic residue Cys285 by traversing the active site. Cleavage of the L2 loop also results into formation of a L2' loop-fragment, L2' is important for the stabilization of the neighboring monomer. However before a caspase has formed the active site cleft, cleavage of the linker is required for activation, as described in chapter 1.2.2.

Structural studies on procaspase-7 and procaspase-8 have revealed the very dynamic nature of the active site forming loop before and after linker processing. [23, 55, 56]. Procaspase-7 and other executioner procaspases have a rather short but highly flexible linker which impairs the formation of a functional substrate binding and active site formation. The cleavage sites are exposed on the dimer surface and are accessible for proteolytic attack. Cleavage of the linker leads to rearrangements of the loops so that the S1, S2 and S4 subsites will be sculpted, the catalytic residue Cys285 will be positioned properly and the oxyanion holes are formed, rendering the binding sites and the active sites functional [55]. The structure of procaspase-8 shows a partially flexible linker which is located on one side of the central β-sheet. Dimerization supposedly triggers conformational changes of the linker and active-site loops,

thus allowing the active site pocket to form. The active site residue Cys285 which is buried by the linker is released and shifts by 6 Å into a substrate accessible position [23].

The active site architecture of caspases has evolved to fulfill several criteria including activation, substrate recognition and specific proteolytic activity. It represents a highly dynamic part of the protein and the formation of the active site cleft is tightly connected with the regulation and activation of the enzyme.

1.2.4.3 Substrate recognition

After the activation of the procaspase, the enzyme is capable of binding its substrates in order to cleave the polypeptide chain specifically after an Aspartate residue. However it should be noted, that substrate binding might also play an important role in procaspase activation by an induced-fit mechanism [62]. The general convention of substrate recognition by proteases is to name its residue to the N-terminal of the scissile bond P_1 and the on to the C-terminal side P_1'. Any residue next to these positions is named $P_2 – P_x$, depending on the position in respect to the first residue (Figure 1.9). The binding pocket that harbors the respective substrate residue is named 'S' denoted with the according number [77]. Caspases have an absolute requirement of an aspartic acid in P_1, a very unique primary specificity for peptidases in general which can be only found in serine proteases. The S_1-pocket is highly conserved among the whole family and is constructed of three charged residues, namely Arg179, Arg341 and Gln283 which form a highly positively charged pocket which is ideally shaped to harbor an aspartic acid and replacement of Asp by Glu reduces the catalytic efficiency by four orders of magnitude [53]. Next to the P_1-residue the binding affinity and specificity is determined by P_2 to P_4 with the exception of caspase-2 which has an additional pocket to bind a fifth residue P_5. The S_2, S_3 and S_4 subsite mainly contribute to the specificity of the individual caspase but are often conserved among caspase subclasses, such as initiator or inflammatory caspases. In addition to the four main binding pockets it has later been discovered, that the first residue after the scissile bond P_1' is as important and has a significant role in substrate binding [78].

A

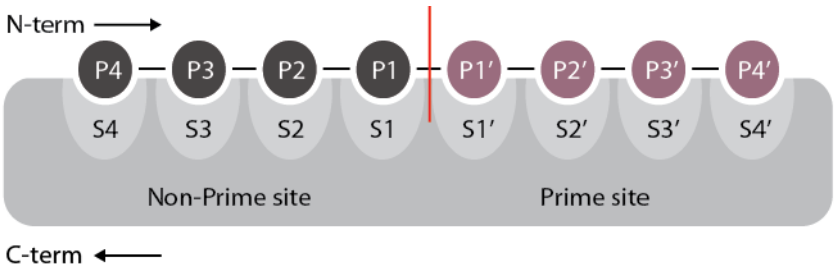

B

Caspase	Optimal substrate sequence	KM	Optimal pH range
Caspase-1	WEHD	4	7.5
Caspase-5	(W/L)EHD	15	7.5 - 8.0
Caspase-4	(W/L)EHD	31	7.0
Caspase-14	WEHD	n.d.	7.5
Caspase-2	VDVAD	n.d.	6.5
Caspase-9	(L/V)EHD	408	6.5 - 7.0
Caspase-8	DEVD/LETD	4	6.5 - 8.5
Caspase-10	(L/V)EXD	42	7.0
Caspase-3	DEVD	5	7.0 - 8.0
Caspase-7	VEHD	15	7.0
Caspase-6	(D/V)EXD	170	7.0 - 7.5

Figure 1-9: Caspase substrate specificity
A) Schematic presentation of a peptidase active site binding to its substrate. The region responsible for substrate binding is called subsite and is divided into primed and non-primed site with respect to the cleavage site. Substrate residues and binding sites that are N-terminal of the cleavage site are called P1-PX and S1 – SX respectively. The C-terminal site is marked by an additional apostrophe. The structure of the active site determines the intrinsic subsite occupancy and specificity [77]. B) Human caspases, their optimal substrate sequence and kinetic properties are listed.

1.2.4.4 Peptide specificity

A combinatorial screen using positional scanning synthetic peptide-based libraries by Thornberry and colleagues in 1997 was the first systematic approach to determine specificity of caspase substrates [28]. Each of the positions (P_1 to P_4) of the substrate was scanned to reveal preferences and derive a general specificity scheme for caspase cleavage. Next to the absolute requirement of an aspartic acid in P_1, caspases have preferences in the other positions including the P_1' position. A simplified substrate sequence for caspases that many papers refer to is D/WEXD.Φ ($P_4P_3P_2P_1.P_1$') with Φ being a small uncharged residue. Figure 1.9 offers a

detailed overview listing all residues for each caspase. It is conspicuous that the sequence specificity is very similar if not the same within subclasses such as inflammatory or executioner caspases. This fact urges the conclusion that caspase activity is to some extent redundant exhibiting overlapping substrate specificity *in vivo*.

From this and other studies came the general idea of caspase-specific consensus recognition in order to predict natural substrates. In addition peptide substrates and inhibitors were developed and used for structural biology, enzyme kinetics, drug development and many other applications in molecular biology. These substrates or inhibitors have usually a tetrapeptide sequence matching a specific caspase coupled to a fluorogenic reporter or a warhead respectively. They are very useful *in vitro* to characterize individual purified caspases, but "they are by no means useful to distinguish between caspases in complex milieu such as cell lysates" [27]. This fact has to some extend been ignored in many studies in dissecting apoptotic pathways, leading to wrong conclusions. Caspase-7 exemplifies this problem very well, where it was shown that virtually any residue can bind at the P_2 ,P_3 and P_4 position although with varying affinities [79]. One can consequently say that there is a significant overlap between individual consensus sequences and the specificity highly depends on the concentration used. The promiscuity of the pseudo specific caspase substrates was further indicated by "showing that caspase-3 was able to cleave most substrates more efficiently than those caspases to which the substrates are reportedly specific" [80]. These finding suggest, that there are additional factors that determine the specificity and local concentrations of caspases.

1.2.5.1 Exosites

Caspase specificities between close homologous such as caspase-3 and -7 can often not be distinguished *in vitro* and all reported positional scanning methods of caspase substrates have only been obtained by *in vitro* techniques. The optimal tetrapeptide substrate for both caspases is DEVD or VEHD and caspase-3 has a significantly higher catalytic activity than caspase-7. A finding that contradicts this result is that PARP (poly[ADP-ribose]polymerase),

a well described natural caspase substrate, possess a much higher affinity for caspase-7 than for the close homologue caspase-3 *in vivo*. This reverses the observed catalytic efficiency of caspases against small synthetic substrates. The enhanced affinity was found to be the result of specific interactions of the large caspase-7 subunit and PARP, which is not present in caspase-3 [81]. This example is the first description of an exosite that essentially determinates substrate recognition and processing. These exosites can to a certain extend explain the discrepancies of cleavage preferences *in vitro* and substrate cleavage found *in vivo* [82]. There is more evidence that implies the existence of exosites in caspase dependent substrate recognition and may to some extend overrule specificity requirements derived from studies with short synthetic peptides [53]. This does not mean, that all caspase cleavage events involve binding to exosites. It was found that caspase-1 cleaves heat denatured pro-IL-1β was cleaved as efficient as the folded precursor [83].

1.2.5.2 Caspase phosphorylation

The first evidence that caspases are regulated through phosphorylation was shown by Michael Cardone and colleagues in 1998, where they found that Caspase-9 was directly phosphorylated at Ser-196 by the kinase Akt, leading to inhibited protein activity [84]. Many more conserved phosphorylation sites have been assigned mainly in upstream caspases that obviously have a crucial role in regulation of apoptosis. A very illustrative example is the phosphorylation and dephosphoylation of caspase-8 regulating neutrophil survival [85]. Neutrophils are the most abundant type of white blood cells and are part of the innate immune system. The *in vivo* life span of neutrophils is 6 to 8 hours with a turnover of about 10^{11} cells per day. Delayed apoptosis in neutrophils is associated with several diseases and if one bears in mind, that apoptosis is a process that takes several hours to be complete it becomes obvious, that it has to be tightly regulated in neutrophils. Neutrophil survival is dynamically regulated through phosphorylation and dephosphorylation at Tyr310 which can consequently be recognized by the tyrosine phosphatase SHP-1 which dephosphoylates caspase-8, permitting apoptosis to proceed. The non-receptor tyrosine kinase Lyn can phosphorylate

caspase-8 on Tyr-397 and Tyr465, rendering it resistant to activational cleavage and inhibiting apoptosis. This mechanism represents a dynamic post translational regulation of apoptosis in neutrophils. Dysregulation of the mechanism is directly linked to tissue damage in sepsis [85].

1.2.5.3 Allosteric mechanisms

Allosteric regulation of proteins and especially enzymes leading to conformational changes is a common way to regulate enzymes independent from the active site. The clear advantage of this mechanism is that even enzyme families with highly conserved active sites gain specificity through regulation of their activity at positions other than the active site. First evidence that caspases are also to some extend regulated through allosteric mechanism was demonstrated for caspase-3 and -7. A conserved allosteric site was discovered in a deep cavity at the dimer interface about 14 Å from the active site [86]. A conserved cysteine in this allosteric site when coupled to a compound renders the caspase inactive. This allosteric site is functionally connected to the active site and binding of a compound traps a zymogen-like conformation. The active site cysteine is dislocated, the L2' loop is pinned over the allosteric site to prevent proper folding of the active site and residues critical for substrate recognition are also dislocated [87]. It was later shown; that this allosteric site is located in a linear circuit of functional residues that connects both active site and a positive cooperativity has been revealed by kinetic analysis. Thus the formation of a dimer itself can be regarded as allosteric control of the active site since the dimer interface and the active site are connected. The small molecule binding site can functionally reverse the procaspase activation suggesting a common regulatory site for the allosteric control of inflammation and apoptosis [88].

1.3 Targeting and analyzing caspases

1.3.1 General strategies of caspase inhibitor design

The intrinsic subsite preferences for all caspases has been extensively studied with positional scanning approaches [89]. Knowledge about substrate specificity has been used to develop caspases inhibitors which resemble the natural substrate. These inhibitors contain three structural components: the P_2-P_4 peptides, the P_1 aspartic acid and a warhead electrophile (e.g.: fluoromethylketone) which reacts with the nucleophilic cysteine. However, peptide inhibitors for caspases are unspecific and have poor drug like properties due to charged peptides. This has prompted researchers to develop molecules that mimic their natural substrates, so called peptidomimetics (Figure 1.10). An alternative approach is the exploration of compound libraries to identify peptidase inhibitors since it does not require knowledge of subsite preferences. A prerequisite for this high throughput screening (HTS) however is the availability of large and chemically diverse compound libraries and requires extensive screening followed by lead optimization to obtain the desired bioavailability and specificity.

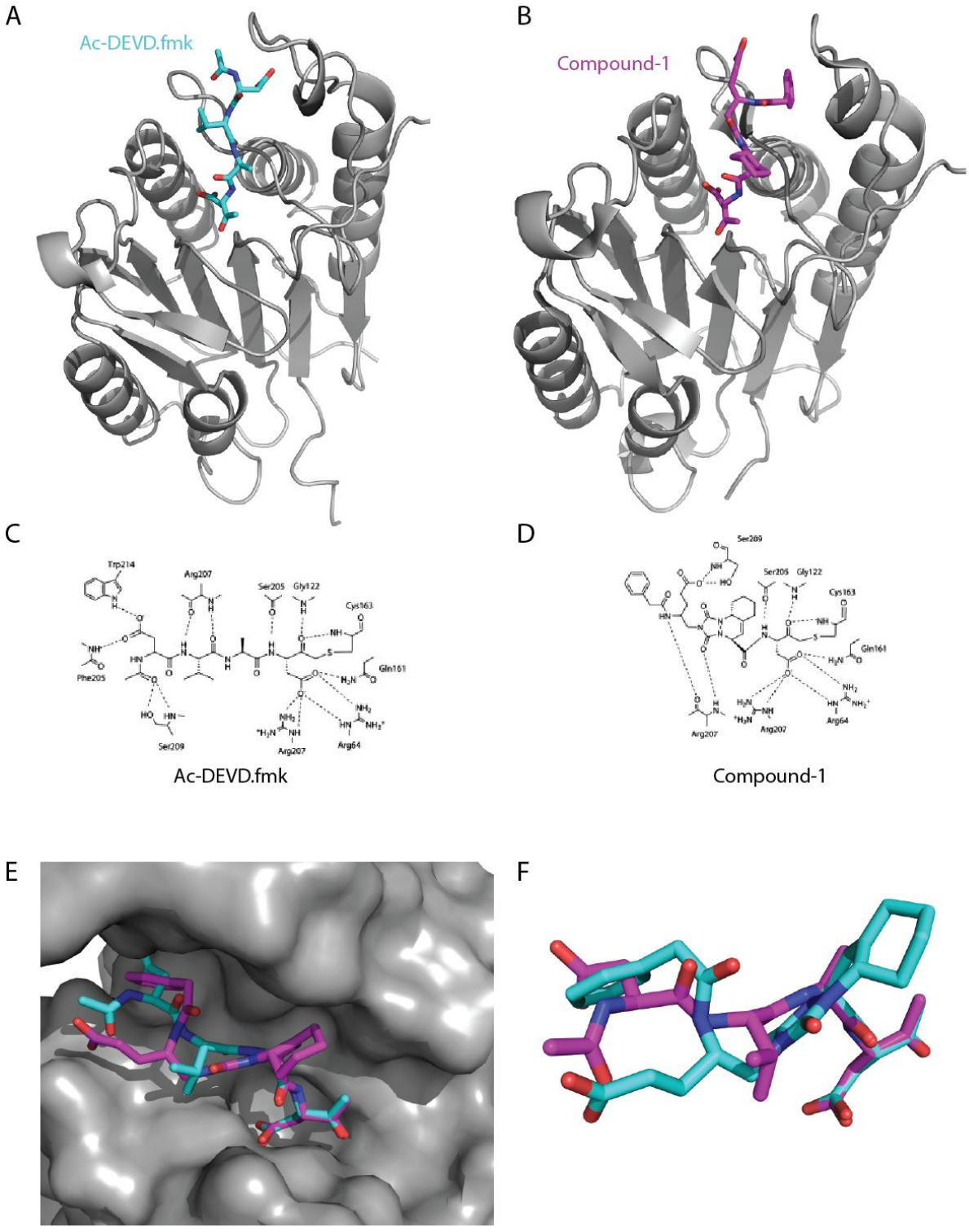

Figure 1-10: Caspase inhibitors

A) Cartoon representation of the structure of caspase-3 (grey) in complex with the peptide inhibitor Ac-DVAD.fmk (cyan) represented as sticks in the active site (PDB entry code 1CP3)[90] B) Cartoon representation of the structure of caspase-3 (grey) in complex with the irreversible inhibitor 'compound-1' (B92, magenta, PDB entry code 3KJF) [91] represented as sticks in the caspase-3 active site. C) Chemical diagram of the hydrogen bonding interactions of Ac-DEVD with caspase-3 D) Chemical diagram of the hydrogen bonding interactions of 'Compound-1' with caspase-3 [C and D adapted from [91]] E) Surface representation of caspase-3 in complex with both inhibitors. F) Structural alignment of the two inhibitors (color coding as in A and B) Ac-DEVD and 'Compound-1'.

1.3.2 Alternative strategies for the development of caspase inhibitors

Many conventional peptidase inhibitors have limited specificity and significant off target effects. This lack of specificity is often the result of highly conserved active sites within a protein family or even other families with similar catalytic mechanisms. This problem also accounts for other highly conserved protein families such as kinases, a class of proteins frequently implicated in many human diseases.

An alternative approach involves inhibitors which target epitopes other than the active site. One example is the endogenous 'X-linked inhibitor of apoptosis protein' (XIAP), which inhibits caspase-3, -7 and -9 [92]. Caspase-3 and-7 are inhibited by the BIR2 domain (Figure 1.11A), which has a binding site outside the active site (exosite) and an unstructured peptide which binds into the active site groove to prevent binding of the natural substrate. Caspase-9 is inhibited by an allosteric mechanism with the BIR3 domain binding the dimerization interface to prevent activation (Figure 1.11B). An advantage of allosteric inhibition is that the inhibitor is not competitive with the substrate and is thus not affected by substrate concentrations. This is particularly compelling if one considers that most peptidases work in substrate saturated environments where inhibition of a competitive inhibitor is weakened.

The same inhibition strategy can be pursued with antibodies or alternative scaffolds such as designed ankyrin repeat proteins (DARPins). These proteins scan larger surface areas and thus enhance the specificity of the interaction. Furthermore, interactions with allosteric sites such as dimer interfaces are possible, similar to the BIR3 domain of XIAP. Although large molecules have several distinct advantages over small molecules their scope of application is limited to extracellular applications until novel methodologies are developed to efficiently deliver proteins across cell membranes. The potential of both approaches would be best exploited if they were combined so that structural studies of large molecules in complex with caspases could provide insight for the rational design of small-molecule inhibitors that mimic the binding interactions [89].

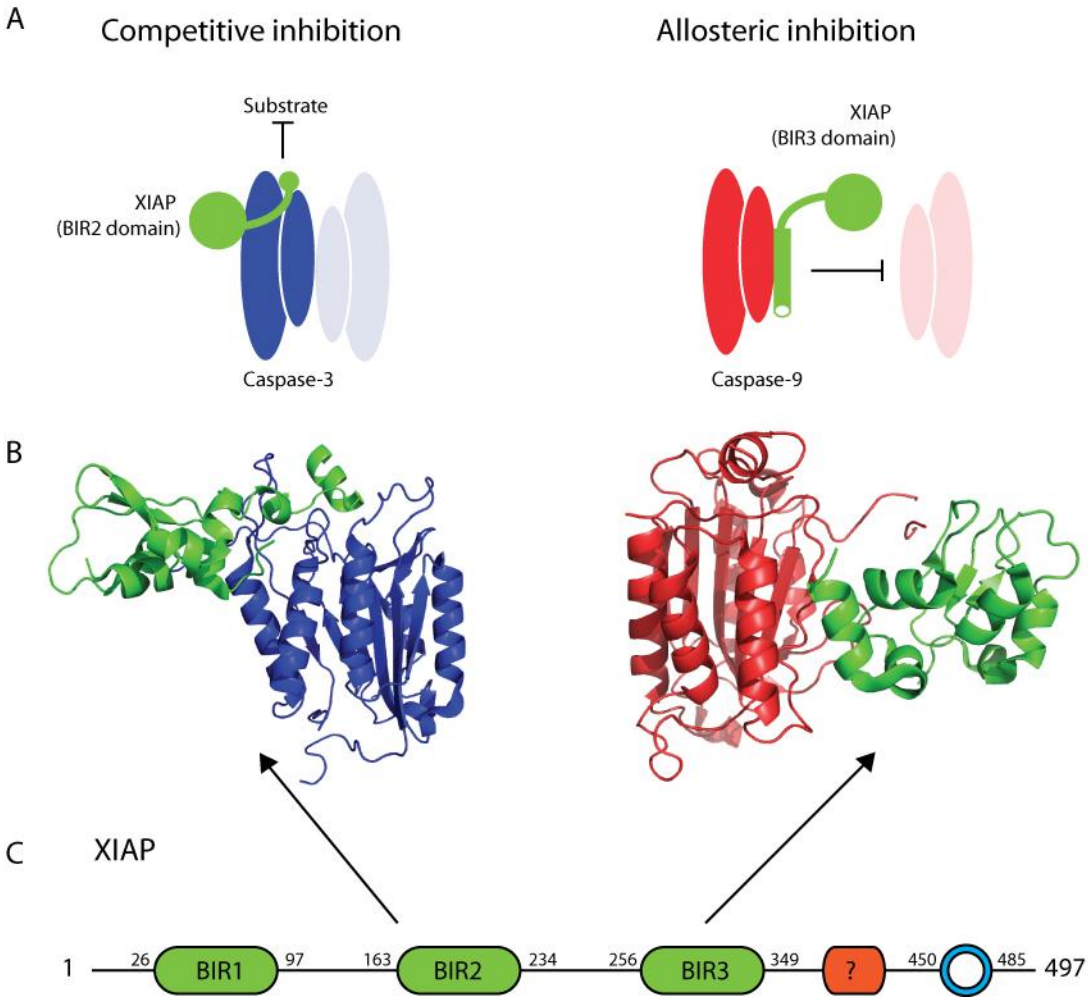

Figure 1-11: Caspase inhibition strategies by nature
A) Schematic sketch of XIAP inhibiting caspase-3 or caspase-9. Color coding is according to 3D structures in (B). B) XIAP (green) inhibits caspase-3 (blue) with is BIR-2 domain with a long loop which binds into the active site cleft and thus competes with substrate binding. Caspase-9 is inhibited by the BIR3 domain which binds the dimerization interface and prevents dimerization. Dimerization is critical for full catalytic activity so inhibition by preventing dimerization is an allosteric mechanism used by nature. C) Domain organization of XIAP with the two BIR domains responsible for caspase inhibition. A caspase cleavages site at residue 242 (SESD) is not indicated. Figure was adapted from [53].

1.3.3 Specific inhibition of caspases

Caspase-1 is involved in the onset of inflammation and is a major target for drug design. Based on the optimal substrate specificity WEHD, several highly specific peptidomimetic molecules have been developed. The most prominent caspase-1 inhibitor, pralnacasan (VX-740 from Vertex Pharmaceuticals) and a derivative VX-765, possess an IC_{50} of 1.3 nM for caspase-1 which is 1000 fold higher than for any other caspase [93]. Although both inhibitors were well tolerated and exhibited strong anti-inflammatory effects in mice, they were

ultimately withdrawn from clinical trials due to liver toxicity [45, 94]. A limitation of caspase peptidomimetics is the absolute requirement of a charged aspartic acid in P_1 which has a negative impact on drug like properties and cell permeability. In order to ameliorate drug like properties and obviate the requirement of an aspartic acid, researchers also used small-molecule caspase inhibitors. However, none of the drugs developed so far have succeeded in clinical trials [45]. A new emerging strategy with high potential to increase the specificity of caspase targeting drugs are allosteric and exosite inhibitors. Allosteric regulators targeting caspase-3 and -7 were developed using tethering or disulfide trapping which revealed two compounds that bound in close proximity to the dimer interface [86]. When bound, these compounds displaced residues in the active site, thereby occluding substrate binding in this region.

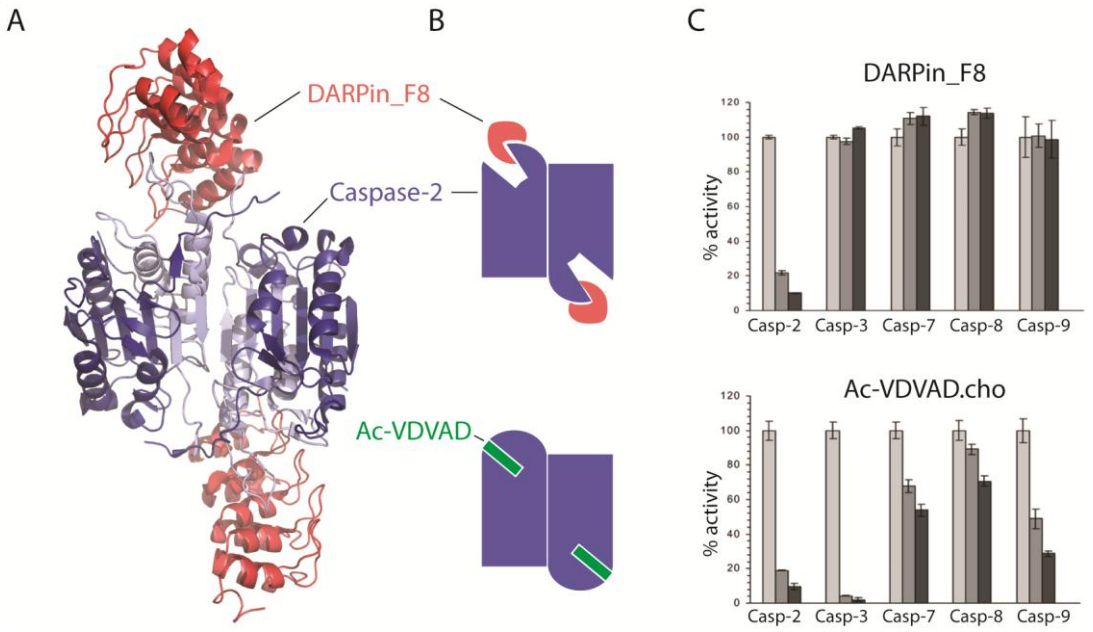

Figure 1-12: Specific allosteric inhibition of caspase-2 by a DARPin
A) Crystal structure of caspase-2 (blue) in complex with the inhibitory DARPin F8 (red) (PDB entry code 2P2C). The DARPin binds loop4 in an inactive conformation leading to allosteric inhibition. B) Inhibition of caspase-2 (blue) DARPin F8 and the short peptide inhibitor VDVAD.fmk (green) is illustrated. The short peptide competes with the caspase-2 substrate while DARPin F8 stabilizes a conformation that is unable to cleave the natural substrate. D) Specificity profile of both the DARPin F8 and VDVAC-CHO inhibitor. The peptide inhibitor is relatively unspecific while DARPin F8 only inhibits caspase-2 but none of the other caspases. Figure is adapted from [95].

The advancement of novel techniques in protein engineering of antibodies and alternative scaffolds, such as nanobodies and DARPins, has added another promising means for developing allosteric protein inhibitors. Antibodies, scFv and especially DARPins have been shown to modulate the function of a diverse array of proteins such as kinases [96] and also caspases (Figure 1.12)[95]. In the latter study, DARPin_F8 was shown to bind to a flexible surface area which includes loop 381 and some residues of the large subunit. Furthermore, the authors revealed that DARPin_F8 inhibits caspase-2 via an allosteric mechanism. Loop 381 appears to be crucial in active site formation and binding of DARPin_F8 stabilizes a distinct conformation in which essential residues in substrate recognition are misaligned. With a K_i of 0.29 nM, this DARPin is a highly potent caspase-2 inhibitor and has an exceptional selectivity profile for other caspase family members. DARPin_F8 is highly specific because is interacts with caspase-2 through a large interface and binds a unique epitope close to the active site. Although it is unlikely this DARPin will make it into clinical trials, structural insights into the inhibition mechanism may assist in the development of small and cell permeable molecules [97].

1.3.4 Specific activation of caspases

Since many diseases, including cancer, occur due to a decreased activity of peptidases a valid therapeutic strategy is to activate peptidases such as procaspase-3 [45]. One approach would be to block endogenous inhibitors which are often up regulated in several diseases. For example, XIAP is up regulated in acute myeloid leukemia (AML) and contributes to chemo resistance [98]. An antisense oligonucleotide (AEG35156) that targets XIAP induces apoptosis in combination with chemotherapy, showing that inhibiting the inhibitors is a viable approach [99].

Many types of cancer cells are resistant to apoptotic stimuli due to overexpression of regulatory proteins such as IAP's or BCL2. However, a very promising finding was that activation of caspase-3 efficiently kills cancer cells despite XIAP overexpression [100]. There are in principle two ways to activate a caspase depending on whether they are executioner or

initiator caspase. Firstly, initiator caspases such as caspase-8 can be activated by induced dimerization via mimicry of the DISC. According to the current understanding of the DISC, caspase-8 can be activated simply be creating a high local concentration of two procaspase-8 monomers leading to autoproteolysis and dimerization. Secondly, executioner caspases such as caspase-3 are believed to be in equilibrium between the active and the inactive state; it is thus necessary to find a compound which either stabilizes the active conformation or destabilizes the inactive conformation [100]. The first compound (PAC1) that activates caspase-3 was reported by BioLineRtx in 2006, yet it remains controversial whether PAC1 directly activates caspase-3 or whether the observed effect is due to a secondary Zinc mediated mechanism [101]. An independent HTS screening led to the discovery of a small molecule (1541) which activates caspase-3 at a concentration of 2.4 μM [102]. Compound-1541 was found to induce apoptosis in cancer cells and a mutational study in the active site revealed that this compound activates caspase-3 through stabilization of the active conformation.

1.3.5 Specific analysis of caspase activities

Positional scanning of the intrinsic subsite preferences has determined the optimal substrate sequences of each caspase [28]. This knowledge provided the basis for the design of caspase substrates in order to profile caspase activity in apoptotic cells. These tetrapeptide sequences were combined with a functional group (7-amino-4-methyl coumarin (AMC)) at the C-terminal. Cleavage of the peptide after the P_1 residue AMC leads to a fluorescent red shift of 125 nm (λ_{ex}= 345 nm, λ_{em}= 440 nm)[103]. This fluorogenic caspase substrate (e.g.: Ac-DEVD.AMC) thus allows profiling of caspase activity by fluorescent measurements. However, because caspases have highly overlapping sequence specificities, this method is unable to determine the activity of a single caspase in complex mixtures such as cell lysates of apoptotic cells [80]. One approach to overcome this limitation would be the isolation of the desired caspase by a specific binding protein such as an antibody or DARPin followed by activity profiling using tetra peptide substrates. Here the specificity is achieved via interaction

of the binding protein with a less conserved surface of the caspase, followed by the addition of highly sensitive substrates capable of detecting the activity of very low enzyme concentrations. In order to realize this approach, it is necessary to have a panel of binding proteins specifically targeting each of the caspases with affinities below the actual concentration of the caspases in an apoptotic cell.

1.4 Designed Ankyrin Repeat Proteins and their applications

1.4.1 Antibodies and the rise of alternative scaffolds

Antibodies have evolved as molecules that recognize antigens specifically in the adaptive immune system. The immunoglobulin fold has proven to bind target molecules with high specificity and affinity in both, *in vivo* and *in vitro* applications. Antibodies can be generated using the immune system of a host animal or with screening approaches of a synthetic library using various display technologies. They are large, multidomain proteins and their disulfide bonds and glycosylation are both indispensable for immune effector functions [104]. Antibodies, especially the IgG format have proven to be very successful therapeutics and represent the most widely used binding molecules [105, 106]. Despite this success, antibodies are rather expensive to produce and often aggregate when fused to effector molecules. They possess disadvantageous biophysical properties including disulfide bonds, a complex molecular composition and are large molecules with a size of about 150 kDa. Research, development and industrial production of antibodies are obfuscated by the high production costs and elaborate screening procedures. Consequently smaller variants such as Fab or scFv fragments have been developed based on the IgG antibodies and can be produced at much lower costs, however they inherit many of the above mentioned limitations [107](Figure 1.13A).

These circumstances gave rise to the development of non-antibody scaffolds and have led to a multitude of alternative scaffolds. Some of the most successful alternative scaffolds include Immunoglobulin-Like β-sandwich (FN3), β-barrel (Lipocalins), single loop (aptamers), α-helical scaffolds (Affibodies) and repeat proteins (DARPins, LRR). Although these proteins differ significantly in their properties and fold, their design and selection are based on the same fundamental principles (Figure 1.13A).

The concept of a molecular scaffold for binding protein was developed in 1993 and is the basic idea of a stable protein core that tolerates extensive surface mutations that allow it to

bind a ligand [108]. Natural evolution has derived many folds with such properties and most are involved in various protein-protein contacts. An alternative scaffold should ideally be highly stable in order to tolerate a large number of mutations forming a contiguous interface. In addition it is generally favorable to have a small protein with no disulfide bonds and with high solubility in order to improve its experimental handling. The choice of a scaffold then requires the design of a highly diverse library and an appropriate selection technique which agrees with the biophysical properties of the desired protein and future application.

This Chapter gives an overview of the development and applications of an alternative scaffold based on the Designed Ankyrin Repeat Proteins (DARPins). A more detailed description of the many diverse alternative scaffolds that have been used to design binding protein is reviewed in [104].

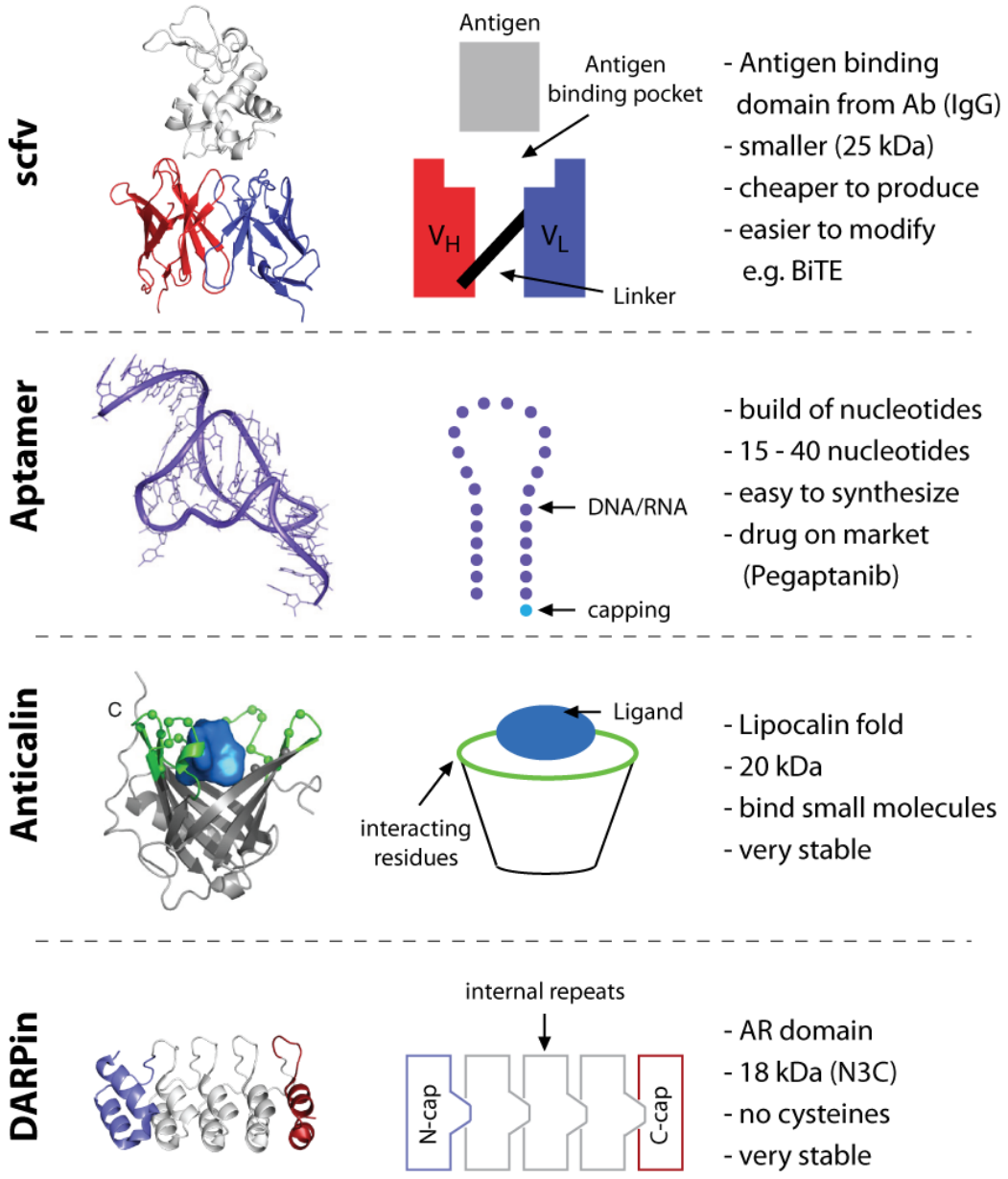

Figure 1-13: Overview of selected alternative scaffolds

1.4.2 Design of DARPins based on ankyrin repeat proteins

The rational for developing DARPins was to overcome all limitations of antibodies and its variants while not compromising on affinity and specificity [104]. The desired properties are high expression yields, stability and solubility, absence of disulfide bonds or free cysteines and favorable folding properties.

DARPins have been designed based on naturally occurring ankyrin repeat proteins which are known to be highly stable and versatile binding molecules with a modular architecture. The fundamental idea was to design a consensus repeat encoding self-compatible repeat modules. Some amino acid positions would be conserved and necessary for folding of the backbone, whereas other positions would be non-conserved surface exposed residues involved in the interaction interfaces [109]. Based on an alignment using sequence databases a consensus sequence was defined. Positions with no or very low sequence preference were chosen as randomized residues (Figure 1.14 D). A second important aspect is the capping of repeat proteins to shield the hydrophobic interface of internal repeats [109]. The capping repeats increase the solvent accessible surface significantly and lead to increased solubility and stability. Assembly of the selected framework leads to modular repeats that form a stable and self-compatible protein fold while allowing randomized residues at the surface [110].

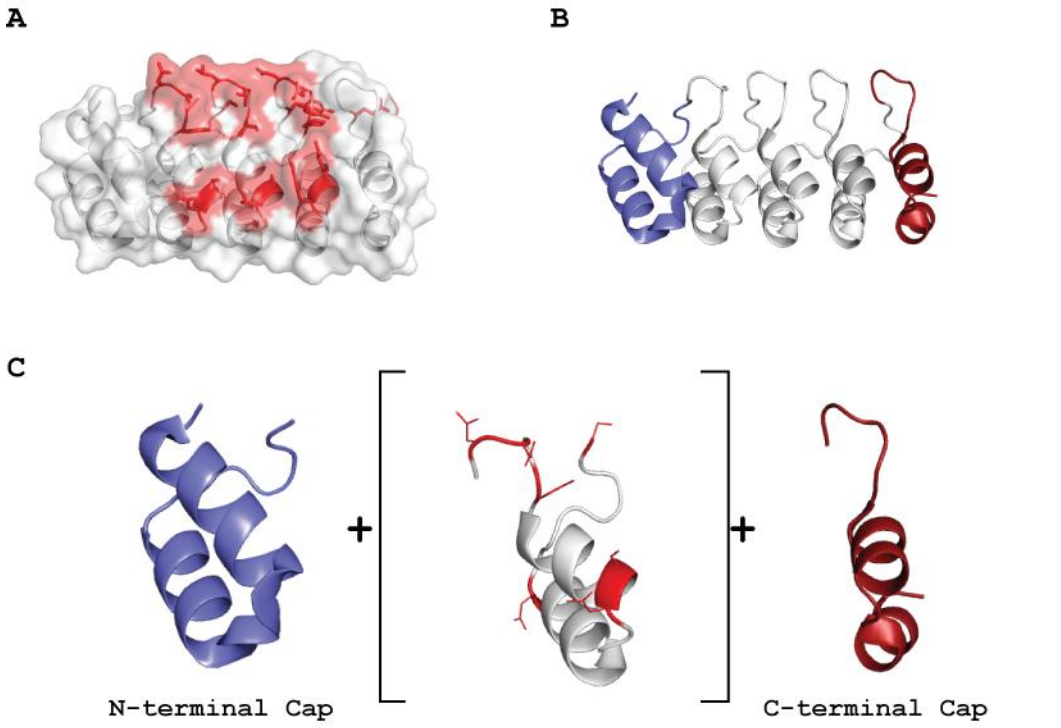

Figure 1-14: Architecture of a DARPin
A) Transparent surface and cartoon representation of DARPin E3_5 (PDB entry code 1MJ0). The randomized positions which build the interaction with the respective side chains interface are shown in red. B) Each DARPin has a N- and C-terminal Cap colored in blue and red respectively. Several repeats (white), in this case three, can be inserted between both caps and form a continuous hydrophobic core which is shielded by the two caps. C) Modular architecture of caps, repeats and the randomized positions (skyred) is shown. D) Sequence of a DARPin with the respective randomized positions in red and the secondary structure. Color coding is adapted from (C). Parts from this figure are adapted from [109].

1.4.3 Stability and folding of DARPins

The first crystal structure of a consensus ankyrin protein was solved by A.Kohl and H.K.Binz et al. [111]. This DARPin (E3_5) showed very favorable biophysical properties with a free energy of unfolding (ΔG) of 14.84 kcal/mol and a midpoint of unfolding of approximately 5 M GdmCl. Further general studies of H.K.Binz et al. with randomly chosen library members [110] showed that the DARPin expression yielded up to 200 mg per liter. They could be purified by immobilized metal-ion affinity chromatography (IMAC) with a single step resulting in high purity. Only 1 of 6 selected binders showed a dimer peak indicating that DARPins are generally monomeric in solution. All DARPins showed cooperative unfolding while exhibiting substantial heat resistance with midpoints between 66 °C and more than 85 °C. The ΔG values for unfolding were calculated between 9.5kcal/mol and 21.1 kcal/mol.

A folding study of a single consensus repeat with flanked capping repeats revealed that the AR is an autonomously folding domain following monoexponential kinetics with $k_{folding}$= 28 sec^{-1} and $k_{unfolding}$=0.9 sec^{-1}. Specific unfolding enthalpy and entropy as well as the temperature slope of the heat capacity are typical for globular protein domains explaining the favorable properties of the consensus framework [112]. The hydrophobic interactions between the helices within a single AR are not well optimized, while hydrophobic stacking is more compact at inter-repeat interfaces. This finding explains the cooperative behavior of the number of internal repeats and thermodynamic stability [110].

In order to address the folding and unfolding behavior of a DARPin as a function of the number of repeats S.K.Wetzel et al. designed a DARPin with identical repeats [113]. While 7 out of 33 amino acids were randomized in the common DARPin library, defined residues were assigned to the variable positions according to sequence statistics and structural considerations [110]. This “averaged structure” revealed that DARPins with three repeats can only be entirely denaturated when boiled in 5 M GdmCl, whereas DARPin with four or more repeats did not denaturate when boiled in 8 M GdmCl. These findings highlight the cooperativity between stability and number of repeats and can be rationalized following the

Ising model. The stability of the AR protein is determined by unfolding rates rather than the folding rates which are monophasic (~400-800 s-1) and almost independent from the number of repeats. The unfolding rates in contrast decrease by a factor of 10^4 with every repeat. This leads to the conclusion that the folding can be considered as a nucleation event where the folding of a single repeat triggers the folding of the entire molecule. The unfolding needs a progressive disruption of all repeats and is consequently dependent on the number of repeats [114].

A study by T.Merz et al. gave more insight to the intramolecular interactions that contribute to the stability of a DARPin by comparing two DARPins at atomic resolution [115]. His findings highlighted the almost crystal-like regularity of a network composed by salt bridges on the surface involving sulfate ions. This suggests that this regular charge network of surface exposed electrostatic interactions contributes to the stability of the protein next to the compact hydrophobic core. Although it is believed that this interaction network is a hidden design feature in this protein family, it can no longer be observed in naturally occurring AR proteins due to functional selection [115].

The contribution of the hydrophobic core and the surface exposed salt bridges are so tremendous that randomization of amino acids in specific positions can be easily tolerated without a critical loss of stability. This case highlights the interplay of stability and functional selection showing that stability is a prerequisite to functional selection.

1.4.4 Target directed DARPin selection with display techniques

The generation of specific binding proteins by immunizing animals is limited to proteins that can be evolved by the respective immune system. Although this approach offers different forms of antibodies or leucine rich repeat proteins (LRR) [116] depending on the host animal it does not allow the directed evolution of alternative scaffolds. This prompted researchers to develop *in vitro* techniques that mimic the classical selection procedure of the immune system

by physically coupling genotype with phenotype. The first display technique was developed in 1985, namely Phage display [117] providing a system of a viral phage which encapsulates DNA and presents the corresponding protein on the surface. Phage display is to date the most commonly used system for directed evolution and is especially attractive because of its high robustness and availability in different laboratories. Different display systems have emerged in recent years using different phages, cells or molecules such as proteins, DNA or RNA.

One main limitation in cell or virus based systems is the absolute requirement of a transformation step in order to integrate DNA into the host. The relative low transformation efficiency that is obtained witch current techniques, limits the library size to less than 10^8 molecules [118]. In contrast one can obtain library sizes of up to 10^{14} molecules with cell free methods such as Ribosome Display (RD) which was first demonstrated by Hanes and Plückthun [119]. The phenotype-genotype coupling is achieved through a stable complex of mRNA, ribosome and the translated protein. The ribosome does not dissociate from the translated RNA due to the absence of a stop codon but allows the translated target protein to fold and exit the ribosomal tunnel owing to a tether sequence incorporated in the RNA library. The complex can then be panned against any target molecule that is usually immobilized on a surface followed by several washing steps. The genetic information of selected binding proteins is then recuperated and reverse transcribed into a more stable DNA library. A more detailed description is shown in figure 1.15. The most recent publication on RD offers an overview and a protocol including all aspects which have to be considered when performing RD selections [120].

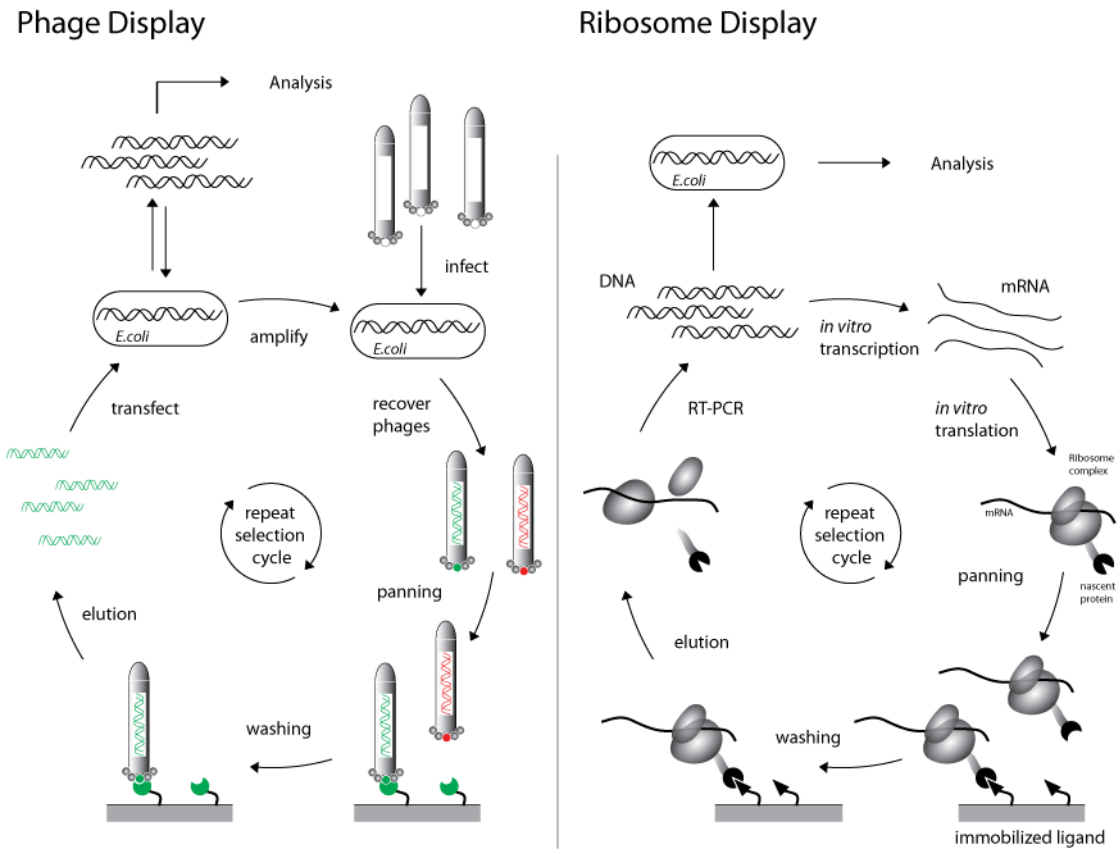

Figure 1-15: Protein display technologies
Both Phage Display (PD) and Ribosome display (RD) couple phenotype with genotype with Phages or Ribosomal complex respectively and allow selection of a protein for a specific binder. Both selection methods require a DNA library of a protein to be selected. In the case of PD, this library is transfected into *E.coli* and subsequently infected by phages. The amplified phages carry a single gene and present the according protein on the surface; this allows selection for a target protein which is immobilized on a surface. The DNA library in RD is transcribed into mRNA and then translated by a Ribosome. A tether sequence stops the translation and allows the formation of a stable complex of mRNA, ribosome and translated proteins which allows the selection against an immobilized target protein. The phage and the ribosome complex are eluted after selection in both PD and RD and the DNA and RNA are recovered respectively. This selection cycle can be repeated multiple times until sufficient enrichment of the library for a target is accomplished. Both selection techniques are followed by cloning of the selected library into *E.coli* with subsequent analysis of single clones by ELISA techniques. Ribosome display drawing was adapted from [121].

We have chosen RD to evolve DARPins against Caspase for several reasons. Firstly, the library based on the DARPin scaffold has a theoretical diversity of 10^{23} molecules, and RD represents the least limiting selection technique in terms of library size. Secondly, RD and DARPins libraries are compatible with high expression and stability of DARPins in the S30 translation system. Finally DARPins show poor display levels using the conventional Phage Display system based on the Sec translocation system due to high folding rates that interfere with translocation to the phage surface. Only recently a novel variant named "SRP Phage

Display" yielded increased surface display of DARPins by exchanging the translocation signal sequence [122]. Third, RD has an additional diversification due to reverse transcription and multiple PCR amplification steps which increase the practical library diversity significantly. This may also lead to unpredictable but favorable framework mutations that can strongly impact affinity [123].

It should be noted that each system has distinct advantages and disadvantages and the appropriate system should be selected carefully depending on the scaffold and the intended properties one aims to obtain. The DARPins scaffold combined with the designed library are highly compatible with RD and many studies have successfully combined the two technologies.

1.4.5 Recent Applications of DARPins

Since the development of the consensus ankyrin repeat protein and the combinatorial library [110], many studies have shown specific and high affinity binding of various target proteins. The first crystal structure of a DARPin in complex with its target protein maltose binding protein (MBP) at a resolution of 2.3 Å gave first insight on the interaction interface mediated by DARPins (Figure 1.16C) [124]. The selected DARPin (off7), a N3C molecule bound to MBP, exhibited a K_D of 4.4 nM and was specific to its target protein. The interactions in the interface were only mediated by randomized surface residues with a total buried surface area of 1.267 $Å^2$. This proof of principle work confirmed the feasibility and opened the door for many different studies and applications.

The first tailor made protein inhibitor was selected against aminoglycoside phosphotransferase (3')-IIIa (APH), and again showed high specificity and affinity and completely inhibited APH *in vitro* and lead to a gene knockout phenotype *in vivo* [96]. This study underlines the potential of DARPins for modulation of intracellular protein function. The crystal structure of APH in complex with its inhibitory DARPin AR_3a revealed an allosteric inhibition mode by binding three α-helices in a displaced conformation. This shows

that DARPins are not limited to active site binding in contrast to small molecules, thus representing a powerful starting point for rational drug design in combination with allosteric inhibition by DARPins [125].

Another highlight was the first DARPin selected against the soluble domain of a membrane protein, the human epidermal growth factor receptor 2 (Her2). The selected DARPins bound to the same epitope as Herceptin with a K_D of 7.3 nM. Her2 is an important target for cancer therapy and diagnosis thus the selected DARPins might be used for the development of diagnostic tests or in cancer treatment [126]. In a subsequent study, the affinity of the best selected Her2 binder was improved to 90 pM by error-prone PCR and affinity maturation. A single point mutation in the framework residue (H53T) leading to a conformational change in relative disposition of the repeat domains resulted in a 3000-fold affinity increase compared to the consensus sequence [123]. This DARPin (H10-2-G3) has the highest affinity so far reported of an AR protein [123, 127].

A central problem in targeting enzymes such as proteases is lack of specificity due to the fact that the binding hotspots are usually the active sites which are known to share homologous structures and overlapping specificities [97]. A study by A. Schweizer and H.Roschitzki-Voser demonstrated the specific inhibition of Caspase-2 with DARPin AR_F8 by avoiding the actual active site and binding an exposed loop that is involved in the formation of the active site. Binding the loop freezes a nonproductive conformation and reveals a conformation of the active site that can be exploited for the design of inhibitory compounds. AR_F8 is the only specific caspases inhibitor to date [95].

The first structure of a DARPin binding an integral membrane protein (AcrB) has been published by G. Sennhauser et.al [128] with a resolution of 2.5 Å, higher than any structure of AcrB before (Figure 1.16B). This study demonstrates that DARPins can be used as crystallization chaperones in order to improve resolution or help the crystallization process by extending the hydrophilic surface [129]. Next to the improved resolution, the selected

DARPin allowed functional studies of substrate transport by stabilizing an inactive conformation.

In total, 18 reports have demonstrated the selection of DARPins against multiple targets including soluble and membrane proteins from various species. Taken together, this confirms that DARPins can in principle be selected against literally any protein for multiple applications. However, these studies represent only a fraction of possible applications that are imaginable for the future.

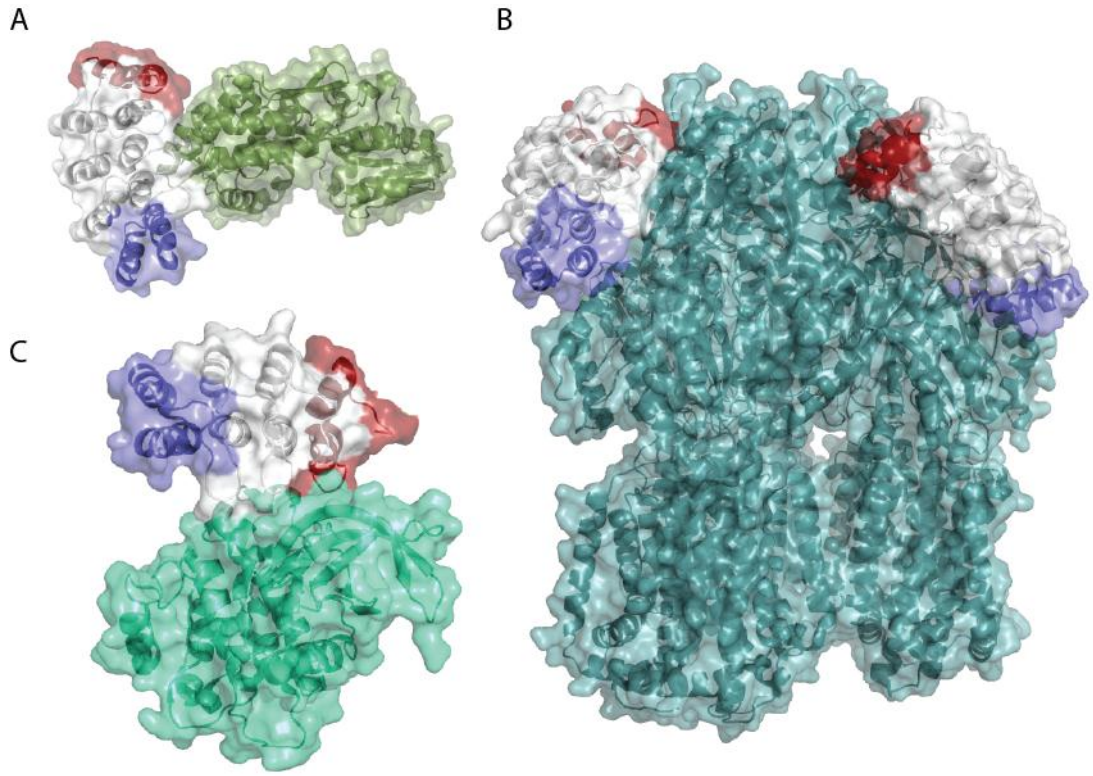

Figure 1-16: Crystal structures of DARPins
The DARPin is colored in blue (N-Cap) white (internal repeats) and red (C-Cap). A) The first DARPin selected was against MBP showing how the interaction is mediated by the randomized positions (PDB entry code 1SVX)[124]. B) First structure of a DARPin in complex with a membrane protein (green)(PDB entry code 2J8S [128]). The membrane protein AcrB is a trimeric protein and binds two DARPins only. C) Structure of the first N2C DARPin in complex with the wild-type PLK-1 kinase domain (green) (PDB entry code 2V5Q [127]).

1.4.6 Applications and future perspective

Alternative scaffolds are expected to replace most applications that have previously been demonstrated by antibodies due to the amelioration of several features such as: stability, expression and purification as well as production costs. In addition, intracellular applications become feasible owing to the fact that most alternative scaffolds do not contain cysteine bonds. As described in several studies [104, 130], possible applications involve five areas:

Therapeutic applications - The vast majority of therapeutic binding molecules on the market or in clinical studies are antibodies and alternative molecules are only slowly entering clinical trials. Antibodies have a long history of research and have clear advantages over other binding proteins. Their bivalent interactions leads to high affinities, they are fully human are well tolerated and have a long serum half-life. However antibodies also have limitations since it is a large multi domain protein with cysteine bonds and glycosylation and are thus rather difficult to handle at relatively high costs. The therapeutic effect that is achieved with antibodies is usually based on blocking a target or by "exerting effector functions" to activate a response of the immune system [131].

DARPins represent an ideal protein class to complement antibodies in blocking or neutralizing target proteins. The absence of an effector domain (Fc) reduces the activation of the immune system and their significantly smaller size is expected to advance tissue penetration. It is further expected that antagonistic DARPins will have an enhanced ability to remove unwanted molecules such as toxins based on their short serum half-life. Although DARPins do not have effector functions, their mode of action is not limited to simply blocking or neutralizing a target. Their single domain architecture does not contain any cysteines, which allows the attachment of diverse molecules affecting their pharmacokinetic properties or even effector domains. Such a conjugated DARPin could thus deliver toxins, cytokines, enzymes or even a second DARPin domain for the recruitment of other effectors (Figure 1.17). This is indeed also possible with antibodies and other binding molecules but the

stability, ease of use and the possibility of introducing site-specific thiol groups constitute clear advantages for the DARPin fold [104, 131].

Chromatography and affinity purification based on specific antibodies is already applied and represents a well-established technique. The antibody is immobilized onto a surface and is able to purify the specific binding partner from complex mixtures such as cell lysates. Protein A is the most prominent example for standard purification of antibodies. Limitations in this field are mostly the high cost of antibody production and the sensitivity of antibodies to harsh washing or reducing conditions. Alternative scaffolds, especially DARPins are highly attractive due to their cheap production costs and the highly stable fold. We can expect significant progress in this field with an increasing number of specific binding proteins in the near future (Figure 1.17).

Crystallization Chaperones facilitate crystallization and crystal packing of a desired target protein. This is in most cases given by reducing conformational heterogeneity, masking hydrophobic surfaces or by mediation of crystal contacts within the crystal lattice. In addition they may provide phase information by molecular replacement or the incorporation of heavy metal derivatives [132]. Immunoglobulins, Fab fragments and scFv's have been successfully used as crystallization chaperones in the past and the potential and success stories of DARPins as crystallization chaperones has been recently reviewed [129] (Figure 1.17). Several structures of DARPins in complex with their target proteins have been solved, but the only example of a DARPin in complex with a previously unknown structure is the kinase Plk-1 [127]. In order to reveal the true potential of DARPins in as crystallization chaperones many more structures and studies are needed.

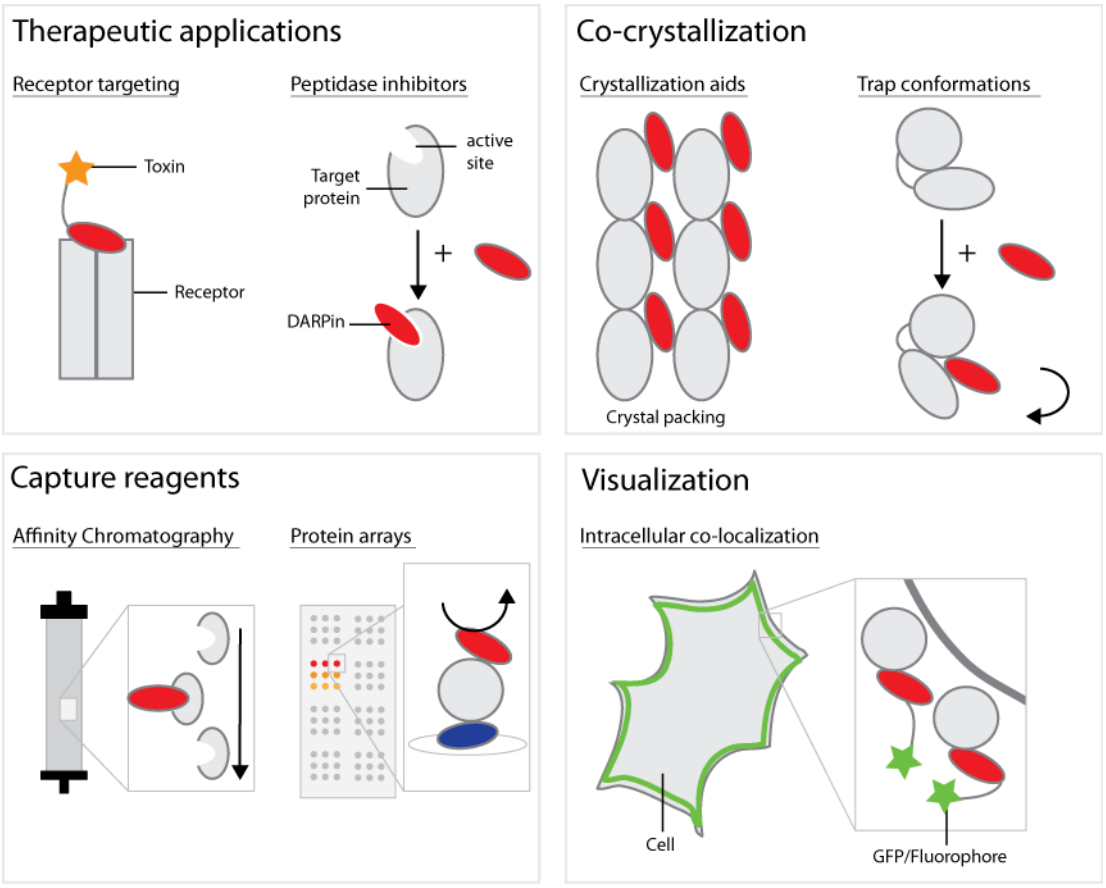

Figure 1-17: Possible applications of DARPins.
Applications as drugs are financially most attractive but many more applications as a technology in research are possible due to their favorable properties.

Diagnostic applications such as ELISA, Flow cytometry and immunohistochemistry are mainly based on antibodies, alternative scaffolds may play a distinct role in the future because they can be produced at lower costs and might have a longer shelf half-life. Additionally cysteine free scaffolds allow specific immobilization to a surface or the attachment of functional groups such as fluorophore by introducing a specific cysteine. Whether alternative scaffolds will replace antibodies in the future will depend on the availability of such molecules in the scientific community.

Intracellular applications could so far not be studied by antibodies due to their cysteine bonds that do not form in the cytoplasm. Alternative scaffolds are thought to have higher potential in this aspect as they can be expressed intracellularly (Figure 1.17). Several studies have shown

that selected synthetic molecules such as aptamers and DARPins can be used to perturb cellular functions [133, 134]. Despite its potential this approach still represents major bottlenecks, since synthetic proteins are not cell permeable and require expression in the host cell.

In summary alternative scaffolds such as DARPins represent a complementary proposition to antibodies in almost all fields. Antibodies are still the most successful molecules in all applications but DARPins are an attractive alternative due to their favorable biophysical properties. While the majority of applications remain in their infancy, the most promising of these appear to target functions which are not possible for antibodies: intracellular applications, protein trafficking, dissection of pathways and sensors of biomarkers [130]. Their success as drugs will depend on the general immunogenic tolerance as therapeutics [135].

2. Expression, purification and kinetic characterization of human caspases

Title:

Expression, purification and kinetic characterization of human caspases

Heidi Roschitzki-Voser[*+], Thilo Schröder[*+], Franziska Frölich[*], Esther Lenherr[*], Andreas Schweizer[1], Rajkumar Ganesan[2], Peer R.E. Mittl[*], Antonio Baici[*], & Markus G. Grütter[*†]

[**Protein Expression and Purification** *Manuscript in preparation*]

Expression, Purification and Kinetic Characterization of Human Caspases

Heidi Roschitzki-Voser[*+], Thilo Schröder[*+], Franziska Frölich[*], Esther Lenherr[*], Andreas Schweizer[1], Rajkumar Ganesan[2], Peer R.E. Mittl[*], Antonio Baici[*], & Markus G. Grütter[*†]

[*] Department of Biochemistry, University of Zürich, Winterthurerstrasse 190, CH-8057 Zürich, Switzerland

[1] Present address: Molecular Partners AG, Wagistrasse 14, CH-8952 Schlieren, Switzerland

[+] These authors contributed equally to this work

[†] Corresponding author: M.G.Grütter, Department of Biochemistry, University of Zürich, Winterthurerstrasse 190,

CH-8057 Zürich, Switzerland.

Tel. +41 44 635 55 80;

Fax. +41 44 635 68 34

Email: gruetter@bioc.unizh.ch

Abstract

Different strategies for the expression, purification and kinetic characterization of caspases have been described previously offering a vast number of protocols. In this work we have systematically revised these protocols and describe a comprehensive optimized expression and purification protocol for caspases 1-9 as well as improved assay conditions for their reproducible kinetic characterization. The here described studies on active site titration revealed that the accuracy is heavily influenced by the presence of DTT in the assay buffer. Furthermore it was found, that the activity of some caspases is not proportional to their enzyme concentration, explaining the discrepancy between the published values of specific activities. Our results contribute to overcome this problem leading to higher reproducibility in expression, purification and kinetic characterization of caspases.

Introduction

Caspases are a conserved family of peptidases that play essential roles in inflammation and apoptosis. They employ a cysteine residue as the catalytic nucleophile and share a stringent specificity for cleaving their substrates after an aspartate in P_1 position. To date twelve different human caspases have been identified and are classified into apoptotic or inflammatory caspases based on their sequence homology and substrate specificity (**Figure 1**). Caspase-1, -4 and -5 are known to be involved in cytokine activation in the inflammatory response. Their main substrates are pro-interleukin-1-β and pro-interleukin-18 which are activated upon caspase cleavage [136]. Caspase-12 which shares high sequence homology with caspase-1 is not expressed as a protease in the majority of the human population due to an early stop codon [137].

The apoptotic caspases can be further subdivided into initiators (caspase-2, -8, -9 and -10) and executioners (caspase-3, -6, and -7). The main substrates for the initiator caspases are the executioner caspases, which once activated cleave many cellular proteins which are important for the integrity of the cell such as PARP, Lamins, various kinases an others to promote apoptosis [138-141]. Caspase-14 is a unique member of the caspase family which has been shown to be involved in proliferation and differentiation of keratinocytes [53, 142, 143].

In cells, caspases are expressed as pro-enzymes containing an N-terminal prodomain and a catalytic domain. The catalytic domain consists of a large (17-20 kDa) and a small (10-12 kDa) subunit connected by a short inter-domain linker (**Figure 1**). Processing of the caspase prodomain and the linker results in the formation of the active enzyme with two substrate-binding sites [48, 144]. All caspases share a highly conserved fold and have a high sequence homology, with the highest identities found within the family of inflammatory caspases (60-80 %).

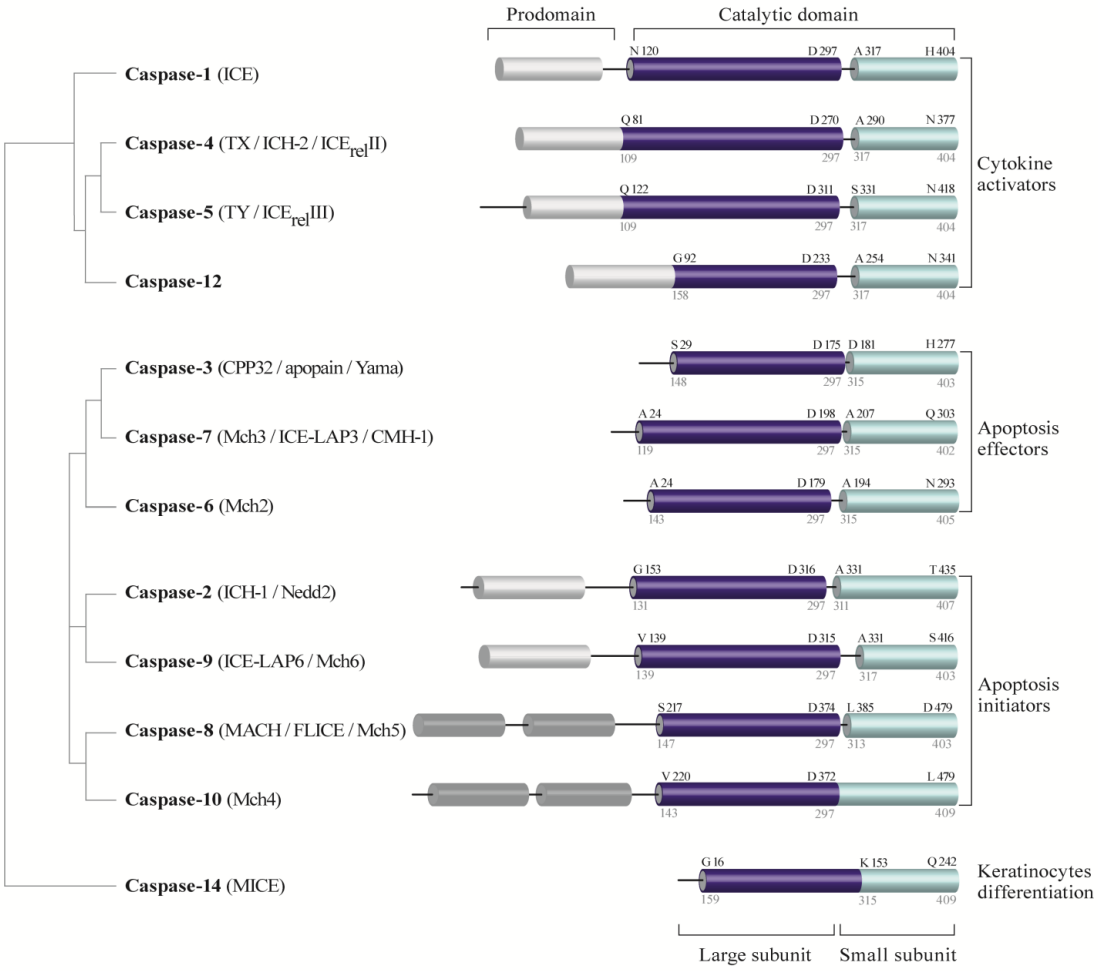

Figure 1: Phylogenetic tree of the caspase family.
The tree is organized based on the sequence similarity and substrate specificity. The sequence numbering highlighted in bold corresponds to the Swiss-Prot entries and numbering in grey represents the caspase-1 nomenclature suggested by Fuentes-Prior and Salvesen 2004 [53].

Given the biological importance of caspases in apoptotic and inflammatory processes and their subsequent pharmaceutical potential, major research efforts in both academia and industry have been focused on investigating the structure and function of these enzymes. These studies have led to the functional classification and description of the role of individual caspases in apoptotic and inflammatory signaling. For the pharmaceutical industry the ultimate goal is to design small molecule substrates and inhibitors, selectively targeting individual caspases. The large scale production and handling of human caspases in their active form is absolutely essential to make further advances in this direction.

Caspases were first isolated from natural sources. For example THP-1 cells, monocytes from human myeloid leukemia cell lines provided the source for caspase-1 and also caspase-3 [5, 145]. Caspase-9 could be isolated from HeLa cells, a human uterine carcinoma cell line [18]. However, caspases could also be expressed in *E.coli* and purified as active enzyme resulting in significantly higher yields. The various procedures have been described in numerous publications all involving the heterologous expression of the catalytic domains.

Here we describe optimized, detailed and consolidated expression and purification protocols for human caspases 1-9 that yield enzymes of equally high purity. Furthermore, we have re-determined the enzymatic activities of all caspases in different conditions and propose optimal protocols for activity measurements and kinetic analyses.

Material and Methods

Expression and purification of human caspases

The plasmids for the expression of caspase-1, -2, -3 -4, -5, -6, -7, -8 and -9 are cloned as indicated in **Table 1**.

Caspase	Gene		Vector
Caspase-1	Large subunit	MA_N_{120} -- D_{297}	pET28a(+)^{kan}
	Small subunit	MGS_A_{317}-- H_{404}_LEHHHHHH	pET28a(+)^{kan*}
Caspase-2	Large subunit	MA_N_{150} -- D_{316}	pET11d^{amp}
	Small subunit	M_A_{331} -- T_{435}	pET11d^{amp}
Caspase-3	Full length	M-S_1 – H_{277}_ALEVLFQGPHHHHHHH	pET28a(+)^{kan}
Caspase-4	Large subunit	M_Q_{81} -- D_{270}_LE	pET21(+)^{amp}
	Small subunit	M_A_{290} -- N_{377}_LEHHHHHH	pET21(+)^{amp}
Caspase-5	Large subunit	M_A_{135} -- D_{311}	pET11d^{amp}
	Small subunit	MGS_S_{331} -- N_{418}_LEHHHHHH	pET28a(+)^{kan*}
Caspase-6	Full length	M_1-N_{293}_LEHHHHHH	pET21(+)^{amp}
Caspase-7	Full length	M_1-Q_{303}_LEHHHHHH	pET23b(+)^{amp}
Caspase-8	Large subunit	MG_E_{218} -- D_{374}	pET11d^{amp}
	Small subunit	M_{383} -- D_{479}	pET11d^{amp}
Caspase-9	Full length	M_1-S_{416}_LEHHHHHH	pET23b(+)^{amp}

Table 1: Constructs for the expression of human caspases.

Expression and purification of caspase- 3, - 6, -7 and -9 (procedure A1a)

The full length gene for caspase-3 was cloned into pET28a(+)^{kan} engineered to carry a C-terminal His7-tag after a 3C cleavage site. The constructs for the expression of human caspase-6, -7 and -9 were obtained from Dr. Guy Salvesen, The Burnham Institute, La Jolla, USA [146]. The gene for caspase-6 was cloned into pET21(+)^{amp}, caspase-7 into pET23b(+)^{amp} and caspase-9 in pET23b(+)^{amp} all containing a C-terminal His6-tag [146]. The caspase-6 construct was mutated at the cleavage site located between the large subunit and the linker (D_{294}VVDNQ$_{299}$ → D_{294}EVDAA$_{299}$) because this cleavage site was only partially processed by bacterial proteases. The mutated construct yielded fully processed homogenous caspase-6 when expressed in *E.coli*. Expression and purification was carried out according to

the protocols established by Stennicke and Salvesen [146, 147]. The plasmids were transformed into BL21 (DE3). Single colonies were used to inoculate a 5ml 2×YT culture (0.5% NaCl, 1% Yeast Extract, 1.6% Tryptone), containing the appropriate antibiotic and was then grown at 37°C overnight (~210rpm). This culture was used to inoculate 500 ml of selective 2×YT medium in 2-liter baffled flasks at an OD600 of 0.02 and grown at 37°C. When the culture reached an OD600 of 0.6 – 0.8 the temperature was lowered to 30°C, expression was performed as listed in **Table 2**.

Caspase	*E.coli* Strain	Temperature	[IPTG]	Time	OD_{600}
Caspase-3	BL21 (DE3)	30°C	0.2 mM	3h	0.6-0.8
Caspase-6	BL21 (DE3)	30°C	0.02 mM	18h	0.6-0.8
Caspase-7	BL21 (DE3)	30°C	0.2 mM	18h	0.6-0.8
Caspase-9	BL21 (DE3)	30°C	0.2 mM	3h	0.6-0.8

Table 2: Expression conditions for human caspase-3, -6, -7 and -9.

Cells were harvested and washed in cell wash buffer (100 mM Tris-HCl, pH 8, 100 mM NaCl) subsequently resuspended in 50 ml lysis buffer (100 mM Tris-HCl, pH 8, 100 mM NaCl, 20 mM Imidazole, 10 units/ml DNaseI). Cells were broken using an EmusliflexTM homogenizer and further purified by immobilized metal ion affinity chromatography (IMAC). Lysate was cleared by centrifugation followed by filtration (0.22 mm syringe filter) and was loaded on a Ni^{2+}-nitrilotriacetic acid (Ni-NTA) (Qiagen, Chatsworth, USA) gravity flow column previously equilibrated with wash buffer (100 mM Tris-HCl, pH 8, 500 mM NaCl, 20 mM Imidazole). Nonspecifically bound protein was washed out with wash buffer and the protein was eluted with elution buffer (100 mM Tris-HCl, pH 8, 100 mM NaCl, 200 mM Imidazole). Fractions containing pure and active caspase were pooled.

Expression, refolding and purification of caspase-1, -2, -4, -5 and -8 (procedure B2a & b)

For separate expression of the individual subunit, the plasmid of each subunit was transformed into BL21-Codon Plus (DE3)-RILtetr, pRareCodon^{cam}. Single colonies were inoculated in 5 ml selective 2×YT medium and grown at 37°C overnight. Overnight cultures were transferred into 500 ml selective 2×YT medium in 2-liter baffled flasks and grown until an OD600 of 0.8 was reached. To express caspase subunits the cells were induced by adding 1 mM IPTG and grown for 4 hours at 37°C. Under these conditions both caspase subunits were highly expressed and localized in the inclusion body fraction where they constituted more than 90% of the total protein.

Cells from 500 ml culture were harvested, washed in 10 mM Tris-HCl, pH 8.0, resuspended in 50 ml lysis buffer (50 mM Tris-HCl, pH 8, 150 mM NaCl, 10 units/ml DNaseI) and incubated for 1 hour at 4°C. The cells were broken using an Emusliflex^{TM} homogenizer and inclusion bodies were pelleted by centrifugation (17000×g for 20 min at 4°C).

The pellets were washed twice in buffer 1 (50 mM Tris-HCl, pH 8, 300 mM NaCl, 1 M Guanidine Hydrochloride 0.1% Triton-X-100) and twice in buffer 2 (50 mM Tris-HCl, pH 8, 300 mM NaCl, 1 M Guanidine Hydrochloride). Between each washing step the pellets were resuspended using an Ultra Turbax blender and pelleted by centrifugation for 20 min at 4°C and 17000×g. The washed inclusion bodies were solubilized by stirring the sample overnight at room temperature in a volume of 3 mL solubilization buffer (6.5 M Guanidine Hydrochloride, 25 mM Tris-HCl, pH 7.5, 5 mM EDTA, 100 mM DTT).

Refolding of active caspases was achieved by rapid dilution. Equimolar amounts of both subunits were combined to a total volume of approximately 6 ml and rapidly diluted in 250 ml of refolding buffer (**Table 3**) to a final concentration of 200-500 µg/ml. Refolding was performed overnight at 20°C, with gentle stirring under nitrogen to avoid oxidation. Unfolded and aggregated protein was removed by centrifugation for 20 min at 4°C, 5000× g and subsequent filtration (0.22 mm syringe filter).

Following refolding, caspase-4 and 5 were further purified by IMAC (B2a), caspase-2 and 8 by anion exchange chromatography and caspase-1 by cation exchange chromatography (B2b).

Caspase	Buffer	pH
Caspase-1	100 mM HEPES, 100 mM NaCl, 100 mM Sodium Malonate, 20% Sucrose, 0.5 M NDSB-201, 10 mM DTT	8.0
Caspase-2	100 mM HEPES, 20% Sucrose, 10 mM DTT	7.5
Caspase-4	100 mM HEPES, 100 mM NaCl, 100 mM Sodium Malonate, 20% Sucrose, 0.1 M NDSB-201, 10 mM DTT	7.5
Caspase-5	100 mM HEPES, 100 mM NaCl, 100 mM Sodium Malonate, 20% Sucrose, 0.1 M NDSB-201, 10 mM DTT	8.0
Caspase-8	100 mM HEPES, 10% Sucrose, 0.1% CHAPS, 10 mM DTT	7.5

Table 3: Refolding conditions for human caspases.

Expression and purification of human caspase-4 and -5 (procedure B2a)

After refolding and filtration caspase-4 and -5 were dialysed against IMAC wash buffer (50 mM Tris-HCl, pH 7.5, 250 mM NaCl, 10% Sucrose, 20 mM Imidazole) in order to reduce the DTT concentration.

The protein solution was loaded on a Ni2+-NTA gravity flow column previously equilibrated with IMAC wash buffer (50 mM Tris-HCl, pH 7.5, 250 mM NaCl, 10% Sucrose, 20 mM Imidazole). The protein sample was loaded twice and the column was subsequently washed with washing buffer (total volume 100x of the bead volume) to remove nonspecifically bound protein. The protein was eluted with 50 mM Tris-HCl, pH 7.5, 150 mM NaCl, 10% Sucrose, 250 mM Imidazole. Fractions containing pure and active caspase are pooled and stored at -80°C.

Expression and purification of human caspase-2 and -8 (procedure B2b)

The refolding solution of caspase-2 and -8 was concentrated 10 fold by ultrafiltration using an stirred cell (Model 8200, Amicon) and a PLG cellulose membrane, 10-30 kDa molecular weight cutoff at 4°C, under nitrogen. The concentrated refolding solution was dialyzed overnight against buffer A (20 mM HEPES pH 7.5, 10% Sucrose) at 4°C in order to reduce the salt concentration and to facilitate binding to the column. Subsequent purification was carried out by anionic exchange chromatography at 4°C using a MonoQ HR 5/5 column (GE Healthcare Life Sciences, Uppsala, Sweden). The protein was eluted with buffer B (20 mM HEPES, pH 7.5, 10% Sucrose, 500 mM NaCl) using a gradient from 0-200 mM NaCl in 20 column volumes. Fractions containing pure and active caspase were pooled.

Expression and purification of human caspase-1 (procedure B2b)

To prevent autoproteolysis, the refolding buffer for caspase-1 was supplemented with 100 mM Sodium Malonate (**Table 3**). The refolding solution was concentrated 10 fold by ultrafiltration (10 kDa molecular weight cutoff) and dialyzed against buffer A (30 mM Na-Ac, pH 5.9, 10% glycerol) in order to facilitate binding to the column. Subsequent purification was carried out by cation exchange chromatography at 4°C using a ResourceS column (GE Healthcare Life Sciences, Uppsala, Sweden) and the protein was eluted with 25% buffer B (72 mM Na-Ac, pH 5.9, 400 mM NaMalonate, 10% Glycerol) corresponding to a final NaMalonate concentration of 100 mM. Fractions containing pure and active caspase-1 were pooled.

Size exclusion chromatography

Size exclusion buffer	20 mM Tris-HCl, pH 7.5, 500 mM NaCl, 5 mM DTT, 10% Sucrose

For analytical purposes and for buffer exchange after IMAC, all caspase were further purified by size exclusion chromatography using a Superdex 200 5/150 GL or a Superdex 200 10/30 GL column respectively (GE Healthcare Life Sciences, Uppsala, Sweden) previously equilibrated with size exclusion buffer.

Kinetic characterization of caspases

Standard caspase assay buffer	20 mM PIPES, pH 7.5, 100 mM NaCl, 1 mM EDTA, 5 mM DTT, 0.1% (w/v) CHAPS, 10% Sucrose
High citrate assay buffer	50 mM Tris-HCl, pH 7.5 (6.5 for caspase-2) 1 M NaCitrate, 5 mM DTT, 10% Sucrose
Caspase-2 assay buffer	100 mM MES, pH 6.5, 10% (w/v) PEG600, 5 mM DTT, 0.1% (w/v) CHAPS

Caspase activity assay

The caspase activity was determined in a fluorometric assay using substrates with the general structure Ac-Xaa-Xaa-Xaa-Asp↓AMC incorporating the sequence previously determined to be optimal for each caspase [28] (**Table 4**). In order to ensure linearity, caspases were assayed at protein concentrations such that not more than 10% of substrate was converted during the measurements. Appropriate dilutions of enzymes (**Table 4**) were added to the reaction mixture containing buffer and substrate at concentrations of $0.2 \cdot K_m$ to $5 \cdot K_m$ in a total assay volume of 100 µl. To analyze the effect of kosmotropic salt on the kinetic properties, the individual caspases were assayed in standard caspase assay buffer as well as in high citrate assay buffer.

AMC release was monitored by measuring the fluorescence at λex = 360 nm and λem = 465 nm using a spectrofluorometer (Tecan Infinite M-1000). Kinetic constants were computed by direct fits of the initial velocity data to Equation 1, where ν is the initial velocity, V the limiting rate and K_m the Michaelis constant. An AMC standard curve was determined for each experiment. Caspase activity was expressed in units per mg active protein (one unit corresponds to the conversion of 1µmol caspase substrate per min).

$$\upsilon = \frac{V[S]}{K_m + [S]}$$ **Equation 1**

For qualitative analysis of enzyme activity during protein purification, 5 µl of peak fractions were diluted in standard assay buffer, the reaction started by adding DMSO-dissolved substrate to a final volume of 100 µl and initial rates of substrate hydrolysis were calculated.

Caspase	Protein Concentration	pH	Preferred Substrates
Caspase-1	10-50 nM	7.5	Ac-WEHD↓AMC
Caspase-2	5-20 nM	6.5	Ac-VDVAD↓AMC
Caspase-3	1-10 nM	7.5	Ac-DEVD↓AMC
Caspase-4	50-100 nM	7.5	Ac-WEHD↓AMC
Caspase-5	50-100 nM	7.5	Ac-WEHD↓AMC
Caspase-6	10-100 nM	7.5	Ac-IETD↓AMC
Caspase-7	10-100 nM	7.5	Ac-DEVD↓AMC
Caspase-8	10-100 nM	7.5	Ac-DEVD↓AMC
Caspase-9	50-100 nM	7.5	Ac-LEHD↓AMC

Table 4: Optimized assay conditions for activity measurements of caspases.

SDS-PAGE analysis

Sodium dodecyl sulfate polyacrylamide gel electrophoresis (SDS-PAGE) 15 % was used to separate the caspase subunits by their size. 15 µl of caspase (~1 mg/ml) was mixed with 5 µl of 4x loading buffer containing 1% β-mercaptoethanol. The samples were boiled at 95°C for 10 min and 10 µl were loaded per lane in a gel (Protean, BioRad).

Enzyme activity in dependence of initial caspase concentrations

The dependence of the enzyme activity on the caspase concentration was determined in standard assay buffer, except for caspase-9, which was assayed in high citrate assay buffer. The individual caspases were analyzed at three different concentrations (1x, 2x and 4x), the lowest (1x) concentrations were: 20 nM caspase-1, 3 nM caspase-2, 1 nM caspase-3, 50 nM caspase-4, 50 nM caspase-5, 100 nM caspase-6, 10 nM caspase-7, 10 nM caspase-8 and 25 nM caspase-9. The substrate concentrations were kept constant at 140 µM. Ac WEHD↓AMC was the substrate used for caspase 1, -4 and -5, Ac-DEVD↓AMC for caspase-3, 7 and -8, Ac-IETD↓AMC for caspase-6, Ac-LEHD↓AMC caspase 9 and Ac-VDVAD↓AMC for caspase-2.

Product formation at different caspase concentrations were plotted against time multiplied by the concentration factor.

Active site titration

In order to obtain reliable kinetic data, active enzymes concentrations were first determined accurately by active site titration, where the caspases were titrated with increasing concentrations of covalent and preferentially irreversible inhibitors and decreasing enzyme activity was measured. A plot of the residual activity versus inhibitor concentrations revealed the active site concentration.

In order to analyze the reversibility of the covalent enzyme-inhibitor complex under reducing conditions, caspase-8 was used as a case study. 75 nM enzyme were titrated with Ac-DEVD-CMK in 3 different assay buffers either without DTT or supplemented with 10 mM and 12 µM, respectively.

The following inhibitors were used for active site titration: Ac-YVAD-CMK (Peptanova, Sandhausen, Germany) for caspase 1, -Ac-WEHD-CHO (Peptanova, Sandhausen, Germany) for 4 and -5, Ac-VDVAD-CHO (Peptanova) for caspase 2, and Ac-DEVD-CMK (R&D Systems, Palo Alto, USA) for caspase 3, -7. -8 and -9.

Results and Discussion

Expression and purification of human caspases

Expression and purification protocols of human caspases have been described in numerous studies and mainly employ two different approaches: (i) the expression of the full length gene in order to obtain soluble protein which is activated upon expression in *E.coli* (**Figure 2, A**) and (ii) the expression of inclusion bodies followed by refolding (**Figure 2, B**). The genes encoding the catalytic domain are cloned either in one single vector (**Figure 2, I**) or in the case of inclusion body formation the two genes encoding the individual subunits are cloned in two different vectors (**Figure 2, II**). Expression of caspases as inclusion bodies requires refolding, processing and/or autoprocessing in order to obtain full catalytic activity and subsequent purification by ion exchange- or affinity chromotography (**Figure 2, a/b**). We have systematically tested the optimal expression and purification strategy for each caspase.

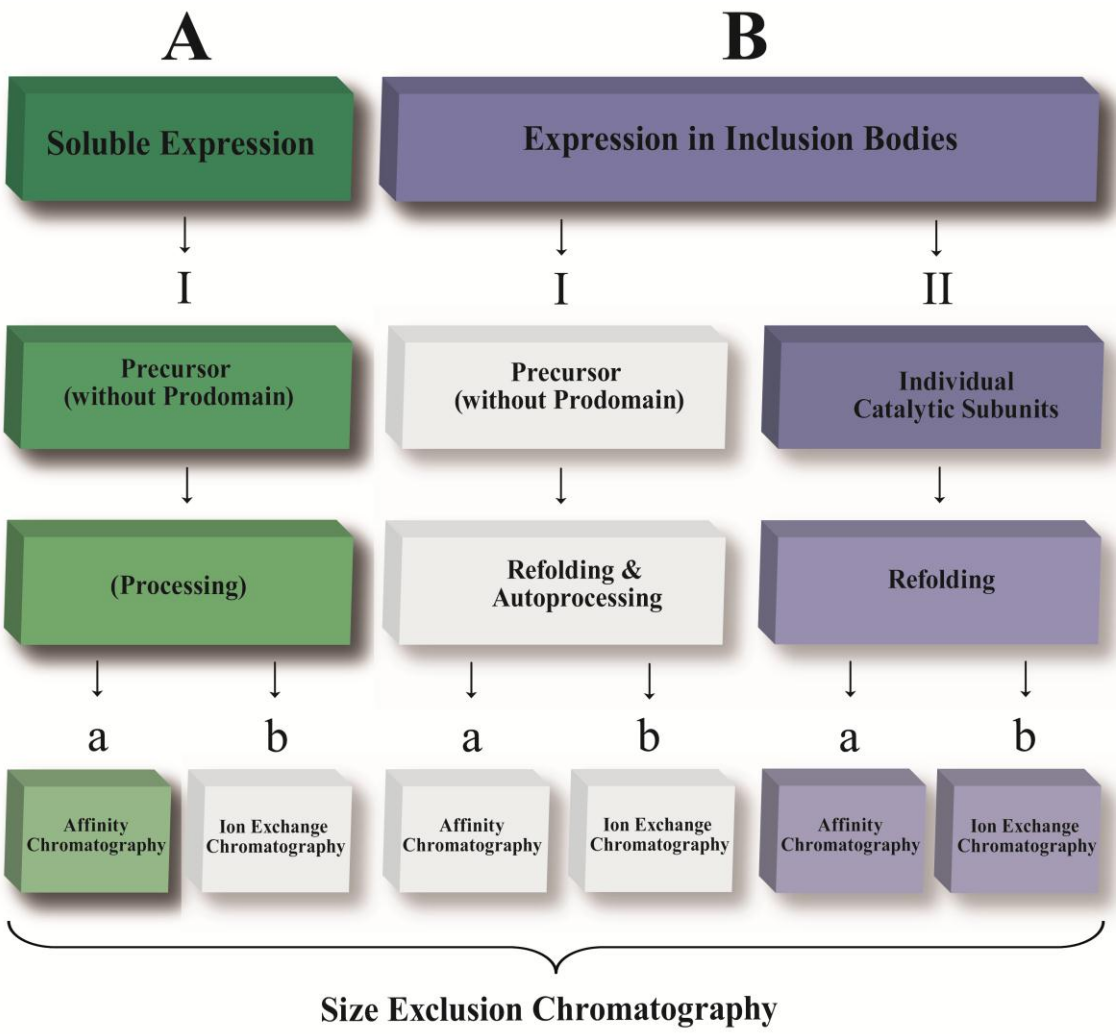

Figure 2: Expression and purification of human caspases at a glance.
A) The strategies for the soluble expression and subsequent purification of caspases. **B)** The expression of inclusion bodies followed by refolding and purification. The genes encoding the catalytic domain are cloned either in one single vector (**I**) or as two genes encoding the individual subunits in two vectors (**II**). The protein, independent of the expression strategy, is subsequently purified using affinity (**a**) or ion exchange chromatography (**b**) followed by size exclusion chromatography. The strategies corresponding to the optimized expression and purification protocols applied in this work are highlighted (in green the strategies for the soluble expression and in blue the expression of inclusion bodies).

Soluble expression and purification of caspases

Soluble expression of a caspase is the method of choice if the respective caspase undergoes maturation in the bacterial host cell. By employing the AIa strategy (Figure 2) several mg of the desired protein can be produced and only one purification step is necessary to obtain highly pure caspase. In the procedures AIa and A1b, the full length construct (lacking the N-terminal peptide) is expressed in the cytosol of *E. coli*. The expressed protein undergoes 'maturation' by cleavage of bacterial proteases. It is crucial that the caspase is entirely cleaved otherwise a heterogenous protein sample will be obtained. We found that caspase-6 is only partially cleaved at the first cleavage site in the inter subunit linker ($D_{294}VVDNQ_{299}$) resulting in two p20 subunits species of slightly different size. We therefore mutated this site to ($D_{294}EVDAA_{299}$) which resulted in fully processed caspase-6. The protein can either be purified by immobilized metal ion affinity chromatography (IMAC) loaded with Ni^{2+} or by ion exchange chromatography. IMAC represents a straight forward purification strategy and thus is the most desired approach, granted the tag does not interfere with downstream applications.

Although the procedure of soluble expression has been proposed for all human caspases [18, 29, 90, 147-151], we find it most suitable for the production of non-autocatalytic executioner caspases-3, -6, -7 and -9 [152] (**Table 5**). Soluble expression of inflammatory caspases results in considerable degradation products due to their autocatalytic activity, especially in the case of caspase-1.

Caspase	*Procedure*
1	BIIb
2	BIIa
3	AIa
4	BIIb
5	BIIb
6	AIa
7	AIa
8	BIIa
9	AIa

Table 5: Optimal expression and purification strategy for human caspase-1 to -9.

Expression of caspases in inclusion bodies and purification

Inclusion body formation is a very common occurrence during heterologous protein expression in *E.coli*. Since inclusion bodies are highly homogeneous their isolation is usually the first purification step [153]. Various protocols for the refolding of human caspases have been described [28, 154, 155] and all approaches yield active enzymes (procedure **B**) [103]. Full length caspase-8 and -10 constructs (lacking the N-terminal domain) can be expressed as inclusion bodies (procedure BI) followed by refolding and autocatalytic processing. The fully processed active caspase is further purified either by affinity chromatography (**a**) [156], ion exchange chromatography (**b**) or it can be directly loaded on a size exclusion column [157]. This approach is limited to caspase-8 and -10 and may lead to heterogeneous protein due to incomplete processing.

We favor the more commonly used strategy for the production of recombinant caspases (procedure **BII**) because it yields higher protein concentrations and very homogenous samples. Both subunits are separately expressed in *E.coli* and subsequently refolded by rapid dilution overnight. The refolded caspase can then be purified by ion exchange chromatography [103] (procedure **BIIb**), which is our method of choice for caspase-8 and -2 (**Table 5**). However, purification by ion exchange chromatography is not straight forward which accounts especially for the inflammatory caspases. They bind to the anionic exchange column (MonoQ HR 5/5) at a conductivity of the buffer below 1.2 mS/cm which requires extensive dialysis after refolding leading to accumulation of degradation products because of their autoproteolytic activity. Therefore, we have developed a new protocol for caspase-1, -4 and -5 based on the study published by Scheer *et al*. [158]. The addition of a malonate ion during refolding and purification prevents the autoproteolysis of the enzyme. Although these caspases can be purified by ion exchange chromatography (**BIIb**), we obtained significantly higher yields by using IMAC purification. The purification by IMAC is therefore preferred (**Table 5**) because it is faster, reduces the risk of protein degradation and it increases the yield of purified protein.

SDS-PAGE analysis of purified caspases

Purified caspases 1-9 were analyzed by SDS-PAGE, as shown in **Figure 3**. For each caspase the small and the large subunit are visible which appear around 10 kDa and 20 kDa respectively. The size can vary by several kDa due to the different molecular composition of each subunit in size. The large subunit of Caspase-9, which contains a CARD domain, appears at a molecular weight of about 30 kDa. Due to their particular amino acid composition the small subunits appear less stained than the large subunits for most caspases. For all caspases, a purity of over 95% was achieved thus allowing the application of protein crystallography and functional and kinetic assays. In the case of caspase-1, degradation products were observed due to autoproteolysis, which could not be entirely prevented by the addition of sodium malonate.

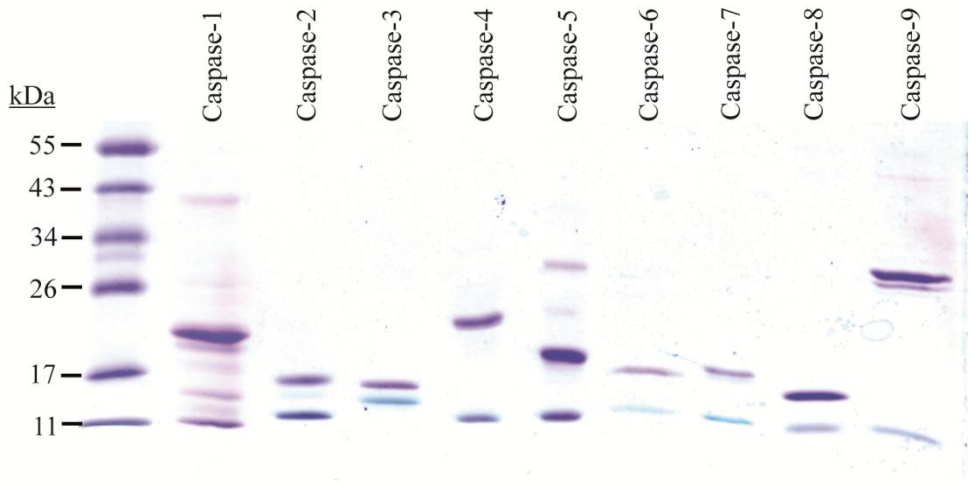

Figure 3: SDS-PAGE analysis of human caspase-1 to -9.
SDS-PAGE (15%) analysis showing purified samples of caspase 1 to 9. The small and large subunits of each caspase are seen as predominant bands.

Size exclusion chromatography analysis of purified caspases

The oligomeroc state of caspases influences their specific activity. Independent of concentration, executioner caspases and caspase-2 exist as stable dimers [159-161] in solution, while caspase-6 can form tetramers [162]. In contrast, initiator and inflammatory

caspases exist in a monomer-dimer equilibrium; however, only the dimeric form has catalytic activity. The oligomeric state of each caspase was therefore analyzed by size exclusion chromatography. The inflammatory caspases **(Figure 4**, left column) appear as monomers, but a shoulder representing a higher molecular weight was observed in the case of caspase-5 due to the detergent NDSB supplemented during purification. On the other hand, the executioner caspases (**Figure 4**, middle lane) were found to be stable dimers as previously described, caspase 6 is partially present as a tetramer [162]. The initiator caspase-2 (**Figure 4**, right column) is a stable dimer and caspase-9 is monomeric, the latter runs at a higher elution volume due to the CARD domain at the amino terminus of the large subunit. As expected, the oligomeric state of caspase-8 is highly dependent on ion and protein concentration and thus occurs in a monomer-dimer equilibrium [161].

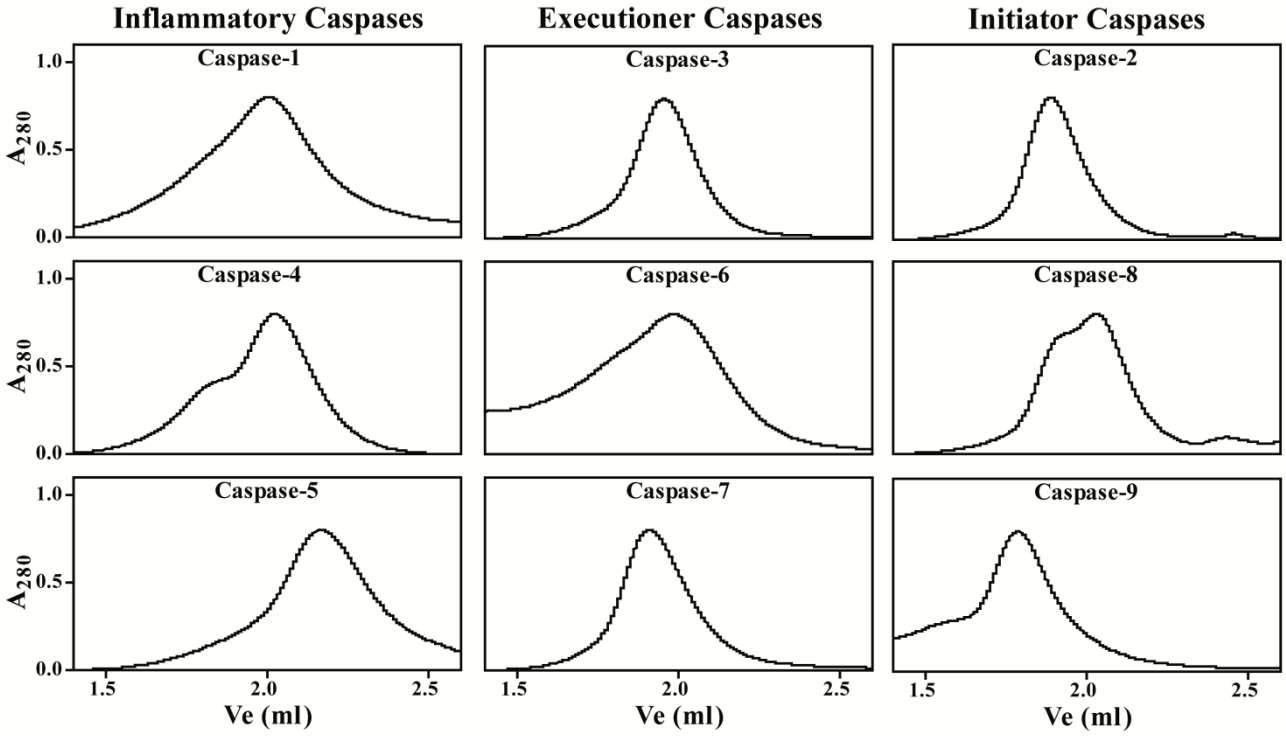

Figure 4: Size exclusion profile of human caspase-1 to -9.
50-100 µg protein was injected onto an analytical Superdex 200 (5/150 GL) column. The absorbance signal at 280nm has been normalized.

Functional analysis of human caspases

In the past, caspases have often been characterized in standardized conditions, which is not in agreement with their biochemical nature leading to a false interpretation of their kinetic properties and specificities. This particularly concerns the correlation of their oligomeric state and their specific activity. Here we pinpoint the described problem for each individual caspases and offer a broad biochemical and kinetic characterization leading to an improved assay protocol for the determination of the enzyme activity. Furthermore we would like to emphasize the importance of a reproducible and accurate determination of the protein concentration. We critically depict active site titration to determine the amount of active sites which are essential for kinetic analysis.

Active site titration

Absorption spectrometry is an inadequate method to determine accurate enzyme concentration since the total amount of both active and inactive protein is measured. To obtain precise concentration values of active protein we used active site titration. This method is based on the titration of the active sites with an irreversible inhibitor; increasing concentrations of a covalent and preferentially irreversible inhibitor are incubated with the enzyme and its activity is recorded. A plot of the residual activity versus inhibitor concentration reveals the active site concentration. Caspase activity is routinely analyzed under reducing conditions to keep the active site cysteine reduced. Therefore, the standard caspase assay buffer is typically supplemented with DTT or another reducing agent such as β-mercaptoethanol or L-cysteine. However, we observed that the presence of DTT is problematic for the determination of the exact protein concentration by active site titrations. Significant enzyme activity was detected even in the presence of a 150-fold excess of inhibitor (**Figure 5A**), indicating reversibility of the covalent enzyme-inhibitor complex under reducing conditions. A similar but less pronounced effect occurred at low DTT concentrations (12 µM), yet the inhibition remained hyperbolic (**Figure 5B**). A linear inhibition curve, which is essential for the accurate titration of the enzyme, was obtained only when DTT free assay buffer was used (**Figure 5C**).

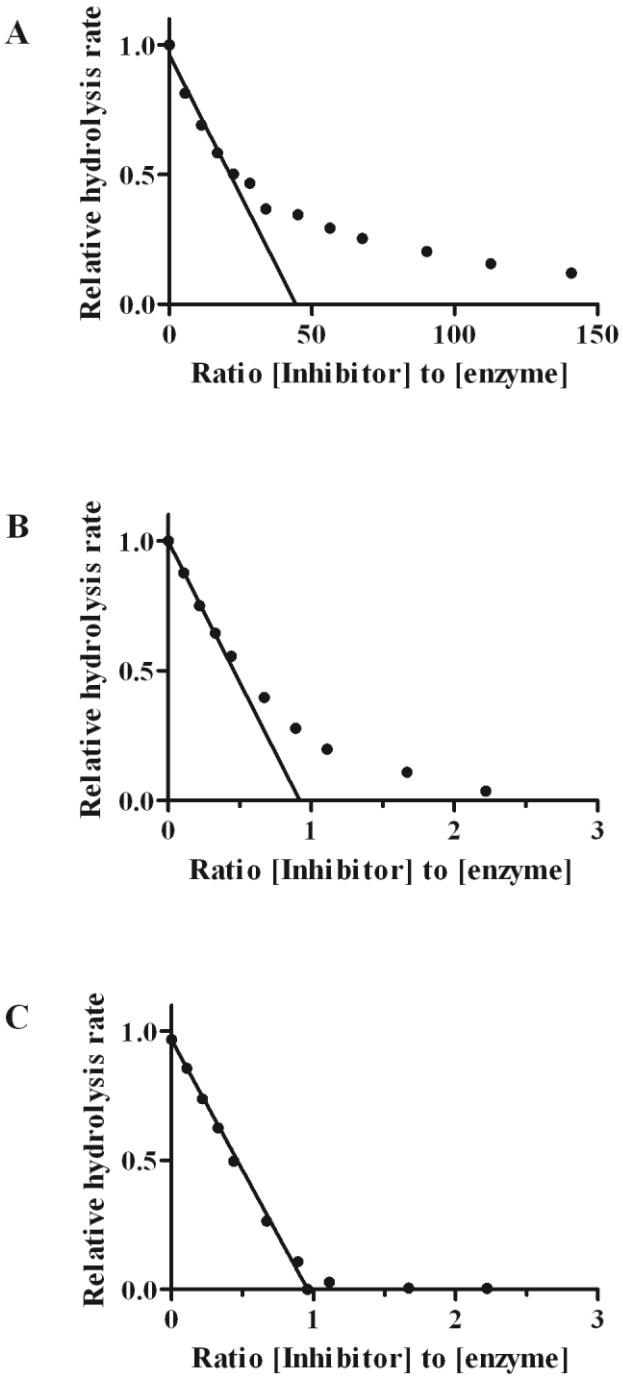

Figure 5: Active site titration of caspase-8 at different DTT concentrations.
Relative hydrolysis rate against the ratio of inhibitor concentration to enzyme concentration are shown at 10 mM (A), 12 µM (B), and no DTT (C). The substrate (Ac-DEVD-AMC) was used at final concentration of 12.3 µM.

Dependence of enzyme activity on caspase concentration

Loss of Enzyme activity due to instability of the protease is commonly observed under *in vitro* assay conditions. To establish the optimal assay conditions and determine the time range in which a particular enzyme is stable, M.J. Selwyn developed a time-course assay to systematically monitor enzyme stability over time [163]. This procedure involves plotting product formation at different enzyme concentrations against time multiplied by the initial enzyme concentration. These progress curves superimpose during the time course where the enzyme is stable.

By applying this method, we systematically analyzed the activity of all caspases at different enzyme concentrations. Relative fluorescence was plotted against time multiplied by the respective enzyme concentration. It is evident from the initial velocity graphs (**Figure 6**) that the dependence of enzyme activity on caspase concentration is not linear for all caspases. In the case of caspase-2, -3, -7 and -9, doubling the enzyme concentration yielded a twofold enzyme activity increase. In contrast, an increase in enzyme activity for caspase-1, -4, -5 and -8 resulted in higher activity (**Figure 6**).

Our results are in agreement with the observed oligomeric state of active caspases described above (**Figure 4**). Caspases which are monomeric in solution or occur in monomer-dimer equilibrium show an exceeding increase of enzyme activity at higher protein concentrations, suggesting that the equilibrium is shifted to the dimer at higher protein concentrations. This hypothesis is supported by the observation that dimeric caspases fail to exhibit this effect. It can also be hypothesized that the tetrameric form of caspase 6 is less active than the dimer.

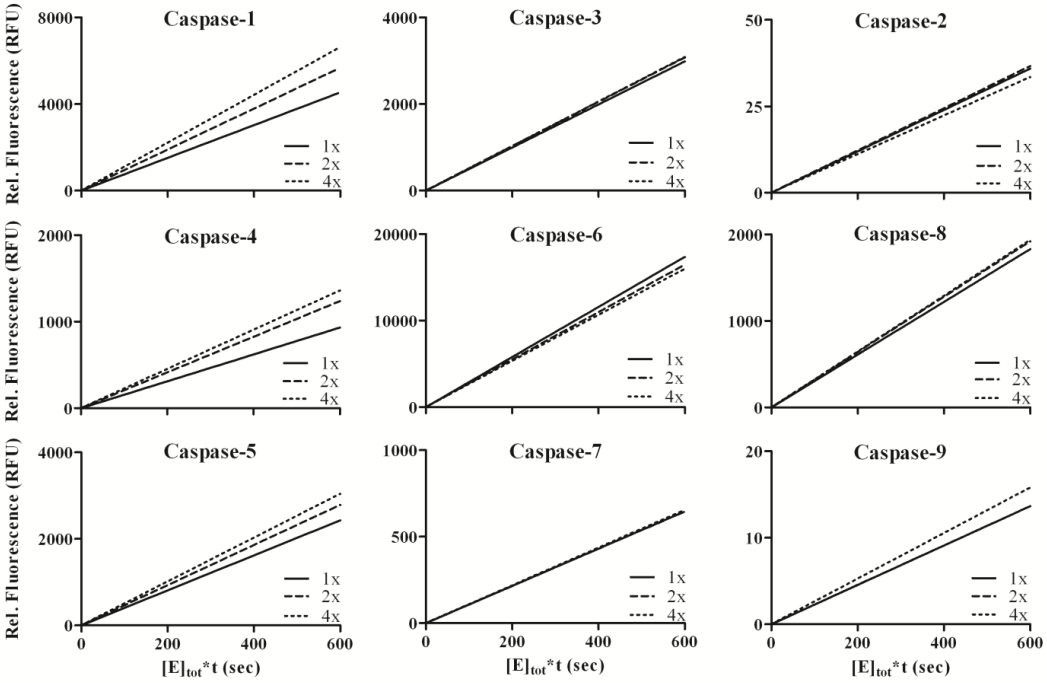

Figure 6: Selwyn-Test of human caspase-1 to -9.
Product formation at different initial caspase concentrations (1x, 2x and 4x enzyme concentrations) were plotted against time multiplied by the concentration factor. The lowest concentrations (1x) were: 20nM caspase-1, 3nM caspase-2, 1nM caspase-3, 50nM caspase-4, 50nM caspase-5, 100nM caspase-6, 10nM caspase-7, 10nM caspase-8 and 25nM caspase-9. The substrate concentrations were kept constant at 140µM. Ac-WEHD↓AMC was the substrate used for caspase-1, -4 and -5, Ac-DEVD↓AMC for caspase-3,-7 and -8, Ac-IETD↓AMC for caspase-6, Ac-LEHD↓AMC caspase-9, and Ac-VDVAD↓AMC for caspase-2. Initial velocities were determined in standard assay buffer except for caspase-9, which was assayed in citrate buffer.

These findings have important implications for the setup and analysis of enzymatic assays for initiator and inflammatory caspases. Catalytic efficiencies should be determined in high citrate assay buffer or at high enzyme concentration using standard assay buffer. Therefore, values that have been obtained in different conditions in the past need to be interpreted with caution.

The effect of kosmotropic salts on caspase activity and specificity

Kosmotropic solutes contribute to the stability of proteins; furthermore, such salts are able to stabilize the dimerization of caspases. Boatright *et al.* previously demonstrated, that kosmotropes significantly enhance the activity of recombinant procaspases-8 and -9 but do not enhance the activity of the executioner procaspases-3 and -7 [59]. This is in line with our observation, that apical caspases are disproportionally more active at higher concentrations.

We set out to systematically analyse the effect of kosmotropic salts on the kinetic properties of caspase-1 to -9. Substrate affinities (K_m values), specific activity and substrate specificity were determined under standard assay conditions and in the presence of high concentrations of kosmotriopic salt (**Table 5** and **Figure 7**).

	K_m Value (µM)		**k_{cat}** (s^{-1})		**Specific Activity** (U/mg)	
	Standard Buffer	Citrate Buffer	Standard Buffer	Citrate Buffer	Standard Buffer	Citrate Buffer
Casp-1	8.6	18.9	1.4	3.7	26'553	77'209
Casp-2	19.9	24.5	0.8	0.7	15'665	13'573
Casp-3	29.8	23.1	8.7	5.7	170'326	111'943
Caps-4	228.1	188.8	0.3	0.5	5'717	8'378
Casp-5	33.9	57.4	0.5	1.3	9'689	24'731
Casp-6	98.7	75.9	0.5	0.4	10'260	7'142
Casp-7	40.3	55.4	3.2	1.0	55'625	18'250
Casp-8	9.7	41.4	0.3	0.4	5'563	7'444
Casp-9	n.d.	189.0	n.d.	0.1	n.d.	1'171

Table 5: The catalytic properties of human caspases.
The assay concentrations of the different enzymes were: 8nM caspase-1, 12nM caspase-2, 5nM caspase-3, 84nM caspase-4, 41nM caspase-5, 180nM caspase-6, 90nM caspase-7, 135nM caspase-8, 125nM caspase-9. Ac-WEHD↓AMC was the substrate used for caspase-1, -4 and -5, Ac-DEVD↓AMC for caspase-3, -7 and -8, Ac-IETD↓AMC for caspase-6, Ac-LEHD↓AMC caspase-9, and Ac-VDVAD↓AMC for caspase-2. One unit (U) corresponds to the conversion of 1µmol substrate per min.

In the presence of sodium citrate a decrease in substrate affinity (slightly higher K_m values) was observed for caspase-1, -5 and -8 and a clearly improved cleavage efficiency (k_{cat} values), resulting in significantly higher specific activities, was measured for caspase-1, -4, -5 and -8.

Although the presence of kosmotrophic salts did not affect the catalytic properties of caspase-2,-3, -6 and -7, a decrease in cleavage efficiency was observed (**Table 5**).

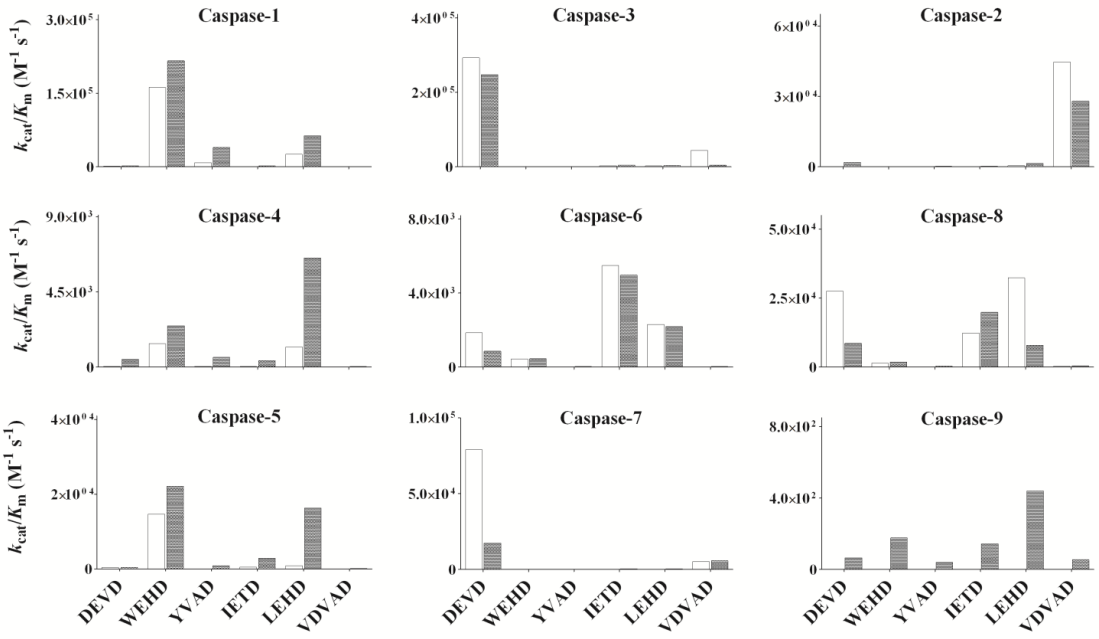

Figure 7: Substrate specificities of human caspases.
Substrate specificities were determined in standard assay buffer (white bars) and high sodium citrate buffer (grey bars). The protein concentrations were: 8nM caspase-1, 12nM caspase-2, 5nM caspase-3, 84nM caspase-4, 41nM caspase-5, 180nM caspase-6, 90nM caspase-7, 135nM caspase-8, 125nM caspase-9.

We further analyzed the effect of kosmotropic salts on substrate specificity for caspase-1 to -9 (**Figure 7**). Here we also noticed that the substrate specificity does not change for dimeric caspases (caspase-2, -3, -6 and -7). However, for all monomeric caspases (caspase-1, -4, -5, -8 and -9) we observed an increase in cleavage efficiency not only for the preferred substrates but also for additional substrates. This effect was found to be particularly pronounced for caspase-4 and -5, which showed significantly increased substrate specificity for LEHD in the presence of sodium citrate (**Figure 7**).

Conclusions

In this study we have refined the established protocols for the expression and characterization of human caspases. Several buffer conditions and constructs have been screened and the optimal conditions for each caspase are herein described. Our study on active site titration, to reliably determine caspase concentration, revealed that the presence of DTT leads to a hyperbolic inhibition curve and thus inaccurate fitting results. Another finding is that the specific activity and specificity of caspases is dependent on their concentration. However, we demonstrated that the activity of some caspases is not proportional to their enzyme concentration. This property accounts in particular for inflammatory caspases (-1, -4, -5), but to some extend also for caspase-8 and caspase-9 which are monomeric in solution but dimerize at higher concentrations. Since a dimer is required for the full enzymatic activity we observe that the specific activity increases at higher concentrations or in presence of kosmotropic salts such as sodium citrate. Furthermore, the presence of kosmotropic salts was found to affect substrate specificity. We thus recommend determining the specific activity of these caspases at high enzyme concentrations or in sodium citrate buffer. In contrast, the executioner caspases (-3, -6, -7) and caspase-2 are dimeric in solution and their specific activity is not dependent on enzyme concentration and can therefore be determined using the standard caspase assay buffer.

In conclusion we show that the protocols described in this study allow for optimal expression, purification and characterization of caspase-1 to -9. Enzyme activities are often cited as specific activities and these values can vary tremendously between laboratories, most likely as a result of different assay conditions and methods used for the determination of caspase concentration. Our results help to overcome this issue leading to a more reproducible characterization of caspases.

Acknowledgements

We gratefully acknowledge Dr. Guy S. Salvesen for the expression plasmids for caspase-6, -7 and -9. We thank the present and former group members for experimentally validating the expression and purification protocols included in this work and for many helpful suggestions and discussions. Christopher Weinert and Andreas Flütsch are acknowledged for providing caspase-1 and -7 for SDS-PAGE and the analytical size exclusion chromatography.

This work was supported by the European Commission Framework 6 Program (CAMP project, LSHG-2006-018830) and by the European Commission Framework 7 Program (FP7-Health-2009-241919-LIVIMODE project). The authors declare no conflict of interest.

References

1. Martinon, F. and J. Tschopp, *Inflammatory Caspases: Linking an Intracellular Innate Immune System to Autoinflammatory Diseases.* Cell, 2004. **117**(5): p. 561-574.

2. Saleh, M., et al., *Differential modulation of endotoxin responsiveness by human caspase-12 polymorphisms.* Nature, 2004. **429**(6987): p. 75-9.

3. Goldberg, Y.P., et al., *Cleavage of huntingtin by apopain, a proapoptotic cysteine protease, is modulated by the polyglutamine tract.* Nat Genet, 1996. **13**(4): p. 442-9.

4. Krippner-Heidenreich, A., et al., *Targeting of the transcription factor Max during apoptosis: phosphorylation-regulated cleavage by caspase-5 at an unusual glutamic acid residue in position P1.* Biochem J, 2001. **358**(Pt 3): p. 705-15.

5. Rao, L., D. Perez, and E. White, *Lamin proteolysis facilitates nuclear events during apoptosis.* J Cell Biol, 1996. **135**(6 Pt 1): p. 1441-55.

6. Tewari, M., et al., *Yama/CPP32 beta, a mammalian homolog of CED-3, is a CrmA-inhibitable protease that cleaves the death substrate poly(ADP-ribose) polymerase.* Cell, 1995. **81**(5): p. 801-9.

7. Denault, J.B. and G.S. Salvesen, *Caspases.* Curr Protoc Protein Sci, 2002. **Chapter 21**: p. Unit 21 8.

8. Denecker, G., et al., *Caspase-14 reveals its secrets.* J Cell Biol, 2008. **180**(3): p. 451-8.

9. Fuentes-Prior, P. and G.S. Salvesen, *The protein structures that shape caspase activity, specificity, activation and inhibition.* Biochem J, 2004. **384**(Pt 2): p. 201-32.

10. Walker, N.P., et al., *Crystal structure of the cysteine protease interleukin-1 beta-converting enzyme: a (p20/p10)2 homodimer.* Cell, 1994. **78**(2): p. 343-52.

11. Wilson, K.P., et al., *Structure and mechanism of interleukin-1 beta converting enzyme.* Nature, 1994. **370**(6487): p. 270-5.

12. Nicholson, D.W., et al., *Identification and inhibition of the ICE/CED-3 protease necessary for mammalian apoptosis.* Nature, 1995. **376**(6535): p. 37-43.

13. Thornberry, N.A., et al., *A novel heterodimeric cysteine protease is required for interleukin-1 beta processing in monocytes.* Nature, 1992. **356**(6372): p. 768-74.

14. Li, P., et al., *Cytochrome c and dATP-dependent formation of Apaf-1/caspase-9 complex initiates an apoptotic protease cascade.* Cell, 1997. **91**(4): p. 479-89.

15. Denault, J.B. and G.S. Salvesen, *Expression, purification, and characterization of caspases.* Curr Protoc Protein Sci, 2003. **Chapter 21**: p. Unit 21 13.

16. Stennicke, H.R. and G.S. Salvesen, *Biochemical characteristics of caspases-3, -6, -7, and -8.* J Biol Chem, 1997. **272**(41): p. 25719-23.

17. Thornberry, N.A., et al., *A combinatorial approach defines specificities of members of the caspase family and granzyme B. Functional relationships established for key mediators of apoptosis.* J Biol Chem, 1997. **272**(29): p. 17907-11.

18. Blanchard, H., et al., *The three-dimensional structure of caspase-8: an initiator enzyme in apoptosis.* Structure, 1999. **7**(9): p. 1125-33.

19. Dang, L.C., et al., *Preparation of an autolysis-resistant interleukin-1 beta converting enzyme mutant.* Biochemistry, 1996. **35**(47): p. 14910-6.

20. Kamens, J., et al., *Identification and characterization of ICH-2, a novel member of the interleukin-1 beta-converting enzyme family of cysteine proteases.* J Biol Chem, 1995. **270**(25): p. 15250-6.

21. Mittl, P.R., et al., *Structure of recombinant human CPP32 in complex with the tetrapeptide acetyl-Asp-Val-Ala-Asp fluoromethyl ketone.* J Biol Chem, 1997. **272**(10): p. 6539-47.

22. Srinivasula, S.M., et al., *Molecular ordering of the Fas-apoptotic pathway: the Fas/APO-1 protease Mch5 is a CrmA-inhibitable protease that activates multiple Ced-3/ICE-like cysteine proteases.* Proc Natl Acad Sci U S A, 1996. **93**(25): p. 14486-91.

23. Talanian, R.V., et al., *Substrate specificities of caspase family proteases.* J Biol Chem, 1997. **272**(15): p. 9677-82.

24. Stennicke, H.R. and G.S. Salvesen, *Caspases: preparation and characterization.* Methods, 1999. **17**(4): p. 313-9.

25. Fink, A.L., *Protein aggregation: folding aggregates, inclusion bodies and amyloid.* Fold Des, 1998. **3**(1): p. R9-23.

26. Rano, T.A., et al., *A combinatorial approach for determining protease specificities: application to interleukin-1beta converting enzyme (ICE).* Chem Biol, 1997. **4**(2): p. 149-55.

27. Rotonda, J., et al., *The three-dimensional structure of apopain/CPP32, a key mediator of apoptosis.* Nat Struct Biol, 1996. **3**(7): p. 619-25.

28. Garcia-Calvo, M., et al., *Purification and catalytic properties of human caspase family members.* Cell Death Differ, 1999. **6**(4): p. 362-9.

29. Fernandes-Alnemri, T., et al., *In vitro activation of CPP32 and Mch3 by Mch4, a novel human apoptotic cysteine protease containing two FADD-like domains.* Proc Natl Acad Sci U S A, 1996. **93**(15): p. 7464-9.

30. Koeplinger, K.A., et al., *Caspase 8: an efficient method for large-scale autoactivation of recombinant procaspase 8 by matrix adsorption and characterization of the active enzyme.* Protein Expr Purif, 2000. **18**(3): p. 378-87.

31. Scheer, J.M., J.A. Wells, and M.J. Romanowski, *Malonate-assisted purification of human caspases.* Protein Expr Purif, 2005. **41**(1): p. 148-53.

32. Pop, C., et al., *Role of proteolysis in caspase-8 activation and stabilization.* Biochemistry, 2007. **46**(14): p. 4398-407.

33. Keller, N., M.G. Grutter, and O. Zerbe, *Studies of the molecular mechanism of caspase-8 activation by solution NMR.* Cell death and differentiation, 2010. **17**(4): p. 710-8.

34. Donepudi, M., et al., *Insights into the regulatory mechanism for caspase-8 activation.* Mol Cell, 2003. **11**(2): p. 543-9.

35. Baumgartner, R., et al., *The crystal structure of caspase-6, a selective effector of axonal degeneration.* Biochemical Journal, 2009. **423**(3): p. 429-439.

36. Selwyn, M.J., *A simple test for inactivation of an enzyme during assay.* Biochim Biophys Acta, 1965. **105**(1): p. 193-5.

37. Boatright, K.M., et al., *A unified model for apical caspase activation.* Mol Cell, 2003. **11**(2): p. 529-41.

3. Development of a caspase specific microarray using DARPins as capture reagents

Introduction

Apoptosis can be monitored with a variety of techniques such as flow cytometry, microscopy and western blot. These techniques visualize the apoptotic phenotype of the cell, formation of membrane complexes or cleavage of apoptotic target proteins. In contrast, it is technically challenging to monitor the activity if a single caspase in the apoptotic pathway. Attempts to dissect the apoptotic pathways are mainly based on western blot analysis and short peptide substrates [29]. The available caspases substrates are unspecific and one substrate is cleaved by several caspases [164]. It is thus not possible to dissect the apoptotic pathway simply by measuring their activity using caspases substrates.

We thus aimed to develop a caspase specific array that allows us to monitor the following aspects: (i) activity of each caspase in different apoptotic stages, (ii) expression levels of caspases during apoptosis and (iii) caspases activity in relation to different apoptotic stimuli. This would allow us to dissect the apoptotic pathway and monitor the contribution of a single caspase to the apoptotic pathway. We regarded the protein microarray setup as very promising as it allows high throughput analysis of a large number of samples while only a small amount of sample and material is required [165]. We thus developed a protein microarray with caspase specific DARPins as capture reagents. Since DARPins are highly selective binding proteins (similar to antibodies) they are ideal molecules to target individual enzymes in a family of homologous proteins.

We have combined a multitude of techniques and protocols to establish a standard procedure of DARPin selection and characterization. We improved current protocols for the characterization of selected DARPins so that a large number of DARPins can be handled with minimal use of material in a time efficient manner. By combining state of art machines and

novel protocols we were able to handle large numbers of DARPins while obtaining highly quantitative data (Figure 3.1). Furthermore we describe the production and optimization of DARPin microarrays and offer possible applications for this technology.

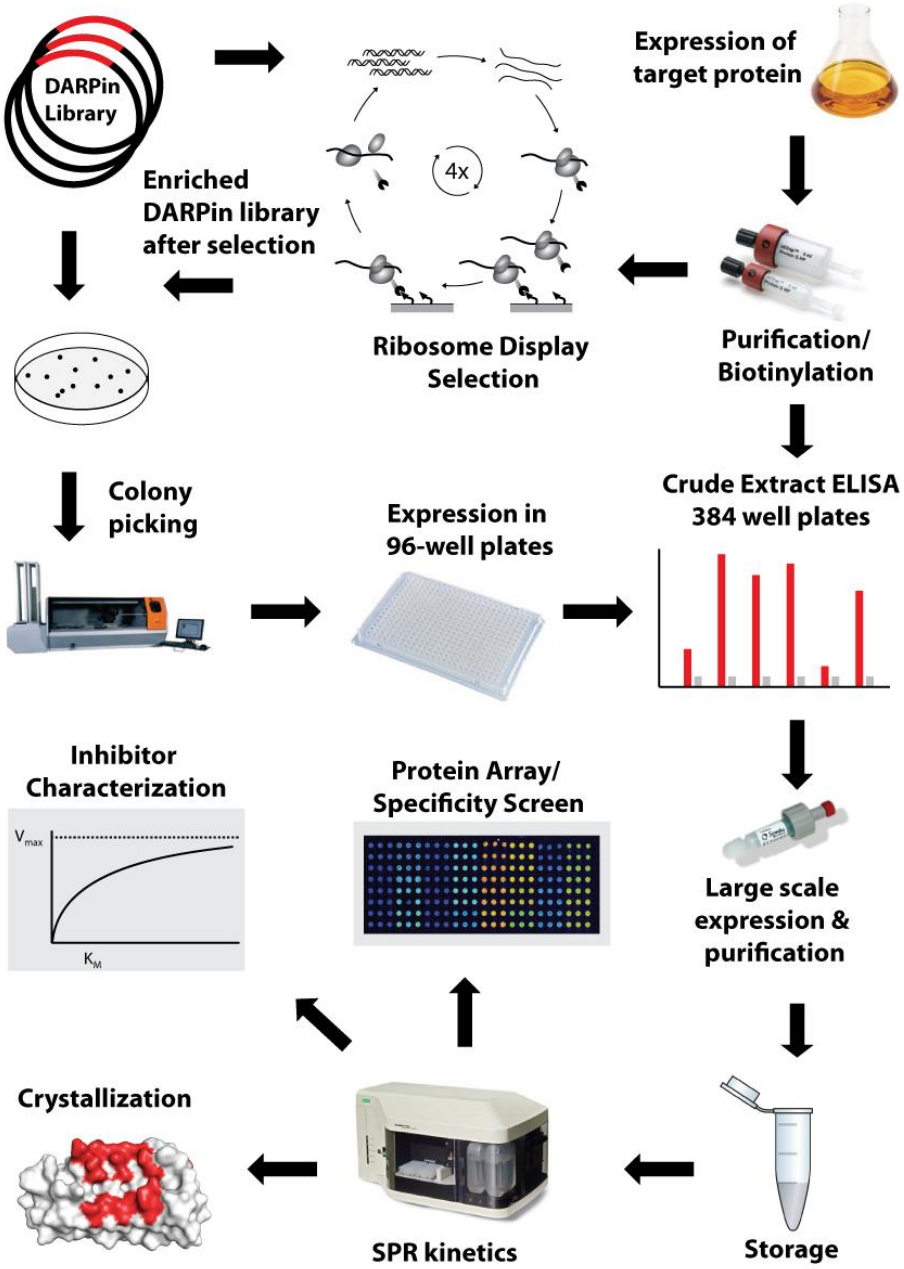

Figure 3-1: Workflow of the selection and characterization of DARPins.

Results

Selection of DARPins against caspases using ribosome display

We used ribosome display for the selection of DARPins based on a library that was described previously [110]. Nine caspases (caspase-1 to -9) were used as target proteins. The selection for each target protein was performed under varying conditions such as addition of inhibitor, chemical additives or k_{off}-maturation. Typically the selection included 4 selection rounds, however in some individual cases three or five selection rounds have been performed (Figure 3.2A). For each caspase we now have an enriched DARPin sub-library which is stored at -20°C. These libraries were further used to identify caspase specific DARPins binders. The analysis of individual clones by Crude Cell Extract ELISA (CEE) (Figure 3.2 B and C) revealed a set of potential binders that were further characterized. We improved several technical aspects during the DARPin characterization this included the use of a colony picker, ELISA washer, liquid suspender and pipetting robot. Furthermore we up scaled the ELISA from a 96 to a 386 well format which significantly reduces the amount of target protein to 1/5 compared to the previous setup. This represents a crucial improvement because the purification of the target protein is often a bottleneck. The usage of auto inducing media increased the expression rate to 99 % compared to previously used media 2YT where only approximately 80 % of the selected constructs expressed the DARPin. Each DARPin obtained a unique name after selection (DX.Y) with X indicating the caspase it binds and Y stands for the succession of discovery; e.g. D1.10 is the tenth DARPin that was identified to bind caspase-1.

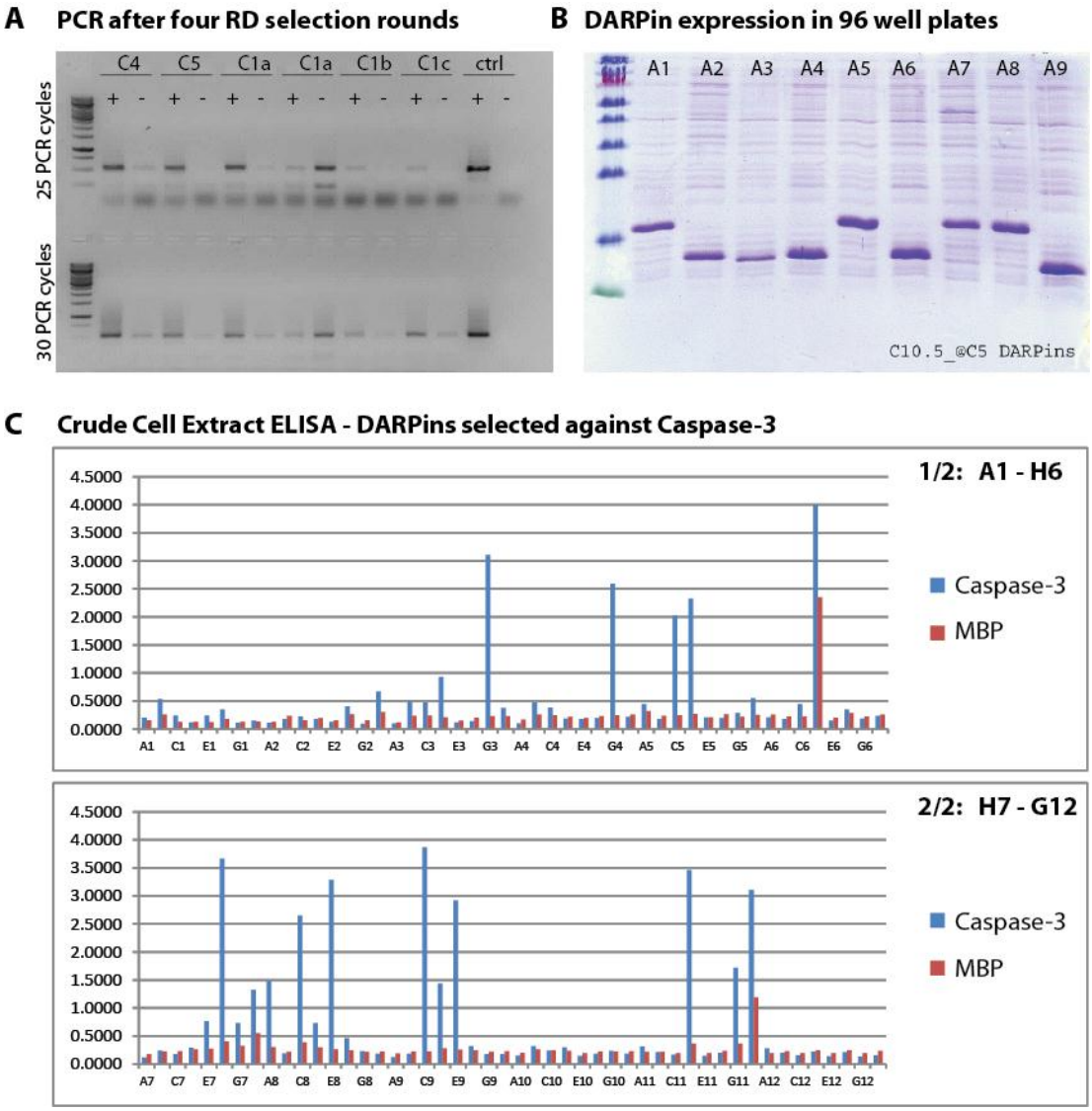

Figure 3-2: Selection of DARPins against caspases
(A) The enrichment of the DARPin library after four RD selection rounds analyzed on a 1% Agarose Gel. C4 indicates selection against caspase-4. (+) indicated selection against the target (-) indicates selection against the surface only. Buffer conditions are indicated by a, b and c with a=WBT, b= WBT + z-WEHD.cho, c= WBT + 30mM NaMalonate (WBT stands for Wash buffer + Tween as indicated in the material and methods section). (B) 15% SDS-PAGE showing N3C and N2C DARPin expression in Crude Cell Extract. (C) Crude Cell Extract ELISA of DARPins selected against caspase-3. Blue bars show the signal against caspase-3 and red bars show signal against the negative control MBP.

High throughput expression and characterization of DARPins

Positive hits from CEE ELISA were expressed in larger volumes to obtain sufficient material and purity for further analysis. Because different DARPins show very different behavior in recombinant *E.coli* cell cultures we used auto-inducing media for high throughput expression. A parallelized expression and purification setup in 24-well plates allowed the purification of 96 different DARPins in one day with a yield of usually more than 1mg per culture (5ml) followed by IMAC purification. The purified DARPins were stored at 4 °C with the antimicrobial additive sodium azide (NaN_3) at a final concentration of 0.03% for further characterization. DARPins stored in these conditions retained their binding capabilities for at least one year. In contrast storage at -20 °C even when cryoprotectants such as sucrose or glycerol were used resulted in precipitated protein after thawing.

Since the strength of a signal in CEE experiments does not directly correlate with binding affinity we further analyzed the selected DARPins by surface plasmon resonance (SPR) after purification by size-exclusion chromatography (SEC). We used the Proteon XPR36 (BioRad [166]) because it allows analysis of up to 24 DARPins within one day. Binding at 8 different concentrations usually in the range from 0.17 to 128 nM was measured. Figure 3.3 shows the SPR kinetics of six different DARPins (DARPin_3.7 to DARPIN_3.13), that were selected against Caspase-3 and expressed in a 5 ml cell culture followed by IMAC purification. From this screen we were able to determine an approximate K_D by equilibrium analysis. Furthermore other kinetic constants such as k_{on} and k_{off} of each individual DARPin could be estimated. Based on this screen we could exclude DARPins with unfavorable kinetic properties. Binders that show slow dissociation rates, as it is the case for DARPIN_3.8 and DARPIN_3.13 (Figure 3.3) were sequenced and used for further analysis. We repeated SPR analysis with selected DARPins which were purified by IMAC and SEC followed by a precise determination of the protein concentration. The results of all SPR screens that have been performed are shown in the comprehensive summary in Table 1. We classified the

DARPins according to their affinity estimated by equilibrium binding measurements of the saturated phase. DARPins with K_D values lower than 10 nM are marked with (+++), DARPins with K_D lower than 100 nM and 1µM were marked with (++) and (+) respectively. No kinetic constants (k_{on} and k_{off}) can be determined from equilibrium measurements and are thus not included in Table 3.1. We were not able to determine the kinetic constants for each DARPin often due to the absence of a fitting equation that was in agreement with the experimental data. A list of the kinetic data of the best DARPins we selected is listed in Table 3.2.

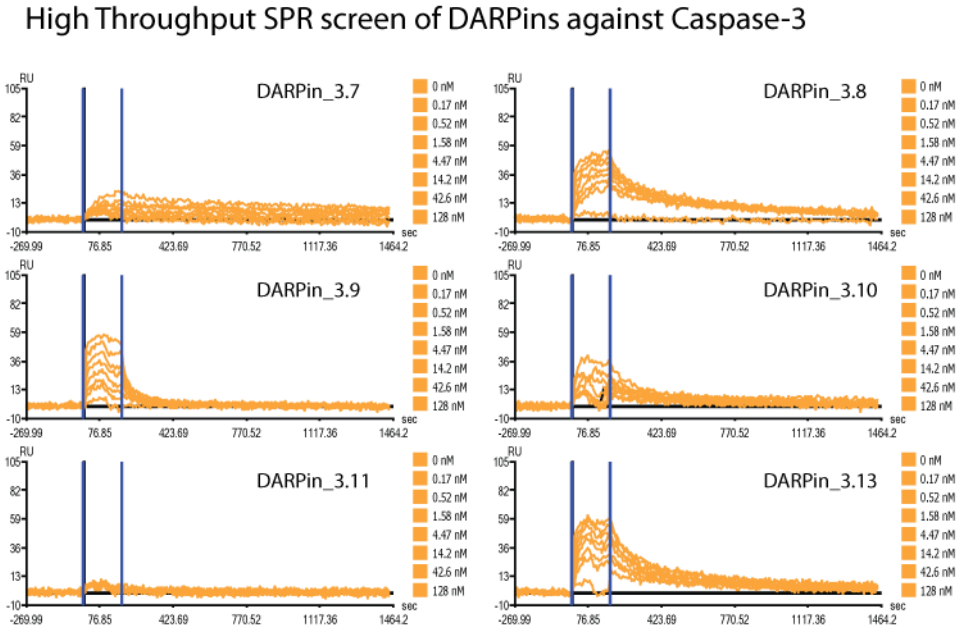

Figure 3-3: SPR analysis of DARPins
High-throughput analysis of selected DARPins. SPR signal for eight concentrations of six DARPins was measured against a surface that was coated with caspase-3.

To measure specificity of the particular DARPin we used the Proteon XPR36 as well. It allows independent coating of 6 lanes with different caspases. The analyte (DARPin) can thus be tested against 6 caspases simultaneously. DARPin_3.8 was particularly interesting for us, because it was found to inhibit caspase-3 (Chapter3). In order to test the specificity of DARPin_3.8 caspase-3 and five other homologous caspases were coated on the SPR chip.

DARPIN_3.8 showed binding to caspase-3 only, indicating that this DARPin is very specific (Figure 3.4).

We initially anticipated to have a least two DARPins that bind different epitopes of the same caspase for sandwich ELISA applications. To confirm this we tested DARPins from different sequence families by competition ELISA. Interestingly we found that literally all DARPin bound to one, or overlapping epitopes (Andreas Flütsch). For caspase-7 as an example we selected 43 different DARPins, but none of them showed uncompetitive behavior to other caspase-7 DARPins.

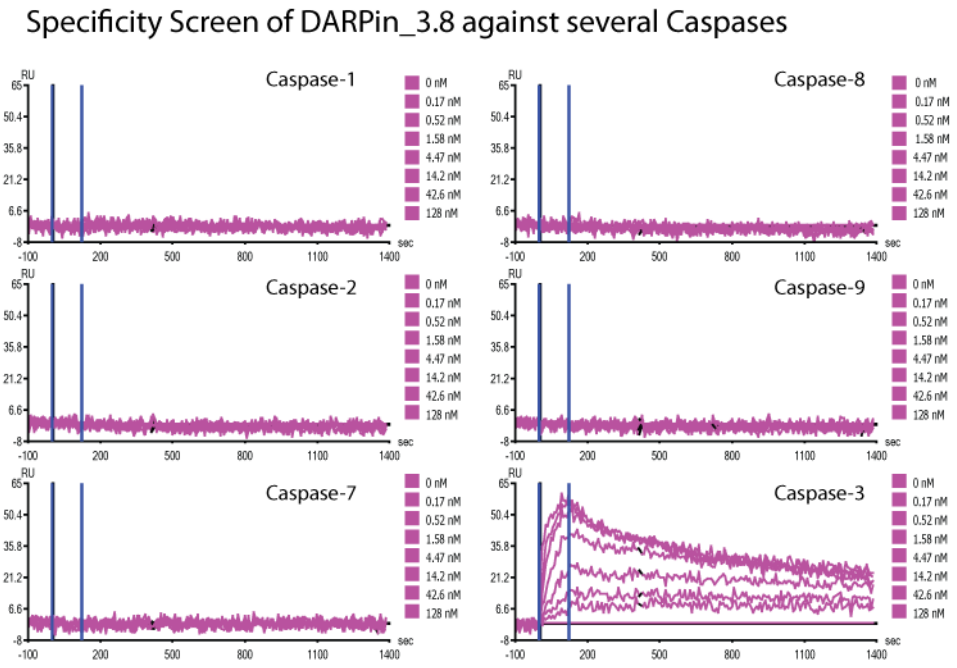

Figure 3-4: SPR specificity analysis
Six different ligands were coated and one DARPin (DARPIN_3.8) was analyzed for binding against each caspase simultaneously.

Due to the overwhelming number of selected DARPins we listed only the most important DARPins for each caspase. As an example, over 130 caspase-1 specific DARPins have been characterized in search for an inhibitor, but not all of them are listed also because they often have almost identical sequences. For every caspase, except for caspase-4 we found specific

and high affinity binders. For completeness we have listed four DARPins that were selected against caspase-4 but SPR experiments have shown that they possess affinities in the low μM range, three orders of magnitude higher than the best binders we have found against the other caspases. Next to binding properties we have also screened for DARPins which either activate or inhibit a caspase. For caspase-1 we found DARPin 1.81 which inhibits the activity significantly. However, even at 1000 fold excess the DARPin reduced the activity by only 50%. From the DARPin library selected against caspase-3 we identified two DARPins which inhibit caspase-3 (DARPin_3.4 and DARPin_3.8), which are described in Chapter 4 in more detail. Furthermore the selection of DARPins against caspase-8 revealed a DARPin which increases the activity of caspase-8, as described in Chapter 5.

DARPin	Properties					Results		
Name	repeats	MW	ExtCoef	pI	Sequenced	SPR	Array	properties
D1.1	N3C	18371.5	16960	5.54	Yes		-	-
D1.4	N3C	18371.5	15470	5.61	Yes	++	+++	-
D1.7	N3C	18341.5	16960	5.54	Yes	++	+++	-
D1.9	N3C	18385.5	16960	5.54	Yes	++	+++	-
D1.10	N3C	18375.5	15470	5.61	Yes		-	-
D1.15	N3C	18320.4	15470	5.54	Yes	+	+++	-
***D1.16**	N3C	18371.5	16960	5.54	Yes	++	+++	-
D1.17	N3C	18384.6	16960	5.44	Yes		-	-
D1.19	N3C	18427.6	16960	5.54	Yes	++	+++	-
D1.21	N3C	18418.6	18450	5.54	Yes		+	-
D1.39	N3C	18371.5	16960	5.54	Yes		+	-
D1.44	N2C	16037.9	16960	5.87	Yes		++	-
D1.53	N3C	18381.6	16960	5.54	Yes		n.d.	-
D1.70	N3C	18165.2	11000	5.4	Yes		n.d.	-
***D1.73**	N3C	18358.4	9970	5.34	Yes	+++	n.d.	-
D1.74	N3C	18262.3	12490	5.4	Yes		n.d.	-
D1.75	N3C	18390.4	9970	5.49	Yes		n.d.	-
D1.76	N3C	18227.4	8480	5.34	Yes		n.d.	-
D1.77	N2C	14652.4	6690	5.29	Yes		n.d.	-
D1.81	N3C	18353.5	24980	5.18	Yes	+	n.d.	Inhibitor
D1.85	N3C	18416.5	12490	5.51	Yes	+	n.d.	-
D1.93	N3C	18440.6	15470	5.27	Yes		n.d.	-
D1.97	N3C	18406.5	20970	5.35	Yes		n.d.	-
D1.100	N3C	18140.2	4470	5	Yes		n.d.	-
***D2.1**	N3C	18417.5	18450	5.28	Yes	+++	+	Inhibitor
D2.2	N2C	14773.7	6990	5.27	Yes	+	+	-
D3.1	N2C	14327.90	0.00	5.64	Yes	-	n.d.	-
D3.2	N2C	14812.60	6990.00	5.55	Yes	-	n.d.	-
D3.3	N2C	14726.50	11000.00	5.45	Yes	+	n.d.	-
D3.4	N2C	14676.40	5500.00	5.84	Yes	+++	n.d.	Inhibitor
D3.4_S76R	N2C	14676.40	5500.00	5.84	Yes	+++	n.d.	Inhibitor
D3.4_I78S	N2C	14676.40	5500.00	5.84	Yes	-	n.d.	No inhibition
D3.5	N2C	14545.20	2980.00	5.55	Yes	-	n.d.	-
D3.6	N2C	14468.20	6990.00	5.29	Yes	+++	n.d.	-
D3.7	N2C	14551.20	5500.00	5.55	Yes	+	n.d.	-
***D3.8**	N3C	17964.10	8480.00	5.51	Yes	-	n.d.	Inhibitor
D3.9	-	-	-	-	No	+	n.d.	-
D3.10	-	-	-	-	No	+	n.d.	-
D3.11	-	-	-	-	No	-	n.d.	-
D3.12	-	-	-	-	No	-	n.d.	-
***D3.13**	N3C	18257.40	9970.00	4.92	Yes	+++	n.d.	-
D4.1	N3C	18096.1	9970	4.99	Yes	-	-	-
D4.2	N3C	18410.5	16960	5.09	Yes	-	-	-
D4.3	N3C	18108	6990	4.95	Yes	-	-	-
D4.4	N2C	14659.2	2980	5.15	Yes	-	-	-
D4.5	N3C	18286.4	5960	5.01	Yes	-	-	-
D5.1	N3C	18598.9	22460	5.7	Yes		+	-
D5.2	N3C	18598.9	22460	5.7	Yes		+	-
D5.3	N3C	18521.6	12950	5.49	Yes		-	-
D5.4	N3C	18280.5	8480	5.39	Yes	+	+++	-
***D5.5**	N3C	14794.5	12490	5.38	Yes	++	+	-
D5.6	N2C	14794.5	12490	5.38	Yes		+	-
***D5.7**	N3C	18356.4	13980	4.89	Yes	++	+++	-
D5.8	N3C	18405.7	17990	4.99	Yes		-	-
D5.11	N2C	14853.4	9970	5.04	Yes	-	+++	-
***D5.15**	N3C	18324.5	19480	4.99	Yes	+++	+++	-
D5.16	N3C	18324.5	19480	4.99	Yes		+++	-
D5.25	N3C	18324.5	19480	4.99	Yes		+++	-
D6.1	N3C	18374.4	7450	5.54	Yes	++	n.d.	-
D6.2	N3C	18088.3	6990	5.35	Yes	+	-	-
D6.3	N3C	18469.7	14440	5.08	Yes	+	-	-
D6.4	N3C	14690.4	4470	5.03	Yes	+	-	-
D6.5	N3C	18469.7	14440	5.08	Yes	+	-	-
D6.6	N3C	18329.7	12950	5.51	Yes	+	-	-
D6.7	N3C	14846.5	8480	5.41	Yes	+	-	-
D6.8	N3C	18209.5	11460	5.41	Yes	++	+	-
D6.9	N3C	18064.3	4470	5.51	Yes	++	+	-

DARPin	Properties							Results
Name	repeats	MW	ExtCoef	pI	Sequenced	SPR	Array	properties
D6.10	N3C	14697.4	6690	5.44	Yes		-	-
***D6.11**	N3C	18300.4	9970	5.46	Yes	++	+++	-
D6.12	N3C	18345.3	7450	5.44	Yes	+	-	-
D6.14	N3C	18345.3	7450	5.44	Yes	+	-	-
D6.15	N3C	18088.3	6990	5.35	Yes	+	n.d.	-
D6.16	N3C	18283.6	11460	5.54	Yes	+	n.d.	-
D6.20	N3C	-	-	-	No	+	++	-
***D6.21**	N3C	18381.5	15470	5.4	Yes	+	+++	-
***D7.1**	N3C	18023.1	2980	4.99	Yes	+++	+++	-
D7.2	N2C	14928	17990	5.79	Yes	n.d.	-	-
D7.3	N2C	14873.6	19480	5.51	Yes	++	+++	-
D7.4	N3C	18211	13980	5.53	Yes	n.d.	-	-
D7.5	N2C	14741.4	5500	5.72	Yes	n.d.	-	-
D7.7	N2C	14930	15470	5.79	Yes	++	++	-
D7.10	N2C	14725	12490	5.43	Yes	+	-	-
D7.14	N2C	14961	15470	5.72	Yes	+++	++	-
D7.17	N2C	15013	17990	5.85	Yes	n.d.	++	-
D7.18	N3C	18273.2	15470	4.74	Yes	++	+++	-
D7.20	N2C	14780.5	12490	5.52	Yes	n.d.	+++	-
D7.31	N3C	18363.5	13980	5.51	Yes	n.d.	-	-
D7.33	N2C	14983.7	17990	5.85	Yes	+	+++	-
D7.40	-	-	-	-	No	++	+++	-
***D7.43**	N3C	14812.6	6990	6.68	Yes	+++	+++	-
D8.1	N3C	18157.4	5500	5.28	Yes	+++	n.d.	-
D8.2	N3C	18122.4	6990	5.38	Yes	+++	n.d.	-
D8.3	N3C	18157.3	6990	5.48	Yes	+++	n.d.	-
***D8.4**	N3C	18190.5	5500	5.3	Yes	+++	n.d.	Activation
D8.7	N3C	18157.4	5500	5.28	Yes	+++	n.d.	-
D9.2	N3C	-	-	-	-	-	-	-

Table 3-1: DARPins selected against human caspases. The best DARPin binders for each caspase are labeled with an asterix (*) in front of the DARPin name.

Protein microarray

The microarray technology has proven to offer a highly parallelized and reproducible setup for diagnostic applications using DNA and RNA molecules as capture reagent [167]. However, in contrast to well-established DNA microarrays, the automation and robustness of protein microarrays needs to be demonstrated before they can be reliably used for diagnostic high-throughput applications [168]. These applications include the identification of biomarkers, screening large numbers of patient samples or the detection of protein expression levels in the cell [169]. The greatest limitation in producing protein microarrays is the availability of capture reagents which are able to bind a molecule in a complex sample even if it is expressed at low concentrations. DARPins are very promising in this regard because they are exceptionally stable and can bind their target protein with high specificity. We describe here the first production of microarrays with DARPins as capture reagents.

For the production of the microarray we used a Piezoelectric non-contact spotter S11 (Scienion, Berlin as illustrated in Figure 3.5A). We developed a very reproducible technique that allows us to screen up to 500 different DARPin with six replicates on one array to screen for binding and specificity. We found that epoxysilane coated slides are most effective and offer a good signal to noise ratio at low costs. The DARPins were covalently immobilized (PBS, pH 7.4) by reacting with epoxysilane via their reactive amino groups. Figure 3.5C shows a schematic overview of DARPin coating and signal readout. Coated microarray slides were stored at 4 °C and saturated humidity for up to one month. The microarray showed an inferior performance after storage longer than one month.

After the immobilization of DARPins on the surface we applied the biotinylated caspase using a hybridization station (2xHS 4800, Tecan Figure 3.5 B). This device allows microarray handling including pre-hybridization, blocking, washing and drying for up to twelve different microarrays in parallel. The caspase which was used for hybridization has been covalently linked to a Cy5 fluorophore. For signal readout of the hybridized microarray we used a confocal laser scanning microscope LS4000 (Tecan, Austria). Figure 3.5D shows a

microarray with fluorescent intensity represented in color, with black being no signal and red being the strongest signal. On this microarray we coated 150 different DARPins that were selected against caspase-1 to caspase-9 and hybridized the slide with caspase-5. As indicated, 32 DARPins that have been selected against caspase-5 have been coated. The majority of those DARPins show a significant signal for caspase-5, whereas two DARPins that have been selected against other caspases (blue box) also show a signal for caspase-5, indicating that they are not specific. Figure 3.5E shows the signal intensity of the average of six replicates that were coated on the chip. Bars in blue or red, are DARPins that were selected against caspase-5. We have set a threshold of 2.5 (Ratio of net intensity/background) to select specific binders with a strong signal. DARPins that excel this threshold can be regarded as specific caspase-5 binders under the given conditions.

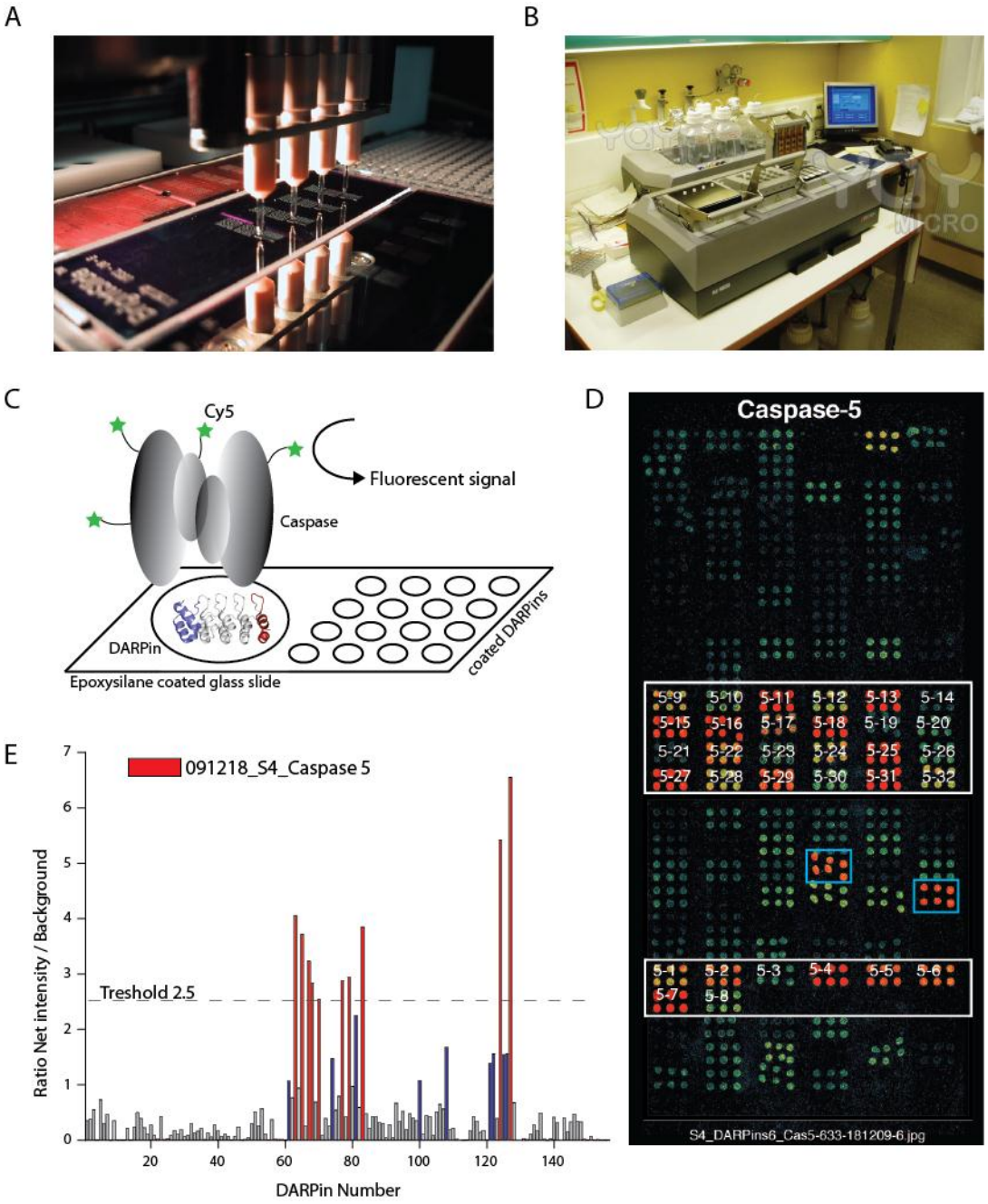

Figure 3-5: Production of protein microarrays

A) Piezoelectric non-contact spotter S11 (Scienion, Berlin). B) Hybridization station (2xHS 4800, Tecan). (C) Schematic view of the microarray interactions. DARPins are immobilized to the epoxysilane coated slides and bind caspases. The caspases are labeled with a Cy5 fluorophore which is used for signal readout. (D) A microarray coated with 150 different DARPin each spotted in replicates of six. The microarray was then incubated with caspase-5 to test DARPin for specificity against caspase-5. (E) Quantification of signal intensity with a confocal scanning laser microscope. Ratio net intensity/background is assigned to each DARPin. A threshold of 2.5 was set to distinguish between specific and non-specific DARPins.

Optimization of microarray printing and readout

Microarray experiments aim to handle large numbers of samples with minimum consumption of material. At the same time, the experiments need to be highly reproducible with optimal results in terms of signal to background ratio. For this we screened several conditions during the procedure of microarray including printing, hybridization and readout. We found that, DARPins are successfully printed in PBS pH 7.3 which is compatible with previously used buffers for DARPin purification. Any additives such as Sucrose increased the viscosity and led to higher failure rates during printing of the protein spots. Addition of sodium azide to a final concentration of 0.03 % did not affect printing or the interaction with a caspase. The ideal protein concentration was 0.5 mg/ml, since higher concentrations also increased the viscosity and lower concentrations decreased the density and thus the resulting signal. As mentioned before we found epoxysilane coated glass slides (Schott Nexterion) are most favorable for our application and offer a good signal to noise ratio at low cost of five CHF per slide. We tested several other slides from different manufacturers; however they did not increase the signal to noise ratio but were significantly more expensive. We also tested which caspase concentration is best for optimal signal. Starting with a concentration of 0.1 mg/ml caspase-1 we used four different dilutions in PBS as illustrated in Figure 3.6A. Increasing concentrations led to increasing background signal, the optimal ratio was found at a dilution of 1:1500 with an average signal intensity over background of approximately eight (Figure 3.6B).

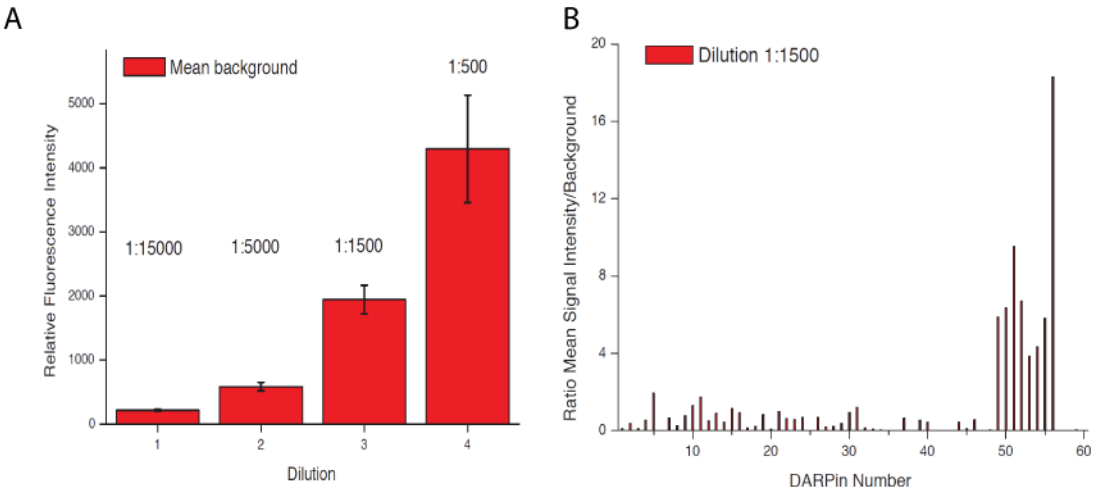

Figure 3-6: Optimization of protein microarrays
(A) Caspase-1 was incubated with the previously coated microarray at different dilutions. Relative fluorescent intensity and mean background are shown. (B) Signal intensity/background of 57 DARPins is shown. Position 49 to 57 are caspase-1 specific DARPins. Caspase-1 was incubated with the microarray at a dilution of 1:1500.

Specificity test of DARPins using protein microarrays

To test the specificity of the selected DARPins we used the microarray technology. Caspases have high sequence homologies thus we were interested whether the selected DARPins distinguish between the homologous proteins. An example is shown for binders of caspase-6 and -7 (Figure 3.7). In total 46 DARPins were coated in replica of 12 spots. This screen indicates that the DARPins are overall very specific. None of the DARPins shows a significant signal against the close homologue. For example D7.18 shows an intense signal for caspase-7, but no signal is visible for caspase-6 (Figure 3.7). The signal intensities that are observed on the microarray are in line with other experimental setups such as SPR and ELISA. As an example D6.11 is the best binder according to the kinetic properties we measured by SPR which is in agreement with the microarray experiment, where D6.11 has the highest signal intensity and thus affinity to caspase-6.

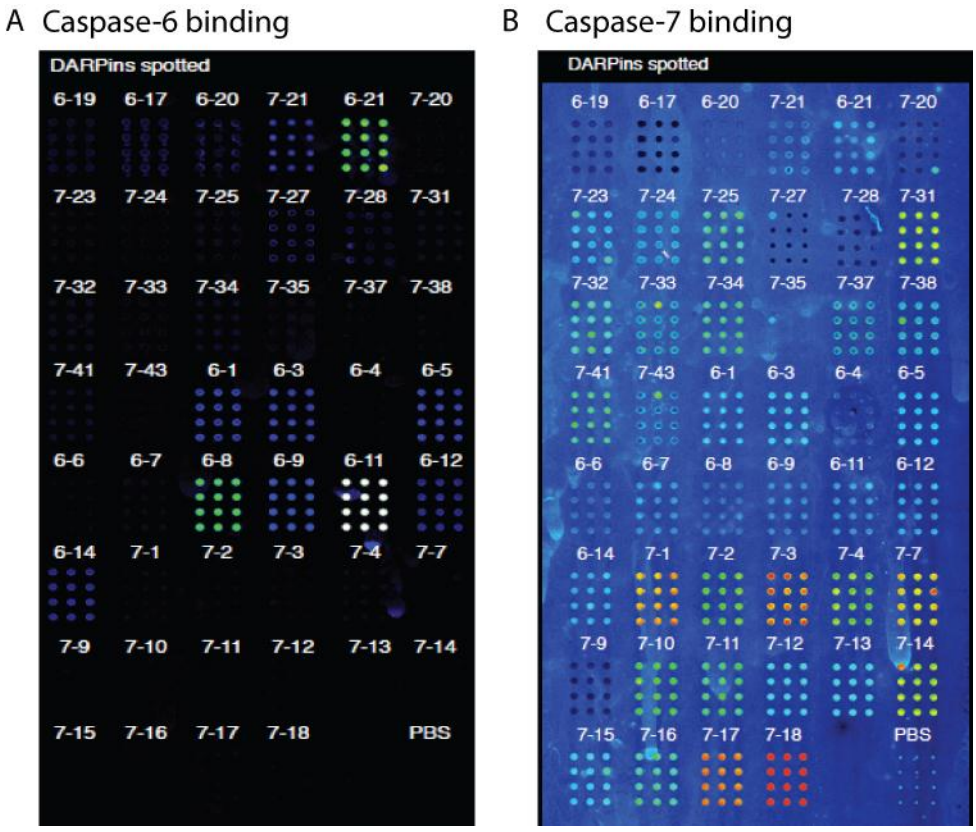

Figure 3-7: Specificity of DARPins tested on microarrays
A set of caspase-6 and caspase-7 DARPin was coated on a microarray and then hybridized with (A) caspase-6 and (B) caspase-7. The intensity of the signal is represented by a rainbow color-coding with black being no signal, red a strong and white an oversaturated signal.

Characterized set of binders against all caspases

With the described DARPin selection and characterization we selected a pool of DARPins against caspase-1 to caspase-9. This set of DARPins can be regarded as a "toolbox" of caspase binders for various applications such as caspase localization, depletion or protein microarrays. An overview of these binders including their kinetic properties is presented in Table 3.2 and the amino acid sequence of the corresponding DARPin is listed in the appendix. For most caspases the kinetic data were evaluated based on the heterogeneous ligand model [170] which gives two possible kinetic values as indicated in Table 3.2. The only case where we could apply the langumir model is DARPin_8.4 which has a K_D of 5.2 nM.

	Kinetic constants						Equilibrium
Binder	$k_{on1}(M^{-1}s^{-1})$	$k_{off1}(s^{-1})$	$K_{d1}(M)$	$k_{on2}(M^{-1}s^{-1})$	$k_{off2}(s^{-1})$	$K_{d2}(M)$	$K_d(M)$
D1.16	1.41E+05	1.22E-03	8.63E-09	2.89E+06	2.82E-03	9.78E-10	-
D1.73	1.03E+05	4.70E-04	4.54E-09	1.20E+06	1.88E-03	5.87E-09	-
D2.1	n.d.	n.d.	4.1E-09	-	-	-	-
D3.8	1.77E+05	2.49E-03	1.41E-08	2.44E+06	1.11E-04	4.57E-11	3.4E-09
D3.13	2.74E+05	1.24E-03	4.51E-09	2.31E+06	7.86E-03	3.41E-09	7.69E-09
D5.15	1.05E+06	1.01E-02	1.00E-08	2.85E+05	5.97E-04	2.10E-09	1.10E-08
D5.16	6.05E+05	1.05E-02	2.13E-08	1.55E+05	9.66E-04	6.23E-09	3.37E-08
D6.11	1.32E+05	0.01	8.99E-08	4.70E+04	3.70E-04	7.88E-09	-
D7.1	1.55E+06	1.10E-02	6.90E-09	1.03E+05	8.41E-04	8.14E-09	-
D7.43	1.90E+06	9.63E-03	5.06E-09	2.21E+05	6.54E-04	2.95E-09	-
D8.4	1.8E+05	9.31E-04	5.2E-09	-	-	-	-
D9.2	-	-	-	-	-	-	-18E-09

Table 3-2: Association, dissociation kinetics and K_D-values of selected DARPins for each caspase.
The affinity of DARPins with two indicated kinetic constants were determined applying the heterogeneous ligand model [170]. D8.4 kinetics were determined using the langumir model.

Discussion

We successfully selected and characterized DARPins against nine human caspases. Several tight binding DARPins were characterized for each caspase with the exception of caspase-4, where the interaction was only observed in the ELISA format but could not be shown in SPR measurements. In the selection and characterization workflow we have optimized several steps based on existing protocols allowing us to handle large sample numbers in one experiment. This included the use of auto-inducing media that resulted in higher expression, higher cell densities and more reproducible expression during DARPin expression in 96-well plates and 100 mL flasks. Furthermore we assisted several steps during the characterization with state of the art machines such as a colony picker and liquid suspender. We based all screens on 384 well plates which led to higher throughput while only a fifth of proteins material was required compared to previously common ELISA screens. The hits we obtained by Crude Cell Extract ELISA screens were analyzed by high throughput SPR measurements which provided high quality data within a short time. This allowed the elimination of most DARPins that do not possess the required kinetic properties. Only DARPins with K_D values lower than 50 nM and slow dissociation rates from their target protein were considered for further characterization.

Our high-throughput selection and characterization yielded a large number of specific DARPins which bind caspases and few also have a functional phenotype when bound to the caspase as described in chapter 4 and 5. We have found DARPins that inhibit caspase-3 (DARPIN_3.4 and DARPIN_3.8) and caspase-1 (D1.81), D1.81 however only inhibited caspase-1 by 50% and we were not able to elucidate the basis of this inhibition. A caspase-8 specific DARPin (D8.4) increased the activity of caspase-8 which is described in chapter 5. These DARPins in complex with their caspase also led to well diffracting crystals for structural studies. Furthermore the selected DARPins are used by Andreas Flütsch as caspase specific binding molecules for the visualization of apoptosis in fixed and living cells.

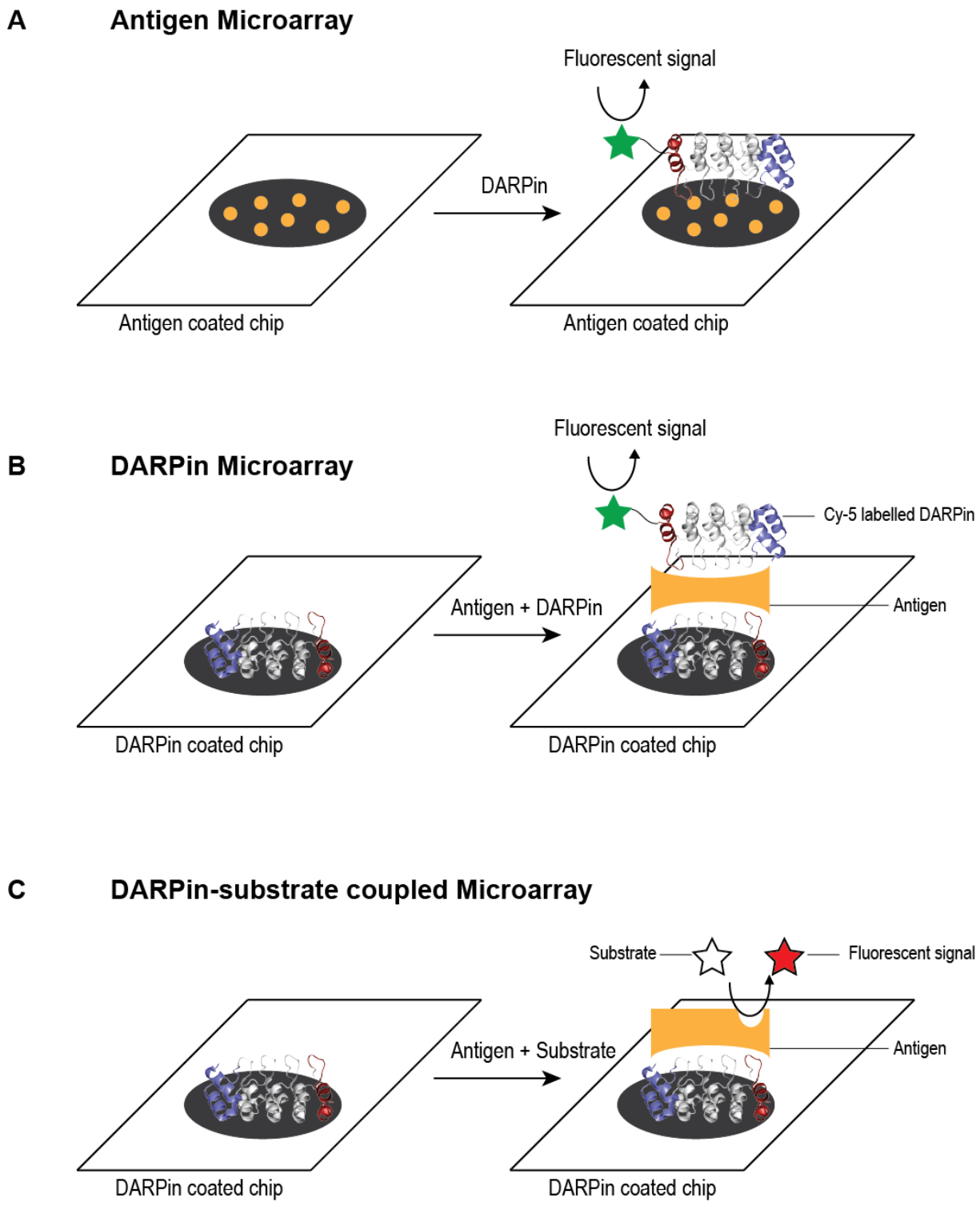

Figure 3-8: Potential formats for a caspase specific DARPin microarray
A) Antigen microarray. The antigen (orange circle) is coated on the surface of the slide. A fluorophore (green star) labeled DARPin is used to detect and quantify the amount of antigen concentration B) DARPin microarray. The DARPin is coated on a microarray followed by addition and incubation with the antigen (orange). A secondary DARPin labeled with a fluorophore is used to detect the antigen. The two DARPins have to detect non-overlapping epitopes. C) DARPin-substrate coupled microarray. As described in B, the antigen is captured by a coated DARPin. The caspase is then quantified by a enzymatic assay, monitoring cleavage of a caspases substrate.

Our initial goal was to select two DARPins against each caspases with high affinity and if possible different binding epitopes. Competition ELISA however showed that most, if not all DARPins bind to the same or overlapping epitope on a particular caspase. This suggests that DARPins in one selection process tend to favor one dominant epitope of the target protein which excludes the application of DARPins in a sandwich assay approach (DARPin microarray) in ELISA or microarray applications (Figure 3.8 B). Other possible microarray setups based on DARPins as capture or detection reagents would be an antigen- or DARPin-enzyme coupled microarray (Figure 3.8 A and C). The DARPin-substrate coupled microarray has the advantage that caspases can be isolated from complex cell lysates of apoptotic cells followed by standard enzyme substrates. The specificity is given by the DARPin-caspase interaction which is quantified by fluorogenic substrates.

In order to use DARPins as capture reagents, we investigated whether they retain their binding properties that have been elucidated in solution. A number of different slide surfaces can be used with the criteria that one maintains the conformation and functionality while achieving maximum binding capacities at low costs. We found that epoxy-derived glass slides fulfill these criteria best and developed our microarrays based on this format in combination with a non-contact spotter.

We were able to print more than 150 different DARPins on one slide and classified the DARPins according to their signal strength, specificity and stability. We saw a clear correlation between affinities that we determined in SPR experiments and signal strength on the microarray indicating that the DARPin fold is generally suitable for array technologies. The compact fold with its extraordinary stability represents a promising alternative to the commonly used antibodies in protein microarrays. We further conducted several experiments to determine specificity of DARPin sets for their target protein and their closest homologs (Table 3.1). Since we had to handle a large amount of DARPins we optimized the purification for microarray experiments. After Ni-NTA purification of each DARPin we exchanged the buffer to PBS, pH 7.3 on a desalting column. The addition of glycerol to prevent dehydration

on the slide was not necessary but complicated the printing process due to the high viscosity. We found that a concentration of 0.5 mg/ml was optimal and we obtained the best signal to noise ration at a 1:1500 dilution of the caspase for incubation with the slides.

Our initial goal was to develop a caspase specific array to dissect the apoptotic caspase pathway because no appropriate techniques are available. Due to the lack of DARPin binders targeting different epitopes for a sandwich based approach for detection we adapted our strategy to a general proof-of-principle of DARPins as capture reagents. Furthermore apoptotic cells in a cell culture are highly heterogeneous and cannot be synchronized. Apoptosis occurs around four hours after the apoptotic stimulus and transmission of the apoptotic signal leading to the activation of executioner caspases is then completed within minutes. This timeframe in a heterogeneous sample is very short and complicates development and application of a caspase specific microarray. Consequently we decided to establish DARPins as capture reagents on microarrays without performing experiments with apoptotic samples.

In summary we have shown, that DARPins can be selected against a whole protein family with high specificity and affinity. DARPins retain their functionality on a surface and are very promising proteins for microarray applications. We were able to use our microarray to classify the selected DARPins according to their specificity and affinity. DARPins in combination with microarrays is an excellent high-throughput method that can be used to characterize an entire collection of proteins for a specific function or biochemistry [165].

Material and Methods

Caspase purification and biotinylation

All caspase have been purified as described in chapter 1 [171]. For ribosome display selection and ELISA experiments we biotinylated the caspase prior to the experiment. For chemical biotinylation of the caspase we used the linker EZ-Link Sulfo-NHS-LC-LC-Biotin (21338, Pierce), containing a reactive group, a 3.05 nm long linker and a biotin moiety. After purification, 1ml of the caspase (10 μM) was either in PBS pH 7.3 or 50 mM HEPES pH 7.5, 150 mM NaCl and was incubated with a seven fold molar excess (1 ml of a 70 μM solution) of biotin on ice for 30 minutes. The reaction was quenched by adding 10 μl of 5M Tris, pH 7.5. The biotinylated protein was then purified by size exclusion chromatography, using a Superdex 200 10/300 GL (GE Healthcare) in PBS at 4 °C. The fractions containing the biotinylated caspase were pooled and frozen in liquid nitrogen after adding sucrose to a final concentration of 10 %. The samples were stored at -80 °C for up to one year until further usage.

Ribosome display selection of DARPins

Cloning and amplification of the N3C DARPin library has been described previously [110]. The library contains N3C and N2C DARPins. The principle of ribosome display selection has been described elsewhere [119, 120]. However, Figure 3.6 shows a schematic drawing of the selection strategy that was developed for selection with focus on specificity and low k_{off} rates. We performed four selection rounds for each caspase and maltose-binding protein (MBP) was coated for pre panning (22 nM) in each round. Furthermore the two most homologous caspases (22 nM) were included into pre-panning in round n°1 and n°3. k_{off} maturation was done in round n°2 and n°4 by adding a 1000 fold excess of unbiotinylated caspase (final concentration of 22 μM, if the caspases was coated at a concentration of 22 nM) for 5 or 10 minutes respectively. After each round we washed the unbound DARPin-Ribosome complex with increasing stringency as indicated in Figure 3.8.

After four selection rounds we cloned the library into a pQE30 vector and this library was used to transfect competent XL-1Blue *E.coli* cells (Stratagene). Single colonies were used for Crude Cell Extract ELISA experiments.

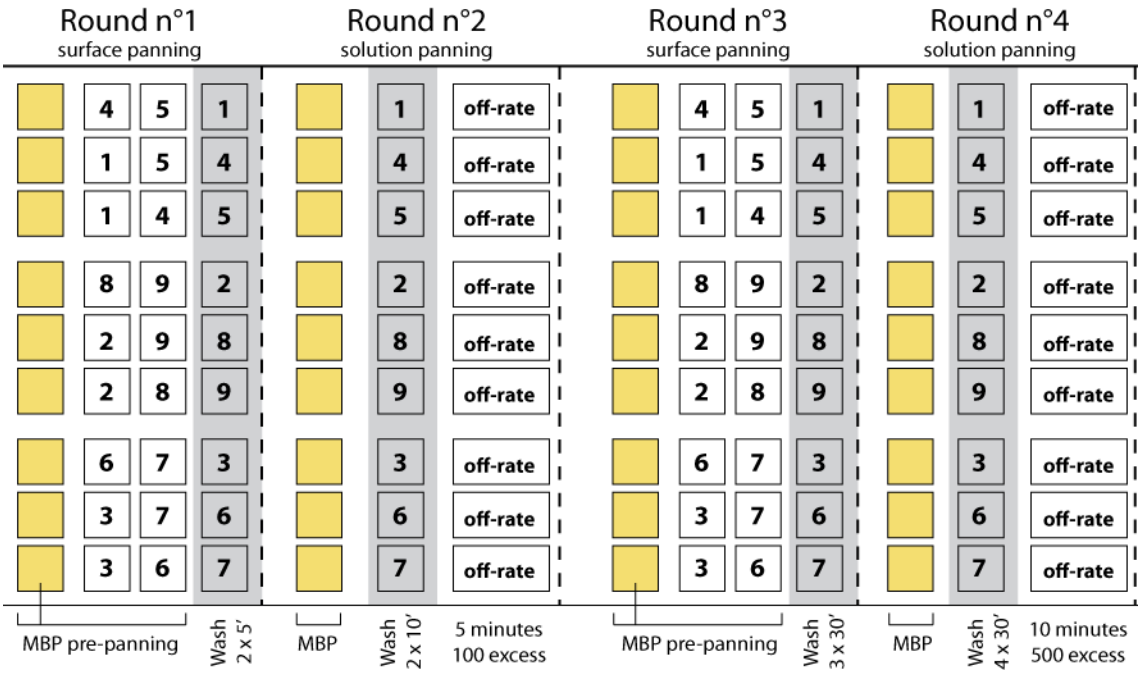

Figure 3-9: Overview of the RD selection strategy
An strategy with alternating conditions each round was used to prevent unspecific enrichment under one condition. The number in the box stands for the respective caspase, with '3' representing caspase-3. Yellow boxes represent pre-panning with MBP, white box pre-panning against other caspases and gray background indicates the target protein for selection. Off-rate selection was done in round n °2 and n°4.

Crude cell extract ELISA

Single colonies each containing one DARPin clone of the selected library were picked and inoculated in 0.9 ml auto-inducing media [172] containing deep 96-well plates (Abgene, UK). The cells were grown over night at 37 °C while shaking at 300 rpm in a shaker (TH15, Edmund Bühler GmbH). Then 200 µl of each well were transferred into a sterile 96 well plate (Nunc) as a backup for further protein expression and plasmid preparation. The remaining 700 µl of cell-suspension was harvested by centrifugation and the cell pellet was lysed with 50 µl B-PER II (78260, Pierce) per well for 30 minutes shaking at room temperature. The lysed

cells were resuspended by adding 950 µl PBS, pH 7.3 and cell debris was removed by centrifugation (20 min, 4500 rpm at 4°C) in a table top centrifuge 5414 (Eppendorf). We took 20 µl of the supernatant an added it to 384 ELISA plate (Nunc) where MBP or a caspases has been coated previously. This plate has been coated with 20 µl of a 22 nM Neutravidin solution (Pierce, 31000), followed by extensive washing. We then added 20 µl of a 100 µM protein solution representing the caspases or MBP as control. After 1h of incubation of the supernatant at room temperature and 3 washing cycles the plate was incubated with mouse anti-RGS-H_4 antibody (34650, Qiagen) at a dilution of 1:2000 in PBS 1% BSA. We then added the secondary antibody (goat-α-mouse IgG alkaline phosphatase conjugate (Sigma, A3562)) followed by four washing cycles and added the substrate di-sodium 4-nitrophenyl phosphate (pNPP; 3 mM di-sodium 4-nitrophenyl phosphate, 50 mM NaHCO3, 50 mM MgCl2.6H2O). The OD was measured at 405 nm using a multi-well plate reader (Infinite M1000, Tecan).

Large scale expression and purification of DARPins

DARPins were expressed in 100 ml media using either 2YT or auto-inducing media starting from a glycerol stock or the 200 µl backup culture after Crude Cell extract ELISA. When expressed in 2YT media we induced expression at an OD_{600nm} between 0.6 - 1 with 0.5 mM Isopropyl β-D-1-thiogalactopyranoside (IPTG) followed by 3h of expression at 37 °C under continuous shaking. Cells were harvested by centrifugation for 7 minutes at 8000rpm, 4°C (Biofuge primo R, Hereaus) and lysed by sonification. The expressed DARPin was purified with common His-tag purification methods using a self-made gravity column consisting of a plastic column (57024, Supelco) and 0.5 ml bead volume of Ni^{2+}-NTA agarose (30210, Qiagen). The DARPins were eluted in PBS, 200 mM Imidazole pH 7.4 and the Imidazole was removed with a PD-10 desalting column (17-0435-01, GE Helthcare). We added sodium azide (NaN_3) to a final concentration of 0.03% to prevent growth of bacteria and fungi. The DARPins solution was further stored at 4 °C.

Kinetic Analysis of DARPins with Surface Plasmon Resonance

For SPR experiments we used the Proteon XPR36 (Bio-Rad Laboratories, Inc.) and all kinetic analysis were made on a NLC sensor chip (Bio-Rad Laboratories, Inc.). We used sterile filtered PBS pH 7.3, 0.005% Tween-20 as a standard buffer for coating and all kinetic measurements. The biotinylated ligand (caspase) was coated on the sensor chip at a concentration of 5 nM and a flow rate of 30 µl per minute. The coating procedure was interrupted once a total of 1000 relative units (RU) were reached on the Proteon monitoring system. We started by coating lane six and continued with lane five and used lane one at last. Twelve different analytes (DARPin) were prepared prior to the experiment and a dilution series was pipetted in the 96 well storage plates, which were sealed to prevent evaporation or contamination with dust particles. For Kinetic analysis we measured every analyte at eight different concentration (0, 0.176, 0.52, 1.58, 4.47, 14.2, 42.6, 128 nM) starting with the lowest concentration. All experiments were performed at 20 °C. Due to the heterogeneity of the system we did not regenerate the chip surface in between every concentration but dissociated the analyte with a long dissociation phase of up to 300 minutes. We used a flow rate of 100 µl per minute, an association phase of 5 minutes and a dissociation phase of 20 minutes. The data were recorded and further processed with the ProteOn Manager 2.1.1 (BioRad). Data evaluation and curve fitting was performed with the same program to determine kinetic and equilibrium constants [166].

Microarray production

Prior to coating the DARPin samples were adjusted to a final concentration of 0.5 mg/ml in PBS, pH 7.4 and filtered (0.22 µm). 15 µl of each DARPin was pipetted into a 384-well plate (Nunc) which was connected to the microarray printer. We used a piezoelectric non-contact spotter S11 (Scienion, Berlin) for microarray slide production. Each spot was printed by shooting three drops of 1.5 nl on the slide surface, with six to twenty replicates. We used epoxysilane coated glass slides (Schott, Nexterion) for most of the experiments. After printing the microarray was stored at 4 °C in saturated humidity for up to one month. The microarray

was hybridized with a diluted biotinylated caspase solution (0.1 mg/ml in PBS pH 7.3) for 1h at room temperature in a hybridization station (2xHS 4800, Tecan). Four different dilutions were used; 1:500, 1:1500, 1:5000 and 1:20000. Hybridization was followed by four washing cycles. In a second step we incubated a fluorophore-conjugated Streptavidin (Alexa-633) followed by four more washing cycles. The microarray was then dried and stored at room temperature protected from light. For scanning of the slides we used a confocal laser scanning microscope LS4000 (Tecan, Austria) with an excitation wavelength of 633 nm and fluorescent detection at 670 nm. Data extraction and image processing and were performed with ArrayPro 4.5 (Media Cybermetics, Bethesda, USA) and Origin (Microcal, Northampton, USA).

4. Specific inhibition of caspase-3 by a competitive DARPin

Title:

Specific inhibition of Caspase-3 by a competitive DARPin: molecular mimicry between native and designed inhibitors.

Thilo Schroeder[1], Jonas Barandun[2], Andreas Flütsch[1], Christoph Briand[1], Peer R.E. Mittl[1], Markus G. Grütter[1]

[**Structure** *Manuscript in preparation*]

Subject area	Protein and nucleic acid structure, function and interaction
Running title	caspase-3 directed DARPins
Title	**Specific inhibition of Caspase-3 by a competitive DARPin: molecular mimicry between native and designed inhibitors.**
Authors	Thilo Schroeder[1], Jonas Barandun[2], Andreas Flütsch[1], Christoph Briand[1], Peer R.E. Mittl[1], and Markus G. Grütter[1]
Affiliation	[1]Department of Biochemistry, University of Zurich, Winterthurerstrasse 190, CH-8057 Zurich, Switzerland [2] present address: Institute of Molecular Biology and Biophysics, Schafmattstrasse 20, ETH Zürich, CH-8093 Zurich, Switzerland.
Corresponding author	[1]Department of Biochemistry, University of Zürich, Winterthurerstrasse 190, CH-8057 Zürich, Switzerland Tel. +41-44-6355580, Fax. +41-44-6356834, Email: gruetter@bioc.unizh.ch
Document	Text pages-28; Figures-7; Tables-3 ; Supplementary figures-5. Words in abstract, 171; characters (including space), 1155
Coordinates	Coordinates and structure factors have been be deposited at the PDB under accession codes 2XZD and 2Y0B.
Keywords	Caspase; DARPin, XIAP, inhibitor, molecular mimicry

Abstract

Dysregulation of apoptosis is associated with several human diseases including cancer, autoimmune diseases and stroke. The main mediators of apoptosis are cysteine proteases (caspases) which propagate death signals to downstream targets. One of the main executioners is caspase-3 which is responsible for the majority of cleavage events in the cell. The potential of caspase 3 as a therapeutic target is an area of high interest and to date, several potent active site peptide inhibitors have been synthesized. However, all these molecules do not only inhibit caspase-3, but also homologous caspases. Here we describe caspase-3 specific inhibitors which have been selected from a library of designed ankyrin repeat proteins (DARPins). The crystal structures presented describe how the high specificity and inhibition is achieved and the kinetic data reveal a competitive inhibition mechanism. We further demonstrate that the mode of inhibition of the DARPins has similarities with that of the natural caspase inhibitor XIAP. However, unlike XIAP, the DARPin inhibitor is specific for caspase-3 alone and therefore does not bind the highly homologous caspase-7.

Introduction

Programmed cell death (apoptosis) is a central process for the development and tissue homeostasis of metazoans. It is characterized by morphological changes such as nuclear fragmentation, membrane blebbing or the formation of apoptotic bodies [1]. In multicellular organisms including humans, improper regulation of apoptosis leads to a variety of pathologies such as cancer, autoimmune diseases and neurodegenerative disorders [2]. Apoptosis is triggered by various internal- and external stimuli, which are propagated by different pathways. Common to all apoptotic pathways are cysteine Asp-specific peptidases (caspases) [3-5]. These proteins are synthesized as inactive pro-enzymes and upon triggering of the cell death machinery they are activated by proteolytic cleavage on the C-terminal side of a well-conserved aspartic acid. Active caspases are dimers of two catalytic subunits and each subunit consists of a p12 and a p17 chain.

Of the eleven known human caspases, caspase-3 occupies a prominent position in the apoptotic cascade. Caspase-3 is activated by intrinsic- or extrinsic death signals and it executes cell death by the cleavage of downstream targets such as PARP-1 [6]. Since apoptosis is a dangerous process for the cell, caspase activation is strictly controlled and all apoptotic signaling pathways are tightly regulated. All caspases recognize tetrapeptide sequences, which are characterized by an aspartic acid at the C-terminus (P1 position) and either tryptophan, aspartic acid or leucine residues at the N-terminus (P4 position) conferring selectivity for caspase-1, -3 and -8, respectively. The P4 selectivity has been attributed to different interactions with residues in loops flanking the P4 binding pocket [7, 8]. However, the selectivity of short peptidic substrates remains controversial. It has been reported that the *in vitro* selectivity of caspase-3 for a substrate harboring a P4 aspartic acid is at least 100-fold higher than for a glutamate or an asparagine [9]. Despite this finding, commercially available peptide substrates failed to exhibit the expected caspase selectivity [10]. Caspase-3 is the most promiscuous and efficient caspase and is more active in cleaving short peptide substrates than the caspase it was originally designed for. [10]. This analysis raised doubt regarding the use

of short peptides to dissect signaling cascades leading to apoptosis. The observation that naturally occurring caspase inhibitors, such as X-linked inhibitor of apoptosis (XIAP), are highly specific for caspase-3 and -7 [11, 12] suggests that specificity can be gained by extending the size of the inhibitor. Caspases are attractive drug targets since they are implicated in various diseases. Selective and potent caspase-specific inhibitors are therefore highly desirable.

In order to develop a caspase-3 specific inhibitor we used the Designed Ankyrin Repeat Protein (DARPin) technology [13]. From a highly diverse library of DARPin molecules, binders that recognize the target molecule can be selected by either ribosome- or phage display [14, 15]. DARPins consist of a N- and C-terminal capping repeat and two or three internal repeats that recognize the target molecule through selected amino acids in randomized positions. DARPins possess several beneficial properties that make them attractive for biotechnological applications. They are thermodynamically stable, easily produced and do not contain cysteine residues allowing intracellular applications [16]. Highly selective DARPins have been successfully selected and described for a variety of different target proteins such as kinase inhibitors [17], crystallization chaperones [18], HIV inhibitors [19] and tumor targeting binding molecules [20].

Here, we report the selection and characterization of DARPins that bind to active caspase-3. Kinetic and binding experiments revealed that DARPins D3.4 and D3.8 are competitive caspase-3 inhibitors that do not recognize other members of the caspase family. The structure of the caspase-3/D3.4 complex provides insight into the inhibition mechanism and presents an analogy to XIAP inhibition.

Results

Selection of caspase-3 specific DARPin binders

A DNA library containing NI_2C and NI_3C DARPins was used to select caspase-3 binders by ribosome display [15]. After four selection rounds, 768 putative binders were screened by crude-cell extract ELISA yielding 29 clones that possessed submicromolar affinities for caspase-3. These high affinity binders were individually expressed, purified and their binding affinities for caspase-3 were determined by surface plasmon resonance (SPR) analysis. Four of the selected DARPins showed affinities below 10 nM (Supplementary Figure 1). Their sequences were aligned and are shown in Figure 1. Although DARPins D3.4 and D3.8 contain 2 and 3 internal repeats, respectively, they possess the highest sequence similarity. Of the 14 randomized positions of the internal repeats 7 residues are identical. When comparing the sequences of DARPin D3.6 and D3.13 only 4 residues in a total of 21 randomized positions are identical. Despite the different numbers of internal repeats all four DARPins possess very high affinities for Caspase-3. SPR analysis revealed that D3.4, D3.6, D3.8 and D3.13 bind caspase-3 with K_D values of 9.6±1.1 nM, 8.8±2.0 nM, 3.4±0.4 nM, and 7.69±0.4 nM, respectively (Table 1). These K_D values were determined based on equilibrium analyses of the SPR signal. We used the heterogeneous ligand model to determine the kinetic values (Table 1), which suggests two epitopes with substantially different binding affinities [21].

Inhibition of Caspase-3 by DARPins D3.4 and D3.8

The inhibitory properties of the purified DARPins were analyzed using two different approaches. Initially the ability of the DARPins to inhibit the hydrolysis of the short chromogenic caspase-3 substrate Ac-DEVD-AMC was measured. These initial tests revealed that D3.4 and D3.8 inhibit the hydrolysis of the standard caspase-3 substrate with K_i values of 16.8±0.3 nM and 6.37±0.2 nM respectively, whereas D3.6 and D3.13 showed no detectable inhibitory activities (Table 1). To characterize the mode of inhibition (competitive versus uncompetitive), specific velocity plot (Supplementary Figure 2) [22] analysis was performed,

which yields the ratio between competitive and uncompetitive inhibitor constants (α) and the turnover rate of free enzyme to inhibited enzyme (β). For both DARPins we determined equal values of $\alpha = \infty$ and $\beta = 0$ demonstrating that D3.4 and D3.8 are purely competitive inhibitors of caspase-3 (Table 1).

In the past, short peptide substrates have been extensively used for the characterization of proteases, because the determination of rate constants is straight forward in those experiments. On the other hand, short peptide substrates represent a rather artificial situation, since these substrates utilize a very limited number of binding interactions. Natural protease substrates are significantly larger and consequently their binding is guided by a broader set of interactions. Therefore, we tested whether the selected DARPins also inhibit the processing of PARP-1, one of the best characterized caspase-3 substrates. The 116 kDa PARP-1 is specifically cleaved by caspases-3 and -7 on the C-terminal side of Asp216 into an 85 kDa and a 31 kDa fragment [23]. The addition of three fold molar excess of D3.4 or D3.8 over caspase-3 inhibited the cleavage of PARP-1 by ~50%, whereas the addition of E3_5, a DARPin that does not bind caspase-3, showed no effect on the cleavage of PARP-1 (Figure 2). However, the addition of a 150 fold molar excess of the caspase-3 DARPin inhibitors did not abolish PARP-1 cleavage completely in contrast to the peptide inhibitor Ac-DEVD.fmk which inhibited cleavage of PARP-1 completely (Figure 2).

Specificity of DARPins D3.4 and D3.8

All commercially available caspase inhibitors are capable of inhibiting both caspases-3 and -7 equally well [10]. We investigated the caspase selectivity of D3.4 and D3.8 by measuring the binding affinity and inhibitory activity against caspase-7 (56% sequence identity with caspase-3) and the more distantly related caspase-6 (41% sequence identity). SPR analysis did not show any detectable binding of the caspase-3 directed DARPins D3.4 and D3.8 to caspases-6 or -7 (Supplementary Figure 3), suggesting that both DARPins are highly specific for caspase-3. These results are consistent with the activity measurements where D3.4 and D3.8 were also unable to inhibit PARP-1 cleavage by caspase-7 (Figure 2). Probing the ability

of D3.4 and D3.8 to inhibit the hydrolysis of chromogenic tetrapeptide substrates by caspases-1, -2, -4, -5, -6, -7, -8, and -9 revealed that only D3.8 has a moderate inhibitory activity against caspase-7 (Figure 3, and Supplementary Figure 4). Addition of 1000 fold excess of D3.8 decreases the activity of caspase-7 to approximately 40%.

Crystal structure analysis of the caspase-3/DARPin D3.4 complex

To understand the inhibition mechanism of caspase-3 by DARPins the crystal structure of the caspase-3/D3.4 complex was determined at 2.1 Å resolution. The details of the structure determination (data collection and refinement) are listed in Table 2. In the crystal structure the asymmetric unit contains one $(p12, p17)_2$ caspase-3 heterotetramer and two D3.4 molecules (Figure 4A). In the complex a surface area of 876 $Å^2$ is buried and a surface complementarity index of 0.74 indicates a very good fit between D3.4 and caspase-3 (Table1). The interface involves residues from the N-terminal capping repeat and the two internal repeats from the DARPin, which form specific hydrogen bonds and hydrophobic interactions with the caspase (Figure 4A). The crystal structure reveals first of all that D3.4 binds in the active site pocket of caspase-3 and prevents substrate molecules from accessing the catalytic residues (Figure 4A). The β-turns of D3.4 point towards the β-strand of caspase-3 that is responsible for the recognition of the substrate by main chain hydrogen bonds (residues 205 to 207). This observation agrees very well with the kinetic analysis of the inhibition mechanism, where also no uncompetitive contribution was observed ($\alpha = \infty$). Therefore, structural and kinetic analyses consistently classify D3.4 as a purely competitive caspase-3 inhibitor (Supplementary Figure 2). Furthermore, the concave side of the DARPin binds to loop-4 of caspase-3 (L4, residues 246 to 258) with the residues in the randomized positions.

When comparing the structure with the previously published caspase-2 inhibitor (DARPin_F8) structure [24] and the natural caspase-3 inhibitor XIAP structure [25] (Figure 4B and C) the following features can be highlighted: (i) DARPin_F8 also binds to loop-4 (also termed 381-loop) however from the backside, (ii) DARPin F8 does not occupy the active site and inhibits caspase-2 specifically by an allosteric mechanism (Figure 4B) (iii) The

BIR2 domain of XIAP inhibits caspase-3 with its N-terminal extension loop and binds in the active site of caspase-3 in the opposite direction when compared to the substrate (Figure 4C). Interestingly, the binding mode of D3.4 shows similarities to the binding of natural substrates (based on inhibitor structures) and the natural inhibitor XIAP. Asp45 of D3.4 is located in the β-turn that connects the N-terminal capping repeat and the first internal repeat of D3.4 and its side chain occupies the S4 pocket of caspase-3 (Figure 5A). It forms a direct hydrogen bond with Asn208-ND2 and two water-mediated hydrogen bonds with Trp214-NE1 and Phe250-N (Figure 5A and Supplementary Figure 5). The main chain carbonyl oxygen of Asp45 forms another water-mediated (Wat10) hydrogen bond with Arg207-N of caspase-3. This atom is normally involved in the formation of an anti-parallel β-sheet with the substrate peptide. Wat10 forms a third hydrogen bond with Tyr204-OH. As a consequence, Thr166 moves towards the active site pocket and forms hydrogen bonds with Trp79-NE1 and Lys111-NZ of D3.4 (Figure 5A and Figure 6A).

The tip of loop-4 of caspase-3 is recognized by the DARPins concave surface (Figure 5B and C). The side chain of Asp44 of D3.4 is buried in the interface and forms two hydrogen bonds with Ser251-OG and Phe252-N. In contrast, the side chains of Lys56 and Arg81 of D3.4 are solvent exposed and form salt bridges with the side chain Asp253 of caspase-3. Hydrophobic interactions seem to play equally important roles. The side chain of Phe256 of caspase-3 nicely fits into a pocket that is formed by Ala46, Val48, Ile78 and Trp79 of D3.4 where the benzyl ring of Phe256 of caspase-3 forms T-stacking interactions with the indole ring of D3.4 Trp79 (Figure 5C). Although the Phe256 binding pocket is mainly hydrophobic, the side chain of Asp77 is located at the bottom of this pocket and forms an intra-molecular salt bridge with Arg81 and a hydrogen bond with Wat26 (Figure 5C).

Comparison of the caspase-3/D3.4 structure with caspase-3 in complex with XIAP and DEVD

The overall structure of caspase-3 is identical to several other caspase structures with rmsd values of 0.39 Å and 0.352 Å, respectively, when comparing the caspase-3/D3.4 structure with the 1.06 Å resolution caspase-3/z-DEVD-cmk (2DKO, [26]) and the caspase-3/XIAP complex structures (1I3O, [25]). Differences between caspase-3/D3.4 and the caspase-3/z-DEVD-cmk structures are observed in the active site pocket. In the caspase-3/D3.4 structure loop-4 of caspase-3 has moved approximately 1 Å out of the active site, whereas Thr166 has moved into the active site compared to the caspase-3/z-DEVD-cmk structure (Figure 6A). The movement of Thr166 is a consequence of the 120° rotation of the Tyr204 side chain. In the caspase-3/z-DEVD-cmk structure Tyr204 points towards Thr166, whereas in the caspase-3/D3.4 complex the Tyr204 side chain occupies the P2 pocket (Figure 6A).

Interestingly, the conformations of Tyr204, Thr166 and loop-4 in the caspase-3/D3.4 complex structure resemble the conformations in the caspase-3/XIAP structure (1I3O) (Figure 6B). In both complexes Tyr204 occupies the S2 pocket and consequently the side chains of Thr166 superimpose well [25]. Furthermore, Tyr204 rests against a hydrophobic patch of the inhibitor, which is formed by Leu141 and Val146 in XIAP and by Ala46 and Ile78 in D3.4 (Figure 6B).

Modeled structure of the caspase-3/D3.8 complex

Based on the sequence alignment and the competitive inhibition we assume that both D3.4 and D3.8 bind to the same epitope with similar interactions. We were not able to crystallize the caspase-3/D3.8 complex and thus calculated a homology model of D3.8 based on a N3C DARPin structure (DARPin E3_5, 1MJ0, [27]). This homology model was aligned with the caspase-3/D3.4 crystal structure (Figure 6C). D3.4 lacks the first internal repeat so that the N-cap of D3.4 was superimposed with the first internal repeat of D3.8 (Figure 6C). D3.8 has two mutations (L56S and S76R) in the interface which are possibly involved in the interaction with caspase-3. All other amino acid changes between D3.4 and D3.8 are located more than 4

Å away from caspase-3. The homology model showed that the Lys56…Asp253 salt bridge is missing in the D3.8/caspase-3 complex (Figure 6D). In D3.8, Lys56 is replaced by serine, which is unable to form a salt bridge as observed in the caspase-3/D3.4 structure. The positive charge of Lys56 in D3.4 may also lead to repulsive interactions with His255 of caspase-7 at the top of loop-4 (Figure 6D). D3.8 in contrast, possesses a weak affinity for caspase-7 which is possibly caused by the L56S mutation. The deletion of a positive charge in caspase-7 is compensated by the positive charge of His255 in caspase-7.

Mutant D3.4_S76R

D3.8 binds caspase-3 with higher affinity and has a lower inhibition constant (K_i= 3.42 nM). Residue Ser76 in D3.4 is located in proximity to the interface but does not interact with caspase-3. Because a bulkier side chain such as Arg, as it is observed in D3.8, could participate in an extended DARPin/caspase-3 interface, we generated the D3.4_Ser76Arg (D3.4_S76R) mutant and characterized its functional and structural properties. The D3.4_S76R mutant has a dissociation and inhibitory constant of K_D^{S76R} = 5.99 ± 0.47 nM and K_i^{S76R} = 3.49 ± 0.03 nM, respectively. Thus, D3.4 Ser76Arg shows an even lower inhibitory constant for caspase-3 compared to D.3.8 (Table 1).

The 2.1 Å resolution crystal structure of the caspase-3/D3.4 Ser76Arg complex revealed that although the overall structure is identical to the caspase-3/D3.4 structure (rmsd of 0.198 Å), the C-terminal capping repeat has shifted by approximately 2 Å (Figure 6E). The newly introduced Arg76 forms two intra-molecular hydrogen bonds with Gly80-O and Gln109-O of the C-terminal capping repeat and an inter-molecular hydrogen bond with Gly60-O of the caspase (Figure 6E). In addition, the weak hydrogen bond between Lys111 and Thr166 as it is seen in the parent structure is broken and Lys111 points into the active site forming an intra-molecular hydrogen bond with Ile78-O and a water-mediated hydrogen bond with Gly165-O of caspase-3. The mediating water molecule is located in direct vicinity of the active site Cys163 (Figure 6E).

Discussion

The development of specific caspase inhibitors has remained a challenging task, due to the similarity between the active sites of caspases. Although the selectivity of caspases for short peptide inhibitors that differ in the P4 positions is well established [28], their selectivity is often insufficient considering the different amounts of active caspases in cells undergoing apoptosis [29]. In 2007 Schweizer *et al*. published the first truly specific caspase inhibitor (AR_F8) which inhibits caspase-2 with an allosteric mechanism by interacting with loop-4 [24].

Using the same technology [13], we identified four caspase-3 DARPins of which two specifically inhibited the enzyme. Kinetic analysis characterized D3.4 and D3.8 as purely competitive inhibitors, corresponding well with the structural findings that show how D3.4 recognizes loop-4 of caspase-3 and occupies the active site substrate binding pocket. The caspase-2 directed DARPin AR_F8 also recognized loop-4, but demonstrated a significant part of uncompetitive inhibition. The different inhibition modes of D3.4 and AR_F8 can be explained by the different epitopes on the caspases. AR_F8 recognizes caspase-2 from the backside of loop-4 and stabilizes a distinct conformation which is not able to bind the substrate, whereas D3.4 binds straight into the active site of caspase-3. Our analysis further showed that D3.4 prevents substrates from accessing the catalytic Cys163 and leaves the conformation of loop-4 almost undisturbed when compared to the caspase-3 inhibitor structure.

Another finding of our study was the superior inhibition of caspase-3 by the closely related D3.8 which inhibits caspase-3 even better than D3.4, however, D3.8 was found to have some residual affinity for caspase-7, probably resulting from Ser56.

DARPin molecules D3.6 and D3.13 bind caspase-3 but do not inhibit hydrolysis and were thus not further analyzed. The IC_{50} value for the inhibition of caspase-7 by D3.8 can be estimated to be in the lower micro-molar range, based on data given in Figure 2. Thus, even inhibitors with a significantly extended interaction surface compared to tetrapeptide inhibitors

can in principle be recognized by the closely related caspases-7, albeit with affinity constants that differ by at least three orders of magnitude. Our inhibition studies using PARP-1 as a caspase substrate revealed that the selected DARPins inhibit the cleavage of PARP-1 specifically. However, the irreversible peptide inhibitor Ac-DEVD.fmk inhibited caspase-3 completely in contrast to the DARPins which reduced the activity of caspase-3 by approximately 50 % even in a 150 fold excess. This can be explained by the fact, that the caspase-3/DARPin complexes exist in an equilibrium and a small fraction of unbound active caspase-3 is sufficient to cleave PARP-1 over a relatively long incubation time of 20 minutes.

Our data suggest that D3.4 and D3.8 bind to the same caspase-3 epitope, since residues that seem to be crucial for the recognition of this epitope, such as Asp45, Ala46, Val48, Ile78, Trp79 and Arg81, are conserved in both molecules. Our crystal structure revealed that D3.4 recognizes caspase-3 by a set of specific hydrogen bonds, salt bridges and hydrophobic contacts. Particularly interesting are the interactions formed by Asp45, which occupies the S4 pocket. So far all structurally characterized caspase-3 specific peptide inhibitors harbor an aspartic acid that occupies this pocket (Figure 7). Although the hydrogen bonding networks are different in the structures of caspase-3 in complex with D3.4, z-DEVD-cmk or XIAP, the positive electrostatic potential explains the preference for a small and negatively charged hydrogen bonding partner like aspartate. Further similarities between the complex structures of caspase-3 with D3.4 and XIAP are seen for Tyr204 (Figure 7). In both structures the Tyr204 side chain points towards Arg341, placing the phenyl ring at van der Waals distance to Cys163-Sγ. On the opposite side the Tyr204 phenyl ring rests against a hydrophobic core, which is composed of caspase-3 residues Leu168 and Phe256 and the side chains of Ala46 and Ile78 from D3.4 or Leu141 and Val146 from XIAP. D3.4 and XIAP are both lacking an aspartic acid that could occupy the S1 pocket of caspase-3, which consequently is filled by water molecules. The same conformation of Tyr204 is also seen in several other structures of caspase-3 in complex with low molecular weight inhibitors that are lacking a P1 aspartate [30, 31]. Conversely, this conformation is different from classical tetrapeptide inhibitors, where the Tyr204 side chain rests against the side chain of Thr166 [26].

The small molecule inhibitor z-DEVD.cmk and D3.4 both run anti-parallel to caspase-3 residues 204-208. The S_4 pocket of caspase-3 is occupied by Asp1 and Asp45 of z-DEVD.cmk and D3.4 respectively and the S_3-S_1 pockets are occupied by residues continuing towards the C-terminus. The main chain of XIAP in contrast runs parallel to caspase-3 with Val 146 and Asp148 binding into the S2 and the S4 pocket respectively. Although the main chains of D3.4 and XIAP run in opposite directions, both inhibitors use very similar interactions to inhibit caspase-3 (Figure 7). Thus, the comparison of the caspase-3/D3.4 crystal structure with the caspase-3/XIAP crystal structure provides an interesting example for the molecular mimicry of natural and designed caspase-3 inhibitors.

In summary, our study presents the development and characterization of a caspase-3 inhibitory DARPin with implications for specificity and inhibition mechanism. D3.4 and the improved variant D3.4_S76R are the first truly specific caspase-3 inhibitors and do not bind its close paralog caspase-7 or any other caspase. The selected DARPin is entirely competitive and prevents substrate binding by directly competing with the substrate. A remarkable finding was that this DARPin inhibits caspase-3 with a similar mechanism compared to XIAP, the natural caspase-3 inhibitor which also inhibits caspase-7. It has previously been postulated that specificity is achieved by two key factors, allosteric regulation and scanning of large volumes of conformational space [32]. While the second aspect holds true, we demonstrate here that specificity can be achieved even when the conserved active site is targeted, provided this is combined with specific surface recognition outside the active site.

Methods

DARPin selection with Ribosome Display

We performed 4 rounds of ribosome display to enrich caspase-3 specific binders based on a N3C and N2C library as described before [15, 33]. Prior to each selection the DARPin-ribosome-mRNA complex was incubated with the closest homologous of caspase-3 (caspase-6 and -7) and Streptavidin for 30 minutes at 4 °C to avoid selection of unspecific DARPins. Biotinylated caspase-3 was immobilized on magnetic particles (Dynabeads, Invitrogen) for solution panning. The DARPin-ribosome-mRNA complex was incubated with 20 µl of beads for 30 minutes at 4 °C in a tube that was previously blocked with TBST-BSA (50 mM TrisHCl pH 7.4, 150 mM NaCl, 0.05 % Tween-20, 0.1 % BSA). The incubation was followed by 4 washing cycles in WBT (50 mM Tris acetate pH 7.4, 150 mM NaCl, 50 mM Magnesium acetate, 0.05 % Tween-20). The RNA was eluted in EB (50 mM Tris acetate pH 7.4, 150 mM NaCl, 25 mM EDTA) and purified and reverse transcribed for amplification for the next selection round. In round three and four we added a 1000 fold excess of unbiotinylated caspase-3 for 10 minutes during the selection to favor the enrichment of DARPins with slow k_{off} rates. After four rounds of selection, we cloned the library in a pQE30 vector (Qiagen), transformed competent XL1 blue cells (Stratagene) and continued with crude cell extract ELISA.

Crude cell extract ELISA

Single colonies each containing one DARPin clone of the selected library were picked and inoculated in 0.9 ml auto-inducing media 5052 [34] containing deep 96-well plates (Abgene, UK). The cells were grown over night at 37 °C while shaking at 300 rpm in a shaker (TH15, Edmund Bühler GmbH). Then 200 µl of each well were transferred into a sterile 96 well plate (449824, Nunc) as a backup for further protein expression and plasmid preparation. The remaining 700 µl of cell-suspension was harvested by centrifugation and the cell pellet was lysed with 50 µl B-PER II (78260, Pierce) per well for 30 minutes shaking at room

temperature. The lysed cells were resuspended by adding 950 µl PBS, pH 7.3 and cell debris was removed by centrifugation (20 min, 4500 rpm at 4°C) in a table top centrifuge 5804 (Eppendorf). We now took 20 µl of the supernatant of four 96 well plates and transferred it to one 384 well ELISA plate (464718, Nunc). This plate has been previously coated with 20 µl of a 22 nM Neutravidin solution (Pierce, 31000) and biotinylated caspase-3, followed by extensive washing. After 1h of incubation at room temperature and 3 washing cycles the plate was incubated with mouse anti-RGS-H_4 antibody (34650, Qiagen) at a dilution of 1:2000 in PBS 1% BSA. We then added the secondary antibody (goat-α-mouse IgG alkaline phosphatase conjugate (Sigma, A3562)) followed by four washing cycles and added the substrate di-sodium 4-nitrophenyl phosphate (pNPP; 3 mM di-sodium 4-nitrophenyl phosphate, 50 mM NaHCO3, 50 mM MgCl2.6H2O). The OD was measured at 405 nm using a multi-well plate reader (Infinite M1000, Tecan).

Expression, purification and biotinylation of Proteins

All DARPins were expressed in auto-inducing media [34] or lysogeny broth media (LB) [13]. The expressed DARPin was purified with common His-tag purification methods using a self-made gravity column consisting of a plastic column (57024, Supelco) and 0.5 ml bead volume of Ni^{2+}-NTA agarose (30210, Qiagen). The DARPins were eluted in PBS, 200 mM Imidazole pH 7.4 and the Imidazole was removed with a PD-10 desalting column (17-0435-01, GE Helthcare). We added sodium azide (NaN_3) to a final concentration of 0.03% to prevent growth of bacteria and fungi. The DARPins solution was further stored at 4 °C. Protocols on expression, purification and characterization of human caspase-1 to caspase-9 are published elsewhere [35].

For chemical biotinylation of the caspase we used the linker EZ-Link Sulfo-NHS-LC-LC-Biotin (21338, Pierce), containing a reactive group, a 3.05 nm long linker and a biotin moiety. After purification, 1ml of the caspase (10 µM) in PBS pH 7.3 was incubated with a seven fold molar excess (1 ml of a 70 µM solution) of biotin on ice for 30 minutes. The reaction was

quenched by adding 10 µl of 5M Tris-HCl, pH 7.5. The biotinylated protein was then purified by size exclusion chromatography, using a Superdex 200 10/300 GL (GE Healthcare) in PBS at 4 °C. The fractions containing the biotinylated caspase were pooled and frozen in liquid nitrogen after adding sucrose to a final concentration of 10 %.

Crystallization, Data Collection and structure modeling

Crystallization

The caspase/DARPin complexes were formed by incubating caspase-3 with a two-fold molar excess of each DARPin for 10 minutes on ice. The complex was purified by size exclusion chromatography (Superdex 200 HR 10/30, Amersham Pharmacia, Sweden) in 50mM Tris pH 8.0 (4 °C), 50 mM NaCl. The samples containing the caspase/DARPin complex were concentrated to 5 mg/ml and 10 mg/ml for D3.4 and D3.4_S76R respectively, using a centrifugal filter device with a molecular weight limit of 15 kDa (Amicon Ultra, Millipore).

Crystals were grown at room temperature using the vapor-diffusion method. 2 µl of concentrated protein solution (5 mg/ml and 10 mg/ml for D3.4 and D3.4_S76R respectively) were mixed with 1 µl of reservoir solution containing 100 mM HEPES buffer, pH 7.3, 70% (v/v) 2-Methyl-2,4-pentanediol (MPD). The mixture was stored at 20 °C and crystals appeared within 24 hours.

Data Collection, Structure Determination and Refinement

Crystals were flash frozen in liquid nitrogen for diffraction analysis and data collection at 100K. No cryoprotectant was necessary for data collection. X-ray diffraction data were collected at the Swiss Light Source (SLS) at the X06SA beamline equipped with a Pilatus 6M fast readout pixel detector (Dectris, Switzerland). XDS was used for data processing and data were scaled with XSCALE [36]. Structure factors were calculated with IDXREF [37]. Both complexes crystallized in the space group $P3_121$. Unit cell dimensions are listed in Table 2. The structures were solved by molecular replacement with the program PHASER [38] using a

high resolution structure of caspase-3 (2DKO, [26]) and a modeled N2C DARPin. The N2C DARPin was generated by homology modeling (MODELLER 9v8 [39]) using the N3C DARPin E3_5 (1MJ0, [27]) as a template. The crystals have a solvent content of 59 % (Matthews coefficient = 3) [40] with two caspase-3 heterodimers bound to two DARPins in the asymmetric unit. Alternating rounds of manual building using COOT [41] and restrained refinement with TLS groups using REFMAC 5.5.01.09 [42]. Water molecules were introduced in the last phase of refinement. The final refinement step we obtained Rfree/Rwork values of 0.185/0.217 for the caspase-3/D3.4 complex and 0.174/0.214 for the caspase-3/D3.4_S76R complex. Data collection and structure refinement statistics are listed in Table 2. Structural superposition was done using COOT [41] and figures were prepared using PyMOL [43].

Site directed Mutagenesis

We used the QuikChange® Site Directed Mutageneis Kit (Stratagene) to incorporate mutations in the DARPin sequence. The following Primers were used to mutate D3.4 to D3.4_S76R fwd: 5'-GGT GCT GAC GTT AAC GCT CGT GAC ATT TGG GGT CGT ACT-3' rev: 5'-AGT ACG ACC CCA AAT GTC ACG AGC GTT AAC GTC AGC ACC-3'. Codon which is underlined indicates the mutation.

SPR measurements

For SPR experiments we used the Proteon XPR36^{TM} (Bio-Rad Laboratories, Inc.) and a NLC sensor chip (Bio-Rad Laboratories, Inc.). We used sterile filtered PBS pH 7.3, 0.005% Tween-20 as a standard buffer for coating and all kinetic measurements. The biotinylated ligand (caspase) was coated on the sensor chip at a concentration of 5 nM and a flow rate of 30 µl per minute. The coating procedure was interrupted once a total of 1000 relative units (RU) were reached on the monitoring system. A dilution series of the analyte (DARPin) was pipetted in 96 deep well microplates (176-6023, Biorad), which were sealed to prevent evaporation or contamination with dust particles. For Kinetic analysis we measured the

analyte at eight different concentrations (0, 0.176, 0.52, 1.58, 4.47, 14.2, 42.6, 128 nM) starting with the lowest concentration. All experiments were performed at 20 °C. We used a flow rate of 100 µl per minute, an association time of 3 minutes and a dissociation time of 20 minutes. The data were recorded and further processed with the ProteOn Manager 2.1.1™ (BioRad). The K_D, k_{on} and k_{off} values were determined using the data analysis tool provided by the ProteON Manager™ 2.1.1 using the heterogeneous ligand model and equilibrium constants [44].

Caspase activity measurements

Specific inhibition of caspase-1 to caspase-9 was measured using peptide substrates from PEPTIDE INSTITUTE Inc. We used AC-DEVD-AMC for caspase-3, -6, -7 and -8, AC-WEHD-AMC for caspase-1, -4 and -5, AC-VDVAD-AMC for caspase-2 and AC-LEHD-AMC for caspase-9. Enzyme and substrate concentrations in the assay were as following considering each caspase as a dimer: caspase-1 (10 nM enzyme; 150 µM substrate), caspase-2 (25 nM; 150 µM), caspase-3 (0.5 nM; 150 µM), caspase-4 (200 nM; 600 µM), caspase-5 (10 nM; 150 µM), caspase-6 (10 nM; 600 µM), caspase-7 (2 nM, 400 µM), caspase-8 (10 nM; 150 µM and caspase-9 (25 nM, 600 µM). DARPin was added in the according molar ratio calculated per caspase active site. For caspase-2 we used 100 mM MES, pH 6.5, 10% PEG600 (w/v), 0.1% CHAPS (w/v), 10 mM DTT and caspase-9 activity was monitored in 50 mM Tris, pH 7.5, 10% Sucrose (w/v) and 1.3 M NaCitrate. For all other caspases we used 20 mM PIPES, pH 6.5, 10% Sucrose (w/v), 0.1% CHAPS (w/v), 10 mM DTT, 150 mM NaCl, 1mM EDTA. AMC release was monitored by measuring the fluorescent at λex = 360 nm and λem = 465 nm using a spectrofluorometer (Infinite M-1000, Tecan).

Specific velocity plot

Inhibition mechanism and K_i values of D3.4, D3.8 and D3.4_S76R have been determined using the specific velocity plot [22] and inhibitor titration. The concentration of caspase-3 was

determined by active site titration as described previously [9]. The caspases inhibitor AC-DEVD-CMK (0-7.6 nM), caspase-3 (~0.5 nM) and the substrate AC-DEVD-AMC (100 μM) were prepared in activity buffer containing no DTT [20 mM PIPES, pH 6.5, 10% Sucrose (w/v), 0.1% CHAPS (w/v), 10 mM DTT, 150 mM NaCl, 1mM EDTA]. Concentrations of DARPins have been determined using amino acid analysis at the Functional Genomic Center, Zurich. The initial velocities of substrate hydrolysis with 0.5 nM caspase-3 (Dimer) have been measured with different DARPin concentrations (D3.4: 8-32 nM, D3.4_S76R: 4-10 nM, D3.8: 2-8 nM) and substrate concentration between 0.2 – 0.8 times K_m (K_m = 24.7 ± 1.8 μM). Graphical analysis of the velocity plot was done with Prism5 (GraphPad Software). The inhibitor titration has been performed using 0.5 nM caspase-3 (Dimer), different DARPin concentrations (D3.4: 0-1000 nM, D3.4_S76R: 0-1000 nM, D3.8: 0-100 nM) and 24 μM substrate. Initial velocities have been fitted according to tight binding inhibition equation which has been described previously [45] to determine K_i values of inhibitor DARPins.

PARP-1 inhibition and Western Blot analysis

A 0.15 μM solution of PARP-1 [50 mM Tris pH 7.5, 150 mM NaCl] was obtained by Prof. Hottiger (University of Zurich) and mixed with caspase-3 or -7 (1.5 μM) and the according DARPin (4.5 to 225 μM) as indicated in Figure 2. The reaction was incubated for 20 minutes at 37°C in 50 mM Tris pH 7.5, 150 mM NaCl, 0.5 mM DTT and stopped by adding SDS sample buffer and heating to 95°C for 5 minutes. The samples were further analyzed by Western Blot analysis.

Western Blot analysis

The sample was subjected onto a 12% SDS-PAGE under reducing conditions for separation and transferred to a nitrocellulose membrane (iBlot®, Invitrogen). The membrane was blocked in High-TBS [50 mM Tris pH 7.5, 500 mM NaCl] containing 5 % w/v nonfat dry milk over night at 4° C. The primary antibody anti-PARP (Cell Signalling, 9542) was

incubated with the membrane in a 1:1000 dilution in High-TBS-T [50 mM Tris pH 7.5, 500 mM NaCl, 0.1 % Tween-20] at 4°C over night. After intensive washing in High-TBS-T we incubated the membrane with anti-rabbit HRP conjugated antibody (Cell Signalling, #7074) for 1 h at room temperature in TBS [50 mM Tris pH 7.5, 150 mM NaCl]. For the chemiluminescent detection we used the SuperSignal West Pico Chemiluminescent Substrate (Piercenet) and recorded the emitted light with a CCD camera.

Modeling of D3.8

Based on inhibition measurements and the sequence alignment, we hypothesized that D3.8 binds to the same epitope as D3.4. We therefore calculated a model of D3.8 in complex with caspase-3. The N3C DARPin E3_5 (PDB entry code 1MJ0) [27] was used as a template to calculate a homology model of D3.8 using the program MODELLER 9v8 [39]. The model of D3.8 was then aligned and superimposed with the structure of the caspase-3/D3.4 crystal structure based on the sequence alignment shown in Figure 1.

Acknowledgements

This work was supported by the Swiss National Science Foundation grant 310030-122342 to M.G.G. We acknowledge Prof. Hottiger for providing samples of PARP-1 for the caspase-3 in vitro inhibition studies. We acknowledge Antonio Baici for discussions and support in the kinetic evaluation of our experiments. Data collection was performed at the Swiss Light Source of the Paul Scherrer Institute. SPR kinetics was measured at the Functional Genomics Center Zurich. T.S. is member of the Molecular Life Science Ph.D. program at the ETH/University of Zurich. A.F. is member of the Biomolecular Structure Ph.D. program at the ETH/University of Zurich.

Competing financial interests

The authors declare that they have no competing financial interest.

References

1. **Wyllie, A.H., J.F. Kerr, and A.R. Currie, *Cell death: the significance of apoptosis.* International review of cytology, 1980. 68: p. 251-306.**
2. **Riedl, S.J. and Y. Shi, *Molecular mechanisms of caspase regulation during apoptosis.* Nature reviews. Molecular cell biology, 2004. 5(11): p. 897-907.**
3. **Earnshaw, W.C., L.M. Martins, and S.H. Kaufmann, *MAMMALIAN CASPASES: Structure, Activation, Substrates, and Functions During Apoptosis.* Annual Review of Biochemistry, 1999. 68(1): p. 383-424.**
4. **Grutter, M.G., *Caspases: key players in programmed cell death.* Current Opinion in Structural Biology, 2000. 10(6): p. 649.**
5. **Riedl, S.J. and Y. Shi, *Molecular mechanisms of caspase regulation during apoptosis.* Nat Rev Mol Cell Biol, 2004. 5(11): p. 897-907.**
6. **Nicholson, D.W., et al., *Identification and inhibition of the ICE/CED-3 protease necessary for mammalian apoptosis.* Nature, 1995. 376(6535): p. 37-43.**
7. **Mittl, P.R.E., et al., *Structure of Recombinant Human CPP32 in Complex with the Tetrapeptide Acetyl-Asp-Val-Ala-Asp Fluoromethyl Ketone.* J. Biol. Chem., 1997. 272(10): p. 6539-6547.**
8. **Rotonda, J., et al., *The three-dimensional structure of apopain/CPP32, a key mediator of apoptosis.* Nat Struct Biol, 1996. 3(7): p. 619-25.**
9. **Stennicke, H.R., et al., *Internally quenched fluorescent peptide substrates disclose the subsite preferences of human caspases 1, 3, 6, 7 and 8.* Biochem J, 2000. 350 Pt 2: p. 563-8.**
10. **McStay, G.P., G.S. Salvesen, and D.R. Green, *Overlapping cleavage motif selectivity of caspases: implications for analysis of apoptotic pathways.* Cell Death Differ, 2008. 15(2): p. 322-31.**
11. **Roy, N., et al., *The c-IAP-1 and c-IAP-2 proteins are direct inhibitors of specific caspases.* Embo J, 1997. 16(23): p. 6914-25.**
12. **Deveraux, Q.L., et al., *X-linked IAP is a direct inhibitor of cell-death proteases.* Nature, 1997. 388(6639): p. 300-4.**
13. **Binz, H.K., et al., *Designing repeat proteins: well-expressed, soluble and stable proteins from combinatorial libraries of consensus ankyrin repeat proteins.* J Mol Biol, 2003. 332(2): p. 489-503.**

14. **Steiner, D., et al.,** ***Signal sequences directing cotranslational translocation expand the range of proteins amenable to phage display.*** **Nat Biotechnol, 2006. 24(7): p. 823-31.**

15. **Zahnd, C., P. Amstutz, and A. Pluckthun,** ***Ribosome display: selecting and evolving proteins in vitro that specifically bind to a target.*** **Nat Methods, 2007. 4(3): p. 269-79.**

16. **Binz, H.K., P. Amstutz, and A. Pluckthun,** ***Engineering novel binding proteins from nonimmunoglobulin domains.*** **Nat Biotechnol, 2005. 23(10): p. 1257-68.**

17. **Amstutz, P., et al.,** ***Intracellular kinase inhibitors selected from combinatorial libraries of designed ankyrin repeat proteins.*** **J Biol Chem, 2005. 280(26): p. 24715-22.**

18. **Sennhauser, G., et al.,** ***Drug export pathway of multidrug exporter AcrB revealed by DARPin inhibitors.*** **PLoS Biol, 2007. 5(1): p. e7.**

19. **Schweizer, A., et al.,** ***CD4-specific designed ankyrin repeat proteins are novel potent HIV entry inhibitors with unique characteristics.*** **PLoS Pathog, 2008. 4(7): p. e1000109.**

20. **Zahnd, C., et al.,** ***Efficient tumor targeting with high-affinity designed ankyrin repeat proteins: effects of affinity and molecular size.*** **Cancer Res, 2010. 70(4): p. 1595-605.**

21. **Morton, T.A., D.G. Myszka, and I.M. Chaiken,** ***Interpreting complex binding kinetics from optical biosensors: a comparison of analysis by linearization, the integrated rate equation, and numerical integration.*** **Anal Biochem, 1995. 227(1): p. 176-85.**

22. **Baici, A.,** ***The specific velocity plot. A graphical method for determining inhibition parameters for both linear and hyperbolic enzyme inhibitors.*** **European journal of biochemistry / FEBS, 1981. 119(1): p. 9-14.**

23. **Lazebnik, Y.A., et al.,** ***Cleavage of poly(ADP-ribose) polymerase by a proteinase with properties like ICE.*** **Nature, 1994. 371(6495): p. 346-7.**

24. **Schweizer, A., et al.,** ***Inhibition of caspase-2 by a designed ankyrin repeat protein: specificity, structure, and inhibition mechanism.*** **Structure, 2007. 15(5): p. 625-36.**

25. **Riedl, S.J., et al.,** ***Structural basis for the inhibition of caspase-3 by XIAP.*** **Cell, 2001. 104(5): p. 791-800.**

26. **Ganesan, R., et al.,** ***Extended substrate recognition in caspase-3 revealed by high resolution X-ray structure analysis.*** **J Mol Biol, 2006. 359(5): p. 1378-88.**

27. **Kohl, A., et al.,** ***Designed to be stable: crystal structure of a consensus ankyrin repeat protein.*** **Proc Natl Acad Sci U S A, 2003. 100(4): p. 1700-5.**

28. **Thornberry, N.A., et al.,** ***A combinatorial approach defines specificities of members of the caspase family and granzyme B. Functional relationships established for key mediators of apoptosis.*** **J Biol Chem, 1997. 272(29): p. 17907-11.**

29. **Berger, A.B., K.B. Sexton, and M. Bogyo,** ***Commonly used caspase inhibitors designed based on substrate specificity profiles lack selectivity.*** **Cell research, 2006. 16(12): p. 961-3.**

30. **Ganesan, R., et al.,** ***In silico identification and crystal structure validation of caspase-3 inhibitors without a P1 aspartic acid moiety.*** **Acta crystallographica. Section F, Structural biology and crystallization communications, 2011. 67(Pt 8): p. 842-50.**

31. **Agniswamy, J., B. Fang, and I.T. Weber,** ***Conformational similarity in the activation of caspase-3 and -7 revealed by the unliganded and inhibited structures of caspase-7.*** **Apoptosis : an international journal on programmed cell death, 2009. 14(10): p. 1135-44.**

32. **Salvesen, G.S. and S.J. Riedl,** ***Caspase inhibition, specifically.*** **Structure, 2007. 15(5): p. 513-4.**

33. **Binz, H.K., et al.,** ***High-affinity binders selected from designed ankyrin repeat protein libraries.*** **Nat Biotechnol, 2004. 22(5): p. 575-82.**

34. **Studier, F.W.,** ***Protein production by auto-induction in high density shaking cultures.*** **Protein Expr Purif, 2005. 41(1): p. 207-34.**

35. **Heidi Roschitzki-Voser, T.S., Franziska Fröhlich, Esther Lenherr, Andreas Schweizer, Peer R.E. Mittl, Antonio Baici, Markus Grütter,** ***Expression, Purification and Kinetic Characterisation of Human Caspases*****. 2011.**

36. **Kabsch, W.,** ***Integration, scaling, space-group assignment and post-refinement.*** **Acta crystallographica. Section D, Biological crystallography, 2010. 66(Pt 2): p. 133-44.**

37. **Potterton, E., et al.,** ***A graphical user interface to the CCP4 program suite.*** **Acta crystallographica. Section D, Biological crystallography, 2003. 59(Pt 7): p. 1131-7.**

38. **McCoy, A.J., et al.,** ***Phaser crystallographic software.*** **Journal of applied crystallography, 2007. 40(Pt 4): p. 658-674.**

39. **Eswar, N., et al.,** ***Comparative protein structure modeling using MODELLER.*** **Current protocols in protein science / editorial board, John E. Coligan ... [et al.], 2007. Chapter 2: p. Unit 2 9.**

40. ***The CCP4 suite: programs for protein crystallography.*** **Acta Crystallogr D Biol Crystallogr, 1994. 50(Pt 5): p. 760-3.**

41. **Emsley, P., et al.,** ***Features and development of Coot.*** **Acta Crystallogr D Biol Crystallogr, 2010. 66(Pt 4): p. 486-501.**

42. **Murshudov, G.N., A.A. Vagin, and E.J. Dodson,** ***Refinement of macromolecular structures by the maximum-likelihood method.*** **Acta crystallographica. Section D, Biological crystallography, 1997. 53(Pt 3): p. 240-55.**

43. **Schrodinger, LLC,** ***The AxPyMOL Molecular Graphics Plugin for Microsoft PowerPoint, Version 1.0.*** **2010.**

44. **Bravman, T., et al.,** ***Exploring "one-shot" kinetics and small molecule analysis using the ProteOn XPR36 array biosensor.*** **Anal Biochem, 2006. 358(2): p. 281-8.**

45. **Szedlacsek, S.E., et al.,** ***A re-evaluation of the kinetic equations for hyperbolic tight-binding inhibition.*** **Biochem J, 1988. 254(1): p. 311-2.**

Figure legends

Figure 1. Sequence alignment of caspase-3 specific DARPin binders

The general DARPin sequence is shown with the consensus (black) and the randomized amino acid positions (red x, any of the 20 natural amino acids except cysteine, glycine or proline; z, any of the amino acids asparagine, histidine or tyrosine). Four DARPin sequences are aligned to the consensus sequence with identical residues represented as a dot and different residues are highlighted by the respective residue acronym. Amino acids involved in the interaction with caspase-3 are colored in orange and differences in the sequence of DARPin_3.4 and DARPin_3.8 (green) are highlighted. A mutation we introduced in this study (DARPin_3.4S76R) is marked by a red box. The sequence number is based on DARPin_3.4, a N2C DARPin which lacks the first internal repeat.

Figure 2. Inhibition of caspase-3 dependent PARP-1 cleavage by DARPin inhibitors

The cleavage of PARP-1 by caspase-3 and -7 was observed on a 12 % SDS-PAGE (upper panel). PARP-1 and cleaved PARP-1 (cPARP-1) was detected by a specific antibody which recognized both forms. Cleavage of PARP-1 could be prevented by pretreating caspase-3 and -7 with a peptide inhibitor (DEVD.fmk). None of the selected DARPins cleave PARP-1. Caspase-3 and -7 have been pretreated with DARPin inhibitors to test the effect on PARP-1 cleavage. The DARPin was added with a 3, 15 or 150-fold molar excess and cleavage was monitored by SDS-PAGE. The selected DARPins do not inhibit the reaction of caspase-7. The catalytic efficiency of caspase-3 in contrast is clearly reduced and approximately 50 % of PARP-1 is cleaved after 20 minutes.

Figure 3. Specificity and inhibition of selected DARPins for caspase-3, -6 and -7

(A) The relative activity of caspase-3 in presence of four different DARPins (D3.4, D3.4_S76R, D3.8 and control DARPin E3_5) is shown. Each DARPin was added in three different concentrations indicated as X-fold molar excess per active site; 10x (black), 100x (light grey) and 1000x (grey). All DARPins inhibit the activity of caspase-3 with the

exception of the control DARPin E3_5. (B) and (C) The relative activity of caspase-6 and -7 in presence of four different DARPins as described in (A). The 1000-fold molar excess of DARPin was not measured for caspase-6 because no effect was visible at a 100-fold excess. D3.8 has a moderate inhibitory affect on caspase-7, all other DARPins are highly specific for caspase-3.

Figure 4. Structure of the caspase-3 in complex with different inhibitors

(A) Stereo view of a cartoon representation of the caspase-3/D3.4 complex. The two subunits of caspase-3 are colored in dark grey (large subunit) and light grey (small subunit), the active site forming loops L1 to L4 (red) and the catalytic residues (green) are highlighted. The D3.4 consists of two capping repeats (N-cap and C-cap; dark blue) and two internal repeats (1st and 2nd repeat, light blue). D3.4 binds in the active site and mainly interacts with loop-4 of caspase-3. (B) The caspase-2 specific DARPin AR_F8 (green, 2P2C) caspase-3/D3.4 structure has been superimposed, caspases are shown in a surface representation (grey). D3.4 (blue) and DARPin AR_F8 (green) both bind to active site loop-4 (red) covering different epitopes. (C) The BIR2-XIAP/caspase-3 structure (yellow, 1I3O) has been superimposed with the caspase-3/D3.4 structure. The C-terminal BIR2 domain of XIAP binds to an exosite on caspase-3 and inhibits the enzyme with the hook, line and linker substructures at the N-terminal. The DARPins repeats, XIAP substructures and loop-4 (red) are indicated.

Figure 5. Molecular Basis of the Interaction

Stereo view of the caspase-3/D3.4 interaction. D3.4 (blue) interacts with caspase-3 (large subunit, dark grey; small subunit, light grey) via hydrogen bonds (dotted line) and hydrophobic interactions. DARPin amino acid side chains are labeled with an additional (‘). The position of the active site cysteine (green) is shown. (A) Asp45’ forms several hydrogen bonds in the active site and binds in to the S4 pocket of caspase-3. Thr166 which is located close to the active site Cys163 forms two hydrogen bonds with the second repeat of the

DARPin (B) The concave site of DARPin_3.4 binds the tip of loop-4 through several hydrogen bonds. (C) Hydrophobic interactions of both molecules. Phe256 binds into a hydrophobic pocket formed by DARPin residues and forms T-stacking interactions with Trp79.

Figure 6. Structural Basis of DARPin_3.4 Binding and Inhibition

With the exception of caspase-3, the labels of all amino acid side chains contain a unique identifier (D3.4(‘), DEVD(°), XIAP(*), D3.4_S76R(^), D3.8($^{\Delta}$), caspase-7($^{\#}$)). (A) Superposition of the caspase-3/z-DEVD.fmk (green, 2DKO) structure and the caspase-3 (dark grey)/3.4 (blue) structure. Several structural differences can be observed. Tyr204 is rotated by approximately 120° in the DARPin bound structure. The position of Thr166 is shifted away from the active site due to the Tyr204 rotation. (B) Superposition of the caspase-3 (light grey)/XIAP_BIR2 (yellow, 1I3O) structure and the caspase-3 /D3.4 (colored as in A) structure. Both caspase-3 inhibitors use similar interactions for the inhibition. The conformation of Tyr204 is very similar in both structures and occupies the P2 pocket of capase-3. This is also the case for Asp45 which occupies the P4 pocket and forms a hydrogen bond with Asn208. (C) Model of D3.8 (dark red, salmon) is superimposed with D3.4 (blue, light blue) which binds to loop-4 (red) of caspase-3 (surface representation, grey). (D) The first internal repeat of D3.4 (blue) is superimposed with the second internal repeat of the modeled D3.8 (salmon) binding to loop-4 of caspase-3 (grey) and caspase-7 (green). Lys56’ forms two hydrogen bonds with Asp253 and causes repulsive interactions with His255$^{\#}$. Ser56$^{\Delta}$ in D3.8 lacks the hydrogen bonds to Asp253 and repulsive interactions to His255$^{\#}$. (E) Superposition of the caspase-3/D3.4 structure with the mutated D3.4_S76R. Surface (grey) and ribbon (black) representation of caspase-3 in complex with both DARPins (D3.4, dark blue; and D3.4_S76R green) is shown. Newly formed hydrogen bonds are indicated with white dotted lines (grey). The mutated residue Arg76^ forms a new hydrogen bond to Gly60-O (see also Table 3). Ile78^ and Lys111^ form new hydrogen bonds leading to structural changes in the flexible C-terminal capping repeat of D3.4.

Figure 7. Schematic representation of caspase-3 inhibition by different inhibitors

(A) The peptide inhibitor Ac-DEVD.fmk occupies the four substrate binding pockets (S1 – S4) of caspase-3 similar to binding of the natural substrate. (B) The BIR2 domain of XIAP occupies the S4 pocket of caspase-3 and Val146 (V) keeps Tyr204 in a position which occupies the S2 pocket. P1 is filled with water and binding of the hook leads to steric hindrance of substrate binding. The BIR2 domain runs in the opposite direction with the N-terminal at the S1 pocket and the C-terminal at the S4 pocket. (C) DARPin_3.4 (blue) uses a similar mechanism to inhibit caspase-3 compared the XIAP. Asp45 binds in the S4 pocket, Ile78 keeps Tyr204 in a locked conformation and S1 is filled with water. Steric hindrance of the 16 kDa DARPin prevents binding of the substrate.

Table 1. Kinetic constants and characteristics of the interaction

Table 2. X-ray data collection and model refinement statistics

Table 3. Hydrogen bonds of the caspase-3 interaction with DARPin_3.4

Supplementary Figures

Supplementary Figure 1.

SPR analysis of the five DARPins binding to caspase-3. Eight different concentrations (0, 0.176, 0.53, 1.6, 4.5, 14.2, 42.7, 128 nM) have been measured by the Proteon XPR on a NLC sensor chip. The relative units (RU) were recorded for the association (3 minutes) and dissociation phase (20 minutes).

Supplementary Figure 2. Characterization of the inhibition type of caspase-3 DARPins

Initial velocities and the specific velocity plot (small figure) are shown. The specific velocity plot shows the behavior of a competitive inhibitor with $\alpha = \infty$ and $\beta = 0$.

Supplementary Figure 3. SPR analysis of selected DARPins

Caspase-3 specific DARPins have been tested on binding against the close homologs caspase-6 and -7. All three caspases have been coated on a Proteon XPR36 NLC chip followed by testing of five DARPins. DARPin_6.21 and DARPin_7.1 are DARPins that have been selected against caspase-6 and -7 respectively. They were used a positive control, to show that the caspases are functional on the surface on the chip. All DARPins that were analyzed how a signal to their devoted caspase only, indicating how specific DARPins interact with their target proteins.

Supplementary Figure 4 Inhibition assay of different caspases

Inhibition assay of the selected DARPins against different caspases (caspase-1, -2, -4, -5, -8 and -9) as described in Figure 3.

Supplementary Figure 5. Binding of Asp45 in the S4 pocket of caspase-3

Surface representation of caspase-3 in complex with three different inhibitors superimposed in the active site. The peptide inhibitor DEVD (green), XIAP (yellow) and DARPin_3.4 (red) share a common mechanism and occupy the S4 pocket with an aspartic acid. Asp45 from the DARPin forms a hydrogen bond with Asn-ND2 and two water mediated hydrogen bonds.

Footnotes

Abbreviations Ac: Acetyl, AMC: 7-amino-4-methyl coumarin, BIR: Baculovirus IAP repeat, cmk: Chloromethyl ketone, LBHB: Low-barrier hydrogen bond, p12: Small subunit of caspase-3, p17: Large subunit of caspase-3, SMAC: Second mitochondrial activator of caspases, XIAP: X-linked inhibitor of apoptosis, Z/Cbz: Benzyloxycarbonyl

Coordinates Coordinates and structure factors have been be deposited to PDB under accession codes 2XZD, 2Y0B.

Figures

Figure 1

Figure 2

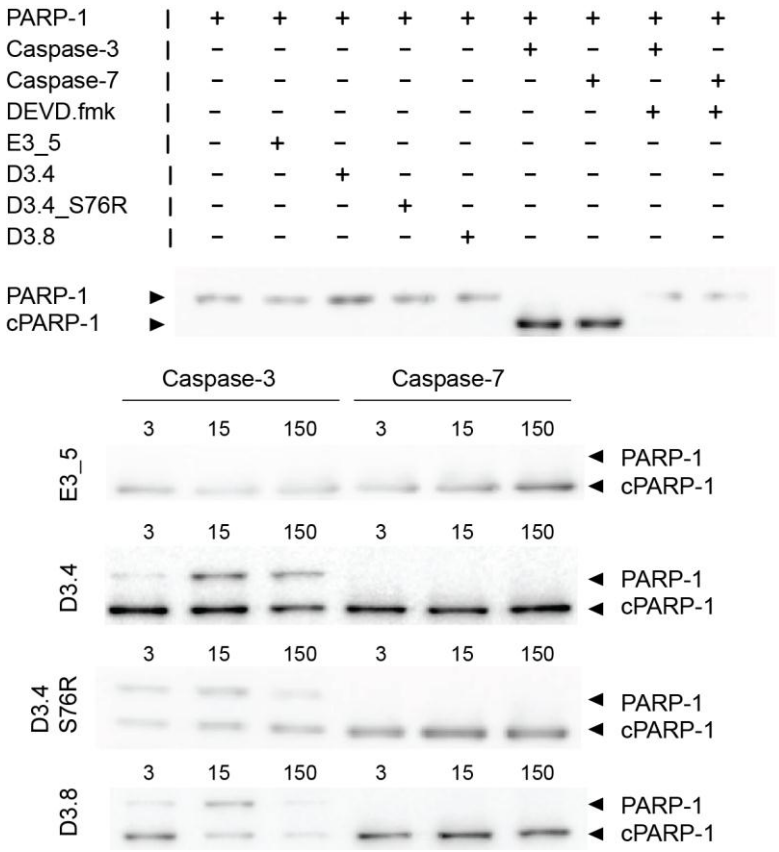
PARP-1 | + + + + + + + + + +
Caspase-3 | − − − − − + − + −
Caspase-7 | − − − − − − + − +
DEVD.fmk | − − − − − − − + +
E3_5 | − + − − − − − − −
D3.4 | − − + − − − − − −
D3.4_S76R | − − − + − − − − −
D3.8 | − − − − + − − − −
PARP-1
cPARP-1
Caspase-3
Caspase-7
3 15 150 3 15 150
E3_5
D3.4
D3.4 S76R
D3.8
PARP-1
cPARP-1

Figure 3A

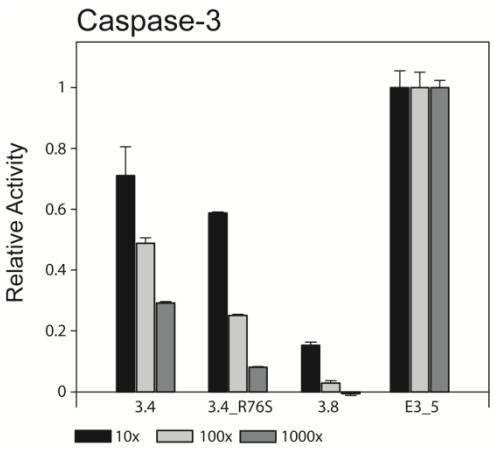

Figure 3B

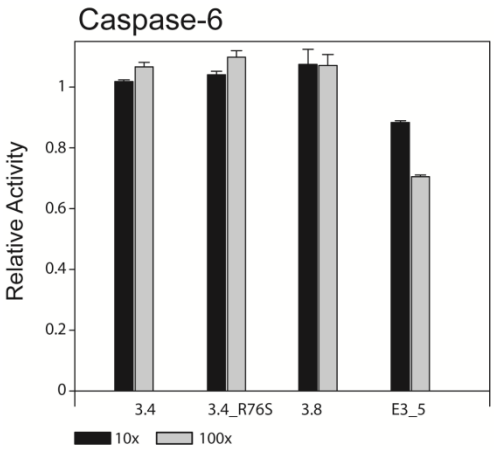

Figure 3C

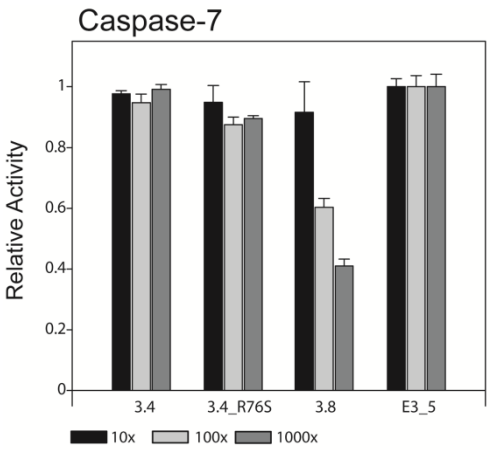

Figure 4A

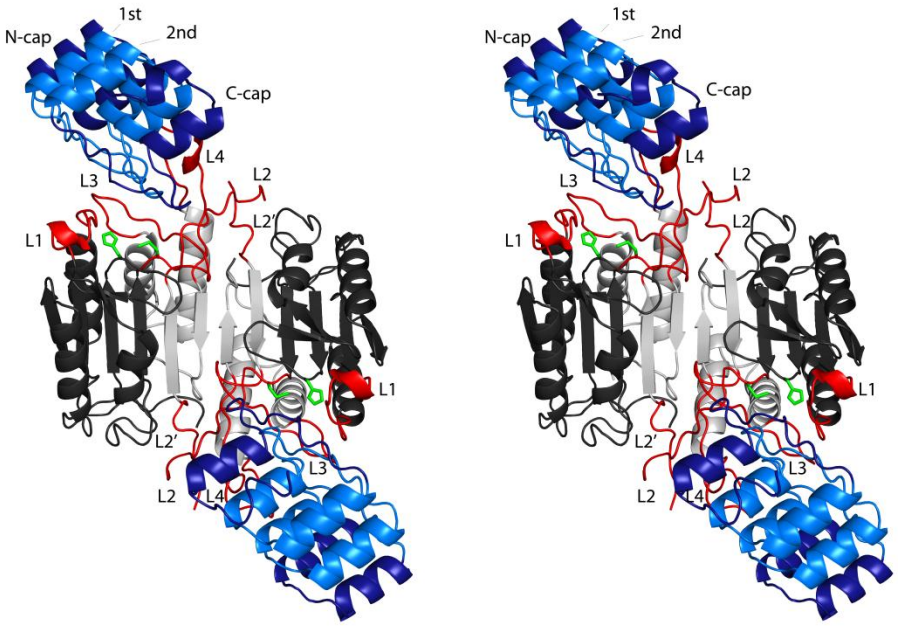
1st
N-cap
2nd
C-cap
L4
L3
L2
L2'
L1
L1
L2'
L3
L2
L4
1st
N-cap
2nd
C-cap
L4
L3
L2
L2
L1
L1
L2'
L3
L2
L4

Figure 4 B

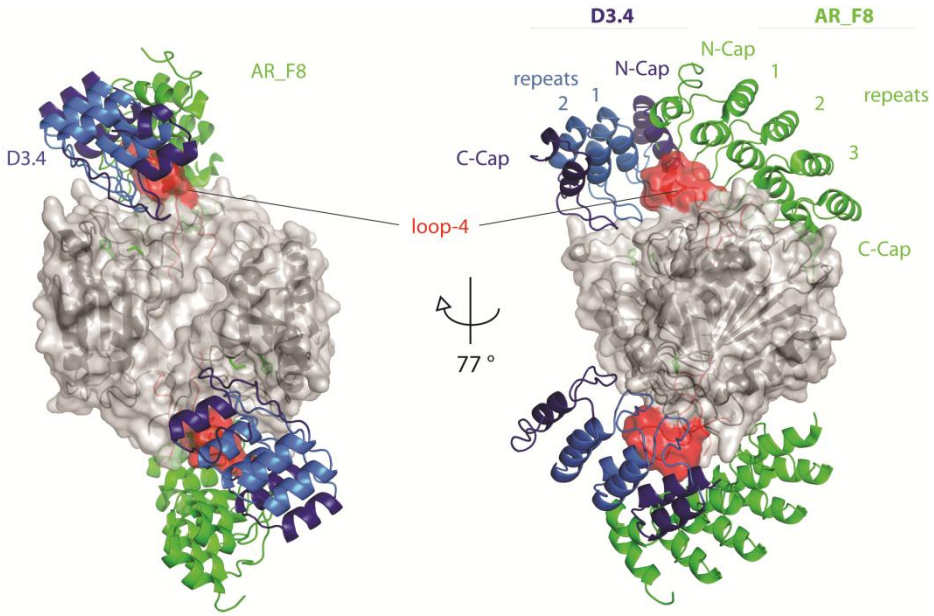

Figure 4 C

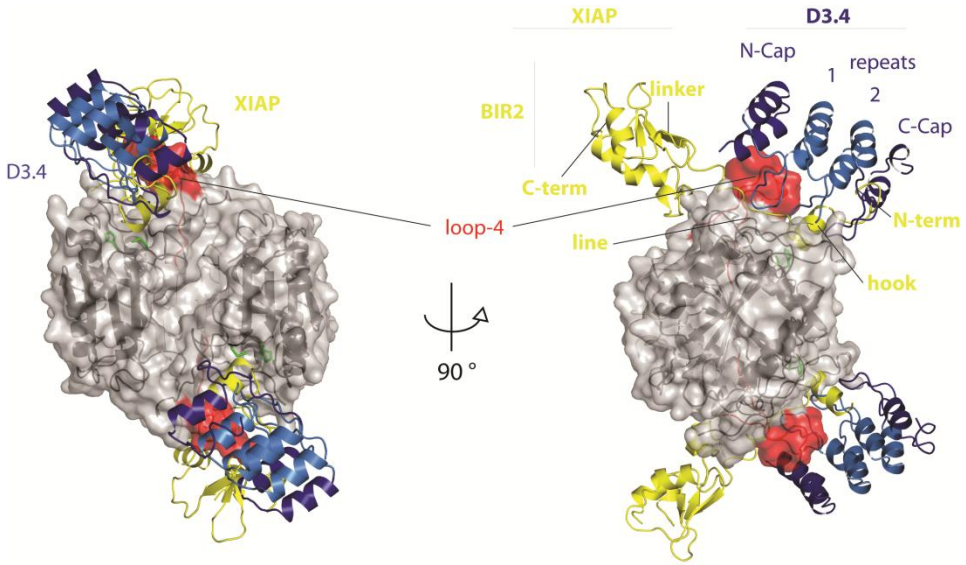

Figure 5 A

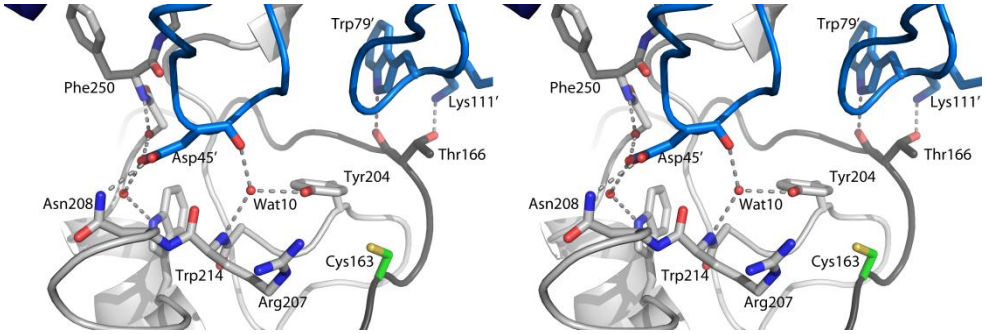

Figure 5 B

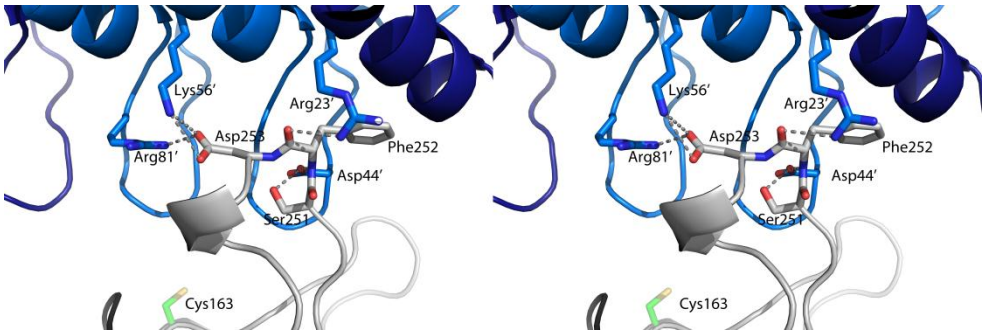

Figure 5 C

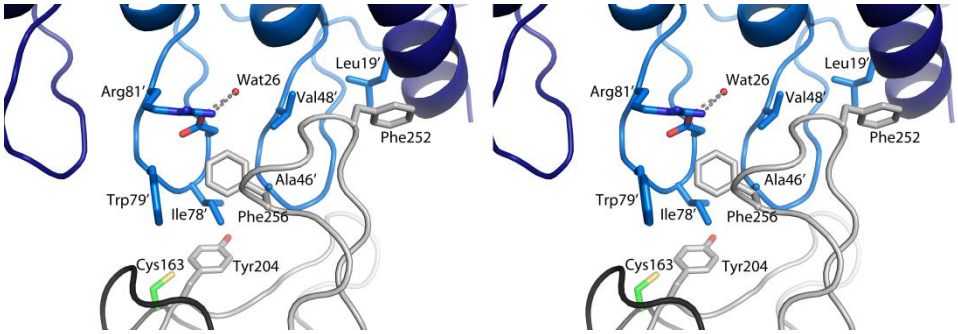

Figure 6 A

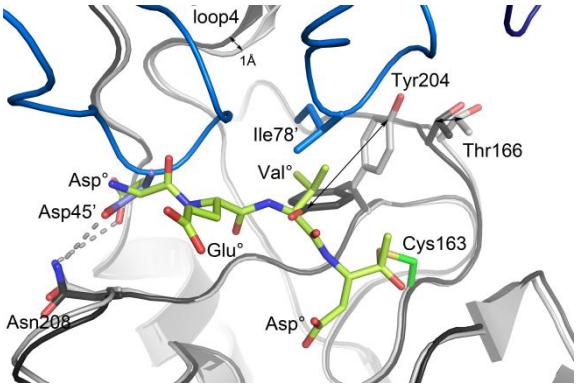

Figure 6 B

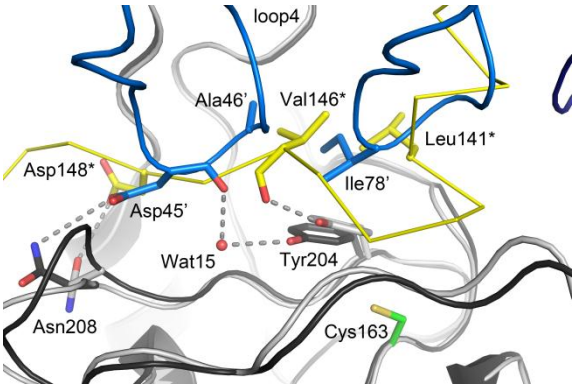

Figure 6 C

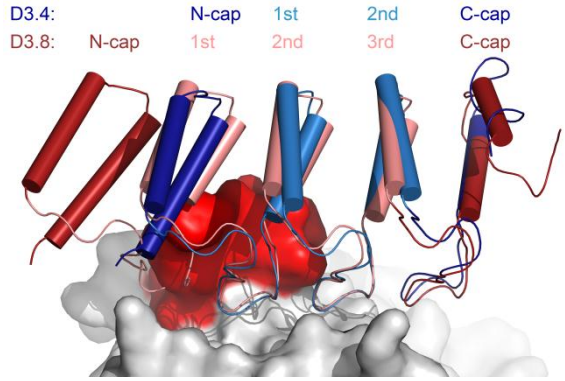

Figure 6 D

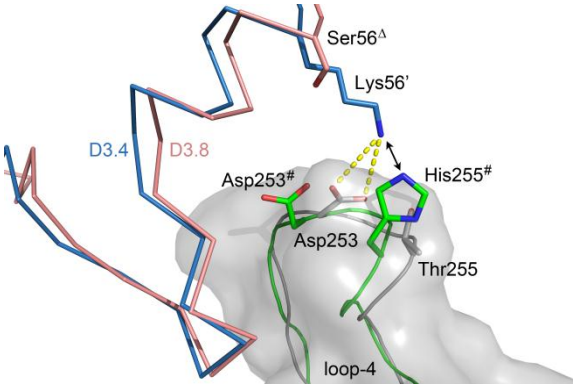

Figure 6 E

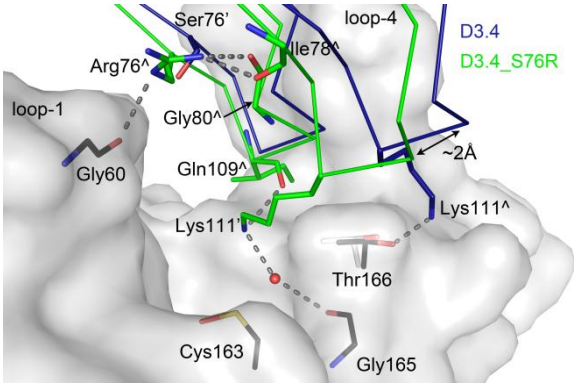

Figure 7

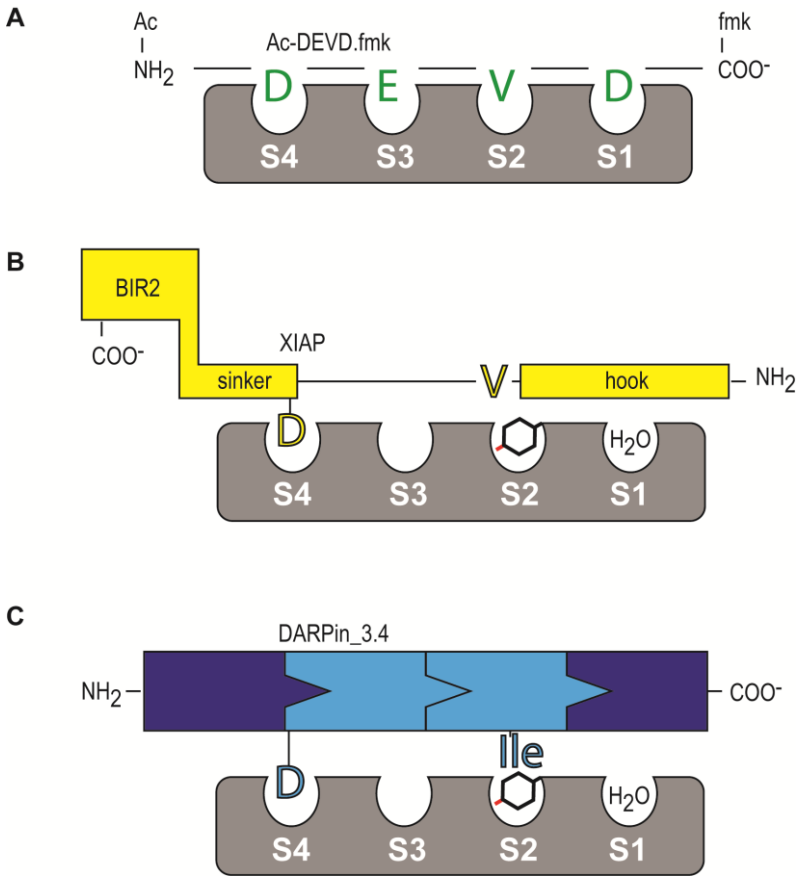
A
Ac
NH2
Ac-DEVD.fmk
fmk
COO-
D
E
V
D
S4
S3
S2
S1
B
BIR2
COO-
XIAP
sinker
V
hook
NH2
D
H2O
S4
S3
S2
S1
C
DARPin_3.4
NH2
COO-
Ile
D
H2O
S4
S3
S2
S1

Table 1: Kinetic constants

	Kinetic						Equlibrium	Inhibition			Interaction		
DARPin	**$k_{on1}(M^{-1s-1})$**	**$k_{off1}(s^{-1})$**	**$K_{D1}(M)$**	**$k_{on2}(M^{-1s-1})$**	**$k_{off2}(s^{-1})$**	**$K_{D2}(M)$**	**$K_D(nM)$**	**$K_I(nM)$**	**α**	**β**	**SC**	**Å²**	**Δ^iG kcal/mol**
D3.4	2.85E+05	8.81E-03	3.09E-08	1.12E+06	1.13E-03	1.01E-09	9.6 ± 1.1	16.76	∞	0	0.740	875.95	-6.1
D3.4_S76R	1.74E+05	4.20E-03	2.42E-08	1.62E+06	7.45E-04	4.61E-10	5.99±0.47	3.49	∞	0	0.725	907.55	-7.1
D3.6	1.48E+05	1.13E-03	7.63E-09	1.46E+06	1.00E-02	6.88E-09	8.8±2.0	-	-	-	-	n.d.	n.d.
D3.8	1.77E+05	2.49E-03	1.41E-08	2.44E+06	1.11E-04	4.57E-11	3.4±0.4	3.42	∞	0	n.d.	n.d.	n.d.
D3.13	2.74E+05	1.24E-03	4.51E-09	2.31E+06	7.86E-03	3.41E-09	7.69±0.4	-	-	-	-	n.d.	n.d.

Table 2: Data and refinement statistics

Structure*	**C3/D3.4 (2XZD)**	**C3/D3.4_S76R (2Y0B)**
Data collection		
Oscillation [°]	0.25	0.2
Space Group	$P3_121$	$P3_121$
Unit cell parameter	a=98 Å	a=98 Å
	b=98.0 Å	b=98.0 Å
	c= 193.6 Å	c= 192.9 Å
	α=β=90.0° γ=120.0°	α=β=90.0° γ=120.0°
Resolution [Å]	49.0 – 2.1	49.0 – 2.1
Wavelength [Å]	1.000	0.92
R_{MEAS} [A][%]	4.9 (69.6)	5.8 (72.2)
R_{OBS} [B][%]	4.2 (60.4)	4.9 (60.9)
Completeness [B][%]	99.3 (99.5)	99.2 (99.5)
$I/\sigma(I)$[B]	15.59 (1.92)	12.94 (1.96)
Refinement		
Resolution [Å]	2.1	2.1
R_{WORK}/R_{FREE}	18.5/21.8	19.1/21.7
No. of protein atoms	5616	5622
No. of water atoms	247	345
B-Factor [$Å^2$]	35.29 ± 11.29	35.75 ± 11.36
Root mean square deviations		
Bond length [Å]	0.011	0.006
Bond angles [°]	1.192	0.941

* Given are the names of caspase-3 DARPin inhibitor complexes and the PDB entry codes in brackets.

Table 3: Hydrogen bonds

DARPin	**Distance**	**Caspase-3**
D:ARG 23 [NH1]	3.19	C:PHE 252 [O]
D:ASP 44 [OD2]	2.69	C:SER 251 [OG]
D:ASP 44 [OD2]	2.97	C:PHE 252 [N]
D:ASP 45 [OD1]	3.1	C:ASN 208 [ND2]
D:ASP 45 [O]	2.5/2.8	C:Wat 10 - TYR 204 [OH]
D:ASP 45 [OD2]	2.6/2.7	C:Wat 12 - Phe 250 [N]
D:ASP 45 [OD2]	2.6/2.9	C:Wat 11 - Trp 214 [NE1]
D:LYS 56 [NZ]	3.38	C:ASP 253 [OD1]
D:LYS 56 [NZ]		C:ASP 253 [OD2]
D:TRP 79 [NE1]	2.87	C:THR 166 [O]
D:ARG 81 [NH2]	2.79	C:ASP 253 [OD2]
D:LYS 111 [NZ]	3.75	C:GLU 167 [OE2]
* D:LYS 111 [NZ]	2.68	C:THR 166 [OG1]
* not present in DARPin_3.4_S76R		
DARPin_3.4_S76R		
D:Arg 76 [NE]	3.3	C:Gly 60 [O]
D:Lys 111 [NZ]	2.7/3.2	C:Wat - Gly 165 [O]

Supplementary Figure 1

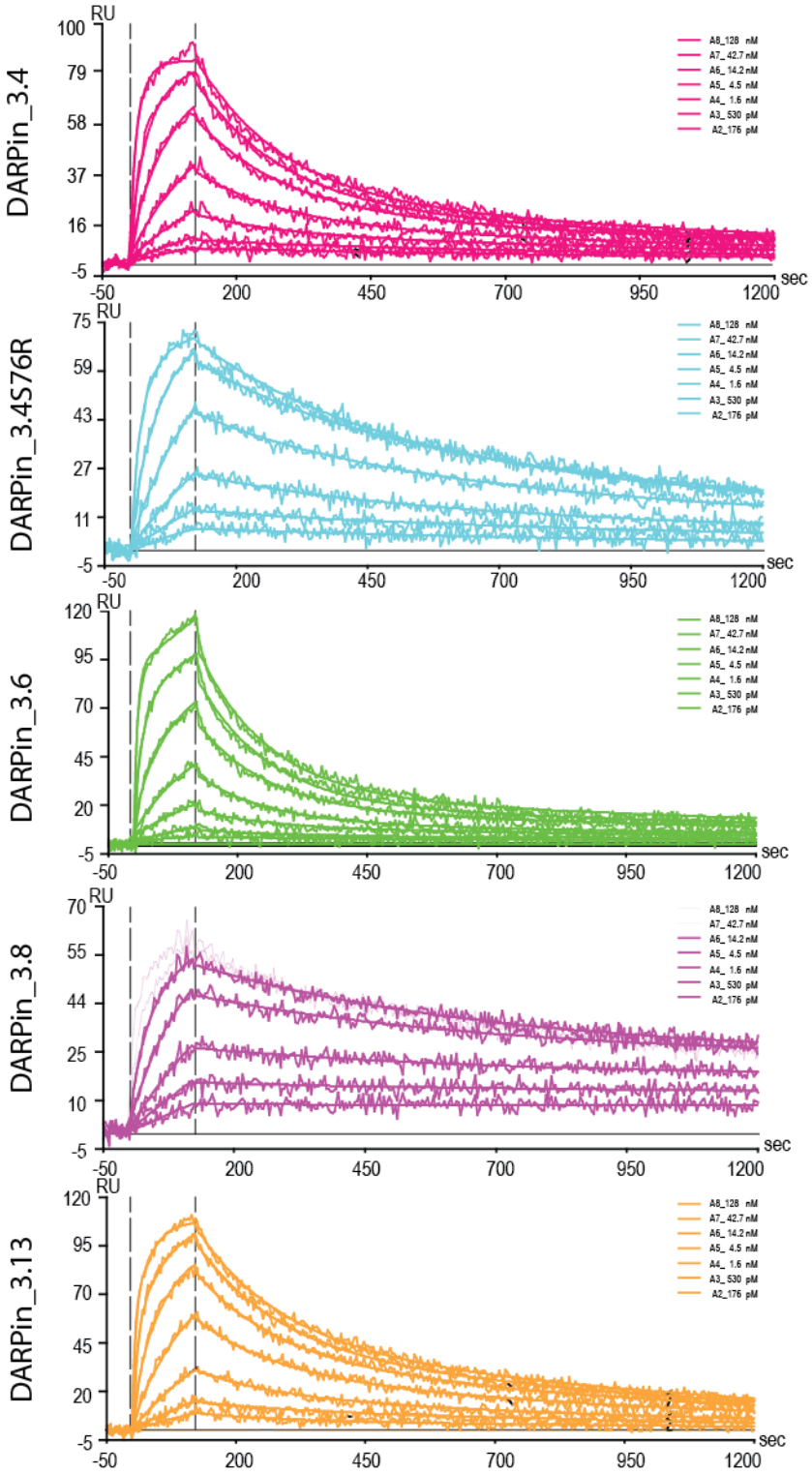

Supplementary Figure 2A

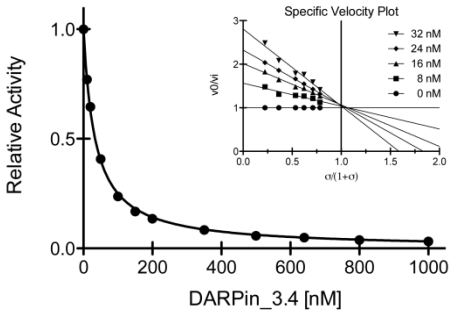

Supplementary Figure 2B

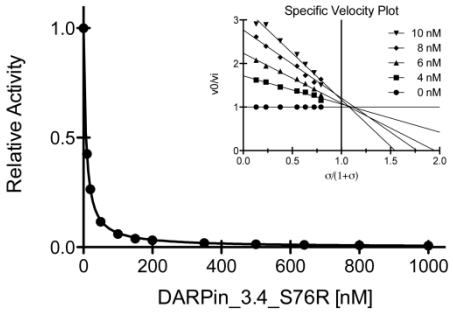

Supplementary Figure 2C

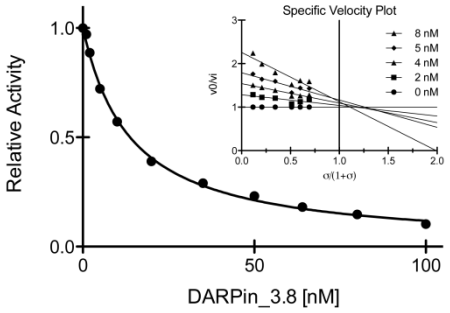

Supplementary Figure 3

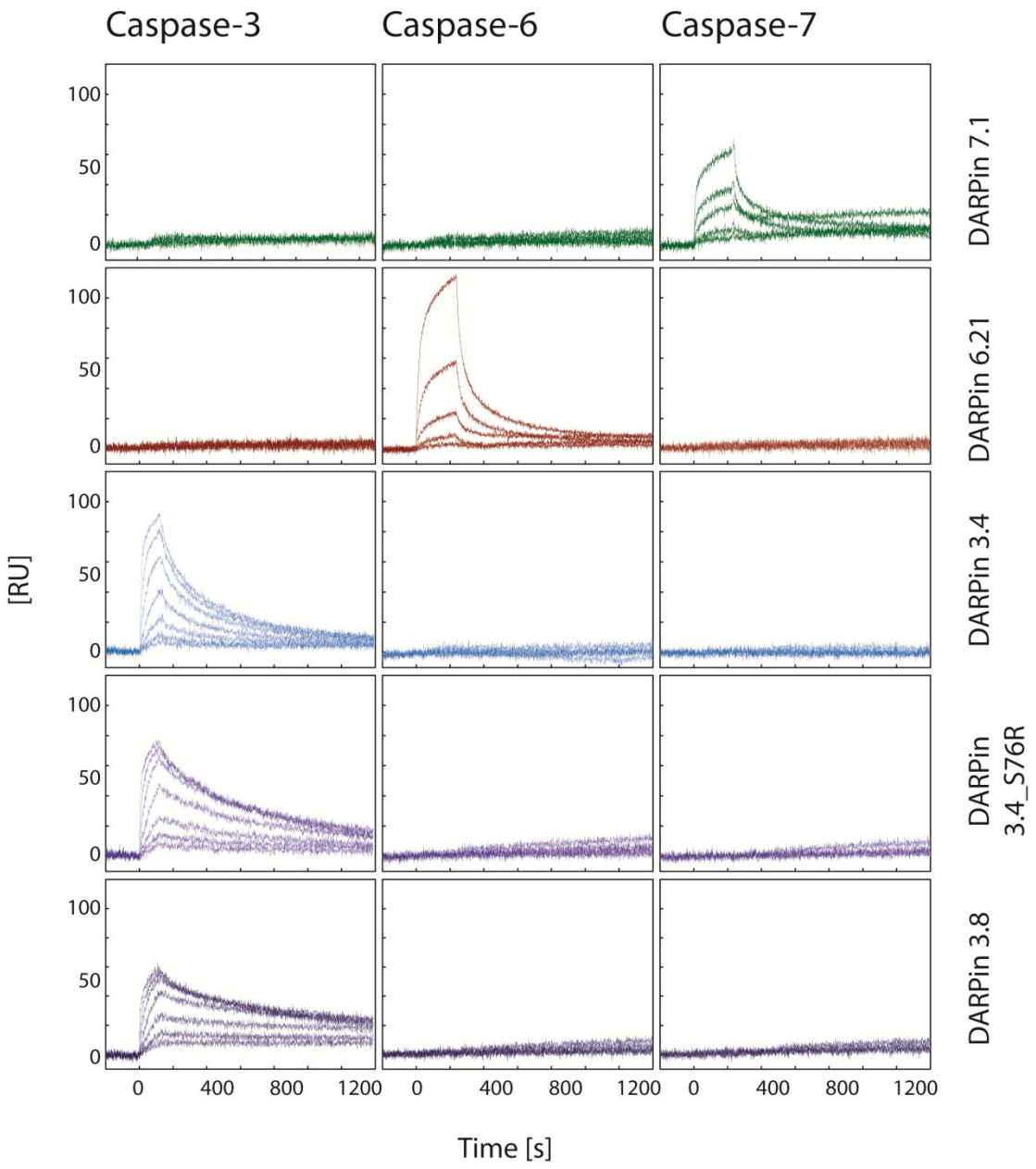

Supplementary Figure 4

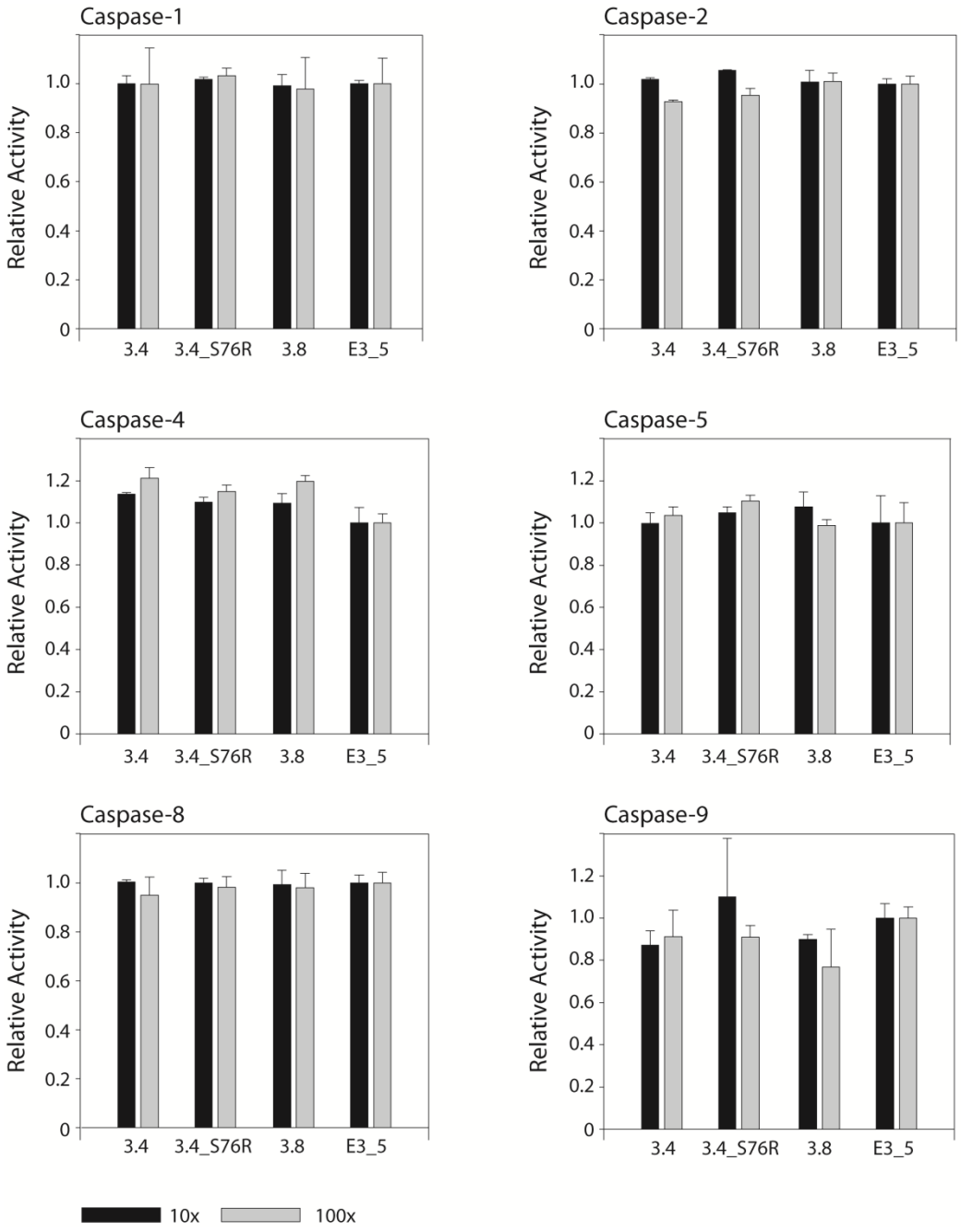

Supplementary Figure 5

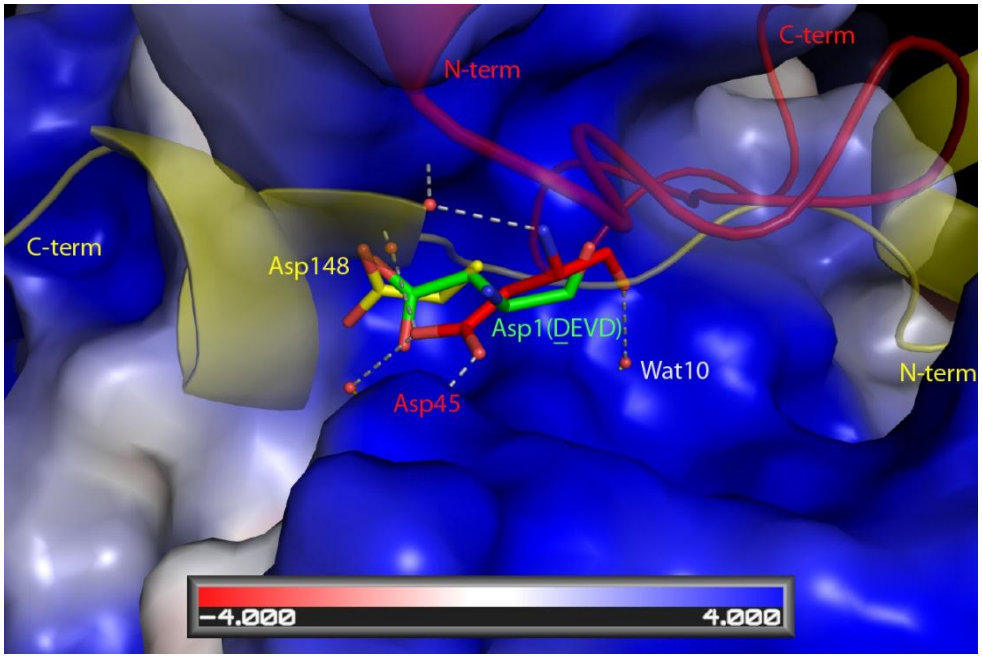

5. A DARPin activator of caspase-8

Introduction

Peptidases are involved in various regulatory pathways in which the signal is relayed by limited proteolysis making the process irreversible [173]. Peptidases control a large number of physiological processes such as cell proliferation, DNA replication, tissue remodeling, homeostasis, apoptosis and inflammation. The deregulation of these highly controlled processes can lead to too little or too much proteolysis and is implicated in many human diseases. Limited proteolysis of a protein can lead to gain, loss or switch of function. An interesting and extensively studied protease cascade that exemplifies these alterations of function is the caspase mediated pathway of cell death and inflammation. Apoptotic initiator caspases, once activated, cleave downstream caspases that are present in the zymogenic inactive form. Once processed, downstream caspases are activated and cleave multiple substrates resulting in most cases in a loss of function of the target protein ultimately leading to cell death [3]. Caspases are present in the cell as inactive zymogens (procaspases), similar to literally all peptidases and require several maturation steps to be active. Initiator caspases such as Caspase-8 and -9 require recruitment to macromolecular activation platforms via their N-terminal prodomains. The high local concentration leads to dimerization and subsequent autocatalytic cleavage of the interdomain linker [62]. Executioner caspases in contrast are constitutively dimeric and are activated by upstream proteolysis of the intra domain linker.

Dysregulation of apoptosis plays a crucial role in many human pathologies and targeting caspases for inhibition or activation are viable strategies to overcome these diseases. MacKenzie *et.al*. have comprehensively addressed this topic and point out general problems and opportunities on how to manipulate caspase activity [45]. While most approaches focus on the inhibition of peptidases, a recent study has highlighted the potential of activating peptidases and their potential in drug discovery [102]. Caspase-8 plays a central role in apoptosis and other signaling pathways (e.g. suppressing or potentiating tumor malignancy [174]) and is therefore a target of high interest.

In this work we have selected a specific caspase-8 binder (DARPin_8.4) from a highly diverse library of designed ankyrin repeat proteins (DARPins) using ribosome display (RD). A crystal structure of the caspase-8/ DARPin_8.4 protein complex revealed that the DARPin binds to helix 2 of caspase-8. Enzymatic characterization showed that this DARPin_8.4 increases the activity of caspase-8 through specific interactions with the active site forming loop1.

Results

Ribosome display selection of DARPins against caspase-8.

DARPins were selected against purified and biotinylated caspase-8 under physiological conditions. We performed two independent selections with four ribosome display rounds. In round one and three we included a pre-panning step against the two closest homologs, namely caspase-2 and caspase-9 (Figure 5.1 A). Both caspases have a sequence homology with caspase-8 of approximately 50% and are also involved in activation of executioner caspases. We additionally included k_{off} maturation during selection to increase selection pressure for DARPins with favorable binding kinetic (Figure 5.1A). In the first RD selection we obtained 4 hits from 192 colonies screened and in the second selection we identified 32 hits from 384 colonies based on a crude cell extract ELISA. We sequenced the 14 strongest hits and the alignment of these DARPins sequences shows that all DARPins have one common ancestor because they differ in only one or two amino acids (Figure 5.1 B).

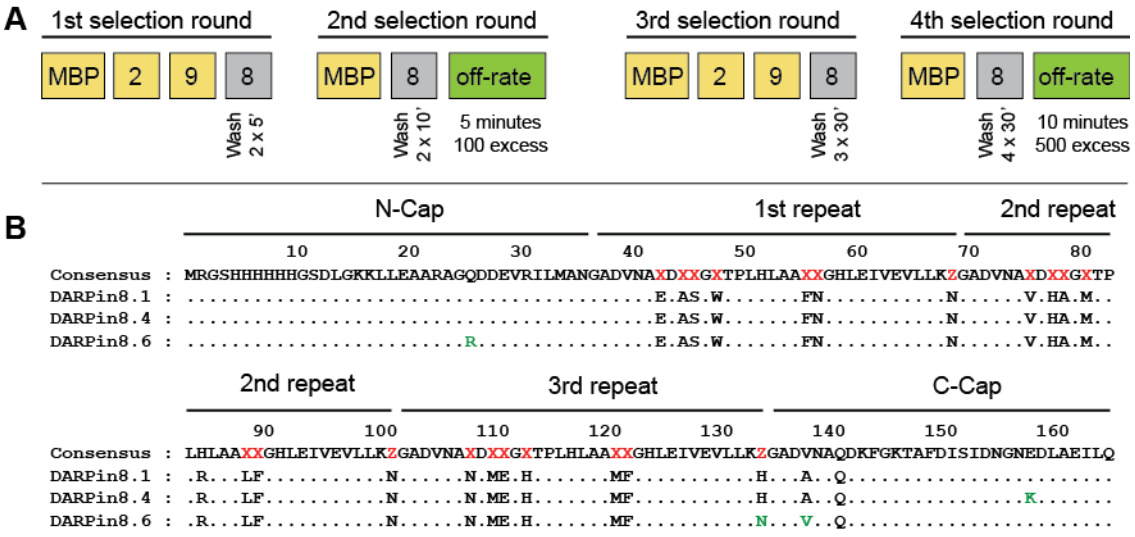

Figure 5-1: DARPin selection against caspase-8
A) The selection strategy consisted of four selection rounds with alternating conditions. Yellow boxes indicate prepanning on MBP, caspase-2 and -9.The grey box shows selection against the target protein caspase-8, followed by washing as indicated. Off-rate selection is shown by the green box. B) Sequence alignment of DARPins DARPin_8.1 from the first selection and DARPin_8.4 and DARPin_8.6 from the second selection by ribosome display. Variable positions in the DARPin consensus sequence (red) are indicated by either X or Z. Amino acids that differ from the other DARPins (green) are shown.

All sequence variation appeared to be either in the C- or N-terminal capping repeat of the DARPin, while all randomized positions were conserved. A DARPin which occurred repeatedly in this pool was DARPin_8.4. This DARPin was also found to be the strongest binder and therefore was further characterized.

DARPin 8.4 binds caspase-8 with high affinity and specificity

In order to determine the thermodynamic properties and binding kinetics of the caspase-8/DARPin_8.4 interaction we applied several techniques. First we revealed that both proteins interact with a 1:1 binding stoichiometry (N= 0.95) with one DARPin binding one caspase-8 monomer using isothermal titration calorimetry (ITC). Binding of both proteins reduced the enthalpy (ΔH=-8477) and is entropically favoured (ΔS= 5.09 kcal/mol) since the Gibbs free energy deceases (Table 5.1). The K_D of the interaction was 47 nM according ITC measurements at 25 °C (Table 5.1).

Kinetics DARPin_8.4				
SPR	**$k_{on}(M^{-1s-1})$**	**$k_{off}(s^{-1})$**	**K_D(M)**	**Δ^iG [kcal/mol]**
	1.8E+05	9.41E-04	5.2E-09	-
ITC	**K_D(M)**	**ΔH [kcal/mol]**	**ΔS [kcal/mol]**	**Δ^iG [kcal/mol]**
	4.7E-08	-8477	5.09	n.d.

Table 5-1: Kinetic data obtained by ITC and SPR

Surface plasmon resonance (SPR) measurements with a Proteon XPR36 allowed precise determination of the kinetic characteristics of the interaction including k_{on} and k_{off} rates. The K_D of the interaction is 5.2 nM at 20 °C based on a fit using the Langmuir model (Table 5.1 and Figure 5.2 C). The high affinity is owing to the slow k_{off} value with 9.41 x 10^{-4}. The resulting k_{on} value is 1.8 x 10^5. We were further interested in the specificity of DARPin_8.4 and thus tested whether it is able to bind other

caspases such as caspase-9, -2, -3 and -7. No interaction was detectable (data not shown) with any other caspase coated on the SPR chip, indicating that DARPin_8.4 is highly specific for caspase-8.

We further analyzed the pH dependency of the caspase-8/DARPin_8.4 interaction by ELISA in different buffers from pH 4 to pH 9.5. DARPin_8.4 binds caspase-8 in a broad pH range (pH 5 – 10) unlike most DARPins that have been selected to date (Figure 5.2 B). The strongest binding was observed between pH 7.5 to 9; binding remains at a significant level between pH 7.5 and pH 5 and becomes insignificant below pH 5.

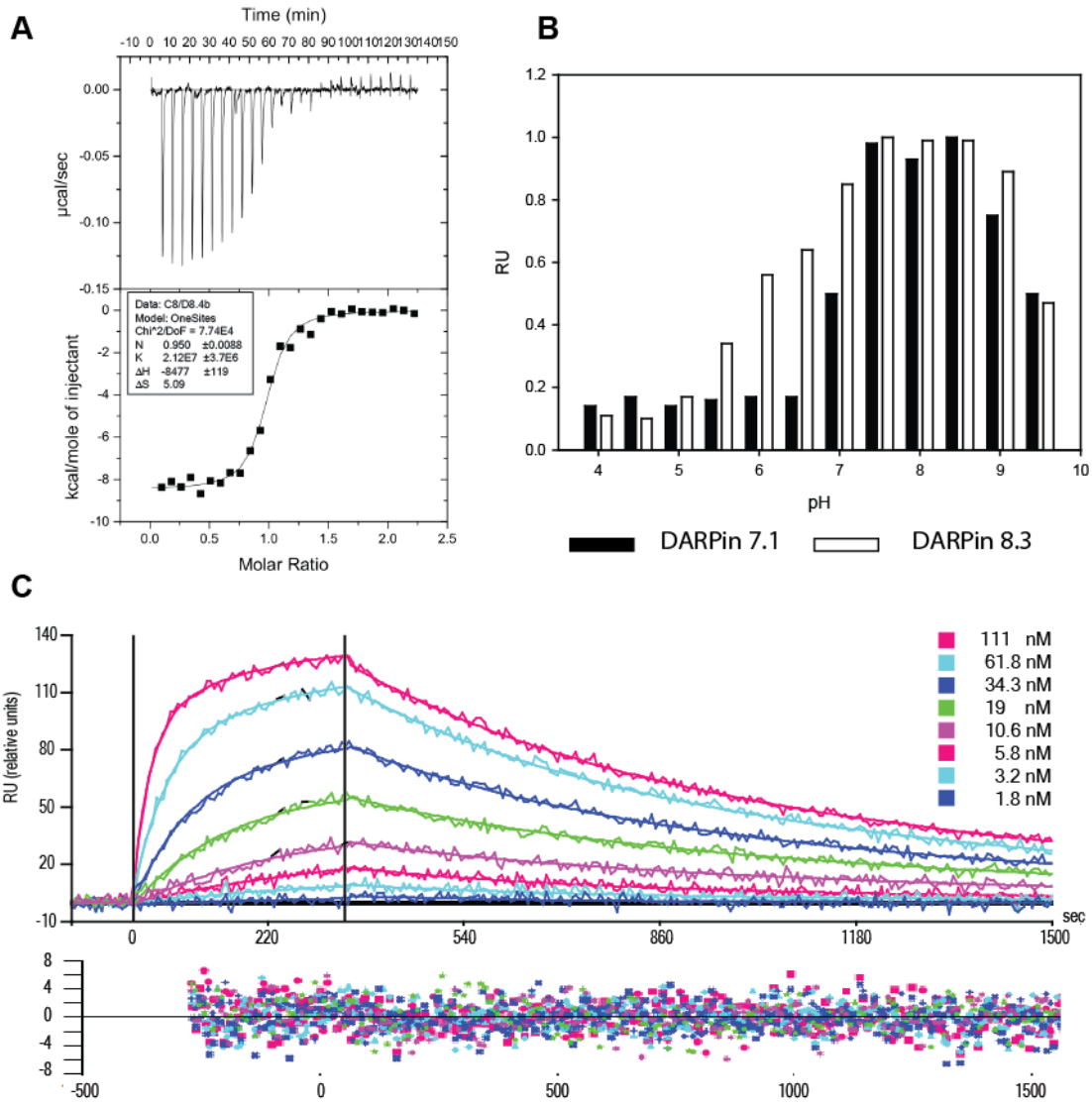

Figure 5-2: Analysis of DARPin binding to caspase-8

A) Top, raw ITC data: eighteen injections of the ligand have been measured and recorded. Bottom, complete binding isotherm: One site model was used to fit the data resulting in values for stoichiometry and enthalpy (black box). B) ELISA profile of the influence of pH on DARPin binding. DARPin_8.4 was compared with DARPin_7.1 which binds caspase-7. Twelve different buffers have been prepared, ranging from pH 4 to pH 9.5. C) SPR profile of DARPin_8.4 against caspase-8 showing eight different concentrations with the according fit. Data were fitted using the Langmuir model with the deviation shown in the lower panel.

Crystal structure of the DARPin_8.4/caspase-8 complex

The DARPin_8.4 caspase-8 complex crystallized in acidic conditions at pH 4.8 showing that the interaction remains intact even at low pH at high protein concentrations. The crystals diffracted to 1.8 Å, the highest resolution for a DARPin structure in complex with its designated target protein so far. The complex crystallized in the space group $P2_12_12_1$ and the crystals have a solvent content of 38.2 %. Crystallographic data are presented in Table 5.2.

Structure	**DARPin_8.4 (2Y1L)**
Data collection	
Space Group	$P2_12_12_1$
Unit cell parameter	a=61.0 Å b=81.60 Å c= 163.2 Å α=β=90.0° γ=120.0°
Resolution [Å]	48.86 – 1.8
Wavelength [Å]	1.000
R_{MEAS} [A][%]	11.1 (58.0) 4.2 (51.5)
Completeness [B][%]	99.4 (98.9)
I/σ(I)[B]	13.29 (3.67)
Refinement	
Resolution [Å]	1.8
R_{WORK}/R_{FREE}	18.0/21.8
No. of protein atoms	6246
No. of water atoms	685
B-Factor [Å^2]	18.4 ± 9.66
Root mean square deviations	
Bond length [Å]	0.009
Bond angles [°]	1.2

Table 5-2: Crystallization and refinement statistics of the caspase-8/D8.4 crystal structure. Values in parentheses represent the highest resolution shell. [A] $R_{MAES}=\Sigma_{hkl}(N/(N-1))\Sigma_1|I_1(hkl)-I(hkl)|\Sigma_{hkl}\Sigma_1I_1(hkl)$. [B] $R_{OBS}=\Sigma_{hkl}\Sigma_1|I_1(hkl)-I(hkl)|/\Sigma hkl\Sigma_1I_1(hkl)$.

The asymmetric unit cell (asu) contains a caspase-8 dimer which consists of two small and two large subunits as it was found in the previous caspase-8 structure (1QTN) [148] and is bound by two DARPins (Figure 5.3 A and B). The crystal has a tight packing and the protein complex is arranged in

layered sheets (Figure 5.3 A). Crystal contacts are mediated mainly by DARPin-DARPin and DARPin-caspase interactions (Figure 5.3 A). One crystal contact is observed between symmetry related caspases. All previously solved structures of caspase-8 crystallized in the space group $P3_121$ with the highest resolution being 1.2 Å [175]. The DARPin/caspase interface has a buried surface area of 934 $Å^2$, this represents one of the largest interfaces observed for DARPin interaction with their target protein [129]. A surface complementarity index of 0.7 indicates a good fit between both proteins. The structure reveals that DARPin_8.4 mainly binds to an extended α-helix (termed α-helix 2) which involves ten residues from Tyr288 to His304 (Figure 5.3 C and Figure 5.4). DARPin_8.4 forms three hydrogen bonds with residues located in the α-helix2 (Glu290, Asp294 and Lys297) which point away from the protein surface (Figure 5.4). It further interacts with residues of the β-strand2, namely Lys282 and Glu280. The C-terminal capping repeat of DARPin_8.4 binds to residues of the active site forming loop1 (Lys246 and Lys250) by forming two hydrogen bonds (Figure 5.4 and Figure 5.5 C). All three internal repeats of the DARPin are involved in the binding interface (Figure 5.3 C); in addition five residues of the C-Cap of DARPin_8.4 also contribute to the interaction. In total, we observe 16 hydrogen bonds (H-bonds) which span the entire interface (Table 5.2 and Figure 5.4).

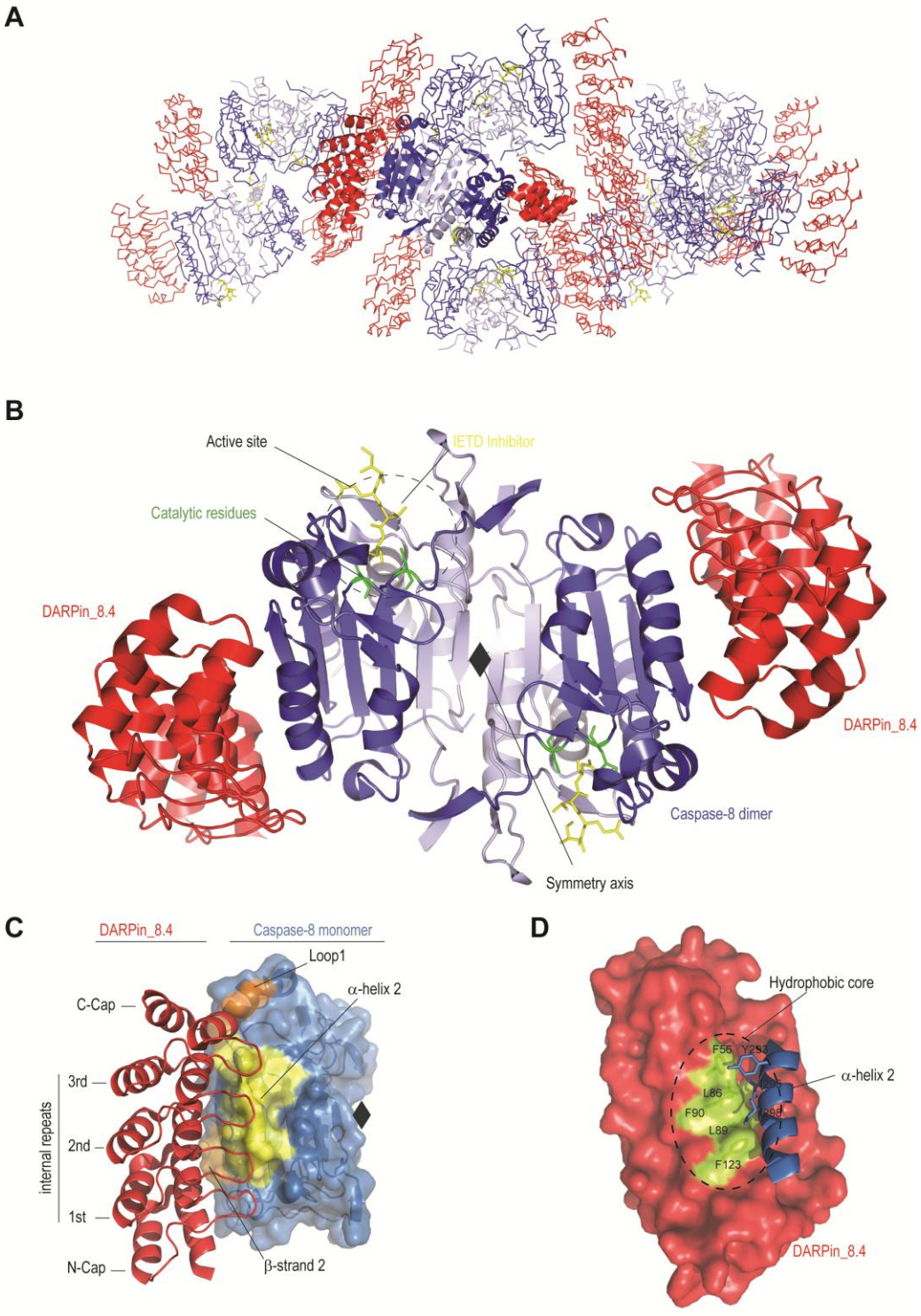

Figure 5-3: Crystal structure of caspase-8 in complex with DARPin_8.4
(A) Crystal packing of the caspase-8/DARPin_8.4 complex (space group $P2_12_12_1$). One complex is shown in cartoon representation and the neighboring complexes are shown in ribbon representation. The caspase-8 dimer is shown in blue (large subunit: dark blue, small subunit: light blue) bound by the active site inhibitor z-IETD.fmk (yellow). Crystal contacts are mediated mainly by DARPin-DARPin and DARPin-caspase interactions but also caspase-caspase interactions. (B) Overview of the caspase-8/DARPin_8.4 complex in a transparent surface and cartoon representation. Color coding as described in (A), residues of the catalytic dyad (Cys285 and His237) are shown in green and the active site is circled (dotted circle). Two DARPin_8.4 (red) molecules bind one caspase-8 dimer. The interface is largely formed by α-helix 2 of caspase-8 and the three internal repeats and the C-Cap (C). DARPin_8.4 interacts with three secondary structure features of caspase-8 (surface representation, blue), α-helix 2 (orange), β-strand 2 and loop 1 (both orange). (D) Surface representation of the DARPin_8.4 surface (red) forming a hydrophobic core (green) with residues and the helix2 of caspase-8 (blue).

The H-bond network surrounds the hydrophobic core which is formed by the amino acids F56, Leu86, Leu89, Phe90 and Phe123 of DARPin_8.4 and Tyr293, Ile295 and Ile298 of caspase-8 (Figure 5.3 C and Figure 4). Residue Ile298 of caspase-8 binds to a pronounced hydrophobic pocket which is formed by Leu86, Leu89 and Phe90 in the core of the caspase-8/DARPin interface (Figure 5.3 D).

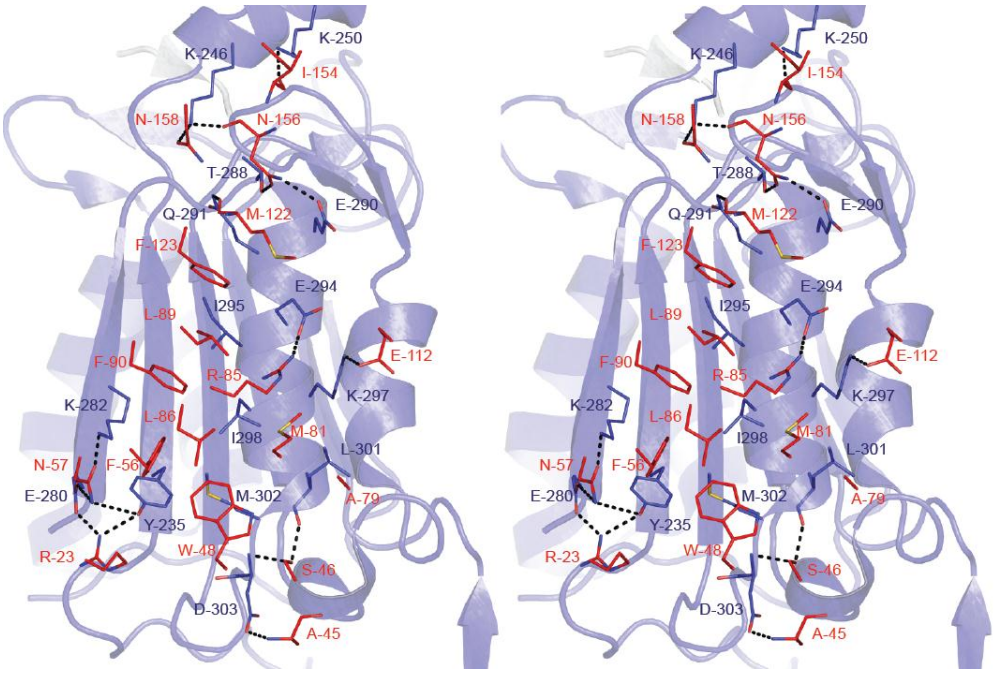

Figure 5-4 Hydrogen bond network of the caspase-8/DARPin_8.4 interaction
Stereo view of Caspase-8 (blue, cartoon representation) and the interacting residues of DARPin_8.4 (red) are shown. H-bonds are indicated by dotted black lines between the two respective side chains.

In total, fifteen residues of caspase-8 are involved in the interaction with DARPin_8.4 of which ten are located in the α-helix2, three in the β-strand2 and two in loop1. A sequence alignment of these residues with ten other caspases revealed that none of the residues is conserved. This finding explains why DARPin_8.4 recognizes caspase-8 with high specificity when binding to an epitope which is unique to caspase-8.

DARPin_8.4	Distance	Caspase-8
D:ARG 23 [NH1]	2.78	C:TYR 235 [OH]
D:ARG 23 [NH1]	2.54	C:GLU 280 [OE1]
D:ASN 57 [ND2]	3.30	C:GLU 280 [OE2]
D:ASN 156 [ND2]	2.62	C:GLU 290 [OE1]
D:ARG 85 [NH2]	2.94	C:GLU 294 [OE1]
D:SER 46 [OG]	2.40	C:LEU 301 [O]
D:ALA 45 [N]	2.69	C:ASP 303 [OD2]
D:ASN 57 [OD1]	2.94	C:TYR 235 [OH]
D:ASN 158 [OD1]	3.12	C:LYS 246 [NZ]
D:ASN 156 [O]	2.55	C:LYS 246 [NZ]
D:ILE 154 [O]	3.09	C:LYS 250 [NZ]
D:ASN 156 [OD1]	2.44	C:THR 288 [OG1]
D:GLU 112 [OE1]	2.95	C:LYS 297 [NZ]
D:SER 45 [OG]	3.04	C:ASP 303 [N]
D:MET 122 [O]	2.60	C:GLN 291 [N]
D:ASN 57 [ND1]	2.3	C:LYS 282 [N]

Table 5-3: Hydrogen bonds formed in the caspase-8/DARPin_8.4 interface

Comparison with previously solved caspase-8 crystal structures

Crystal structures in complex with selected protein binders such as antibodies or DARPins often reveal novel structural conformations that are stabilized by the respective binder [176]. In order to investigate whether caspase-8 in complex with DARPin_8.4 shows a novel conformation we compared the structure with previously published structures of caspase-8 alone. The superposition with the highest resolved crystal structure of caspase-8 in complex with the inhibitor z-IETD.fmk (pdb code: 1QTN) [175] shows that DARPin_8.4 binds to a previously observed conformation (Figure 5.5 A). No significant differences can be observed in the overall structure with an RMSD of 0.717. One exception is loop 2 which is shifted by approximately 1 Å in the caspase-8/DARPin_8.4 structure (Figure 5.5 A). A closer look at the residues that are involved in the interface indicates that only side chains of four amino acids (Lys250, Glu290, Glu294 and Lys297) have different rotamer positions. However, both crystal structures differ with an rmsd of 3.2 from the solution structure of monomeric procaspase-8, which was determined by nuclear magnetic resonance (NMR) spectroscopy [23] (Figure 5.5 A). While

the core of the monomeric procaspase-8 has the typical caspase fold with low flexibility, the active site forming loops display high flexibility [23]. Loop1 is rotated by approximately 90° compared to the position found in the crystal structure and occupies part of the substrate binding site together with the linker (Figure 5.5 B and C). Cleavage of the linker results in the formation of two new active site forming loops, loop2 and loop2' which stabilizes active site in the second monomer [76] (Figure 5.5 A). Furthermore it allows the formation of the dimer interface and loop1 is now able to rotate into the substrate-bound conformation. DARPin_8.4 recognizes caspase-8 in an inhibitor (or substrate)-bound conformation by interacting with loop1 (Figure 5.5 B). Three hydrogen bonds are formed between DARPin_8.4 residues Ile154, Glu156, Glu158 and capase-8 residues Lys246 and Lys250 (Figure 5.5 C).

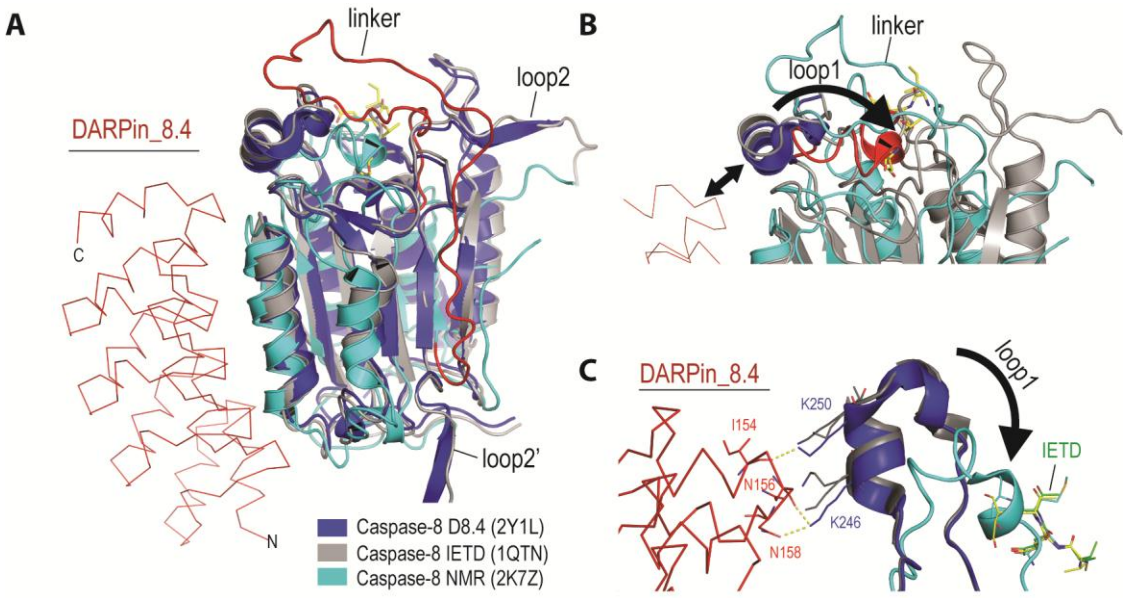

Figure 5-5: Comparison of different caspase-8 structures
(A) Superposition of the caspase-8/DARPin_8.4 crystal structure (blue) with the previously solved caspase-8/inhibitor crystal structure (grey, 1QTN) and the NMR structure of the monomeric procaspase-8 (cyan, 2K7Z). The position of DARPin_8.4 is indicated by the red ribbon representation. The position of the active site bound inhibitor z-IETD.fmk in sticks (yellow) is indicated. The linker connecting the large and small subunit of procaspase-8 is presented as a red loop. (B) Close up view of the active site of all three structures superimposed. Loop1 (red) of procaspase-8 is rotated by ~90° into the active site. (C) The C-Cap of caspase-8 (red) forms three hydrogen bonds with loop1 of caspase-8 and locks the helix in a substrate bound position as it is shown by the caspase-8/z-IETD.fmk structure (grey). The rotation of loop1 in the solution structure (cyan) is indicated leading to a steric clash with the inhibitor.

DARPin_8.4 induces dimerization of caspase-8

As previously observed, binding of a DARPin can alter the activity of an enzyme [95]. We tested whether the presence of DARPin_8.4 has an influence on the activity of caspase-8 and observed that a 10-fold excess of DARPin_8.4 leads to a 4-fold increase in activity compared to caspase-8 alone (Figure 5.6).

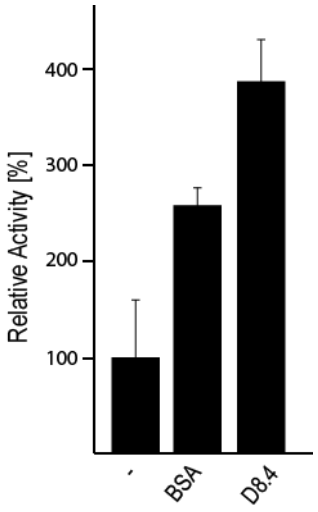

Figure 5-6: Caspase-8 activity is influenced by DARPin_8.4
Relative activity of caspase-8 in presence of different DARPin constructs. Bovine serum albumin (BSA) or DARPin_8.4 have been added to the caspase-8 activity reaction.

The activity of caspase-8 is highly dependent on the monomer-dimer equilibrium with the dimer representing the catalytically active form. The ratio of monomer to dimer of caspase-8 in solution depends on the concentration and presence of an inhibitor [161]. The dissociation constant of the dimer interface of caspase-8 is 50 μM and decreases to 5 μM when bound to an inhibitor [161]. All caspase-8 crystal structures that have been solved, show caspase- 8 in an active conformation in complex with an inhibitor, including the structure (1QTN) [175] shown in Figure 5.5. Since we see no conformational difference in the caspase-8/IETD and caspase-8/DARPin_8.4 structures we assume, that the DARPin_8.4 binds to the active conformation of caspase-8. Interactions with Lys246 and Lys250 of the active site loop locks this loop in an active conformation. The NMR structure of the uncleaved caspase-8 monomer shows loop1 in an inactive conformation [23] (Figure 5.5 B) and several other intermediate conformations might exist. Since binding of an inhibitor induced

dimerization of the caspase monomer, we wanted to test, whether binding of DARPin_8.4 shows the same effect by binding to loop1. In order to test this hypothesis we performed an ultracentrifugation (UZ) experiment which allows us to resolve and quantify the monomer-dimer equilibrium. At a concentration of ~15 μM, 4% of caspase-8 is present as dimer and 96% is monomeric. In the presence of DARPin_8.4 however, we observe that the equilibrium is shifted to the dimer, with approximately 20% dimer and 80% monomer (Table 5.4). This finding supports the hypothesis that DARPin_8.4 recognizes and locks the active substrate bound conformation of loop1, leading to dimerization of caspase-8.

Sample		**Monomer**	**Dimer**
DARPin_8.4 [78mM]	measured size [kDa]	20 ± 4	-
	proportion [%]	99	-
	theoretical size [kDa]	18.5	36
Caspase-8 [15,5 mM]	measured size [kDa]	29 ± 3.4	63 ± 7
	proportion [%]	96	3.7
	measured size [kDa]	29	58
Caspase-8 [15,34 mM]	measured size [kDa]	42.7 ± 5	83.2 ± 9
	proportion [%]	79.8	19.6
	measured size [kDa]	47.5	94

Table 5-4: Analytical Ultracentrifugation
Analytical ultracentrifugation experiments to determine the oligomeric state of caspase-8, DARPin_8.4 and the complex of both proteins.

Discussion

Caspase-8 is a very attractive drug target due to its central role in the apoptotic cascade. Not only the inhibition of caspase-8 is a viable strategy to combat diseases, but also activation of caspase-8 is highly interesting since evading of the apoptotic cascade is regarded as one hallmark of cancer [41]. Caspase-8 is present as an inactive zymogen (procaspase-8) in the cytoplasm and requires activation through an oligomerization platform (DISC) to obtain full catalytic activity. The main event at the DISC is the formation of a caspase-8 dimer followed by linker cleavage, loop rearrangement and formation of the active site.

In order to activate caspase-8 specifically in *in vitro* experiments we have developed a novel approach which aims to dimerize caspase-8 based on specific interaction with DARPins. For this we have selected DARPins against caspase-8 using ribosome display and have identified DARPin_8.4 as a very potent binder. Interestingly we have obtained the same DARPin multiple times in two independent selections with only few mutations in the DARPin framework which are most likely due to reverse transcription of RNA to DNA or PCR amplification. The fact that this DARPin has been favored during selection probably due to the high affinity of 5.2 nM and particularly the slow k_{off} rate of 9.31 10^{-4} x s^{-1}. In the ITC experiment we observed a K_D of 47 nM which is significantly different from the K_D determined by SPR. A possible explanation is the experimental setup since ITC measures the affinity in solution whereas SPR measures the affinity on a surface of a dextran coated chip. Furthermore protein interactions are very sensitive to pH, temperature and buffer conditions and small differences can result in different affinities. SPR measurements have been performed at 20 °C whereas ITC was performed at 25 °C which might be the reason for the two different K_D-values. Furthermore ITC is not the method of choice for low nM affinities; since the resolution limit with 10 to 50 nM is above the affinity we measured by SPR.

The caspase-8/DARPin_8.4 complex is significantly more stable than other DARPin protein interactions we have seen so far. We were still able to observe an interaction at pH 5.5. Therefore we were able to crystallize the complex in a broad range of conditions. The best crystals were obtained at

pH 4.8 and diffracted to 1.8 Å resolution. The 1.8 Å structure illustrates the composition and interface of the complex and explains why this interaction has a low K_D and is relatively insensitive against pH changes. The interface is one of the largest interfaces observed for DARPins so far (934 $Å^2$), with both hydrogen bonds and hydrophobic interactions contributing to the interaction strength. The curvature of the convex caspase-8 surface perfectly fits with the concave DARPins interface with a surface complementary index of 0.7. The epitope of caspase-8 involves α-helix2, the active site forming loop 1 and three residues of the β-strand 2. We assume that the hydrophobic core is essential in the interaction next to the 16 hydrogen bonds. The residues Ile298, Ile295 and Tyr293 of caspase-8 form a hydrophobic core with a hydrophobic patch on the DARPin surface.

The superposition of our structure with a previously determined high resolution crystal structure reveals that no conformational differences can be observed. Merely loop2 shows moderate structural rearrangements and four amino acid side chains have different rotamer positions. An interesting finding is that the residues involved in the interaction are generally not conserved, except for Thr288. This is a strong indication that the interaction of DARPin_8.4 is specific for caspase-8 and that DARPin_8.4 does not bind any of the other caspases. This has also been supported by SPR measurements (data not shown) where no signal was observed for any of the caspases tested except for caspase-8. A residue which is not directly involved in the interaction (Tyr293) has recently been discovered to be essential for the regulation of caspase-8 activity [85]. Tyr293 is constitutively phosphorylated in neutrophils and dephosphorylation by the tyrosine kinase SHP-1 allows the activation of caspase-8. Tyr293 sits at the upper end of helix-2 and points towards loop1 and the active site residues (Figure 5.4). It is involved in hydrophobic interactions with the DARPin_8.4. The DARPin could be used for intracellular visualization of phosphorylation events if DARPin_8.4 is able to bind the dephosphorylated caspase-8 only. This hypothesis however, needs further experimental evidence.

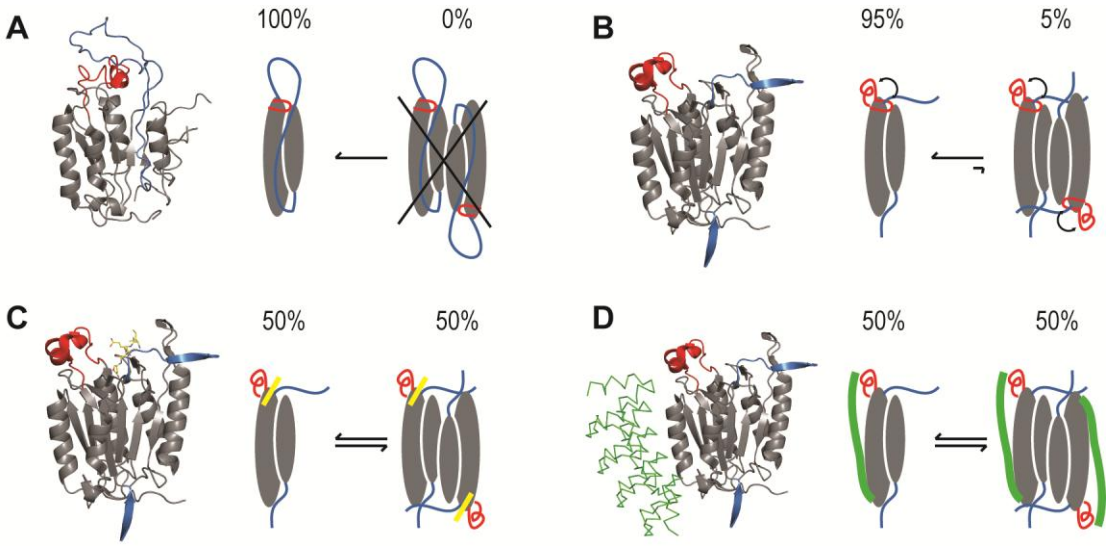

Figure 5-7: Schematic representation of caspase-8 monomer-dimer equilibrium
Caspase-8 (grey) in monomer-dimer equilibrium in different states is shown. Loop1 (red), the linker (blue), the peptide inhibitor z-IETD.fmk (yellow) and DARPin_8.4 (green) green are highlighted in color. (A) The procaspase-8 is present as a monomer only; the linker prevents dimerization and blocks the active site. (B) No crystal structure of the apo form of cleaved caspase-8 is available, but ultracentrifugation experiments revealed that it is almost exclusively present as monomer with only residual activity. Due to the absence of inhibitor, the active site forming loops including loop1 might be flexible and can adapt several conformations. (C) The K_D for caspase-8 dimerization decreases when bound to an inhibitor and the equilibrium is balanced at ~5µM [175]. (D) A similar effect is observed for DARPin_8.4, which locks loop1 in a ligand bound conformation. The equilibrium shifts towards the dimer.

The DARPin selection against caspase-8 by ribosome display was performed in the absence of inhibitor. In contrast, the caspase-8/DARPin_8.4 complex crystallized only in the presence of the inhibitor z-IETD.fmk which is known to stabilize the active site forming loops. The crystal structure of the complex revealed that DARPin_8.4 binds to an inhibitor/substrate bound conformation of caspase-8. Our kinetic analysis of the interaction using ITC and SPR was performed in the absence of inhibitor. This indicates that DARPin_8.4 interacts with caspase-8 in the presence and absence of inhibitor. The crystal structure showed the interaction of DARPin_8.4 with the active site forming loop1, which represents the inhibitor/substrate bound form. The NMR structure of procaspase-8 [23] shows loop1 in an inactive conformation, with the linker which prevents formation of the active site (Figure 5.5 A). Based on the crystal structure and the solution structure we can conclude that loop1 can be present in both conformations if no inhibitor or substrate is bound. Binding of DARPin_8.4 locks loop1 in the active conformation.

Procaspase-8 is monomeric in solution and exists in a monomer-dimer equilibrium after linker processing. The K_D of the interface is ~50 μM and binding of an inhibitor decreases the affinity to ~5 μM [161]. Binding of a substrate or inhibitor thus induces dimerization of caspase-8. This is in line with our finding, that caspase-8 has a higher activity when DARPin_8.4 is bound. The DARPin_8.4 locks loop1 in a substrate bound conformation and thus facilitates dimerization and substrate binding. The activity increases by a factor of 4 upon DARPin_8.4 binding which agrees well with the finding that the amount of dimer increases by a factor of 5, as it was found by ultracentrifugation experiments. The different conformation of the active site loops and the effect on the monomer-dimer equilibrium is illustrated in Figure 5.7.

In summary we have successfully selected and characterized a DARPin which specifically interacts with caspase-8. Binding of DARPin_8.4 increases the activity of caspase-8 significantly. Based on a high resolution structure we were able to uncover the molecular basis of this finding. The interaction increases the activity of caspase-8 by locking loop1 in a substrate bound conformation promoting the formation of a caspase-8 dimer. This study provides new evidence on the dynamic nature of caspase-8 active site loops and dimer formation.

Material and Methods

Ribosome Display and DARPin selection

We performed 4 rounds of Ribosome Display to enrich caspase-8 specific binders based on a N3C and N2C library as described previously [120, 124]. To exclude cross specific DARPins that would also bind the most homologous caspases, -2 and -9 we included them as a prepanning step in each round, prior to incubation with the according caspase (Figure 1A). Biotinylated caspase-8 was immobilized on magnetic particles (Dynabeads, Invitrogen) for solution panning or on streptavidin coated plates (Maxisorb, Nunc) for surface panning (no inhibitor was added). The DARPin-ribosome-mRNA complex was incubated with 20 µl of beads for 30 minutes at 4 °C in a tube that was previously blocked with TBST-BSA (50 mM TrisHCl pH 7.4, 150 mM NaCl, 0.05 % Tween-20, 0.1 % BSA). The incubation was followed by 4 washing cycles in WBT (50 mM Tris acetate pH 7.4, 150 mM NaCl, 50 mM Magnesium acetate, 0.05 % Tween-20). The RNA was eluted in EB (50 mM Tris acetate pH 7.4, 150 mM NaCl, 25 mM EDTA) and purified and reverse transcribed for amplification for the next selection round. In round three and four we added a 1000 fold excess of unbiotinylated caspase-3 for 10 minutes during the selection to favor the enrichment of DARPins with slow K_{off} rates. After four rounds of selection, we cloned the library in a pQE30 vector (Qiagen), transformed competent XL1 blue cells (Stratagene) and continued with crude cell extract ELISA.

Crude cell extract ELISA

Single colonies each containing one DARPin clone of the selected library were picked and inoculated in 0.9 ml auto-inducing media ZYM-5052 [172] containing deep 96-well plates (Abgene, UK). The cells were grown over night at 37 °C while shaking at 300 rpm in a shaker (TH15, Edmund Bühler GmbH). Then 200 µl of each well were transferred into a sterile 96 well plate (Nunc) as a backup for further protein expression and plasmid preparation. The remaining 700 µl of cell-suspension was harvested by centrifugation and the cell pellet was lysed with 50 µl B-PER II (78260, Pierce) per well for 30 minutes shaking at room temperature. The lysed cells were resuspended by adding 950 µl PBS, pH 7.3 and cell debris was removed by centrifugation (20 min, 4500 rpm at 4°C) in a table top centrifuge 5804 (Eppendorf). We took 20 µl of the supernatant an added it to 384 ELISA plate (Nunc).

This plate has been previously coated with 20 µl of a 22 nM Neutravidin solution (Pierce, 31000) and biotinylated caspase-8, followed by extensive washing. After 1h of incubation at room temperature and 3 washing cycles the plate was incubated with mouse anti-RGS-H_4 antibody (34650, Qiagen) at a dilution of 1:2000 in PBS 1% BSA. We then added the secondary antibody (goat-α-mouse IgG alkaline phosphatase conjugate (Sigma, A3562)) followed by four washing cycles and added the substrate di-sodium 4-nitrophenyl phosphate (pNPP; 3 mM di-sodium 4-nitrophenyl phosphate, 50 mM NaHCO3, 50 mM MgCl2.6H2O). The OD was measured at 405 nm using a multi-well plate reader (Infinite M1000, Tecan).

Protein expression, purification and biotinylation

DARPin_8.4 were expressed in auto-inducing media [172] or lysogeny broth media (LB) [110]. The expressed DARPin was purified with common His-tag purification methods using a self-made gravity column consisting of a plastic column (57024, Supelco) and 0.5 ml bead volume of Ni^{2+}-NTA agarose (30210, Qiagen). DARPin_8.4 was eluted in PBS, 200 mM Imidazole pH 7.4 and the Imidazole was removed with a PD-10 desalting column (17-0435-01, GE Helthcare). We added sodium azide to (NaN_3) a final concentration of 0.03% to prevent growth of bacteria and fungi. For crystallization we mixed both caspase-8 and DARPin_8.4 in a ratio of 1:2 and removed the excess of DARPin by size exclusion chromatography on a Superdex 200 10/300 GL (GE Healthcare) in 20 mM Tris pH7.5, 20 mM Nacl. The fractions containing the complex of caspase-8 and DARPin_8.4 were pooled and concentrated to 15 to 21 mg/ml and used for crystallization.

For chemical biotinylation of the caspase we used the linker EZ-Link Sulfo-NHS-LC-LC-Biotin (21338, Pierce), containing a reactive group, a 3.05 nm long linker and a biotin moiety. After purification, 1ml of caspase-8 (10 µM) in PBS pH 7.3 was incubated with a seven fold molar excess (1 ml of a 70 µM solution) of biotin on ice for 30 minutes. The reaction was quenched by adding 10 µl of 5 M Tris-HCl, pH 7.5. The biotinylated protein was then purified by size exclusion chromatography, using a Superdex 200 10/300 GL (GE Healthcare) in PBS at 4 °C. The fractions containing the

biotinylated caspase were pooled and frozen in liquid nitrogen after adding sucrose to a final concentration of 10 %.

Isothermal Titration Calorimetry

Purified caspase-8 were dialyzed against the assay buffer PBS, pH7.3 and 0.005% Tween 20. The protein concentration was determined using absorption spectroscopy at 280 nm combined with amino acid analysis at the Functional Genomics Center Zurich (FGCZ), Switzerland. A MicroCal VP-ITC device (Microcal, GE Healthcare, USA) was used to record isothermal titration calorimetry profiles and integrated with the software Origin. The sample cell contained 1.4 ml of either 5 or 10 μM monomeric caspase-8 at a temperature of 25 °C. 10 μl of DARPin_8.4 was titrated at a concentration of 115.1 μM with an injection interval of 300 seconds until saturation was reached.

Surface Plasmon Resonance

For SPR experiments we used the Proteon XPR36^{TM} (Bio-Rad Laboratories, Inc.) and a NLC sensor chip (Bio-Rad Laboratories, Inc.). We used sterile filtered PBS pH 7.3, 0.005% Tween-20 as a standard buffer for coating and all kinetic measurements. The biotinylated caspase-8 was coated on the sensor chip at a concentration of 5 nM and a flow rate of 30 μl per minute. The coating procedure was interrupted once a total of 1600 relative units (RU) was reached on the monitoring system. A dilution series of the analyte (DARPin) was pipetted in 96 deep well microplate (176-6023, Biorad), which were sealed to prevent evaporation or contamination with dust particles. For Kinetic analysis we measured the analyte at eight different concentrations (0, 1, 1.8, 3.2, 5.8, 10.6, 19.08, 34.3, 61.8, 111.1 and 200 nM) starting with the lowest concentration. All experiments were performed at 20 °C. We used a flow rate of 100 μl per minute, an association phase of 5 minutes and a dissociation phase of 20 minutes. The data were recorded and further processed with the ProteOn Manager 2.1.1^{TM} (BioRad). The K_D, k_{on} and k_{off} values were determined using the data analysis tool provided by the ProteON Manager^{TM} 2.1.1 using the langumir model and equilibrium constants [166].

Crystallography

The caspase-8/DARPin_8.4 complex was formed by incubating caspase-8 with DARPin_8.4 in a ratio of 1:2 for 10 minutes on ice. The complex was purified on a Superdex 200 HR 10/30 (Amersham Pharmacia, Sweden) size exclusion chromatography column in 20 mM Tris pH 7.5 (4°C), 20 mM NaCl. The samples were concentrated to 15 to 21 mg/ml using an Amicon Ultra (Millipore, 10 kDa MWCO).

Prior to crystallization of the complex, we incubated the protein solution with the tetra peptide aldehyde inhibitor Ac-DEVD-CHO in a 1:2 ration (Two inhibitor molecules per active site). Crystals were grown at room temperature using the vapor-diffusion method. The protein solution (21 mg/ml) was mixed with an equal volume of reservoir solution containing 100 mM citric acid, pH 4.9, 200 mM Li_2SO_4 and 22.4 % PEG 4000. For cryoprotection, the crystals were equilibrated in the reservoir buffer and 10 – 15 % ethylene glycerol and subsequently flash frozen in a nitrogen stream at -170 °C.

X-Ray Diffraction, Data Collection, Structure Determination and Refinement

Data were collected at the Swiss Light Source (SLS) at the X06SA beamline equipped with a Pilatus 6M fast readout pixel detector. XDS [177] was used for data processing and structure factors were calculated with IDXREF [178]. The complex crystallized in the orthorhombic space group $P2_12_12_1$ with unit cell dimensions a= 61 Å b= 81.6 Å, c=163.2 Å and $\alpha=\beta=\gamma=90.0°$.

The crystal structure was solved by molecular replacement (MR) using PHASER [179]. We used a previously published high resolution structure of caspase-8 1QDU [148] and N3C DARPin 2QYJ [115] as templates for MR. For refinement of the structures we used REFMAC 5.5.01.09 [180]. Data reduction parameters are presented in Table 5.2.

Caspase Activity measurements

Specific activity of caspase-8 was measured using the peptide substrates AC-DEVD-AMC from PEPTIDE INSTITUTE Inc. (www.**peptide**.co.jp/en/). Enzyme concentration was 10 nM and Substrate concentration was 150 μM and the assay was performed in standard caspase activity buffer containing 20 mM PIPES, pH 6.5, 10% Sucrose (w/v), 0.1% CHAPS (w/v), 10 mM DTT, 150 mM NaCl, 1mM EDTA. AMC release was monitored by measuring the fluorescent at λex = 360 nm and λem = 465 nm

using a spectrofluorometer (Infinite M-1000, Tecan). For activation measurements DARPin was added in the according molar ratio and the initial velocity was recorded.

Ultracentrifugation

Protein samples were dialyzed against PBS pH 7.3 at 4°C over night and equilibrated to 20°C prior to analysis by ultracentrifugation. We used an Optima XL-1 (Beckman Coulter, Fullerton, CA, USA) and a TI50 rotor using epoxy centerpieces (12mm) with sapphire windows. Absorption was measured at 280 nM and results were analyzed using Sedfit [181].

Coordinates

The atomic coordinates for the caspase-8 DARPin_8.4 complex have been deposited at the Protein Data Bank with the accession code 2Y1L.

6. APPENDIX

HIV-1 protease inhibition potential of functionalized polyoxometalates

Bioorganic & Medicinal Chemistry Letters 21 (2011) 1162–1166

Contents lists available at ScienceDirect

Bioorganic & Medicinal Chemistry Letters

journal homepage: www.elsevier.com/locate/bmcl

HIV-1 protease inhibition potential of functionalized polyoxometalates

Andreas Flütsch [b], Thilo Schroeder [b], Markus G. Grütter [b], Greta R. Patzke [a,*]

[a] Institute of Inorganic Chemistry, University of Zurich, Winterthurerstrasse 190, CH-8057 Zurich, Switzerland
[b] Department of Biochemistry, University of Zurich, Winterthurerstrasse 190, CH-8057 Zurich, Switzerland

ARTICLE INFO

Article history:
Received 22 October 2010
Revised 20 December 2010
Accepted 21 December 2010
Available online 25 December 2010

Keywords:
Polyoxometalates
HIV-1 protease inhibition
Functionalized polyoxotungstates
Anti-HIV drugs

ABSTRACT

Polyoxometalates (POMs) are interesting biomedical agents due to their versatile anticancer and antiviral properties, such as remarkable anti-HIV activity. Although POMs are tunable and easily accessible inorganic drug prototypes in principle, their full potential can only be tapped by enhancing their biocompatibility, for example, through organic functionalization. We have therefore investigated the HIV-1 protease inhibition potential of functionalized Keggin- and Dawson-type POMs with organic side chains. Their inhibitory performance was furthermore compared to other POM types, and the buffer dependence of the results is discussed. In addition, chemical shift mapping NMR experiments were performed to exclude POM–substrate interactions. Whereas the introduction of organic side chains into POMs is a promising approach in principle, the influence of secondary effects on the reaction system also merits detailed investigation.

Polyoxometalates (POMs) are transition metal oxide clusters that are preferably formed with W, Mo and V in their high oxidation states.[1] Their ever growing number of complex structural architectures brings forward an impressive application potential that attracts widespread research attention, for example, with respect to key technological applications,[2] (electro)catalytic processes,[3] magnetic materials[4] and nanotechnology.[5] Another special feature of POMs is their versatile bioactivity that leads to antibacterial, anticancer and antiviral properties.[6] These have been widely reviewed over the past years and POMs have been proven to be active against a wide range of viruses, including different influenza strains, Dengue fever virus and SARS coronavirus.[7] They have furthermore been tested as promising anti-HIV agents since the full outbreak of the AIDS epidemic in the 1980s. The first breakthrough was reported in 1988 when the first in vivo studies on humans were performed with the $[NaSb_9W_{21}O_{86}]^{18-}$ polyanion (commonly abbreviated as HPA-23).[8] However, HPA-23 caused severe side effects at higher dosages that forced the patients to discontinue the therapy.[8] Since then, the search for 'second generation' anti-HIV POMs with reduced toxicity was continued and the $[PTi_2W_{10}O_{40}]^{7-}$ polyanion (abbreviated as PM-19) was, for example, identified as a potential antiviral drug capable of inhibiting the replication of HIV-1[9] and herpes simplex virus (HSV)[10] in vitro.

Despite the multitude of empirical investigations on the antiviral activity of POMs, little is known about their interaction mechanisms with viruses or cells.[11] Concerning the anti-HIV activity, Inoue et al. investigated the inhibition of HIV-1 reverse transcriptase (RT) by various POMs.[12] Interestingly, cell culture experiments showed that the anti-HIV-1 activity of the POMs under consideration was not correlated with their HIV-1 RT inhibition.[12] A follow-up study by the same group identified the Keggin- and Dawson-POM types as possible 'lead compounds' for anti-HIV activity.[13] In 2001, a novel inhibition mechanism of HIV-1 protease by Dawson-type POMs was proposed in a pioneering study by Hill et al.[14] The high activity of the niobium-substituted tungstate α_2-$[P_2W_{17}NbO_{62}]^{7-}$ was explained with its binding to the flexible hinge regions on the surface of the HIV-1 protease. As most organic HIV-1 protease inhibitors bind into the active site, larger inorganic cluster molecules, such as POMs, would thus open up new ways of inhibition. Such alternative interaction pathways of POMs with HIV-1 protease would render them less sensitive towards the frequently occurring mutations of HIV-1, thereby circumventing the problem of therapeutic resistance in current AIDS therapy.[15] In addition, most anti-AIDS drugs are costly compounds that have to be administered in inconveniently high doses several times a day. POMs would offer economic advantage over the current anti-AIDS drugs in principle, because they can easily be synthesized from readily available precursors in a few synthetic steps.

The following years witnessed further reports on antiviral POMs[6a] and new insights were obtained regarding the interaction of POMs with human/bovine serum albumin[16] or protein kinase CK2.[17] Nevertheless, the fundamental issue of POM toxicity still remains to be overcome in order to turn them into powerful, versatile and low-cost inorganic anti-HIV agents. However, the development of hybrid and functionalized POMs is now proceeding rapidly[18] and thus provides new inspirations for research on inorganic anti-HIV agents together with the incorporation of antiviral

* Corresponding author. Tel.: +41 44 635 4691; fax: +41 44 635 6802.
E-mail address: greta.patzke@aci.uzh.ch (G.R. Patzke).

0960-894X/$ - see front matter © 2010 Elsevier Ltd. All rights reserved.
doi:10.1016/j.bmcl.2010.12.103

POMs into biomacromolecular matrices as an additional strategy.[19] The increasing gap between these growing classes of novel POMs and their biomedical characterization inspired us to screen a selected variety of POM types with respect to their inhibitory effect on HIV-1 protease. Firstly, we compared the inhibitory potential of POMs with different cluster sizes. We then focused on Keggin- and Dawson-type POMs with different organic side chains in order to evaluate the influence of the functionalization on the inhibitory performance. In addition, we placed emphasis on methodological issues: the results are critically discussed with respect to their considerable buffer dependence. Furthermore, we present NMR studies in solution to exclude the possibility of POM–substrate interactions.

All POMs were synthesized according to published procedures and they are summarized in Table 1. Figure 1 illustrates the structural motifs (Keggin- and Dawson-type) for the majority of the investigated POMs and their organically substituted derivatives. They have emerged from recently developed novel functionalization approaches.[20] POM 1 has been included as a representative of 'sandwich-type' lacunary POM building blocks with embedded transition metal cations. POMs 2–5 are based on the recently discovered $\{Ln_6W_{63}\}$ cluster[21] as the largest polyoxotungstate type among the present selection. These compounds are of general interest, because the incorporation of lanthanoid cations into POMs is promising with respect to their potential double function as diagnostic (e.g., luminescence or MRI) and therapeutic agents.[16a,22] POM 20 (Preyssler type) bears resemblance to the Dawson type due to the arrangement of its five PW_5 units into a Dawson-related surface. POM 28 (Lindqvist type) as the most compact and smallest structure type rounds off the 'classic' POM spectrum.

The POMs were characterized by IR spectroscopy and other analytical methods if required (e.g., NMR or single crystal structure determination) and they were stable under the applied experimental conditions. HIV-1 protease was expressed in *Escherichia coli* BL21 (DE3) pLysS cells and purified by anionic exchange and size exclusion chromatography according to literature protocols (for further experimental details cf. Supplementary data).[23] Given that

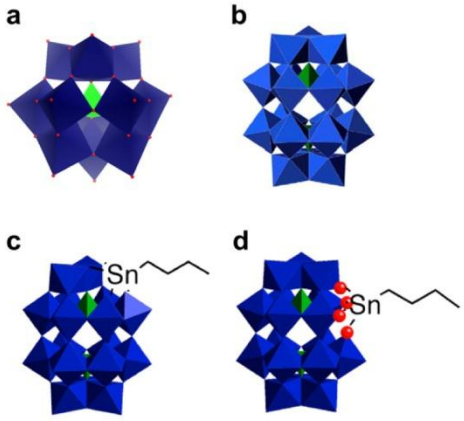

Figure 1. Overview of the most important POM types investigated in the present study: (a) Keggin type, (b) Dawson type, (c) α_2-substituted Dawson type, (d) α_1-substituted Dawson type.

HIV-1 protease has an autocatalytic activation site as well as autoprotolytic activity,[24] special attention must be paid to the high purity of the protein to precisely determine its concentration and to prevent possible interaction of the POMs with degraded protease fragments during the protease assays. For that reason, the substitution of one single amino acid, namely glutamine at position 7 to lysine (Q7K), has been performed to reach a 100-fold increase of the protein stability.[24] This residue is located in the first loop after the first β-strand in the protein and at a considerable spatial distance to the flexible hinge regions that were proposed as POM binding sites.[14] Therefore, it can be practically excluded that the use of the HIV-1 mutant Q7K affects the inhibitory potential of the POMs in comparison with the wild type. The introduction of the positively charged lysine might even exert a productive elec-

Table 1
Survey of the POMs screened for HIV-1 protease inhibition

No.	Formula	Cations	Type	Solvent	Ref.
1	$[Na_3Cu_3(H_2O)_9(AsW_9O_{33})_2]^{9-}$	Na_9	Dimer	H_2O	28
2	$[Cs\subset Tb_6As_6W_{63}O_{218}(H_2O)_{14}(OH)_4]^{25-}$	$Na_{21}Cs_4$	Hexamer	H_2O	21
3	$[Cs\subset Dy_6As_6W_{63}O_{218}(H_2O)_{14}(OH)_4]^{27-}\cdot Cl_2$	$Na_{22}Cs_5$	Hexamer	H_2O	21
4	$[Cs\subset Ho_6As_6W_{63}O_{218}(H_2O)_{14}(OH)_4]^{27-}\cdot Cl_2$	$Na_{22}Cs_5$	Hexamer	H_2O	21
5	$[Cs\subset Er_6As_6W_{63}O_{218}(H_2O)_{14}(OH)_4]^{25-}$	$Na_{21}Cs_4$	Hexamer	H_2O	21
6	α_2-$[P_2W_{17}O_{61}SnR]^{7-}$ (R = $C_3H_5O_2$)	TBA_6H	Dawson	DMSO	20
7	α_2-$[P_2W_{17}O_{61}SnR]^{6-}$ (R = C_4H_6O)	TBA_6	Dawson	DMSO	20
8	α_2-$P_2W_{17}O_{61}SnR]^{7-}$ (R = C_6H_8NO)	TBA_7	Dawson	DMSO	20
9	α_2-$[P_2W_{17}O_{61}SnR]^{7-}$ (R = C_4H_9)	TBA_6H	Dawson	DMSO	20
10	α_2-$[P_2W_{17}O_{61}SnR]^{7-}$ (R = $C_{18}H_{32}N_3O_5S$)	TBA_7	Dawson	DMSO	20
11	α_2-$[PW_{11}O_{39}SnR]^{4-}$ (R = $C_3H_5O_2$)	TBA_4	Keggin	DMSO	20
12	α_2-$[PW_{11}O_{39}SnR]^{4-}$ (R = C_4H_9)	TBA_4	Keggin	DMSO	20
13	α_2- $[PW_{11}O_{39}SnR]^{4-}$ (R = $C_{18}H_{32}N_3O_5S$)	TBA_4	Keggin	DMSO	20
14	α_1-$[P_2W_{17}O_{61}SnR]^{7-}$ (R = $C_3H_5O_2$)	TBA_6H	Dawson	DMSO	20
15	α_1-$[P_2W_{17}O_{61}SnR]^{7-}$ (R = C_6H_8NO)	TBA_7	Dawson	DMSO	20
16	α_1-$[P_2W_{17}O_{61}SnR]^{7-}$ (R = C_4H_9)	TBA_6H	Dawson	DMSO	20
17	α_2-$[P_2V_3W_{15}O_{62}R]^{7-}$ (R = $C_{13}H_{19}N$)	TBA_5	Dawson	DMSO	20
18	$[H_2W_{12}O_{42}]^{6-}$	$(NH_4)_6$	Individual	H_2O	23
19	$[NaSb_9W_{21}O_{86}]^{18-}$	$(NH_4)_{18}$	Individual	H_2O	29
20	$[NaP_5W_{30}O_{110}]^{14-}$	K_{14}	Preyssler	H_2O	29
21	α/β-$[P_2W_{18}O_{62}]^{6-}$	K_6	Dawson	H_2O	29
22	α_1-$[LiP_2W_{17}O_{61}]^{9-}$	K_9	Monolacunary Dawson	H_2O	29
23	α_2-$[P_2W_{17}O_{61}]^{10-}$	K_{10}	Monolacunary Dawson	H_2O	29
24	α_1-$[P_2W_{17}(NbO_2)O_{61}]^{7-}$	K_7	Dawson	H_2O	14
25	α_1-$[P_2W_{17}(NbO_2)O_{61}]^{7-}$	K_7	Dawson	H_2O	14
26	$[PW_{12}O_{40}]^{3-}$	NaH_2	Keggin	H_2O	30
27	$[PTi_2W_{10}O_{40}]^{7-}$	K_7	Keggin	H_2O	31
28	$[Pr(W_5O_{18})_2]^{9-}$	K_9	Lindqvist	H_2O	32

trostatic effect upon the binding of the highly negatively charged POMs to the protease. Standardized protease assays[25] were performed as described in the Supplementary data and an influence of POM absorbance on the measurements was excluded. The protease substrate was dissolved in dimethyl sulfoxide (DMSO) and two different buffer solutions were applied: buffer 1 contained a final DMSO concentration of 10%, whereas the DMSO content of buffer 2 was 1% (for details cf. Supplementary data). The stability of the protease during the assays was confirmed by Selwyn tests,[26] known as the standardized enzymatic stability test till date, under both buffer conditions. The inhibitory potential of all POMs was analyzed in triplicate measurements with Saquinavir as a standard inhibitor under both buffer conditions. Furthermore, the ingredients of the two different buffers were compared under the above conditions using POM 25 with a known high inhibitory activity[14] (cf. Table 1 and Table S-1). The higher concentration of DMSO and the additional detergent Nonidet P-40 obviously exerted the most significant influence on the measured inhibition (cf. Fig. S-1). Although the additional detergent Nonidet P-40 is supposed to stabilize the protease during the assay,[25] the enzymatic reaction also worked in the detergent-free buffer 2 with a lower DMSO concentration. Most importantly, these buffer additive tests show that the POM-induced protease inhibition is not a mere artefact arising from precipitation of protease or substrate during the reaction.

The relative activity of HIV-1 protease Q7K in buffers 1 and 2 is shown in Figure 2: the POMs were added in a 10- or 100-fold excess relative to the protease in buffer 1 and the relative protease activity remained higher than 70% in all reactions, whereas Saquinavir applied in an 1:1 ratio led to 100% inhibition. This excludes experimental setup errors and indicates that no inhibition of the enzymatic reaction by POMs occurred under these conditions. Especially for POMs 24 and 25, this result was unexpected in comparison with their previously reported high potential for HIV-1 protease inhibition.[14]

However, changing the conditions to buffer 2 completely altered the overall activity pattern. Although the use of detergent at 10% DMSO concentration had been reported to exert a stabilizing effect on HIV protease activity,[22] buffer 1 with 1% DMSO and less ingredients was sufficient to keep the protease active. A decline of the enzymatic reaction was observed in almost all experiments, in line with the preceding results:[14] POMs 21, 24 and 25 led to total protease inhibition as well as POMs 9, 12, 14 and 16. For a more detailed discussion of the results obtained in buffer 2, the POMs are classified into water-soluble POMs (1–5, 18–28) and functionalized DMSO-soluble POMs (6–17) with organic side chains. Interestingly, previous studies have pointed out that DMSO influences enzymatic reactions in a rather complex manner that varies widely—from stimulation to inhibitory effects—for the different systems under investigation.[27] However, this does not apply for the pristine HIV-1 protease in the present case and the DMSO dependence of POM-induced HIV-1 protease inhibition in contrast to its general inhibition by Saquinavir points to differences in the interaction mechanisms of organic and inorganic inhibitors, as had been suggested in earlier studies.[14]

A comparison of the water-soluble POMs with significant inhibitory potential (20–25) indicates that POMs related to the Dawson type are generally superior to the remaining POM architectures investigated in this study. POMs 21, 24 and 25 are Dawson structures and POMs 22 and 23 are monolacunary Dawson POMs (α_1- and α_2-isomers, respectively). In comparison with the Dawson type POMs, even the most prominent POMs, namely the aforementioned HPA-23 (POM 19) that was implemented in the first clinical studies[8] and the well-known anti-HIV agent PM-19 of the Keggin type (POM 27),[9] displayed a remarkably lower inhibitory effect.

Concerning POMs 2–5, their larger cluster size did not promote HIV-1 protease inhibition. Likewise, the dimeric structure of POMs 1 and 28 did not bring forward significant inhibitory activity—nor did the smaller $[H_2W_{12}O_{42}]^{6-}$ anion (POM 18) that performed even slightly worse than the Keggin compounds of related size (POMs 26 and 27). These results render the Dawson type especially promising for construction of functionalized antiviral POMs, provided that the above-mentioned buffer influence is taken into account. The dimensions of the Dawson cluster indeed appear to be in the appropriate range for POM/protein interactions as indicated in preceding theoretical studies.[14]

A more detailed comparison of the inhibitory effect among the DMSO-soluble POMs can be found in Figure 3: POMs 11–13 are Keggin type derivatives, whereas POMs 6–10 and 14–17 are Dawson type POMs that were functionalized with organic side chains at the α_1- (POMs 14–16) and α_2-position (POMs 6–10 and 17), respectively. A first glance at Figure 3 shows that the distinction between Keggin and Dawson type POMs is evened out through the introduction of organic residues: the Keggin type POM 12 with a butyl side chain induced complete inhibition of the protease activity (Fig. 3c). Generally, the introduction of a butyl side chain exerted the strongest inhibitory effect among the DMSO-soluble POMs, regardless of the POM framework or the Dawson regiosomer. This effect is even maintained with a 10-fold excess of the butyl-substituted POM 9. In the case of a propionic acid residue, the Keggin type derivative can as well compete with its Dawson analogs in terms of inhibitory effect (Fig. 3a). In parallel, the attach-

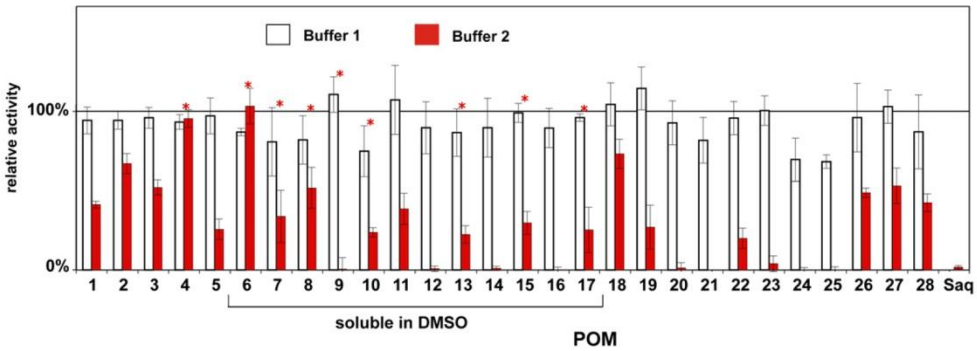

Figure 2. Relative activity of HIV-1 protease in the presence of different POMs as potential inhibitors (cf. Table 1). The reactions were performed in buffer 1 and buffer 2, respectively, and the total reaction volume was 200 µl. POMs were added to a concentration of 3 µM or 300 nM (asterisk). The activity of the protease in reactions without POMs was defined as 100% (Saq = Saquinavir).

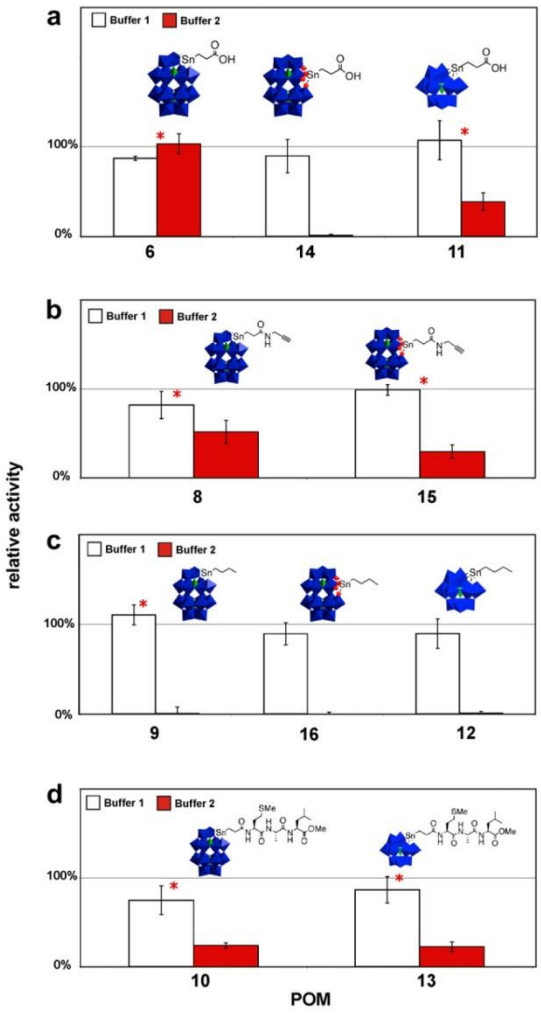

Figure 3. Relative activity of HIV-1 protease Q7K in reactions with DMSO-soluble POMs modified with organic side chains (red asterisks: POMs in 10-fold excess vs. protease, all other POMs were added in 100-fold excess); (a) POM 6, POM 14 and POM 11, (b) POM 8 and POM 15, (c) POM 9, POM 16 and POM 12, (d) POM 10 and POM 13.

ment of a more complex peptide-based side chain significantly reduced the protease activity irrespective of the POM host structure (Keggin or Dawson type, cf. Fig. 3d).

Although these results have to be interpreted with caution due to the limited number of POMs involved in the present study in comparison with the manifold experimental variables (such as buffer composition and POM concentration), their entirety indicates that the functionalization of POMs with organic moieties exerts a productive effect on their potential for HIV-1 protease inhibition.

All in all, the Dawson type POMs displayed the most promising overall inhibitory performance in the present study and it seems that the generally high antiviral potential of this 'classic' type is difficult to obtain with many newly discovered larger polyoxotungstates such as the investigated $\{Ln_6W_{63}\}$ type.[21] In this context, our recent luminescence studies on the interaction of $\{Eu_6W_{63}\}$ and $\{Tb_6W_{63}\}$ with human/bovine serum albumine[16a] also showed that their protein binding modes differ considerably from those of the smaller decatungstate cluster, thus pointing to the POM size as an important factor in structure–activity relationships. However, the introduction of organic side chains may be an important tool to modify structure activity relationships among the different POM cluster types in order to amplify the antiviral potential of POMs in general. This is supported by the fact that the introduction of a butyl group into the Keggin type (POM 12) drastically improves the inhibitory performance in comparison with the pristine Keggin POM 26. Such 'amphiphilic' POMs with unpolar organic substituents turned out to perform quite well in HIV-1 protease inhibition. For that reason, the inhibitory potential of the pristine organic compounds might also be tested as a reference.

However, this result also raises a critical point that should be taken into account for future studies: based on the present buffer additive tests, an interaction of the POMs with the substrate cannot be completely excluded. In order to detect possible interactions of the peptide substrate with POMs, we used solution NMR techniques. In particular, chemical shift mapping 600 MHz proton spectra were recorded on an approx. 100 μM peptide solution at pH 5.0 (100 mM acetate buffer) at 27 °C both in the absence and in the presence of POM 24 that displays significant HIV-1 protease inhibition.[14] The two samples were prepared from the same peptide stock solution, to one of which POM 24 was added. The pH was carefully controlled, and differed by less than 0.1 pH units in the two samples. The region of aliphatic protons displayed very little differences, whereas some amide protons experienced small shift changes. Nevertheless, the observed differences in the spectra were very minor (Fig. 4). From these changes we estimate that the K_d is likely to be in the molar range, strongly disfavoring a specific interaction with reasonable affinity and indicating the presence of a low-affinity, non-specific interaction. We conclude from these data that while a low-affinity non-specific interaction of the POM with the peptide does occur, its strength is so weak that it cannot be the reason for the observed inhibition of the substrate cleavage by the HIV-1 protease.

The ultimate proof of POM–protease interactions would certainly be the crystallization of a POM–protein complex. This challenging goal has never been reached over several decades of anti-HIV studies with POMs. Another option would be a pull-down experiment: POMs linked to beads that are incubated with HIV-1 protease or with substrate, respectively, followed by washing steps and analysis of the residues. This, however, would be a study in its own right, because POM/bead linking methods would have to be developed or, alternatively, HIV-1 protease would have to be stabilized during the coupling.

In summary, the present screening study outlines several methodological issues in the screening of POMs for anti-HIV-1 protease activity that have to be considered in follow-up experiments, namely the composition of the buffer system and the exclusion of POM/substrate interactions. Optimization studies, however, are now worthwhile, because we demonstrated that the functionalization of Dawson and Keggin type POMs with organic moieties is likely to enhance the inhibitory potential and to amplify the range of antiviral POM types, thus rendering them more biocompatible. Further studies concerning the cytotoxicity and cellular uptake of antiviral POMs are under way.

Acknowledgements

This work was supported by the Swiss National Science Foundation (SNSF Professorship PP002-114711/1) and financial support from the University of Zurich is gratefully acknowledged. We are grateful to Prof. Emmanuel Lacôte, Prof. Serge Thorimbert and Prof. Bernold Hasenknopf (UPMC Univ Paris 6, Institut Parisien de Chimie Moléculaire (UMR CNRS 7201)) for supporting us with functionalized polyoxometalates for the present study. We thank

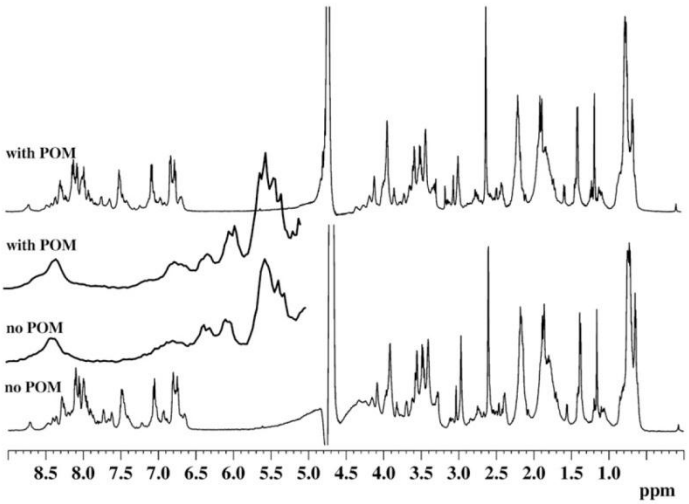

Figure 4. Proton spectra of the peptide substrate in absence (bottom spectrum) and presence (top spectrum) of POM 24, recorded at 600 MHz, $T = 300$ K. The expansion on the left displays the region from 8.2 to 8.8 ppm, and highlights the typically encountered minor changes in the spectra.

Dr. Firasat Hussain for experimental help regarding POM synthesis and Prof. Dr. Oliver Zerbe (Institute of Organic Chemistry, University of Zurich) for his support with the NMR studies. Furthermore, we are grateful to Dr. Jovan Pavlovic (Institute of Medical Virology, University of Zurich, Switzerland) for providing a template plasmid containing the HIV-1 wild type genome. Saquinavir was obtained through the AIDS Research and Reference Reagent Program, Division of AIDS, NIAID, NIH.

Supplementary data

Supplementary data (expression and purification of HIV-1 protease, synthesis and inhibitor screening of POMs as well as additive screen test comparing the different buffers) associated with this article can be found, in the online version, at doi:10.1016/j.bmcl.2010.12.103.

References and notes

1. (a) *Polyoxometalates: From Platonic Solids to Antiretroviral Activity*; Pope, M. T., Müller, A., Eds.; Kluwer: Dordrecht, 1994; (b) Pope, M. T. *Heteropoly and Isopoly Oxometalates*; Springer: Berlin, 1983; (c) Hill, C. L. *Compr. Coord. Chem. II.* **2003**, *4*, 679.
2. *Polyoxometalate Chemistry: From Topology via Self-Assembly to Applications*; Pope, M. T., Müller, A., Eds.; Kluwer: Dordrecht, 2001.
3. Keita, B.; Nadjo, L. *J. Mol. Catal. A: Chem.* **2007**, *262*, 190.
4. Kögerler, P.; Tsukerblat, B.; Müller, A. *Dalton Trans.* **2010**, *39*, 21.
5. Long, D. L.; Burkholder, E.; Cronin, L. *Chem. Soc. Rev.* **2007**, *36*, 105.
6. (a) Hasenknopf, B. *Front. Biosci.* **2005**, *10*, 275; (b) Rhule, J. T.; Hill, C. L.; Judd, D. A.; Schinazi, R. F. *Chem. Rev.* **1998**, *98*, 327; (c) Gerth, H. U. V.; Rompel, A.; Krebs, B.; Boos, J.; Lanvers-Kaminsky, C. *Anticancer Drugs* **2005**, *16*, 101.
7. (a) Shigeta, S.; Mori, S.; Yamase, T.; Yamamoto, N. *Biomed. Pharmacother.* **2006**, *60*, 211; (b) Shigeta, S.; Mori, S.; Kodama, E.; Kodama, J.; Takahashi, K.; Yamase, T. *Antivir. Res.* **2003**, *58*, 265; (c) Shigeta, S.; Mori, S.; Watanabe, J.; Soeda, S.; Takahashi, K.; Yamase, T. *Antimicrob. Agents Chemother.* **1997**, *41*, 1423.
8. Moskovitz, B. L. et al. *Antimicrob. Agents Chemother.* **1988**, *32*, 1300.
9. Take, Y.; Tokutake, Y.; Inouye, Y.; Yoshida, T.; Yamamoto, A.; Yamase, T. *Antiviral Res.* **1991**, *15*, 113.
10. Dan, K.; Miyashita, K.; Seto, Y.; Fujita, H.; Yamase, T. *Pharmacol. Res.* **2002**, *46*, 357.
11. (a) Ni, L.; Greenspan, P.; Gutman, R.; Kelloes, C.; Farmer, M. A.; Boudinot, F. D. *Antiviral Res.* **1995**, *32*, 141; (b) Berry, J. P.; Galle, P. *Exp. Mol. Pathol.* **1990**, *53*, 255.
12. Inouye, Y.; Tokutake, Y.; Kunihara, J.; Yoshida, T.; Yamase, T.; Nakata, A.; Nakamura, S. *Chem. Pharm. Bull.* **1992**, *40*, 805.
13. Inouye, Y.; Fujimoto, Y.; Sugiyama, M.; Yoshida, T.; Yamase, T. *Biol. Pharm. Bull.* **1995**, *18*, 1000.
14. Judd, D. A.; Nettles, J. H.; Nevins, N.; Snyder, J. P.; Liotta, D. C.; Tang, J.; Ermolieff, J.; Schinazi, R. F.; Hill, C. L. *J. Am. Chem. Soc.* **2001**, *123*, 886.
15. (a) Knipe, D. M.; Howley, P. M.; Griffin, D. E.; Lamb, R. A.; Martin, M. A.; Roizman, B.; Straus, S. E. *Field's Virology*; Lippincott, Williams & Wilkins: Philadelphia, 2007; (b) Santos, A. F.; Soares, M. A. *Viruses* **2010**, *2*, 503.
16. (a) Zheng, L.; Ma, Y.; Zhang, G. J.; Yao, J. N.; Bassil, B. S.; Kortz, U.; Keita, B.; de Oliveira, P.; Nadjo, L.; Craescu, C. T.; Miron, S. *Eur. J. Inorg. Chem.* **2009**, 5189; (b) Hungerford, G.; Hussain, F.; Patzke, G. R.; Green, M. *Phys. Chem. Chem. Phys.* **2010**, *12*, 7266.
17. Prudent, R.; Moucadel, V.; Laudet, B.; Barette, C.; Lafanechere, L.; Hasenknopf, B.; Li, J.; Bareyt, S.; Lacôte, E.; Thorimbert, S.; Malacria, M.; Gouzerh, P.; Cochet, C. *Chem. Biol.* **2008**, *15*, 683.
18. (a) Dolbecq, A.; Dumas, E.; Mayer, C. R.; Mialane, P. *Chem. Rev.* **2010**, *110*, 6009; (b) Carraro, M.; Modugno, G.; Sartorel, A.; Scorrano, G.; Bonchio, M. *Eur. J. Inorg. Chem.* **2009**, *34*, 5164.
19. Geisberger, G.; Paulus, S.; Carraro, M.; Bonchio, M., Patzke, G. R. *Chem. Eur. J.*, in press.
20. (a) Li, J.; Huth, I.; Chamoreau, L. M.; Hasenknopf, B.; Lacôte, E.; Thorimbert, S. *Angew. Chem., Int. Ed.* **2009**, *48*, 2035; (b) Boglio, C.; Micoine, K.; Derat, E.; Thouvenot, R.; Hasenknopf, B.; Thorimbert, S.; Lacôte, E.; Malacria, M. *J. Am. Chem. Soc.* **2008**, *130*, 4553.
21. Hussain, F.; Spingler, B.; Conrad, F.; Speldrich, M.; Kögerler, P.; Boskovic, C.; Patzke, G. R. *Dalton Trans.* **2009**, *23*, 4423.
22. Zhongfeng, L.; Weisheng, L.; Xiaojing, L.; Fengkui, P.; Yingxia, L.; Hao, L. *Magn. Res. Imaging* **2007**, *25*, 412.
23. (a) Ido, E.; Han, H. P.; Kezdy, F. J.; Tang, J. *J. Biol. Chem.* **1991**, *266*, 24359; (b) Clemente, J. C.; Coman, R. M.; Thiaville, M. M.; Janka, L. K.; Jeung, J. A.; Nukoolkarn, S.; Govindasamy, L.; Agbandje-McKenna, M.; McKenna, R.; Leelamanit, W.; Goodenow, M. M.; Dunn, B. M. *Biochemistry* **2006**, *45*, 5468.
24. Rosé, J. R.; Salto, R.; Craik, C. S. *J. Biol. Chem.* **1993**, *268*, 11939.
25. Hoffmann, D.; Assfalg-Machleidt, I.; Nitschko, H.; von der Helm, K.; Koszinowski, U.; Machleidt, W. *Biol. Chem.* **2003**, *384*, 1109.
26. Selwyn, M. J. *Biochim. Biophys. Acta* **1965**, *105*, 193.
27. (a) Rammler, D. H. *Ann. N. Y. Acad. Sci.* **1967**, *141*, 291; (b) Monder, C. *Ann. N. Y. Acad. Sci.* **1967**, *141*, 300.
28. Choi, K.-Y.; Matsuda, Y. H.; Nojiri, H.; Kortz, U.; Hussain, F.; Stowe, A. C.; Ramsey, C.; Dalal, N. S. *Phys. Rev. Lett.* **2006**, *96*, 107202-1.
29. Ginsberg, A. P. In *Inorganic Syntheses*; John Wiley & Sons, 1990; Vol. 27.
30. Allmann, R.; D'Amour, H. *Z. Kristallogr.* **1975**, *141*, 161.
31. Domaille, P. J.; Knoth, W. H. *Inorg. Chem.* **1983**, *22*, 818.
32. Liu, Y. N.; Shi, S.; Mei, W. J.; Tan, C. P.; Chen, L. M.; Liu, J.; Zheng, W. J.; Ji, L. N. *Eur. J. Med. Chem.* **2008**, *43*, 1963.

DARPin Sequences

DARPins selected against Caspase-1:

>p1.1_GSDLGKKLLEAARAGQDDEVRILMANGTDVNATDKHGHTPLHLAAYRGHLEIVEVLLKYGADVNALDDYGMTPLHVA
AWAGHLEIVEVLLKHGADVNAWDADGTTPLHLAAHTGHLEIVEVLLKYGADVNAQDKFGKTAFDISIDNGNEDLAEILQKLN
>p1.4_GSDLGRKLLEAARAGQDDEVRILMANGADVNATDKHGHTPLHLAAYRGHLEIVEVLLKYGADVNALDDYGMTPLHVA
AWAGHLEIVEVLLKHGADVNAWDADGTTPLHLAAHTGHLEIVEVLLKHGADVNAQDRFGKTAFDISIDNGNEDLAEILQKLN
>p1.7_GSDLGKKLLEAARAGQDDEVRILMANGADVNATDKHGHTPLHLAAYRGHLEIVEVLLKYGADVNALDDYGMTPLHVA
AWAGHLEIVEVLLKHGADVNAWDADGTTPLHLAAHTGHLEIVEVLLKYGADVNAQDKFGKTAFDISIDNGNEDLAEILQKLN
>p1.9_GSDLGRKLLEAARAGQDDEVRILMANGADVNATDKHGHTPLHLAAYRGHLEIVEVLLKYGADVNALDDYGMTPLHVA
AWSGHLEIVEVLLKHGADVNAWDADGTTPLHLAAHTGHLEIVEVLLKYGADVNAQDKFGKTAFDISIDNGNEDLAEILQKLN
>p1.10_GSDLGKKLLEATRAGQDDEVRILMANGADVNATDKHGHTPLHLAAYRGHLEIVEVLLKYGADVNALDDYGMTPLHV
AAWAGHLEIVEVLLKHGADVNAWDADGTTPLHLAAHTGHLEIVEVLLKHSADVNAQDKFGKTAFDISIDNGNEDLAEILQKLN
>p1.15_GSDLGRKLLEAARAGQDDEVRILMANGADVNATDKHGHTPLHLAAYRGHLEIVEVLLKYGADVNALDDYGMTPLHV
AAWAGHLEIVEVLLKHGADVNAWDADGTTPLHLAAHTGHLEIVEVLLKNGADVNAQDKFGKTAFDISIDNGNEDLAEILQKLN
>p1.16_GSDLGKKLLEAARAGQDDEVRILMANGADVNATDKHGHTPLHLAAYRGHLEIVEVLLKYGADVNALDDYGMTPLHV
AAWAGHLEIVEVLLKHGADVNAWDADGTTPLHLAAHTGHLEIVEVLLKYGTDVNAQDKFGKTAFDISIDNGNEDLAEILQKLN
>p1.17_GSDLGKKLLEAARAGQDDEVRILMADGADVNAIDKHGHTPLHLAAYRGHLEIVEVLLKYGADVNALDDYGMTPLHV
AAWAGHLEIVEVLLKHGADVNAWDADGTTPLHLAAHTGHLEIVEVLLKYSADVNAQDKFGKTAFDISIDNGNEDLAEILQKLN
>p1.19_GSDLGRKLLEAARAGQDDEVRILMVNGADVNATDKHGHTPLHLAAYRGHLEIVEVLLKYGADVNALDDYGMTPLHV
AAWAGHLEIVEVLLKHGADVNAWDTDGTTPLHLAAHTGHLEIVEVLLKYGADVNAQDKFGKTAFDISIDNGNEDLAEILQKLN
>p1.21_GSDLGRKLLEAARAGQDDEVRILMANGADVNATDKHGHTPLHLAAYRGHLEIVEVLLKYGADVNALDDYGMTPLHV
AAWAGHLEIVEVLLKHGADVNAWDADGTTPLHLAAHTGHLEIVEVLLKYGADVNAQDKFGKTAFDISIDYGNEDLAEILQKLN
>p1.39_GSDLGKKLLEAARAGQDDEVRILMANGADVNATDKHGHTPLHLAAYRGHLEIVEVLLKYGADVNALDDYGMTPLHV
AAWAGHLEIVEVLLKHGADVNAWDADGTTPLHLAAHTGHLEIVEVLLKYGADVNAQDKFGKTTFDISIDNGNEDLAEILQKLN
>p1.53_GSDLGRKLLEAARAGQDDEVRILMANGADVNAIDKHGHTPLHLAAYRGHLEIVEVLLKYGADVNALDDYGMTPLHV
AAWAGHLEIVEVLLKHGADVNAWDADGTTPLHLAAHTGHLEIVEVLLKYGADVNAQDKFGKTAFDISIDNGNEDLAEILQKLN
>p1.70_GSDLGKKLLEAARAGQDDEVRILMANGADVNATDVHGHTPLHLAAHVGHLEIVEVLLKHGADVNAADKIGWTPLHV
AGHSGHLEIVEVLLKHGADVNAWDDDGDTPLHLAAFDGHLEIVEVLLKNGADVNAQDKFGKTAFDISIDNGNEDLAEILQKLN
>p1.73_GSDLGKKLLEAARAGQDDEVRILMANGADVNAFDQHGHTPLHLAAYDGHLEIVEVLLKYGADVNAFDSEGWTPLHV
AAFSGHLEIVEVLLKHGADVNAFDYSGFTPLHLAAHSGHLEIVEVLLKNGADVNAQDKFGKTAFDISIDNGNEDLAEILQKLN
>p1.74_GSDLGKKLLEAARAGQDDEVRILMANGADVNATDVHGHTPMHLAAHVGHLEIVEVLLKHGADVNAADKIGWTPLHV
AGHSGHLEIVEVLLKHGADVNAWDDDGDTPLHLAAFDGHLEIVEVLLKYSADVNAQDKFGKTAFDISIDNGNEDLAEILQKLN
>p1.75_GSDLGKKLLEAARAGQDDEVRILMANGADVNAFDHHGHTPLHLAAYDGHLEIVEVLLKYGADVNAFDSEGWTPLHV
AAFSGHLEIVEVLLKHGADVNAFDYSGFTPLHLAAHSGHLEIVEVLLKHGADVNAQDKFGKTAFDISIDNGNEDLAEILQKLN
>p1.76_GSDLGKKLLEAARAGQDDEVRILMANGTDVNATDTEGHTPLHLAAFGGHLEIVEVLLKHGADVNANDAFGWTPLHV
VAMAGHLEIVEVLLKYGADVNAVDIFGYTPLHLAADHGHLEIVEVLLKHGADVNAQDKFGKTAFDISIDNGNEDLAEILQKLN
>p1.77_GSDLGKKLLEAARAGQDDEVRILMANGADVNALDDYGDTPLHLAAAWGHLEIVEVLLKHGTDVNAQDVVGHTPLHL
AAMAGHLEIVEVLLKLGADVNAQDKFGKTAFDISIDNGNEDLAEILQKLN
>p1.81_GSDLGKKLLEAARAGQDDEVRILMANGADVNATNWNGNTPLHLAASFGRLEIVEVLLKNGADVNAKDLWGDTPLHL
AAAWGHLEIVEVLLKYGADVNATDDLGDTPLHLAAHWGHLEIVEVLLKYGADVNAQDKFGKTAFDISIDNGNEDLAEILQKLN
>p1.85_GSDLGKKLLEAARAGQDDEVRILMANGADVNADDHNGVTPLHLAASWGHLEIVEVLLKHGADVNANDHYGFTPLHL
AAWSGHLEIVEVLLKNGADVNAQDHLCQTPLHLAAFFGHLEIVEVLLKHGADVNAQDKFGKTTFDISIDNGNEDLAEILQKLN
>p1.93_GSDLGKKLLEAARAGQDDEVRILMANGADVNAQDRHGHTPLHLATFDGHLEIVEVLLKHGADVNASDWIGWTPLHV
ATFSGHLEIVEVLLKYGADVNAIDDRGDTPLYLAAVTGHLEIVEVLLKYGADVNAQDKFGKTAFDISIDNGNEDLAEILQKLN
>p1.97_GFDLGKKLLEAARAGQDDEVRILMANGADVNADDTRGHTPLHLTAWYGHLEIVEVLLKHGADVNASDWIGWTPLHV
AAFSGHLEIVEVLLKYGADVNAYDDVGTAPLHLAASHGHLEIVEVLLKNGADVNAQDKFGKTAFDISIDNGNEDLAEILQKLN
>p1.100_GSDLGKKLLEAARAGQDDEVRILMANGADVNAQDTLGDTPLHLAAAFGHLEIVEVLLKHGADVNAYDEFGYTPLH
LATLGHLEIVEVLLKHGADVNAEDLQGDTPLHLAAFAGHLEIVEVLLKYGADVNAQDKFGKTAFDISIDNGNEDLAEILQKLN

DARPins selected against Caspase-2:

>2.1_GSDLGKKLLEAARAGQDDEVRILMANGADVNATDWLGHTPLHLAAKTGHLEIVEVLLKYGADVNAWDNYGATPLHLAA
DNGHLEIVEVLLKHGADVNAKDYEGFTPLHLAAYDGHLEIVEVLLKYGADVNAQDKFGKTAFDISIDNGNEDLAEILQKLN
>2.2_GSDLGKKLLEAARAGQDDEVRILMANGADVNAVDMFGQTALHLAASDGHLEIVEVLLKNGSDVNASDHWGFTPLHLAA
LLGHLEIVEVLLKYGADVNAQDKFGKTAFDISIDNGNEDMAEILQKLN

DARPins selected against Caspase-3:

>p3.1_GSDLGKKLLEAAHAGQDDEVRILMANGADVNANDDIGLTPLHLAAAIGHLEIVEVLLKNGADVNAEDRRGWTPCTLA
ANAGHLEIVEVLLKHGADVNATDRRGITPLHLAAWTGHLEIXEVLLKYGADVNTQXKFXXTAFXISIXNXXEDLAEILXKLN

>p3.2_GSDLGKKLLEAARAGQDDEVRILMANGADVNARDETGFTPLAADAGHLEIVEVLLKHGADVNAADRRGQTPLHLAAK
LGHLEIVEVLLKHGADVNAQDKFGKTAFDISIDNGNEDLAEILQKLN
>p3.3_GSDLGKKLLEAAHAGQDDEVRILMANGADVNAFDETGHTPQHLTADTGHLEIVEVLLKHGADVNAMDHLGWTPLHLA
ADAGHLEIVEVLLKNGADVNASDDFGSAPLHLAAIHGHLEIVEVLLKNGADVNAQDKFGKTAFDISIDNGNEDLAEILQKLN
>p3.4_GSDLGKKLLEATRAGQDDEVRILMANGADVNAMDDAGVTPLHLAAKRGHLEIVEVLLKHGADVNASDIWGRTPLHLA
ATVGHLEIVEVLLEYGADVNAQDKFGKTAFDISIDNGNEDLAEILQKLN
>p3.6_GSDLGKKLLEAARAGQDDEVRILMANGADVNAVDDAGITPLHLAAKVGHLEIVEVLLKYGADVNALDIWGRTPLHLA
ARSGHLEIVEVLLKHGADVNARDVRGLTPLHLAAKRGHLEIVEVLLKNGADVNAQDKFGKTAFDISIDNGNEDLAEILQKLN
>p3.8_GSDLGKKLLEAARAGQDDEVRILMANGADVNANDFVGKTLHLAASVGHLEIVEVLLKHGADVNAADDAGVTSLHLAA
SYGHLEIVEVLLKNGADVNARDIWGRTPLHLAAVSGHLEIVEVLLKYGADVNAQDKFGKTAFDISIDNGNEDLAEILQKLN
>p3.13_GSDLGKKLLEAALAGQDDEVRILMANGADVNADDDTGITPLYLAAWKGHLEIVEVLLKYDADVNANDILGRTPLHL
AARLGHLEIVEVLLRYGADVNASDIEGTTPLHLAANAGHLEIVEVLLKNGADVNAQDKFGKTTFDISIDNGNEDLAEILQKLN

DARPins selected against Caspase-4:

>p4.1_GSDLGKKLLEAARAGQDDEVRILMANGADVNAADDFGSTPLHLATDGHLEIVEVLLKYGADVNAFDHEGDTPLHLAA
WVGHLEIVEVLLKYGADVNAQDYGDTPLHLAALRGHLEIVEVLLKHGADVNAQDKFGKTAFDISIDNGNEDLAEILQKLN
>p4.2_GSDLGKKLLEATRAGQDDEVRILMANGADVNTADDFGSTPLHRATDGHLEIVEVLLKYGADVNAFDHEGDTPLHLAA
WVGHLEIVEVLLKYGADVNAIDHDGYTPLHLAAKWGYLEIVEVMLKHGADVNAQDKFGKTAFDISIDNGNEDLAEILQKLN
>p4.3_GSDLGKKLLEATRAGQDDEVRILMTNGADVNAADDFGSTPLHLATDGHLEIVEVLLKYGADVNAADTWGDTPLHLAA
MEGHLEIVEVLLKNGADVNAKDHEGETPRHLAAVNGHLEIVEVLLKNGADVNAQDKFGKTAFDISIDNGNEDLAEILQKLN
>p4.4_GSDLGRKLLEAARAGQDDEVRILMANGADVNAADDFGSTPLHLATDGHLEIVEVLLKYGADVNAIDHDGYTPLHLAA
FRAHLEIVEVLLKNGADVNAQDKFGKTAFDISIDNGNEDLAEILQKLN
>p4.5_GSDLGKKLLEAARAGQDDEVRILMANGADVNARDTFGLTPLHLAAFRGHLEIVEVLLKYGADVNAADYFGETPLHLA
ADVGHLEIVEVLLKYGADVNTDDIEGATPLHLAANTGHLEIVEVLLKYGADVNAQDKFGKTAFDISIDNGNEDLAEILQKLN
>p4.6_GSDLGKKLLEADRADQDDEVRILMANVADVNADDDMGSTPLHLAAVHGHLEIVEVLLKHGADVNALDLAGHTPLHLS
ANLGHLEIVEVLLKHGADVNAQDKFGKTAFDISIDNGNEDLAEILQKLN
>p4.7_GSDLGKKLPEAARAGQDDEVRILMANGADVNANDISGKTPLHLAALTGHLEIVEVLLKNSADVNADDVHGYTPLHLA
AQTGHLEIVEVLLKHGADVNAQDKFGKTAFDISIDNGNEDLAEILQKLN

DARPins selected against Caspase-5:

>p5.1_GSDLGKKLLEAARAGQDDEVRILMANGADVNTIDHHGKTPLHLAAYRGHLEIVEVLLKYGADVNAKDKWDSTPLHLA
AWNGHLEIVEVLLKYGADVNAMDSDGMTPLHLAAKWGYLEIVEVLLKHGADVNAQDKFGKTAFDISIDNGNEDLAEILQKLN
>p5.2_GSDLGKKLLEAARAGQDDEVRILMANGADVNTIDHHGKTPLHLAAYRGHLEIVEVLLKYGADVNAKDKWDSTPLHLA
AWNGHLEIVEVLLKYGADVNAMDSDGMTPLHLAAKWGYLEIVEVLLKHGADVNAQDKFGKTAFDISIDNGNEDLAEILQKLN
>p5.3_GSDLGKKLLEAARAGQDDEVRILMANGADVNATDNFGDTPLHLAAWRGHLEIVEVLLKNGADVNANDFYGNTPLHLV
AYKGHLEVVEVLLKYGADVNAEDYSGRTPLHLTAHHGHLEIVEVLLKYGADVNAQDKFGKTAFDISIDNGNEDLAEILQKLN
>p5.4_GSDLGKKLLEAARAGQDDEVRILMANGADVNAKDRLGETPLHLAAFDGHLEIVEVLLKHGADVNANDQMGKTPLHLA
ADAGHLEIVEVLLKYGADVNAIDIWGDTPLHLAAVHGHLEIVEVLLKYGADVNAQNKFGKTAFDISIDNGNEDLAEILQKLN
>p5.5_GSDLGKKLLEAARAGQDDEVRILMANGADVNAWDTLGETPLHLAALTGHLEIVEVLLKHGADVNAYDHFGATPLHLA
AWEGHLEIVEVLLKHGADVNAQDKFGKTAFDISIDNGNEDLAEILQKLN
>p5.6_GSDLGKKLLEAARAGQDDEVRILMANGADVNAWDTLGETPLHLAALTGHLEIVEVLLKHGADVNAYDHFGATPLHLA
AWEGHLEIVEVLLKHGADVNAQDKFGKTAFDISIDNGNEDLAEILQKLN
>p5.7_GSDLGKKLLDAARTGQDDEVRILMANGADVNALDWFGSTPLHLAAYDGHLEIVEVLLMNGTDVNADDHYGKTPLHLA
AIEGHLEIVEVLLKHGADVNADDLWGDTPLHLAADLGHLDIVEVLLKHGADVNAQDKFGKTAFDISIDNGNEDLAEILQKLN
>p5.8_GSDLGKKLLEAARAGQDDEVRILMANGADVNALDWFGITPLHLAAWMGHLEIVEVLLKNGADVNADDHYGKTPLHLA
AIEGHLEIVEVLLKHGADVNADDLWGDTPLHLVAILGHLEIVEVLLKNGADDNAQDKFGKTAFDISIDNGNEDLAEILQKLN
>p5.11_GSDLGKKLLEAARAGQDDEVRILMANGADVNATDWFGDTPLHLAAQYGHLEIVEVLLKHGADVNAYDEFGTTPLHL
AAYDGHLEIVEVLLKNGADVNAQDKFGKTAFDISIDNGNEDLAEILQKLN
>p5.13_GSDLGKKLLEAARAGQDDEVRILMANGADVNAKDRLGETPLHLAAFDGHLEIVEVLLKHGADVNANDQMGKTPLHL
AADAGHLEIVEVLLKYGADVNAIDIWGDTPLHLAAVHGHLEXVEVLLKYGADVNAQNKFGKTAFDISIDNGNEDLAEILQKLN
>p5.15_GSDLGRKLLEAARAGQDDEVRILMANGADVNADDWLGSTPLHLAAVAGHLEIVEVLLMNGADVNADDHYGKTPLHL
AAIEGHLEIVEVLLKHGADVNADDLWGDTPLHLAAKWGYLEIVEVLLKHGADVNAQDKFGKTAFDISIDNGNEDLAEILQKLN
>p5.16_GSDLGRKLLEAARAGQDDEVRILMANGADVNADDWLGSTPLHLAAVAGHLEIVEVLLMNGADVNADDHYGKTPLHL
AAIEGHLEIVEVLLKHGADVNADDLWGDTPLHLAAKWGYLEIVEVLLKHGADVNAQDKFGKTAFDISIDNGNEDLAEILQKLN
>p5.18_GSDLGKKLLEAARAGQDDEVRILMANGADVNADDWLGSTPLHLAAVAGHLEIVEVLLMNGADVNADDHYGKTPLHL
AAIEGHLEIVEVLLKHGADVNADDLWGDTPLHLAALIGHLEIVEVLLKYGADVNAQDKFGKTAFDISIDNGNVDLAEILQKLN
>p5.25_GSDLGRKLLEAARAGQDDEVRILMANGADVNADDWLGSTPLHLAAVAGHLEIVEVLLMNGADVNADDHYGKTPLHL
AAIEGHLEIVEVLLKHGADVNADDLWGDTPLHLAAKWGYLEIVEVLLKHGADVNAQDKFGKTAFDISIDNGNEDLAEILQKLN
>p5.27_GSDLGRKLLEAARAGQDDEVRILMANGADVNADDWLGSTPLHLAAVAGHLEIVEVLLMNGADVNADDHYGKTPLHL
AAIEGHLEIVEVLLKHGADVNADDLWGDTPLHLAAVDGHLEIVEVLLKYGAEVNAQDKFGKTAFDISIDNGNEDLAEILQKLN

>p5.29_GSDLGKKLLEAARAGQDDEVRILMANGADVNADDWLGSTPLHLAAVAGHLEIVEVLLMNGADVNADDHYGKTPLHL
VAIEGHLEIVEVLLKHGADVNADDLWGDTPLHLAAVDGHLEIVEVLLKHGADVNAQDKFGKTAFDISIDNGNEDLAEILQKLN
>p5.31_GSDLGRKLLEAARAGQDDEVRILMANGADVNADDWLGSTPLHLAAVAGHLEIVEVLLMNGADVNADDHYGKTPLHL
AAIEGHLEIVEVLLKHGADVNADDLWGDTPLHLAAKWGYLEIVEVLLKHGADVNAQDKFGKTAFDISIDNGNEDLAEILQKLN

DARPins selected against Caspase-6:

>p6.1_GSDLGKKLLEAARAGQDDEVRILMANGADVNANDYQGNTPLHLAAQHDHLEIVEVLLKNGADVNTADHFGYTPLHLA
AGYGHLEIVEVLLKHGADVNAEDSHGRTPVHLAAYIGHLEIVEVLLKYGANVNAQDKFGKTAFDISIDNGNEDLAEILQKLN
>p6.2_GSDLGKKLLEAARAGQDDEVRILMANGADVNASDNTGWTPLHLAALAGHLEIVEVLLKHGADVNAIDSDGVPPLHLA
AHVGHLEIVEVLLKNGADVNAQDVILGYTPLHLAASVGHLEIVEVLLKHGADVNAQDKFGKTAFDISIDNGNEDLAEILQKLN
>p6.3_GSDLGKKLLEAARAGQDDEVRILMANGADVNAVDQYGNTPLHLVATMGHLEIVEVLLKNGADVNATDWEGMTPLHLA
AYDGHLEIVEVLLKYGADVNARDMYGYTPLHLAAYSCHLEIVEVLLKNGADVNAQDKFGKTAFDISIDNGNEDLAEILQKLN
>p6.4_GSDLGKKLLEAARAGQDDEVRILMANGADVNAVDQYGNTPLHLVATMGHLEIVEVLLKNGADVNAYDLDGSTPLHLA
AIIGHLEIVEVLLKYGADVDAQDKFGKTAFDISIDNGNEDLAEILQKLN
>p6.5_GSDLGKKLLEAARAGQDDEVRILMANGADVNAVDQYGNTPLHLVATMGHLEIVEVLLKNGADVNATDWEGMTPLHLA
AYDGHLEIVEVLLKYGADVNARDMYGYTPLHLAAYSCHLEIVEVLLKNGADVNAQDKFGKTAFDISIDNGNEDLAEILQKLN
>p6.6_GSDLGKKLLEAARAGQDDEVRILMANGADVNAKDYMGWTPLHLAAHFGHLEIVEVLLKYGADVNASDFLGYTPLHLA
AGYGHLEIVEVLLKNGADVNASDILGRTPLHLAASMGHLEIVEVLLKYGADVNAQDKFGKTAFDISIDNGNEDLAEILQKLN
>p6.7_GSDLGKKLLEAARAGQDDEVRILMANGADVNANDDNGDTPLHLTAFFGHLEIVEVLLKYGADVNAKDKHGYTPLHLT
AWAGHLEIVEVLLKNGADVNAQDKFGKTAFDISIDNGNEDLAEILQKLN
>p6.8_GSALGKKLLEAARAGQDDEVRILMANGADVNAKDMTGDTSLHLAATNGHLEIVEVLLKYGADVNAYDSRGFTPLHLA
ALMGHLEIVEVLLKYGADVNAWDVSGSTPLHLAAFTGHLEIVEVLLKYGADVNAQDKFGKTAFDISIDNGNEDLAEILQKLN
>p6.9_GSDLGKKLLEAARAGQDDEVRILMANGADVNAKDVAGLTPLHLAAQNGHLEIVEVLLKHGADVNASDFLGYTPLHLA
AGYGHLEIVEVLLKNGADVNASDILGRTPLHLAASMGHLEIVEVLLKYGADVNAQDKFGKTAFDISIDNGNEDLAEILQKLN
>p6.10_GSDLGKKLLEAARAGQDDEVRIPMANGADVNANDDTGRTPLHLAAMMGHLEIVEVLLKYGADVNATDIWGATPLHR
AALNGHLEIVEVLLKNGTDVNAQDKFGKTAFDISIDNGSEDLAEILQKLN
>p6.11_GSDLGKKLLEAARAGQDDEVRILMANGADVNAHDIDGTTPLHLAAVHGHLEIVEVLLKHGADVNAYDSRGYTPQHL
AAMYGHLEVVEVLLKNGADVNARDDNGMTPLHLAAWSGHLEIVEVLLKNGADVNAQDKFGKTAFDISIDNGNEDLAEILQKLN
>p6.12_GSDLGKKLLEAARAGQDDEVRILMANGADVNANDYQGNTPLHLAAQHDHLEIVEVLLKNGADVNAADHFGYTPLHL
AAGYGHLEIVEVLLKHGADVNAEDSHGRTPVHLAAYIGHLEIVEVLLKYGADVNAQDKFGKTAFDISIDNGNEDLAEILQKLN
>p6.14_GSDLGKKLLEAARAGQDDEVRILMANGADVNANDYQGNTPLHLAAQHDHLEIVEVLLKNGADVNAADHFGYTPLHL
AAGYGHLEIVEVLLKHGADVNAEDSHGRTPVHLAAYIGHLEIVEVLLKYGADVNAQDKFGKTAFDISIDNGNEDLAEILQKLN
>p6.15_GSDLGKKLLEAARAGQDDEVRILMANGADVNASDNTGWTPLHLAALAGHLEIVEVLLKHGADVNAIDSDGVPPLHL
AAHVGHLEIVEVLLKNGADVNAQDVILGYTPLHLAASVGHLEIVEVLLKHGADVNAQDKFGKTAFDISIDNGNEDLAEILQKL
>p6.16_GSDLGRKLLEAARVGQDDEVRILMANGADVNAADYAGMTPLHLSANSGHLEIVEVLLKYGADVNAGDTFGWTPLHL
TANRGHLEIIEVLVKYGADVNALEKGGNSPLHLAAMISHLEIVEVLLKYGADVNARDKFGKTAFDISIDNGNEDLAEILQKLN
>p6.21_GSDLGKKLLEAARAGQDDEVRILMANGADVNARDIDGTTPLHLAAVWGHLEIVEVLLRNGADVNAYDSRGYTPLHL
AAMYGHLEVVEVLLKHGADVNARDDNGMTPLHLAAWSGHLEIVEVLLKNGADVNAQDKFGKTAFDISIDNGNEDLAEILQKLN

DARPins selected against Caspase-7:

>p7.1_GSDLGKKLLEAARAGQDDEVRILMANGADVNANDATGNTPLHLAAEEGHLEIVEVLLKYGADVNAVDADGSTPLHLA
ALFGHPEIVEVLLKNGADVNAADFYGHTPLHLAALFGHLEIVEVLLKNGADVNAQDKFGKTAFDISIDNGNEDLAEILQKLN
>p7.2_GSDLGKKLLEAARAGQDDEVRILMANGTDVNARDWHGWTPLHLAAWHGHLEIVEVLLKYGADVNAHDTTGNTPLHLA
AHVGHLEIVEVLLKNGADVNAQDKFGKTAFDISIDNGNEDLAEILQKLN
>p7.3_GSDLGKKLLEAARAGQDDEVRILMANGADVNAKDTHGWTPLHLAAWYGHLEIVEVLLKNGADVNADDHLGTTPLHLA
AVWGHLEIVEVLLKYGADVNAQDKFGKTAFDISIDNGNEDLAEILQKLN
>p7.4_GSDLGKKLLEAARAGQDDEVRILMANGTDVNAADYAGMTPLHLSANSGHLEIVEVLLKYGADVNAGDTFGWTPLHLA
AWHGHLEIVEVLLKNGADVNATDLHGTTPLHLAAHMGHLEIVEVLLKHGADVNAQDKFGKTAFDISIDNGNEDLAEILQKLN
>p7.5_GSDLGKKLLEAARAGQDDEVRILMANGADVNASDTFGWTPLHLAAFHGHLEIVEVLLKHGADVNASDTFGNTPLHLA
ARLGHLEIVEVLLKHGADVNAQDKFGKTAFDISIDNGNEDLAEILQKLN
>p7.7_GSDLGKKLLEAARAGQDDEVRILMANGADVNAYDFYGWTPLHLAAWYGHLEIVEVLLKHGADVNANDKHGSTPLHLA
AHTGHLEIVEVLLKHGADVNAQDKFGKTAFDISIDNGNEDLAEILQKLN
>p7.10_GSDLGKKLLEAARAGQDDEVRILMANGADVNATDKWGWTPLHLAAFHGHLEIVEVLLKNGADVNALDXXGSTPLHL
AAXXGXLEIVEVLLKYGADVNAQDKFGKTAFDISIDNGNEDLAEILQKLN
>p7.14_GSDLGKKLLEAARAGQDDEVRILMANGADVNAHDRYGWTPLHLAAFHGHLEIVEVLLKYGADVNANDYLGTTPLHL
AAHWGHLEIVEVLLKNGADVNAQDKFGKTAFDISIDNGNEDLAEILQKLN
>p7.17_GSDLGKKLLEAARAGQDDEVRILMANGTDVNARDWHGWTPLHLATWHGHLEIVEVLLKYGADVNAHDTTGNTPLHL
AAHMGHLEIVEVLLKHGADVNAQDKFGKTAFDISIDNGNEDLAEILQKLN
>p7.18_GSDLGKKLLEAARAGQDDEVRILMANGADVNADDAWGQTPLHLAAQNGHLEIVEVLLKHDADVNATDWVGMTPLHL
AADDGHLEIVEALLKYGADVNAYDQLGNTPLNLAATDGHLEIVEVLLKYGADVNAQDKFGKTAFDISIDNGNEDLAEILQKLN

>p7.20_GSDLGKKLLEAARAGQDDEVRILMANGADVNARDDDGWTPLHLAAWYGHLEIVEVLLKHGADVNALDSLGTTPLHL
AAINGHLEIVEVLLKHGADVNAKDKFGKTAFDISIDNGNEDLAEILQKLN
>p7.31_GSDLGKKLLEAARAGQDDEVRILMANGADVNAIDHQGLTPLHLAAQNGHLEIVEVLLKHGADVNAEDWYGWTPLHL
AAFHGHLEIVEVLLKHGADVNANDYLGTTPLHLAAVTGHLEIVEVLLKHGADVNAQDKFGKTAFDISIDNGNEDLAEILQKLN
>p7.33_GSDLGKKLLEAARAGQDDEVRILMANGTDVNARDWHGWTPLHLAAWHGHLEIVEVLLKYGADVNAHDTTGNTPLHL
AAHMGHLEIVEVLLKHGADVNAQDKFGKTAFDISIDNGNEDLAEILQKLN
>p7.43_GSDLGKKLLEAARAGQDDEVRILMANGADVNANDKHGWTPLHLAAFFGHLEIVEVLLKNGADVNAVDNMGTTPLHL
AAHMGRLEIVEVLLKYGADVNAQDKFGKTAFDISIDNGNEDLAEILQKLN

DARPins selected against Caspase-8:

>p8.1_GSDLGKKLLEAARAGQDDEVRILMANGADVNAEDASGWTPLHLAAFNGHLEIVEVLLKNGADVNAVDHAGMTPLRLA
ALFGHLEIVEVLLKNGADVNANDMEGHTPLHLAAMFGHLEIVEVLLKHGADANAQDKFGKTAFDISIDNGNEDLAEILQKLN
>p8.2_GSDLGKKLLEAARAGQDDEVRILMANGADVNANDLAGWTPLHLAAFLGHLEIVEVLLKNGADVNASDLNGKTPLHLA
AVFGHLEIVEVLLKHGADVNAVDDAGHTPLHLAALFGHLEIVEVLLKYGAEVNAQDKFGKTAFDISIDNGNEDLAEILQKLN
>p8.3_GSDLGKKLLEAARAGQDDEVRILMANGADVNAVDDRGMTPLHLAALNGHLEIVEVLLKNGADVNAADNTGWTPLHLA
ALRGHLEIVEVLLKHGADVNAQDHAGTTPLHLATYLGHLEIVEVLLKNGADVNAQDKFGKTAFDISIDNGNEDLAEILQKLN
>p8.4_GSDLGKKLLEAARAGRDDEVRILMANGADVNAEDASGWTPLHLAAFNGHLEIVEVLLKNGADVNAVDHAGMTPLRLA
ALFGHLEIVEVLLKNGADVNANDMEGHTPLHLAAMFGHLEIVEVLLKNGADVNAQDKFGKTAFDISIDNGNEDLAEILQKLN
>p8.5_GSDLGKKLLEAARAGQDDEVRILMANGADVNAEDASGWTPLHLAAFNGHLEIVEVLLKNGADVNAVDHAGMTPLRLA
ALFGHLEIVEVLLKNGADVNANDMEGHTPLHLAAMFGHLEIVEVLLKHGADVNAQDKFGKTAFDISIDNGNEDLAEILQKLN
>p8.6_GSDLGKKLLEAARAGQDDEVRILMANGADVNAEDASGWTPLHLAAFNGHLEIVEVLLKNGADVNAVDHAGMTPLRLA
ALFGHLEIVEVLLKNGADVNANDMEGHTPLHLAAMFGHLEIVEVLLKHGADANAQDKFGKTAFDISIDNGNKDLAEILQKLN
>p8.7_GSDLGKKLLEAARAGQDDEVRILMANGADVNAEDASGWTPLHLAAFNGHLEIVEVLLKNGADVNAVDHAGMTPLRLA
ALFGHLEIVEVLLKNGADVNANDMEGHTPLHLAAMFGHLEIVEVLLKHGADANAQDKFGKTAFDISIDNGNEDLAEILQKLN
>p8.8_GSDLGKKLLEAARAGQDDEVRILMANGADVNAEDASGWTPLHLAAFNGHLEIVEVLLKNGADVNAVDHAGMTPLRLA
ALFGHLEIVEVLLKNDADVNANDMEGHTPLHLAAMFGHLEIVEVLLKHGADVNAQDKFGKTAFDISIDNGNEDLAEILQKLN
>p8.9_GSDLGKKLLEAARAGQDDEVRILMANGADVNAEDASGWTPLHLAAFNGHLEIVEVLLKNGADVNAVDHAGMTPLRLA
ALFGHLEIVEVLLKNGADVNANDMEGHTPLHLAAMFGHLEIVEVLLKHGADANAQDKFGKTAFDISIDNGNEDLAEILQKLN
>p8.10_GSDLGKKLLEAARAGQDDEVRILMANGADVNAEDASGWTPLHLAAFNGHLEIVEVLLKNGADVNAVDHAGMTPLRL
AALFGHLEIVEVLLKNGADVNANDMEGHTPLHLAAMFGHLEIVEVLLKNGADVNAQDKFGKTAFDISIDNGNEDLAEILQKLN

DARPins selected against Caspase-9:

>p9.3_GSDLGKKLLEAACAGQDXEVRILMANGADVNAWDNVGSTPLHLAGSNGHLEIVEVLLKYGADVNADDHFGDTPLHLA
AKQGHLEIVEVLLKNGADXNAFDXXGNXPLHLXXXYGHLEIVEXLLXNGADVNAQDKFXKTAFXISIXXGXEDLXEILXKLN
>p9.4_GSDLGKKLLEAARAGQDDEVHILMANGADVNALDIFGGTPLHLAADDGHLEIVEVLLKYGADVNATDVSGLTPLHLA
ANWGHLEIVEVLLKYGADVGADDITGETPLHLAARDGHLEIVEVLLRHGADVNAQDKFGKTAFDISIDNGNEDLAEILXKLN

* Each DARPin contains a purification tag and antibody recognition sequence (MRGSHHHHH) at the N-terminus of the sequence.

7. BIBLIOGRAPHY

1. Kerr, J.F., A.H. Wyllie, and A.R. Currie, *Apoptosis: a basic biological phenomenon with wide-ranging implications in tissue kinetics.* Br J Cancer, 1972. **26**(4): p. 239-57.
2. Wyllie, A.H., J.F. Kerr, and A.R. Currie, *Cell death: the significance of apoptosis.* International review of cytology, 1980. **68**: p. 251-306.
3. Taylor, R.C., S.P. Cullen, and S.J. Martin, *Apoptosis: controlled demolition at the cellular level.* Nat Rev Mol Cell Biol, 2008. **9**(3): p. 231-41.
4. Ellis, R.E., J.Y. Yuan, and H.R. Horvitz, *Mechanisms and functions of cell death.* Annual review of cell biology, 1991. **7**: p. 663-98.
5. Thornberry, N.A., et al., *A novel heterodimeric cysteine protease is required for interleukin-1 beta processing in monocytes.* Nature, 1992. **356**(6372): p. 768-74.
6. Cerretti, D.P., et al., *Molecular cloning of the interleukin-1 beta converting enzyme.* Science, 1992. **256**(5053): p. 97-100.
7. Malorn, W., *MORPHOLOGICAL ASPECTS OF APOPTOSIS*, S.F. Walter Malorni, and Carla Fiorentini, Editor. 2009, Walter Malorni, Stefano Fais, and Carla Fiorentini.
8. Alberts, B., *Molecular Biology of the Cell*. Vol. V. 2008: Garland Science.
9. Yu, H.S., et al., *Arsenic induces tumor necrosis factor alpha release and tumor necrosis factor receptor 1 signaling in T helper cell apoptosis.* The Journal of investigative dermatology, 2002. **119**(4): p. 812-9.
10. Luthi, A.U., et al., *Suppression of interleukin-33 bioactivity through proteolysis by apoptotic caspases.* Immunity, 2009. **31**(1): p. 84-98.
11. Degterev, A. and J. Yuan, *Expansion and evolution of cell death programmes.* Nature reviews. Molecular cell biology, 2008. **9**(5): p. 378-90.
12. Horvitz, H.R., S. Shaham, and M.O. Hengartner, *The genetics of programmed cell death in the nematode Caenorhabditis elegans.* Cold Spring Harbor symposia on quantitative biology, 1994. **59**: p. 377-85.
13. Metzstein, M.M., G.M. Stanfield, and H.R. Horvitz, *Genetics of programmed cell death in C. elegans: past, present and future.* Trends in genetics : TIG, 1998. **14**(10): p. 410-6.
14. Riedl, S.J. and Y. Shi, *Molecular mechanisms of caspase regulation during apoptosis.* Nature reviews. Molecular cell biology, 2004. **5**(11): p. 897-907.
15. Fulda, S. and K.M. Debatin, *Extrinsic versus intrinsic apoptosis pathways in anticancer chemotherapy.* Oncogene, 2006. **25**(34): p. 4798-811.
16. Green, D.R. and G. Kroemer, *The pathophysiology of mitochondrial cell death.* Science, 2004. **305**(5684): p. 626-9.
17. Wang, X., *The expanding role of mitochondria in apoptosis.* Genes & development, 2001. **15**(22): p. 2922-33.
18. Li, P., et al., *Cytochrome c and dATP-dependent formation of Apaf-1/caspase-9 complex initiates an apoptotic protease cascade.* Cell, 1997. **91**(4): p. 479-89.
19. Acehan, D., et al., *Three-dimensional structure of the apoptosome: implications for assembly, procaspase-9 binding, and activation.* Mol Cell, 2002. **9**(2): p. 423-32.
20. Daniel, P.T., et al., *The kiss of death: promises and failures of death receptors and ligands in cancer therapy.* Leukemia : official journal of the Leukemia Society of America, Leukemia Research Fund, U.K, 2001. **15**(7): p. 1022-32.
21. Chan, C.W. and F. Housseau, *The 'kiss of death' by dendritic cells to cancer cells.* Cell Death Differ, 2008. **15**(1): p. 58-69.
22. Nagata, S., *Apoptosis by death factor.* Cell, 1997. **88**(3): p. 355-65.
23. Keller, N., et al., *Structural and biochemical studies on procaspase-8: new insights on initiator caspase activation.* Structure, 2009. **17**(3): p. 438-48.

24. Muzio, M., et al., *An induced proximity model for caspase-8 activation.* J Biol Chem, 1998. **273**(5): p. 2926-30.
25. Hanahan, D. and R.A. Weinberg, *The hallmarks of cancer.* Cell, 2000. **100**(1): p. 57-70.
26. Hengartner, M.O., *The biochemistry of apoptosis.* Nature, 2000. **407**(6805): p. 770-6.
27. Timmer, J.C. and G.S. Salvesen, *Caspase substrates.* Cell Death Differ, 2007. **14**(1): p. 66-72.
28. Thornberry, N.A., et al., *A combinatorial approach defines specificities of members of the caspase family and granzyme B. Functional relationships established for key mediators of apoptosis.* J Biol Chem, 1997. **272**(29): p. 17907-11.
29. Talanian, R.V., et al., *Substrate specificities of caspase family proteases.* J Biol Chem, 1997. **272**(15): p. 9677-82.
30. Luthi, A.U. and S.J. Martin, *The CASBAH: a searchable database of caspase substrates.* Cell Death Differ, 2007. **14**(4): p. 641-50.
31. Igarashi, Y., et al., *CutDB: a proteolytic event database.* Nucleic acids research, 2007. **35**(Database issue): p. D546-9.
32. Coleman, M.L., et al., *Membrane blebbing during apoptosis results from caspase-mediated activation of ROCK I.* Nature cell biology, 2001. **3**(4): p. 339-45.
33. Croft, D.R., et al., *Actin-myosin-based contraction is responsible for apoptotic nuclear disintegration.* J Cell Biol, 2005. **168**(2): p. 245-55.
34. Lamkanfi, M. and V.M. Dixit, *IL-33 raises alarm.* Immunity, 2009. **31**(1): p. 5-7.
35. Ziegler, U. and P. Groscurth, *Morphological features of cell death.* News in physiological sciences : an international journal of physiology produced jointly by the International Union of Physiological Sciences and the American Physiological Society, 2004. **19**: p. 124-8.
36. Samejima, K. and W.C. Earnshaw, *Trashing the genome: the role of nucleases during apoptosis.* Nature reviews. Molecular cell biology, 2005. **6**(9): p. 677-88.
37. Nicholson, D.W., *From bench to clinic with apoptosis-based therapeutic agents.* Nature, 2000. **407**(6805): p. 810-6.
38. Borden, E.C., H. Kluger, and J. Crowley, *Apoptosis: a clinical perspective.* Nature reviews. Drug discovery, 2008. **7**(12): p. 959.
39. Srikanth, C.V., et al., *Salmonella pathogenesis and processing of secreted effectors by caspase-3.* Science, 2010. **330**(6002): p. 390-3.
40. Wurzer, W.J., et al., *Caspase 3 activation is essential for efficient influenza virus propagation.* Embo J, 2003. **22**(11): p. 2717-28.
41. Hanahan, D. and R.A. Weinberg, *Hallmarks of cancer: the next generation.* Cell, 2011. **144**(5): p. 646-74.
42. Fesik, S.W., *Promoting apoptosis as a strategy for cancer drug discovery.* Nature reviews. Cancer, 2005. **5**(11): p. 876-85.
43. Ashkenazi, A., *Targeting death and decoy receptors of the tumour-necrosis factor superfamily.* Nature reviews. Cancer, 2002. **2**(6): p. 420-30.
44. Garcia-Calvo, M., et al., *Inhibition of human caspases by peptide-based and macromolecular inhibitors.* J Biol Chem, 1998. **273**(49): p. 32608-13.
45. MacKenzie, S.H., J.L. Schipper, and A.C. Clark, *The potential for caspases in drug discovery.* Curr Opin Drug Discov Devel, 2010. **13**(5): p. 568-76.
46. Yuan, J., et al., *The C. elegans cell death gene ced-3 encodes a protein similar to mammalian interleukin-1 beta-converting enzyme.* Cell, 1993. **75**(4): p. 641-52.
47. Alnemri, E.S., et al., *Human ICE/CED-3 protease nomenclature.* Cell, 1996. **87**(2): p. 171.
48. Walker, N.P., et al., *Crystal structure of the cysteine protease interleukin-1 beta-converting enzyme: a (p20/p10)2 homodimer.* Cell, 1994. **78**(2): p. 343-52.
49. Meergans, T., et al., *The short prodomain influences caspase-3 activation in HeLa cells.* Biochem J, 2000. **349**(Pt 1): p. 135-40.
50. Grutter, M.G., *Caspases: key players in programmed cell death.* Curr Opin Struct Biol, 2000. **10**(6): p. 649-55.

51. Denault, J.B. and G.S. Salvesen, *Caspases.* Current protocols in protein science / editorial board, John E. Coligan ... [et al.], 2002. **Chapter 21**: p. Unit 21 8.
52. Krumschnabel, G., et al., *The enigma of caspase-2: the laymen's view.* Cell Death Differ, 2009. **16**(2): p. 195-207.
53. Fuentes-Prior, P. and G.S. Salvesen, *The protein structures that shape caspase activity, specificity, activation and inhibition.* Biochem J, 2004. **384**(Pt 2): p. 201-32.
54. Sulpizi, M., et al., *Reaction mechanism of caspases: insights from QM/MM Car-Parrinello simulations.* Proteins, 2003. **52**(2): p. 212-24.
55. Riedl, S.J., et al., *Structural basis for the activation of human procaspase-7.* Proc Natl Acad Sci U S A, 2001. **98**(26): p. 14790-5.
56. Chai, J., et al., *Crystal structure of a procaspase-7 zymogen: mechanisms of activation and substrate binding.* Cell, 2001. **107**(3): p. 399-407.
57. Rodriguez, J. and Y. Lazebnik, *Caspase-9 and APAF-1 form an active holoenzyme.* Genes & development, 1999. **13**(24): p. 3179-84.
58. Salvesen, G.S. and V.M. Dixit, *Caspase activation: the induced-proximity model.* Proc Natl Acad Sci U S A, 1999. **96**(20): p. 10964-7.
59. Boatright, K.M., et al., *A unified model for apical caspase activation.* Mol Cell, 2003. **11**(2): p. 529-41.
60. Shi, Y., *Caspase activation: revisiting the induced proximity model.* Cell, 2004. **117**(7): p. 855-8.
61. Donepudi, M. and M.G. Grutter, *Structure and zymogen activation of caspases.* Biophys Chem, 2002. **101-102**: p. 145-53.
62. Keller, N., M.G. Grutter, and O. Zerbe, *Studies of the molecular mechanism of caspase-8 activation by solution NMR.* Cell Death Differ, 2010. **17**(4): p. 710-8.
63. Kischkel, F.C., et al., *Cytotoxicity-dependent APO-1 (Fas/CD95)-associated proteins form a death-inducing signaling complex (DISC) with the receptor.* Embo J, 1995. **14**(22): p. 5579-88.
64. Krammer, P.H., *CD95's deadly mission in the immune system.* Nature, 2000. **407**(6805): p. 789-95.
65. Tsujimoto, Y., *Role of Bcl-2 family proteins in apoptosis: apoptosomes or mitochondria?* Genes to cells : devoted to molecular & cellular mechanisms, 1998. **3**(11): p. 697-707.
66. Pan, G., K. O'Rourke, and V.M. Dixit, *Caspase-9, Bcl-XL, and Apaf-1 form a ternary complex.* J Biol Chem, 1998. **273**(10): p. 5841-5.
67. Martinon, F., K. Burns, and J. Tschopp, *The inflammasome: a molecular platform triggering activation of inflammatory caspases and processing of proIL-beta.* Mol Cell, 2002. **10**(2): p. 417-26.
68. Tinel, A. and J. Tschopp, *The PIDDosome, a protein complex implicated in activation of caspase-2 in response to genotoxic stress.* Science, 2004. **304**(5672): p. 843-6.
69. Yuan, S., et al., *Structure of an apoptosome-procaspase-9 CARD complex.* Structure, 2010. **18**(5): p. 571-83.
70. Riedl, S.J. and G.S. Salvesen, *The apoptosome: signalling platform of cell death.* Nature reviews. Molecular cell biology, 2007. **8**(5): p. 405-13.
71. Salvesen, G.S. and S.J. Riedl, *Structure of the Fas/FADD complex: a conditional death domain complex mediating signaling by receptor clustering.* Cell cycle, 2009. **8**(17): p. 2723-7.
72. Wang, L., et al., *The Fas-FADD death domain complex structure reveals the basis of DISC assembly and disease mutations.* Nat Struct Mol Biol, 2010. **17**(11): p. 1324-9.
73. Holler, N., et al., *Two adjacent trimeric Fas ligands are required for Fas signaling and formation of a death-inducing signaling complex.* Molecular and cellular biology, 2003. **23**(4): p. 1428-40.
74. Scott, F.L., et al., *The Fas-FADD death domain complex structure unravels signalling by receptor clustering.* Nature, 2009. **457**(7232): p. 1019-22.
75. Carl Branden, J.T., *Introduction to Protein Structure.* 1/1/1999. **Second Edition**.

76. Shi, Y., *Mechanisms of caspase activation and inhibition during apoptosis.* Mol Cell, 2002. **9**(3): p. 459-70.
77. Schechter, I. and A. Berger, *On the active site of proteases. 3. Mapping the active site of papain; specific peptide inhibitors of papain.* Biochem Biophys Res Commun, 1968. **32**(5): p. 898-902.
78. Stennicke, H.R., et al., *Internally quenched fluorescent peptide substrates disclose the subsite preferences of human caspases 1, 3, 6, 7 and 8.* Biochem J, 2000. **350 Pt 2**: p. 563-8.
79. Agniswamy, J., B. Fang, and I.T. Weber, *Plasticity of S2-S4 specificity pockets of executioner caspase-7 revealed by structural and kinetic analysis.* Febs J, 2007. **274**(18): p. 4752-65.
80. McStay, G.P., G.S. Salvesen, and D.R. Green, *Overlapping cleavage motif selectivity of caspases: implications for analysis of apoptotic pathways.* Cell Death Differ, 2008. **15**(2): p. 322-31.
81. Germain, M., et al., *Cleavage of automodified poly(ADP-ribose) polymerase during apoptosis. Evidence for involvement of caspase-7.* J Biol Chem, 1999. **274**(40): p. 28379-84.
82. Thornberry, N.A. and Y. Lazebnik, *Caspases: enemies within.* Science, 1998. **281**(5381): p. 1312-6.
83. Sleath, P.R., et al., *Substrate specificity of the protease that processes human interleukin-1 beta.* J Biol Chem, 1990. **265**(24): p. 14526-8.
84. Cardone, M.H., et al., *Regulation of cell death protease caspase-9 by phosphorylation.* Science, 1998. **282**(5392): p. 1318-21.
85. Jia, S.H., et al., *Dynamic regulation of neutrophil survival through tyrosine phosphorylation or dephosphorylation of caspase-8.* J Biol Chem, 2008. **283**(9): p. 5402-13.
86. Hardy, J.A., et al., *Discovery of an allosteric site in the caspases.* Proc Natl Acad Sci U S A, 2004. **101**(34): p. 12461-6.
87. Hardy, J.A. and J.A. Wells, *Dissecting an allosteric switch in caspase-7 using chemical and mutational probes.* J Biol Chem, 2009. **284**(38): p. 26063-9.
88. Scheer, J.M., M.J. Romanowski, and J.A. Wells, *A common allosteric site and mechanism in caspases.* Proc Natl Acad Sci U S A, 2006. **103**(20): p. 7595-600.
89. Drag, M. and G.S. Salvesen, *Emerging principles in protease-based drug discovery.* Nature reviews. Drug discovery, 2010. **9**(9): p. 690-701.
90. Mittl, P.R., et al., *Structure of recombinant human CPP32 in complex with the tetrapeptide acetyl-Asp-Val-Ala-Asp fluoromethyl ketone.* J Biol Chem, 1997. **272**(10): p. 6539-47.
91. Wang, Z., et al., *Kinetic and structural characterization of caspase-3 and caspase-8 inhibition by a novel class of irreversible inhibitors.* Biochim Biophys Acta, 2010. **1804**(9): p. 1817-31.
92. Deveraux, Q.L. and J.C. Reed, *IAP family proteins--suppressors of apoptosis.* Genes & development, 1999. **13**(3): p. 239-52.
93. Siegmund, B. and M. Zeitz, *Pralnacasan (vertex pharmaceuticals).* IDrugs : the investigational drugs journal, 2003. **6**(2): p. 154-8.
94. Fischer, U. and K. Schulze-Osthoff, *Apoptosis-based therapies and drug targets.* Cell Death Differ, 2005. **12 Suppl 1**: p. 942-61.
95. Schweizer, A., et al., *Inhibition of caspase-2 by a designed ankyrin repeat protein: specificity, structure, and inhibition mechanism.* Structure, 2007. **15**(5): p. 625-36.
96. Amstutz, P., et al., *Intracellular kinase inhibitors selected from combinatorial libraries of designed ankyrin repeat proteins.* J Biol Chem, 2005. **280**(26): p. 24715-22.
97. Salvesen, G.S. and S.J. Riedl, *Caspase inhibition, specifically.* Structure, 2007. **15**(5): p. 513-4.
98. Carter, B.Z., et al., *Regulation and targeting of antiapoptotic XIAP in acute myeloid leukemia.* Leukemia : official journal of the Leukemia Society of America, Leukemia Research Fund, U.K, 2003. **17**(11): p. 2081-9.
99. Carter, B.Z., et al., *XIAP antisense oligonucleotide (AEG35156) achieves target knockdown and induces apoptosis preferentially in CD34+38- cells in a phase 1/2 study of patients with*

relapsed/refractory AML. Apoptosis : an international journal on programmed cell death, 2011. **16**(1): p. 67-74.
100. Walters, J., et al., *A constitutively active and uninhibitable caspase-3 zymogen efficiently induces apoptosis.* Biochem J, 2009. **424**(3): p. 335-45.
101. Putt, K.S., et al., *Small-molecule activation of procaspase-3 to caspase-3 as a personalized anticancer strategy.* Nature chemical biology, 2006. **2**(10): p. 543-50.
102. Wolan, D.W., et al., *Small-molecule activators of a proenzyme.* Science, 2009. **326**(5954): p. 853-8.
103. Garcia-Calvo, M., et al., *Purification and catalytic properties of human caspase family members.* Cell Death Differ, 1999. **6**(4): p. 362-9.
104. Binz, H.K., P. Amstutz, and A. Pluckthun, *Engineering novel binding proteins from nonimmunoglobulin domains.* Nat Biotechnol, 2005. **23**(10): p. 1257-68.
105. Pluckthun, A., *Escherichia coli producing recombinant antibodies.* Bioprocess technology, 1994. **19**: p. 233-52.
106. Winter, G., *Synthetic human antibodies and a strategy for protein engineering.* FEBS Lett, 1998. **430**(1-2): p. 92-4.
107. Worn, A. and A. Pluckthun, *Stability engineering of antibody single-chain Fv fragments.* J Mol Biol, 2001. **305**(5): p. 989-1010.
108. Wu, T.T., G. Johnson, and E.A. Kabat, *Length distribution of CDRH3 in antibodies.* Proteins, 1993. **16**(1): p. 1-7.
109. Forrer, P., et al., *A novel strategy to design binding molecules harnessing the modular nature of repeat proteins.* FEBS Lett, 2003. **539**(1-3): p. 2-6.
110. Binz, H.K., et al., *Designing repeat proteins: well-expressed, soluble and stable proteins from combinatorial libraries of consensus ankyrin repeat proteins.* J Mol Biol, 2003. **332**(2): p. 489-503.
111. Kohl, A., et al., *Designed to be stable: crystal structure of a consensus ankyrin repeat protein.* Proc Natl Acad Sci U S A, 2003. **100**(4): p. 1700-5.
112. Devi, V.S., et al., *Folding of a designed simple ankyrin repeat protein.* Protein Sci, 2004. **13**(11): p. 2864-70.
113. Wetzel, S.K., et al., *Folding and unfolding mechanism of highly stable full-consensus ankyrin repeat proteins.* J Mol Biol, 2008. **376**(1): p. 241-57.
114. Forrer, P., et al., *Consensus design of repeat proteins.* Chembiochem, 2004. **5**(2): p. 183-9.
115. Merz, T., et al., *Stabilizing ionic interactions in a full-consensus ankyrin repeat protein.* J Mol Biol, 2008. **376**(1): p. 232-40.
116. Pancer, Z., et al., *Somatic diversification of variable lymphocyte receptors in the agnathan sea lamprey.* Nature, 2004. **430**(6996): p. 174-80.
117. Smith, G.P., *Filamentous fusion phage: novel expression vectors that display cloned antigens on the virion surface.* Science, 1985. **228**(4705): p. 1315-7.
118. Leemhuis, H., et al., *New genotype-phenotype linkages for directed evolution of functional proteins.* Curr Opin Struct Biol, 2005. **15**(4): p. 472-8.
119. Hanes, J. and A. Pluckthun, *In vitro selection and evolution of functional proteins by using ribosome display.* Proc Natl Acad Sci U S A, 1997. **94**(10): p. 4937-42.
120. Zahnd, C., P. Amstutz, and A. Pluckthun, *Ribosome display: selecting and evolving proteins in vitro that specifically bind to a target.* Nat Methods, 2007. **4**(3): p. 269-79.
121. Amstutz, P., et al., *In vitro display technologies: novel developments and applications.* Curr Opin Biotechnol, 2001. **12**(4): p. 400-5.
122. Steiner, D., et al., *Signal sequences directing cotranslational translocation expand the range of proteins amenable to phage display.* Nat Biotechnol, 2006. **24**(7): p. 823-31.
123. Zahnd, C., et al., *A designed ankyrin repeat protein evolved to picomolar affinity to Her2.* J Mol Biol, 2007. **369**(4): p. 1015-28.

124. Binz, H.K., et al., *High-affinity binders selected from designed ankyrin repeat protein libraries.* Nat Biotechnol, 2004. **22**(5): p. 575-82.
125. Kohl, A., et al., *Allosteric inhibition of aminoglycoside phosphotransferase by a designed ankyrin repeat protein.* Structure, 2005. **13**(8): p. 1131-41.
126. Zahnd, C., et al., *Selection and characterization of Her2 binding-designed ankyrin repeat proteins.* J Biol Chem, 2006. **281**(46): p. 35167-75.
127. Bandeiras, T.M., et al., *Structure of wild-type Plk-1 kinase domain in complex with a selective DARPin.* Acta Crystallogr D Biol Crystallogr, 2008. **64**(Pt 4): p. 339-53.
128. Sennhauser, G., et al., *Drug export pathway of multidrug exporter AcrB revealed by DARPin inhibitors.* PLoS Biol, 2007. **5**(1): p. e7.
129. Sennhauser, G. and M.G. Grutter, *Chaperone-assisted crystallography with DARPins.* Structure, 2008. **16**(10): p. 1443-53.
130. Park J. Sheldon, C.R.J., *Protein Engineering and Design*. 2010: CRC Press.
131. Stumpp, M.T., H.K. Binz, and P. Amstutz, *DARPins: a new generation of protein therapeutics.* Drug Discov Today, 2008. **13**(15-16): p. 695-701.
132. Tereshko, V., et al., *Toward chaperone-assisted crystallography: protein engineering enhancement of crystal packing and X-ray phasing capabilities of a camelid single-domain antibody (VHH) scaffold.* Protein science : a publication of the Protein Society, 2008. **17**(7): p. 1175-87.
133. Kawe, M., et al., *Isolation of intracellular proteinase inhibitors derived from designed ankyrin repeat proteins by genetic screening.* J Biol Chem, 2006. **281**(52): p. 40252-63.
134. Fabbrizio, E., et al., *Inhibition of mammalian cell proliferation by genetically selected peptide aptamers that functionally antagonize E2F activity.* Oncogene, 1999. **18**(30): p. 4357-63.
135. Sheridan, C., *Pharma consolidates its grip on post-antibody landscape.* Nat Biotechnol, 2007. **25**(4): p. 365-6.
136. Martinon, F. and J. Tschopp, *Inflammatory Caspases: Linking an Intracellular Innate Immune System to Autoinflammatory Diseases.* Cell, 2004. **117**(5): p. 561-574.
137. Saleh, M., et al., *Differential modulation of endotoxin responsiveness by human caspase-12 polymorphisms.* Nature, 2004. **429**(6987): p. 75-9.
138. Goldberg, Y.P., et al., *Cleavage of huntingtin by apopain, a proapoptotic cysteine protease, is modulated by the polyglutamine tract.* Nat Genet, 1996. **13**(4): p. 442-9.
139. Krippner-Heidenreich, A., et al., *Targeting of the transcription factor Max during apoptosis: phosphorylation-regulated cleavage by caspase-5 at an unusual glutamic acid residue in position P1.* Biochem J, 2001. **358**(Pt 3): p. 705-15.
140. Rao, L., D. Perez, and E. White, *Lamin proteolysis facilitates nuclear events during apoptosis.* J Cell Biol, 1996. **135**(6 Pt 1): p. 1441-55.
141. Tewari, M., et al., *Yama/CPP32 beta, a mammalian homolog of CED-3, is a CrmA-inhibitable protease that cleaves the death substrate poly(ADP-ribose) polymerase.* Cell, 1995. **81**(5): p. 801-9.
142. Denault, J.B. and G.S. Salvesen, *Caspases.* Curr Protoc Protein Sci, 2002. **Chapter 21**: p. Unit 21 8.
143. Denecker, G., et al., *Caspase-14 reveals its secrets.* J Cell Biol, 2008. **180**(3): p. 451-8.
144. Wilson, K.P., et al., *Structure and mechanism of interleukin-1 beta converting enzyme.* Nature, 1994. **370**(6487): p. 270-5.
145. Nicholson, D.W., et al., *Identification and inhibition of the ICE/CED-3 protease necessary for mammalian apoptosis.* Nature, 1995. **376**(6535): p. 37-43.
146. Denault, J.B. and G.S. Salvesen, *Expression, purification, and characterization of caspases.* Curr Protoc Protein Sci, 2003. **Chapter 21**: p. Unit 21 13.
147. Stennicke, H.R. and G.S. Salvesen, *Biochemical characteristics of caspases-3, -6, -7, and -8.* J Biol Chem, 1997. **272**(41): p. 25719-23.

148. Blanchard, H., et al., *The three-dimensional structure of caspase-8: an initiator enzyme in apoptosis.* Structure, 1999. **7**(9): p. 1125-33.
149. Dang, L.C., et al., *Preparation of an autolysis-resistant interleukin-1 beta converting enzyme mutant.* Biochemistry, 1996. **35**(47): p. 14910-6.
150. Kamens, J., et al., *Identification and characterization of ICH-2, a novel member of the interleukin-1 beta-converting enzyme family of cysteine proteases.* J Biol Chem, 1995. **270**(25): p. 15250-6.
151. Srinivasula, S.M., et al., *Molecular ordering of the Fas-apoptotic pathway: the Fas/APO-1 protease Mch5 is a CrmA-inhibitable protease that activates multiple Ced-3/ICE-like cysteine proteases.* Proc Natl Acad Sci U S A, 1996. **93**(25): p. 14486-91.
152. Stennicke, H.R. and G.S. Salvesen, *Caspases: preparation and characterization.* Methods, 1999. **17**(4): p. 313-9.
153. Fink, A.L., *Protein aggregation: folding aggregates, inclusion bodies and amyloid.* Fold Des, 1998. **3**(1): p. R9-23.
154. Rano, T.A., et al., *A combinatorial approach for determining protease specificities: application to interleukin-1beta converting enzyme (ICE).* Chem Biol, 1997. **4**(2): p. 149-55.
155. Rotonda, J., et al., *The three-dimensional structure of apopain/CPP32, a key mediator of apoptosis.* Nat Struct Biol, 1996. **3**(7): p. 619-25.
156. Fernandes-Alnemri, T., et al., *In vitro activation of CPP32 and Mch3 by Mch4, a novel human apoptotic cysteine protease containing two FADD-like domains.* Proc Natl Acad Sci U S A, 1996. **93**(15): p. 7464-9.
157. Koeplinger, K.A., et al., *Caspase 8: an efficient method for large-scale autoactivation of recombinant procaspase 8 by matrix adsorption and characterization of the active enzyme.* Protein Expr Purif, 2000. **18**(3): p. 378-87.
158. Scheer, J.M., J.A. Wells, and M.J. Romanowski, *Malonate-assisted purification of human caspases.* Protein Expr Purif, 2005. **41**(1): p. 148-53.
159. Pop, C., et al., *Role of proteolysis in caspase-8 activation and stabilization.* Biochemistry, 2007. **46**(14): p. 4398-407.
160. Keller, N., M.G. Grutter, and O. Zerbe, *Studies of the molecular mechanism of caspase-8 activation by solution NMR.* Cell death and differentiation, 2010. **17**(4): p. 710-8.
161. Donepudi, M., et al., *Insights into the regulatory mechanism for caspase-8 activation.* Mol Cell, 2003. **11**(2): p. 543-9.
162. Baumgartner, R., et al., *The crystal structure of caspase-6, a selective effector of axonal degeneration.* Biochemical Journal, 2009. **423**(3): p. 429-439.
163. Selwyn, M.J., *A simple test for inactivation of an enzyme during assay.* Biochim Biophys Acta, 1965. **105**(1): p. 193-5.
164. Berger, A.B., K.B. Sexton, and M. Bogyo, *Commonly used caspase inhibitors designed based on substrate specificity profiles lack selectivity.* Cell research, 2006. **16**(12): p. 961-3.
165. Hall, D.A., J. Ptacek, and M. Snyder, *Protein microarray technology.* Mech Ageing Dev, 2007. **128**(1): p. 161-7.
166. Bravman, T., et al., *Exploring "one-shot" kinetics and small molecule analysis using the ProteOn XPR36 array biosensor.* Anal Biochem, 2006. **358**(2): p. 281-8.
167. Heller, M.J., *DNA microarray technology: devices, systems, and applications.* Annual review of biomedical engineering, 2002. **4**: p. 129-53.
168. Joos, T. and J. Bachmann, *Protein microarrays: potentials and limitations.* Frontiers in bioscience : a journal and virtual library, 2009. **14**: p. 4376-85.
169. Heuer, J.G., D.J. Cummins, and B.T. Edmonds, *Multiplex proteomic approaches to sepsis research: case studies employing new technologies.* Expert Rev Proteomics, 2005. **2**(5): p. 669-80.
170. Khalifa, M.B., et al., *BIACORE data processing: an evaluation of the global fitting procedure.* Anal Biochem, 2001. **293**(2): p. 194-203.

171. Heidi Roschitzki-Voser, T.S., Franziska Fröhlich, Esther Lenherr, Andreas Schweizer, Peer R.E. Mittl, Antonio Baici, Markus Grütter, *Expression, Purification and Kinetic Characterisation of Human Caspases*. 2011.
172. Studier, F.W., *Protein production by auto-induction in high density shaking cultures.* Protein Expr Purif, 2005. **41**(1): p. 207-34.
173. Turk, B., *Targeting proteases: successes, failures and future prospects.* Nature reviews. Drug discovery, 2006. **5**(9): p. 785-99.
174. Stupack, D.G., *Caspase-8 as a therapeutic target in cancer.* Cancer letters, 2010.
175. Watt, W., et al., *The atomic-resolution structure of human caspase-8, a key activator of apoptosis.* Structure, 1999. **7**(9): p. 1135-43.
176. Wilson, I.A. and R.L. Stanfield, *Antibody-antigen interactions: new structures and new conformational changes.* Curr Opin Struct Biol, 1994. **4**(6): p. 857-67.
177. Kabsch, W., *Integration, scaling, space-group assignment and post-refinement.* Acta crystallographica. Section D, Biological crystallography, 2010. **66**(Pt 2): p. 133-44.
178. Potterton, E., et al., *A graphical user interface to the CCP4 program suite.* Acta crystallographica. Section D, Biological crystallography, 2003. **59**(Pt 7): p. 1131-7.
179. McCoy, A.J., et al., *Phaser crystallographic software.* Journal of applied crystallography, 2007. **40**(Pt 4): p. 658-674.
180. Murshudov, G.N., A.A. Vagin, and E.J. Dodson, *Refinement of macromolecular structures by the maximum-likelihood method.* Acta crystallographica. Section D, Biological crystallography, 1997. **53**(Pt 3): p. 240-55.
181. Schuck, P., et al., *Size-distribution analysis of proteins by analytical ultracentrifugation: strategies and application to model systems.* Biophysical journal, 2002. **82**(2): p. 1096-111.

8. CURRICULUM VITAE

Personal Data

Name	Thilo Schroeder
Date of birth	03.05.1981
Place of birth	Bad Soden im Taunus

Education, studies and professional development

08/1991 – 08/2000	High school diploma, *Klostergymnasium Großkrotzenburg*
10/2000 - 09/2001	Obligatory Military Service, *Paramedic*
10/2001 - 10/2003	Vordiplom in Biology, *Technical University of Darmstadt* *Major Field: Molecular biology*
10/2003 - 10/2006	Dipl.-Ing. Biotechnology, *ESBS/ULP Strasbourg, France* *Major Field: Protein biochemistry, process engineering*
04/2007 – present	PhD in Biochemistry, *University of Zurich* *Major Field: Structural biology and protein engineering*
04/2007 – present	Life Science Zurich Graduate School, *ETH |University Zurich* *Member of the PhD Program in Molecular Life Science*
10/2009 – present	Head SiROP Global, *A Network of Universities with a joint UROP Program*

Scientific Internships

07/2004 - 09/2004	University of Edinburgh; *Institute of molecular plant science* Project: 'Reactive oxygen species (ROS) regulating cell growth of *Neurospora crassa*'
06/2005 - 09/2005	Micromet AG, Munich; *Division of Production and Purification* Project: 'Production, purification and analysis of scAntibodies and BITE® molecules'
10/2005 - 12/2005	IGBMC, Strasbourg; *Integrated Structural Biology* Project: 'Structural studies of human tissue non-specific alkaline phosphatase and genotype-phenotype correlation in hypophosphatasia'
02/2006 - 10/2006	University of Sydney, *School of Molecular Bioscience* Project: 'Investigation of protein interactions mediated by zinc fingers'

Extracurricular activities

06/2005	Representative of France "*Bright Europe Students Conference"* (Brussels)
09/2006 - 10/2007	Vice-President of the ESBS Alumni Association *Organisation of a scientific conference with 200 participants*
10/2007 – present	Advisory Board of the ESBS Alumni Organisation
08/2007	Novartis Biotechnology Leadership Camp 2007
10/2007 – 09/2009	Head - SiROP University of Zurich *SiROP - Student Research Opportunities Program*
10/2009 – present	President - SiROP Global Association *A Network of Universities with a joint UROP Program*

Scientific Publications

- HIV-1 Protease Inhibition Potential of Functionalized Polyoxometalates.
  A. Flütsch, T. Schroeder, M.G. Gruetter, G.R. Patzke*; *Bioorg. Med. Chem. Lett.*, DOI: 10.1016/j.bmcl.2010.12.103.

- Protein-protein interactions: analysis of a false positive GST pulldown result.
  S. Wissmueller, J. Font, C.W. Liew, E. Cram, T. Schroeder, J. Turner, M. Crossley, J.P. Mackay, J.M. Matthews; Proteins: Volume 79, Issue 8, pages 2365–2371, August 2011

- Systematic Biochemical and Kinetic Characterization of human Caspases.
  H.V. Roschitzki-Voser*, & T. Schroeder*, A. Schweizer, P.R.E. Mittl, M.G. Gruetter;
  ** contributed equally. Manuscript in preparation*

- Specific inhibition of Caspase-3 by a competitive DARPin: molecular mimicry between native and designed inhibitors.
  T. Schroeder, J. Barandun, A. Flütsch, P.M. Mittl, M.G. Gruetter;
  Manuscript in preparation

- A DARPin activator of caspase-8
  T. Schroeder, J. Barandun, A. Flütsch, M.G. Gruetter
  Manuscript in preparation

9. ACKNOWLEDGEMENTS

I owe my deepest gratitude to my “Doktorvater” Prof. Markus Grütter who gave me all the freedom and support I needed for my PhD thesis. I am also grateful to my supportive committee members Prof. Ben Schuler and Prof. Jürgen Rühe. Furthermore I would like to thank Peer Mittl and Christophe Briand for their scientific support and guidance throughout my thesis.

This thesis would not have been possible without the support of my colleagues, collaborators and students thus I am grateful to all for scientific discussions and general support. This especially concerns Andreas Flütsch, Jonas Barandun, Heidi Roschitzki-Voser, Christopher Weinert, Sara Züger, Dominik Zahn, Markus Müller, Cyrille Delley and Markus Seeger. Many more colleagues contributed to the great scientific atmosphere in the lab including Florence Bourquin, Damien Morger, Anshumali Mittal, Michael Hohl, Georg Hausamann, Peter Gutte, Magdalena Burkowska, Céline Stutz-Ducommun, Jana Popp, Martin Bühlmann, Beat Blattmann, Chaithanya Madhurantakam, Frank Kroner and Thomas Heitkamp. I am also indebted to former colleagues in the lab such as Daniel Frey, Gabi Sennhauser, Oliv Eidam, Tobias Merz and Brian Brissoni who have been always willing to help me throughout my thesis.

I have shared great moments with friends I have made in the last 4 ½ years. We have not missed out on enjoying our time in the institute besides long hours and often stressful weeks. I thank Schwami, Sebastian, Löschi, Andi, Jonas and many more for making this time most enjoyable.

Beside my thesis I have met inspiring people during the development of SiROP, especially Dominic Frutiger. I would like to thank everyone who believed in our success and supported us in hard times. This project would have not been possible without the generosity of Prof. Markus Grütter who gave me the autonomy to organize my time and workload at any time.

I am indebted to my family, especially my mother and father who showed me how to life with integrity. They allowed me to grow up in an open, stimulating environment and facilitated me a higher education.

I owe my deepest gratitude to my wonderful girlfriend ‘Ness’ who was on my side during the last five years and supported me at any time. I look forward to many more fulfilling years somewhere in the world.